COMMUNICATIONS QUARTERLY

THE JOURNAL OF COMMUNICATIONS TECHNOLOGY

Fall 1992 $9.95

- Using the NASA Advanced Communications Satellite
- A "Synthesizer Simulator" for 6-Meter FM Operation
- The Drake R-8 Receiver
- The 4:1 Balun
- Long-Path Propagation
- Observing the Sun
- The EXJAY
- The Effects of Antenna Height on Other Antenna Properties

ISSN 1053-9433

Simple Operation
Advanced Technology

Within Budget - Without Compromise

Just when you thought great audio and tough as nails construction were luxury features available only on the most expensive models, and just when you thought simple, intuitive operation was a thing of the past, along comes the Alinco VHF-FM HT, DJ -180T.

A different offset can be stored in each memory channel, and most other functions can also be stored independently in each memory channel. CTCSS encode and decode comes standard. As most QSO's on 2- meter are done through repeaters, these special features make the DJ-180T the most practical HT to own. Alinco has once again combined high-technology with low-cost.

Check out the affordable technology of the 90's. Check out ALINCO.

Also Available
DJ-580T Dual Bander

Incredibly Tough !

Photo for Demonstration only- Abuse to the transceiver will void the warranty.

- Receive 130.0- 173.9 MHz
- CTCSS encode/decode built-in
- 2 watts standard, 5 watts with optional EBP- 28N battery pack
- High/Low power selection
- Selectable frequency step for quick QSY
- Standard DTMF keyboard
- Low battery indicator
- "Busy" channel LCD indicator
- Key Lock/ PTT Lock functions
- Auto Power Off
- Instant QSY to Call channel
- Monitor button
- Scan Modes
- Battery Saver design
- Supplied with Ni-Cd battery pack EBP-26N for 2 watts output, wall charger, belthook, and strap.
- Optional accessories: EBP'28N Battery pack for 5 watts output, EDH-11 Drycell case, EDC-45 Quick charger, EMS-9 Speaker-microphone, EME-12/13 Headset with VOX/PTT. EME-15 Tie-pin microphone, EDH-12 DC Jack adaptor .EBC-6 Mobile bracket, ESC-18/19 Soft case, EJ-14U 50ch Memory unit, EJ-15U 200ch Memory unit.

ALINCO ELECTRONICS INC.

ALINCO ELECTRONICS INC.
438 Amapola Avenue, Unit 130, Torrance, CA 90501
Tel. (310) 618-8616 Fax (310) 618-8758

Specification and features are subject to change without notice or obligation.

Majestic

New horizons in HF communications —from Kenwood

KENWOOD U.S.A. CORPORATION
COMMUNICATIONS & TEST EQUIPMENT GROUP
P.O. BOX 22745, 2201 E. Dominguez
Street, Long Beach, CA 90801-5745

KENWOOD ELECTRONICS CANADA INC.
6070 Kestrel Road, Mississauga,
Ontario, Canada L5T 1S8

KENWOOD

...pacesetter in Amateur Radio

Kenwood's TS-450S is a triumph in transceiver technology. Covering all nine HF amateur bands—in SSB, CW, AM, FM and FSK modes—with powerful 100W output (40W for AM), it's ready to take the lead in all HF communications. Advanced features—with the option of adding a digital signal processor—give you the edge in performance. Yet the compact, lightweight construction makes it a winner for DX-peditions.

- **AIP system**
  Kenwood's exclusive AIP (Advanced Intercept Point) circuit raises the receiver's intermodulation dynamic range to 108dB, while lowering the noise floor level.
- **Superior interference reduction controls**
  IF shift, AF notch, dual noise blankers, CW reverse mode, and pitch control. IF filter settings can be stored in memory.
- **Ultra-fine tuning (SSB, CW and FSK modes)**
  By engaging the FINE key, the operator can tune precisely in 1Hz steps, thanks to the Direct Digital Synthesizer (DDS).
- **Automatic antenna tuner (built-in or option)**
  The internal antenna tuner can automatically establish the optimum match between 20 and 150 ohms in the 80 to 10 meter band. The optional AT-300 automatic external tuner covers 160-10m, and can also be used to tune single-wire antennas.
- **Optional digital signal processor**
  The DSP-100 provides signal modulation of unerring precision. In SSB operation, unwanted sidebands can be effectively suppressed, while in CW mode the rise and decay times of CW waveforms can be tailored for optimum clarity.

The TS-450S can be computer-controlled with the optional IF-232C and HamWindows software. See your Authorized Dealer for more details.

TS-450S
HF Transceiver

COMMUNICATIONS QUARTERLY

THE JOURNAL OF COMMUNICATIONS TECHNOLOGY

CONTENTS

Volume 2, Number 4 — Fall 1992

Cover photo courtesy of NASA. See Using The NASA Advanced Communications Technology Satellite, page 13.

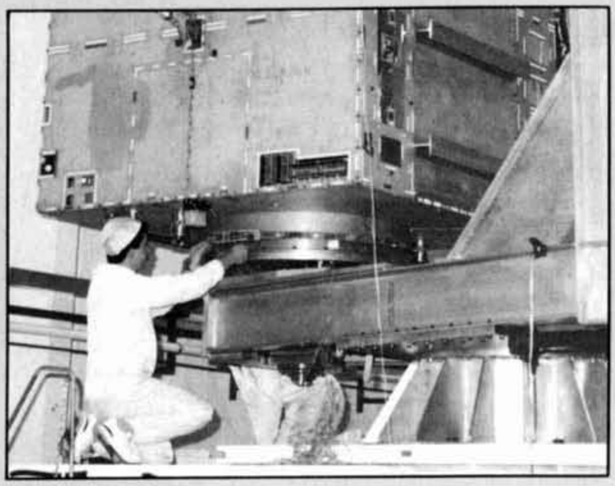

Krueger, page 13

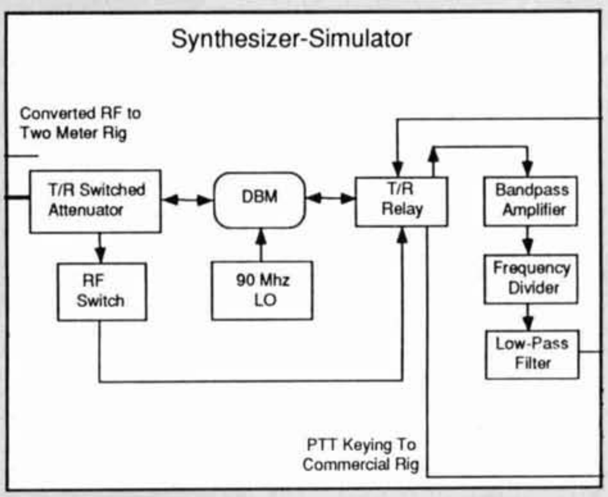

Witmer, page 41

Sevick, page 23

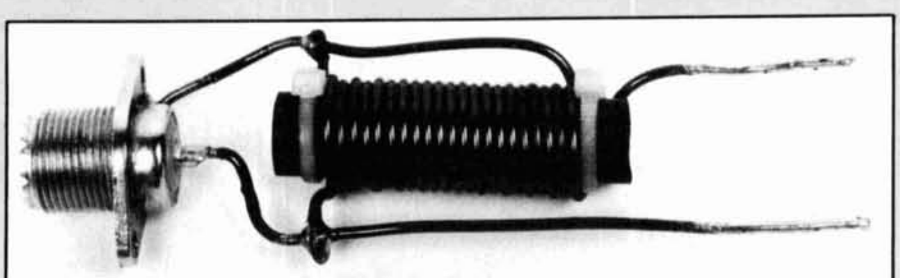

EDITORIAL

It's Time To Clean Up Our Act

Obscenity, indecent language, profanity. There used to be a time when these words had clear-cut definitions. When Clark Gable as Rhett Buttler spoke those immortal words, "Frankly, my dear, I don't give a damn," to Vivian Leigh's Scarlett O'Hara in MGM's rendition of *Gone With the Wind* in the 1940s, it was considered scandalous. Now, even G-rated movies have children making lewd gestures and using off-color words that would have sent my mother rushing for a bar of soap to wash out my mouth.

What ever happened to the "Seven Dirty words" you couldn't say on the air—radio or television?

How many of us have become inured to obscenity, indecent language, and profanity because of its pervasiveness in our culture? How does our apathy affect the youngest members of our society?

Just last night, at my son's soccer game, several of the children (fifth and sixth graders) complained to the coaches and referee about a teammate who was swearing on the field. The child, who happened to be the ref's son, should have received a yellow warning card for foul language that, if repeated, would have resulted from his expulsion from the game. The ref let the incident go, the coaches stewed on the sidelines, and the children seemed demoralized by the lack of adult intervention.

As most of us know, some amateur radio operators are not immune to letting fly with a few on-air expletives. But those who do, might wish to choose their words more carefully in the future.

A recent issue of the "W5YI Report" featured as its lead story a piece about an amateur radio operator who was issued a $2,000 fine for indecent language.* The newsletter noted that it is believed this is the first monetary forfeiture ever issued for an over-the-air amateur service speech violation not linked to an additional, easier to prove offense. The amateur in question, a General Class operator from Tennessee, is charged with using obscene and indecent language during an on-the-air argument on the 20-meter ham band on June 29, 1992, between the hours of 3:53 and 4:22 p.m.—a time when children might be listening in.

Although the Supreme Court has ruled that obscene speech is not protected by the First Amendment, rulings concerning indecent language and profanity are somewhat more nebulous.

In an interview with W5YI's Fred Maia, Mary Beth Richards, Chief of the FCC's Enforcement Division, stated that: "The court has said that obscene speech is not protected by the First Amendment. In indecent speech, the government has to find a compelling interest in order to take action against indecent speech. The Commission has found that the compelling governmental interest is to protect children and that has been upheld. If you can show that there is a likelihood of children listening, then the Commission can take action against indecent speech."

According to Richards, the Commission has not taken action against any of the lesser language violations (i.e., profanity) listed in the FCC's rule Section 97.113(d) at this time. She said that the FCC's recent ruling was an indication that the Commission would continue to take action on obscene or indecent transmissions that occur when there is a reasonable certainty that children are in the audience—reviewing each violation on a case-by-case basis.

As is true of many of the dilemmas people tend to get themselves into, we can be our own worst enemies when it comes to bad language. I myself have used inappropriate words or phrases in front of my 12-year-old son. Do I want my son to use such language? Of course not! Am I surprised to hear such language is commonplace to my son and his peers? Not really. But what, besides monitoring my own speech, can I do, can any of us do, to ensure that our children are protected form obscene and indecent language.

As amateur radio operators, we can both

(Continued on page 8)

*"Amateur Issued $2,000 Fine for Indecent Language," *W5YI* Report, Vol. 14, Issue #19, October 1, 1992, page 1.

A publication of
CQ Communications, Inc.
76 North Broadway
Hicksville, NY 11801-USA

Editorial Offices: P.O. Box 465, Barrington, NH 03825. Telephone/Fax: 603-664-2515.
Business Offices: 76 North Broadway, Hicksville, NY 11801. Telephone: (516) 681-2922. FAX: (516) 681-2926.
Communications Quarterly is published four times a year (quarterly) by *CQ Communications, Inc.* Subscription prices: Domestic—one year $29.95, two years $56.95. Foreign—one year $39.95, two years $76.95. Foreign Air Mail—one year $60.95, two years $118.95. Allow six weeks for change of address.
Second-class postage paid at Hicksville, NY and additional mailing offices.
Postmaster: Please send change of address to Communications Quarterly, CQ Communications, Inc., 76 North Broadway, Hicksville, NY 11801. ISSN 1053-9344

WE'VE GOT EVERYTHING UNDER CONTROL

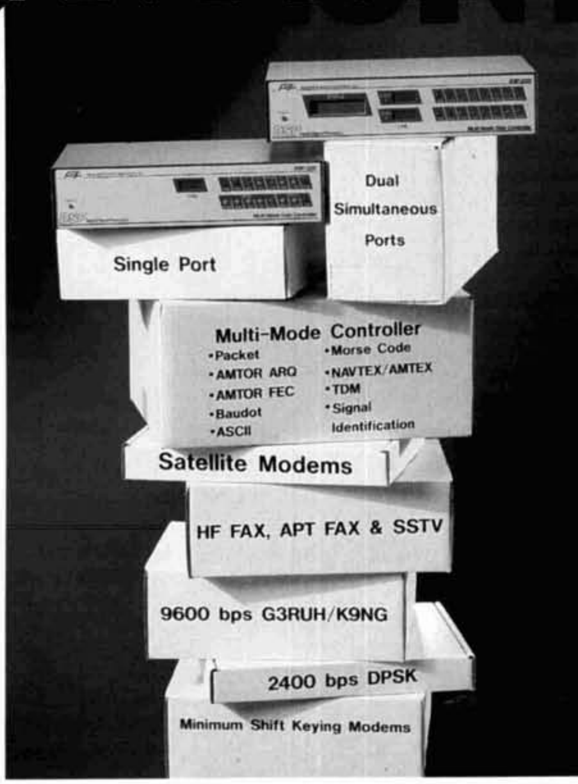

In the world of multi-mode contollers, nothing tops the DSP-2232 or DSP-1232 from AEA. When you choose either the dual port DSP-2232 or single port DSP-1232, you'll have just what you need to couple HF or VHF/UHF (or both) transceivers with a personal computer or computer terminal. Each converts incoming analog signals into digital data by means of a 12-bit, high speed converter.

Developed by AEA — with over 10 years of multi-mode controller development experience — the DSP-2232/1232 are the most advanced and versatile controllers available anywhere. They give you the capability to control all legal Amateur digital modes popular on both HF and VHF. New modems only require new software which can be installed with an EPROM chip, or downloaded from a telephone BBS binary file into the DSP's RAM. You won't need to replace your DSP-2232 or DSP-1232 as no new hardware or modifications will be needed as new modes become available.

Whatever you've thought about doing in Amatuer radio, it's here in the DSP-2232 /1232. All PK-232 MBX modems (Packet, AMTOR, etc.). All satellite modems (PSK, 4800 bps PACSAT, G3RUH 9600 bps, U022 equalized, 400 bps OSCAR-13). Analog modems for HF FAX, FAX APT, and SSTV. 9600 bps K9NG/G3RUH for terrestrial and satellite use. Each also offers internal RAM for uploading modems, up to 36 simultaneous packet connections, EPROM up to 2 Mbits, software selectable radio ports, Mailbox accessible through both ports, dedicated printer port, RTTY digital noise gate, ARQ tolerance command, etc.

The DSP-2232 adds even more control with its dual port gateway, front panel LCD showing connect and packets status, retrieval, call sign connected to, last call monitored and "marquee" display of received RTTY signals.

Get control of your digital operating position with the DSP-2232 or DSP-1232 from AEA. You'll be on top of the Amatuer radio world, too.

To connect with the AEA dealer nearest you or for product sheets, call (800) 432-8873.

Advanced Electronic Applications, Inc.
PO Box C2160, 2006 - 196th St. SW, Lynnwood, WA 98036 Sales: (206) 774-5554

AEA

Connect with us

We Carry the Full Line of MFJ Products

DISCOVER

TEK 453 Oscilloscope

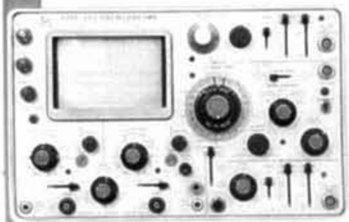

- Dual Trace 5 mV/div - 10 V/div calibrated deflection factors
- DC - 50 MHz bandwidth a t 20 mV/divCalibrated time base 0.1 μsec/div to 5 sec/div
- Calibrated X-Y operation 5 mV /div to 10 V/div in 11 steps
- Calibrated mixed sweep & sweep delay
- 8 x 10 div CRT
- Probes and accessories available at extra cost

Only $395

HP5245L/5253B

- Measures Ratio and Multiple Ratio
- Accurate Timebase (2 Parts in 10^{10})
- All Solid State Design
- DC to 50 MHz (Expandable to 18 GHz)
- Measures Period, Multiple Period & Average

HP5253B

- Extends the range of the 5245L &5246L Counters to 500 MHz
- Frequency range 50-500 MHz
- Input voltage range of 50 mV RMS to 1 V RMS (-13 dBm to +13 dBm)
- Maximum input is 2 V RMS or 100 VDC
- Stability and accuracy of thebasic counters are retained

Only $29

HP 612A Signal Generator

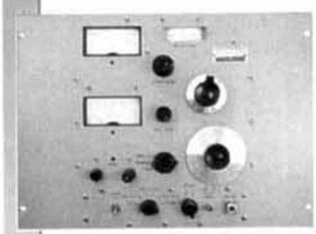

- Frequency range from 450 to 1,230 MHz in one band; accuracy is within ± 1%
- Output voltage from 0.1 μV to 0.5 V into 50 Ω; dial is calibrated in V and dBm
- Internal modulation of 400 and 1000 Hz

Only $249

Bird 6104 RF Absorption Wattmeter

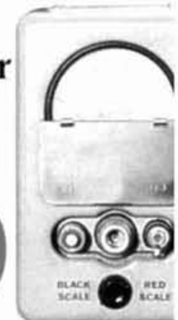

- Nominal 50 Ω input impedance
- VSWR 1.1 maximum DC to 512 MHz for Load
- Power scales 0-2/0-6/0-20/0-60 W
- Power Rating: 60 W in four ranges
- Frequency Range: 25 to 512 MHz for Wattmeter
- Accuracy: ± 5% of full scale from 25 to 512 MHz

Only $149

HP410B Voltmeter

- Ranges of 0-1000 VDC and 0-300 VAC over 20 Hz to 700 MHz frequency range
- Accuracy of ± 3% full scale
- Resistance Range of .2 Ω to 500 mΩ

Only $149

HP 411A RF Millivoltmeter

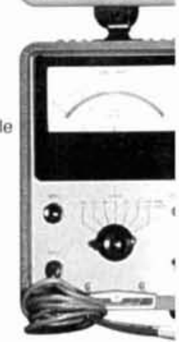

- Measures from 0.01 V RMS to 10 V RMS full scale
- Frequency range from 500 kHz to 1 GHz
- Accuracy of ± 3% of full scale (from 500 kHz to 50 MHz)
- Two linear voltage scales, 0 to 1 and 0 to 3 calibrated in RMS; dB scale is calibrated from +3 to -12 dB, 0 dB = 1 mW in 50 Ω

Only $99

GR 1606A R.F. Bridge

Ideal for measurement of antennas, lines, networks and components from 400KHz to 60MHz. Resistance range of 0-1000Ω. Reactance range of ± 5000Ω at 1MHz. Reactance varies inversely as frequency varies. Requires use of detector & generator. This is the all time favorite of R.F. engineers. These sell out fast…get yours while they last!

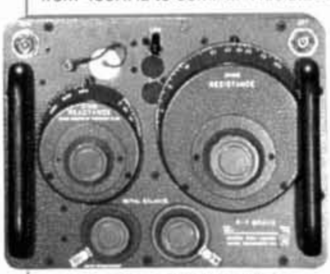

Only $495

HP 608C Signal Generator

- 10 MHz to 480 MHz
- 0.1 μV - 0.5 V output level
- 0 - 95% AM MOD; + CW or Pulse
- ± 0.5% Frequency Accuracy

Only $195

Call, Write or Fax for a FREE Copy of Our Latest Catalog!

Visiting the Dallas Area? Stop by Our Retail Store…1801 Reserve St. Open Mon-Fri 10-6, Sat 9-3

EDITORIAL

(from page 4)

support and work with the FCC in the effort to clean up the airwaves. This is imperative if we wish to continue to promote ham radio as an exciting educational activity for children. How will we convince more teachers to incorporate amateur radio into their curriculums, if they have to worry what kind of language their students will encounter when they tune in? How comfortable will parents feel about introducing their children to an activity whose communications are sprinkled with vulgarities?

In all fairness to those of us who use the ham bands, there are sometimes only vague boundaries between what is acceptable or unacceptable language. Because of the way our language has changed over the last few decades, this can be extremely difficult to determine. Words that were never before used in casual conversation are now part of the vernacular. What some might deem acceptable language, others might consider profane, indecent, or even obscene. Amateur radio operators will need very specific instructions from the FCC about what constitutes obscene speech, indecent language, and profanity, and what consequences hams will face if they indulge in such speech on the air.

It's important for those of us who are concerned about this issue to work together with the FCC to decide what type of language we as amateurs wish to tolerate on the air. We are always quick to write to the commission to defend our privileges to operate in certain ways, experiment, and retain our allotted spectrum. Should we be any less diligent when faced with the specter of obscenity? If we don't take a stand, we are abdicating our responsibility to protect our children from the offensive speech that seems to be permeating our lives—just as the referee did at the soccer game.

It's sad to think our children might be shocked by the language that they hear on the ham bands. It's even sadder to think that foul language is so much a part of their lives that they won't.

Terry Littlefield, KA1STC
Editor

LETTERS

Please give credit where credit is due

It is a disappointment to see that some authors in Communications Quarterly are careless about giving credit to authors whose work they have used, and that some authors are using obsolete reference material. Two papers in the Summer 1992 issue are examples.

Haviland gives much new and useful information in his article "Supergain Antennas." But his Fig. 4 is just Fig. 11.13a from the 1950 edition, or any newer edition including 1988, of the book "Antennas" by Kraus. Although Haviland references my early work on superdirective antennas (the term supergain is incorrect, and is deprecated), important papers on "Fundamental Limitations in Antennas," and on "Superconducting Antennas" were overlooked. See superdirectivity references below.

Michaels, in "How Short Can You Make a Loaded Antenna," repeats the calculations and results in my seminal papers published in 1975, in the IEEE Transactions on Communications, and in the Transactions on Vehicular communications; see references below. Because these references use more accurate impedance formulas, the results should be more useful than those given by Michaels. Reprints are available from the author.

Robert C. Hansen
P.O. Box 570215
Tarzana, CA 91357

REFERENCES

1. R.C. Hansen, "Fundamental Limitations in Antennas," Proc. IEEE, Vol. 69, Feb. 1981, pp. 170-182.
2. R.C. Hansen, "Some New Calculations on Antenna Superdirectivity," Proc. IEEE, Vol. 69, Oct. 1981, pp. 1365-1366.
3. R.C. Hansen, "Superconducting antennas," Trans. IEEE, Vol. AES-26, March 1990, pp. 345-355.
4. R.C. Hansen, "Optimum inductive loading of short whip antennas," Trans. IEEE, Vol. VT-24, May 1975, pp. 21-29.
5. R.C. Hansen, "Efficiency and matching tradeoffs for inductively loaded short antennas," Trans. IEEE, Vol. COM-23, April 1975, pp. 430-435.

ASTRON CORPORATION

9 Autry
Irvine, CA 92718
(714) 458-7277 • FAX (714) 458-0826

ASTRON POWER SUPPLIES

• HEAVY DUTY • HIGH QUALITY • RUGGED • RELIABLE •

MODEL VS-50M

SPECIAL FEATURES

- SOLID STATE ELECTRONICALLY REGULATED
- FOLD-BACK CURRENT LIMITING Protects Power Supply from excessive current & continuous shorted output
- CROWBAR OVER VOLTAGE PROTECTION on all Models except RS-3A, RS-4A, RS-5A, RS-4L, RS-5L
- MAINTAIN REGULATION & LOW RIPPLE at low line input Voltage
- HEAVY DUTY HEAT SINK • CHASSIS MOUNT FUSE
- THREE CONDUCTOR POWER CORD except for RS-3A
- ONE YEAR WARRANTY • MADE IN U.S.A.

PERFORMANCE SPECIFICATIONS

- INPUT VOLTAGE: 105-125 VAC
- OUTPUT VOLTAGE: 13.8 VDC ± 0.05 volts (Internally Adjustable: 11-15 VDC)
- RIPPLE Less than 5mv peak to peak (full load & low line)
- All units available in 220 VAC input voltage (except for SL-11A)

SL SERIES

• LOW PROFILE POWER SUPPLY

MODEL	Colors Gray	Colors Black	Continuous Duty (Amps)	ICS* (Amps)	Size (IN) H × W × D	Shipping Wt. (lbs.)
SL-11A	•	•	7	11	2⅝ × 7⅝ × 9¾	12
SL-11R	•	•	7	11	2⅝ × 7 × 9¾	12
SL-11S	•	•	7	11	2⅝ × 7⅝ × 9¾	12
SL-11R-RA		•	7	11	4¾ × 7 × 9¾	13

RS-L SERIES

• POWER SUPPLIES WITH BUILT IN CIGARETTE LIGHTER RECEPTACLE

MODEL	Continuous Duty (Amps)	ICS* (Amps)	Size (IN) H × W × D	Shipping Wt. (lbs.)
RS-4L	3	4	3½ × 6⅛ × 7¼	6
RS-5L	4	5	3½ × 6⅛ × 7¼	7

RM SERIES

MODEL RM-35M

• 19" RACK MOUNT POWER SUPPLIES

MODEL	Continuous Duty (Amps)	ICS* (Amps)	Size (IN) H × W × D	Shipping Wt. (lbs.)
RM-12A	9	12	5¼ × 19 × 8¼	16
RM-35A	25	35	5¼ × 19 × 12½	38
RM-50A	37	50	5¼ × 19 × 12½	50
RM-60A	50	55	7 × 19 × 12½	60
• Separate Volt and Amp Meters				
RM-12M	9	12	5¼ × 19 × 8¼	16
RM-35M	25	35	5¼ × 19 × 12½	38
RM-50M	37	50	5¼ × 19 × 12½	50
RM-60M	50	55	7 × 19 × 12½	60

RS-A SERIES

MODEL RS-7A

MODEL	Colors Gray	Colors Black	Continuous Duty (Amps)	ICS* (Amps)	Size (IN) H × W × D	Shipping Wt. (lbs.)
RS-3A		•	2.5	3	3 × 4¾ × 5¾	4
RS-4A	•	•	3	4	3¾ × 6½ × 9	5
RS-5A		•	4	5	3½ × 6⅛ × 7¼	7
RS-7A	•	•	5	7	3¾ × 6½ × 9	9
RS-7B	•	•	5	7	4 × 7½ × 10¾	10
RS-10A	•	•	7.5	10	4 × 7½ × 10¾	11
RS-12A	•	•	9	12	4½ × 8 × 9	13
RS-12B		•	9	12	4 × 7½ × 10¾	13
RS-20A	•	•	16	20	5 × 9 × 10½	18
RS-35A	•	•	25	35	5 × 11 × 11	27
RS-50A	•		37	50	6 × 13¾ × 11	46

RS-M SERIES

MODEL RS-35M

MODEL	Continuous Duty (Amps)	ICS* (Amps)	Size (IN) H × W × D	Shipping Wt. (lbs.)
• Switchable volt and Amp meter				
RS-12M	9	12	4½ × 8 × 9	13
• Separate volt and Amp meters				
RS-20M	16	20	5 × 9 × 10½	18
RS-35M	25	35	5 × 11 × 11	27
RS-50M	37	50	6 × 13¾ × 11	46

VS-M AND VRM-M SERIES

MODEL VS-35M

• Separate Volt and Amp Meters • Output Voltage adjustable from 2-15 volts • Current limit adjustable from 1.5 amps to Full Load

MODEL	Continuous Duty (Amps) @13.8VDC	Continuous Duty (Amps) @10VDC	Continuous Duty (Amps) @5VDC	ICS* (Amps) @13.8V	Size (IN) H × W × D	Shipping Wt. (lbs.)
VS-12M	9	5	2	12	4½ × 8 × 9	13
VS-20M	16	9	4	20	5 × 9 × 10½	20
VS-35M	25	15	7	35	5 × 11 × 11	29
VS-50M	37	22	10	50	6 × 13¾ × 11	46
• Variable rack mount power supplies						
VRM-35M	25	15	7	35	5¼ × 19 × 12½	38
VRM-50M	37	22	10	50	5¼ × 19 × 12½	50

RS-S SERIES

MODEL RS-12S

• Built in speaker

MODEL	Colors Gray	Colors Black	Continuous Duty (Amps)	ICS* Amps	Size (IN) H × W × D	Shipping Wt. (lbs.)
RS-7S	•	•	5	7	4 × 7½ × 10¾	10
RS-10S	•	•	7.5	10	4 × 7½ × 10¾	12
RS-12S	•	•	9	12	4½ × 8 × 9	13
RS-20S	•	•	16	20	5 × 9 × 10½	18
SL-11S	•	•	7	11	2¾ x 7⅝ x 9¾	12

*ICS—Intermittent Communication Service (50% Duty Cycle 5min. on 5 min. off)

JRC NRD-535D

"Best Communications Receiver"
World Radio TV Handbook 1992

"Unsurpassed DX Performance"
Passport to World Band Radio 1992

Setting the industry standard once again for shortwave receivers, the NRD-535D is the most advanced HF communications receiver ever designed for the serious DXer and shortwave listener. Its unparalleled performance in all modes makes it the ultimate receiver for diversified monitoring applications.

Designed for DXers by DXers! The NRD-535D (shown above with optional NVA-319 speaker) strikes the perfect balance between form and function with its professional-grade design and critically acclaimed ergonomics. The NRD-535D is the recipient of the prestigious World Radio TV Handbook Industry Award for "Best Communications Receiver."

- Phase-lock ECSS system for selectable-sideband AM reception.
- Maximum IF bandwidth flexibility! The Variable Bandwidth Control (BWC) adjusts the wide and intermediate IF filter bandwidths from 5.5 to 2.0 kHz and 2.0 to 0.5 kHz—continuously.
- Stock fixed-width IF filters include a 5.5 kHz (wide), a 2.0 kHz (intermediate), and a 1.0 kHz (narrow). Optional JRC filters include 2.4 kHz, 300 Hz, and 500 Hz crystal type.
- All mode 100 kHz – 30 MHz coverage. Tuning accuracy to 1 Hz, using JRC's advanced Direct Digital Synthesis (DDS) PLL system and a high-precision magnetic rotary encoder. The tuning is so smooth you will swear it's analog! An optional high-stability crystal oscillator kit is also available for ±0.5 ppm stability.
- A superior front-end variable double tuning circuit is continuously controlled by the CPU to vary with the receive frequency automatically. The result: Outstanding 106 dB Dynamic Range and +20 dBm Third-Order Intercept Point.
- Memory capacity of 200 channels, each storing frequency, mode, filter, AGC and ATT settings. Scan and sweep functions built in. All memory channels are tunable, making "MEM to VFO" switching unnecessary.
- A state-of-the-art RS-232C computer interface is built into every NRD-535D receiver.
- Fully modular design, featuring plug-in circuit boards and high-quality surface-mount components. No other manufacturer can offer such professional-quality design and construction at so affordable a price.

JRC *Japan Radio Co., Ltd.*

Japan Radio Company, Ltd., New York Branch Office – 430 Park Avenue (2nd Floor), New York, NY 10022, USA Tel: (212) 355-1180 / Fax: (212) 319-5227

Japan Radio Company, Ltd. – Akasaka Twin Tower (Main), 17-22, Akasaka 2-chome, Minato-ku, Tokyo 107, JAPAN Tel: (03) 3584-8836 / Fax: (03) 3584-8878

Paul E. Krueger, *N1JDH*
The MITRE Corporation
202 Burlington Road
Bedford MA, 01730

USING THE NASA ADVANCED COMMUNICATIONS TECHNOLOGY SATELLITE

The Army technology demonstrations

The history of satellite communications is that of extraordinary growth and development of new technology. Within the decade of the 1980s we watched the United States maintain its edge in satellite technology, despite competition from foreign governments and industries. We also witnessed many advances in digital satellite communications, with one notable exception; the satellite transponder. In the 1990s, the United States' ability to maintain its position as the leader in satellite technology will require innovative thinking and a commitment by both government and industry. The National Aeronautics and Space Administration (NASA), with the support of Congress, has made that commitment for the government. It is time for the commercial satellite industry to contribute its fair share. Although many members of this nation's commercial satellite industry are investing resources and planning experiments for the ACTS program, there are some notable exceptions.

In this article, I will discuss the NASA advanced communications technology satellite (ACTS) program and its efforts to advance satellite technology. One of the major technological thrusts is the introduction of digital technology to the satellite transponder in the form of on-board processing. I will also discuss the involvement of the United States Army's Space Command with the ACTS program and its innovative use of this newly available technology. The United States Army has been a leader in the development and uses of satellite technology to support the defense of the United States and its allies.

The NASA ACTS Program

The NASA ACTS program was initiated to develop and promote advanced communications satellite technology throughout the commercial satellite industry. ACTS will apply this technology in multiple frequency bands. NASA believes that realization of this goal will result in growth in capacity and effective use of the frequency spectrum. The agency also hopes ACTS will help maintain the United States' preeminence in satellite communications.

The ACTS system uses multiple, hopping

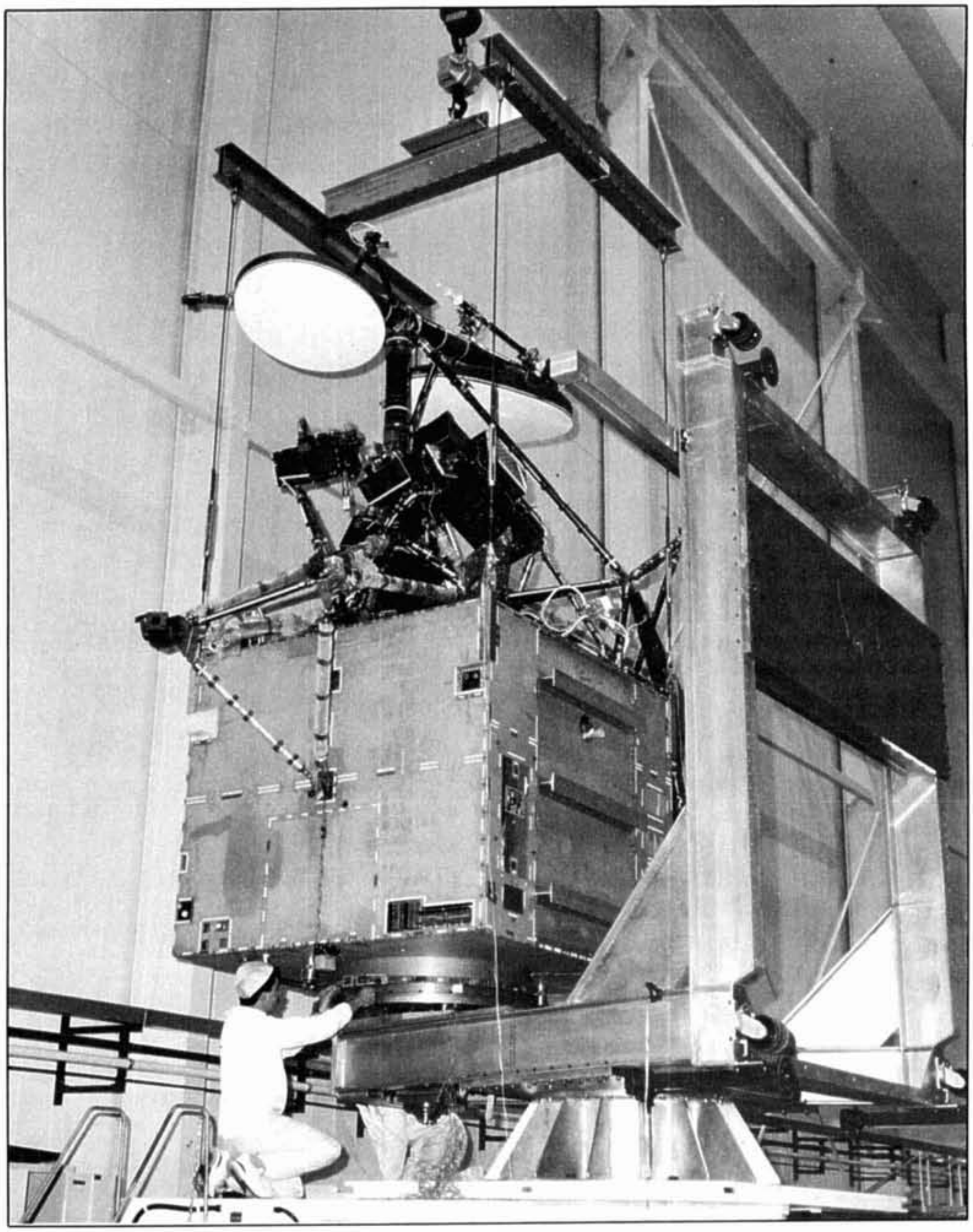

Photo courtesy of NASA

spot beams, and on-board switching and processing systems. Technologies stimulated by the ACTS program and integrated into the ACTS system include:

1. A multibeam antenna with rapidly reconfigurable hopping beams,
2. A baseband processor with individual circuit switched routing,
3. A microwave switch matrix with dynamic reconfiguration at intermediate frequencies,
4. The use of Ka-band components,
5. Implementation of demand assigned multiple access (DAMA) network control,
6. Implementation of adaptive compensation for signal level changes.

The system consists of the ACTS, the NASA ground station and satellite control center, and experimenter terminals. The satellite's original launch date was February 1993, but due to changes in shuttle manifests it's now scheduled for launch in June 1993. Residing in a geostationary orbit at 100 degrees west longitude, ACTS will maintain its position within 0.05 degrees in latitude and longitude. Range variations won't exceed ± 20 kilometers and the drift rate won't exceed ± 1.2 meters per second. The satellite will not compensate for Dop-

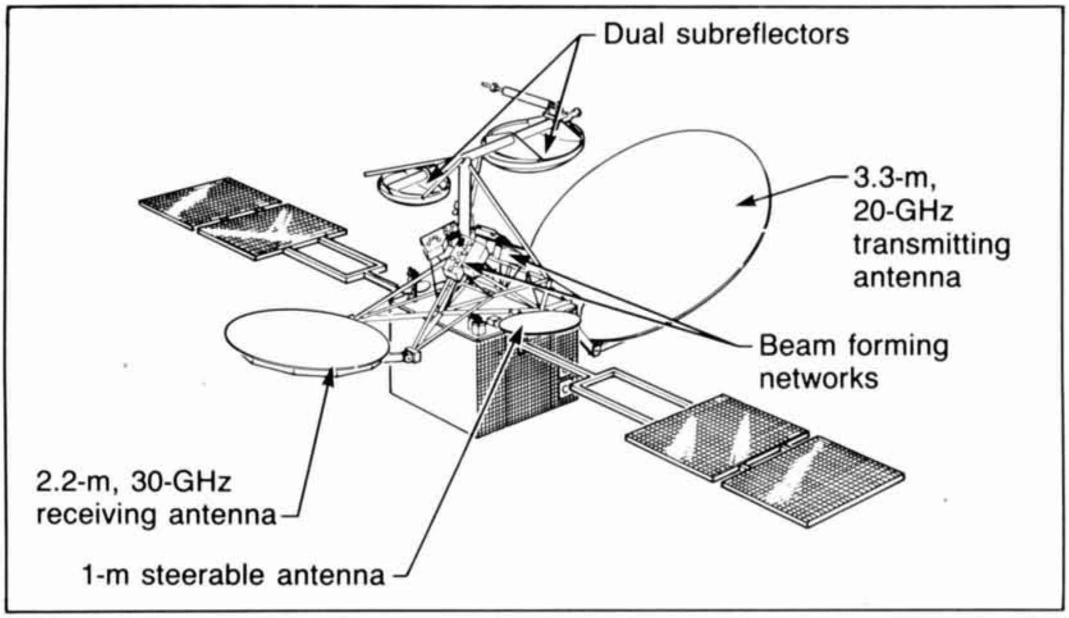

Figure 1. ACTS spacecraft configuration.

pler shift or timing variations, the earth stations are responsible for those functions.

ACTS has two basic operating modes—baseband processing or repeater—and three antennas. The two hopping beam antennas are stationary; one antenna transmits and the other one receives. These antennas provide approximately the same gain and coverage to both the uplink and downlink. The hopping beam receive antenna is a parabolic dish 2.2 meters in diameter and the hopping beam transmit antenna is a parabolic dish 3.3 meters in diameter. The third antenna is a steerable type 1-meter in diameter and provides somewhat less gain. **Figure 1** shows the ACTS spacecraft configuration; **Figure 2** illustrates the ACTS multibeam antenna coverage.

The NASA ground station, located at the NASA Lewis Research Center in Cleveland, Ohio includes the master control station, the reference terminal, two traffic termi-

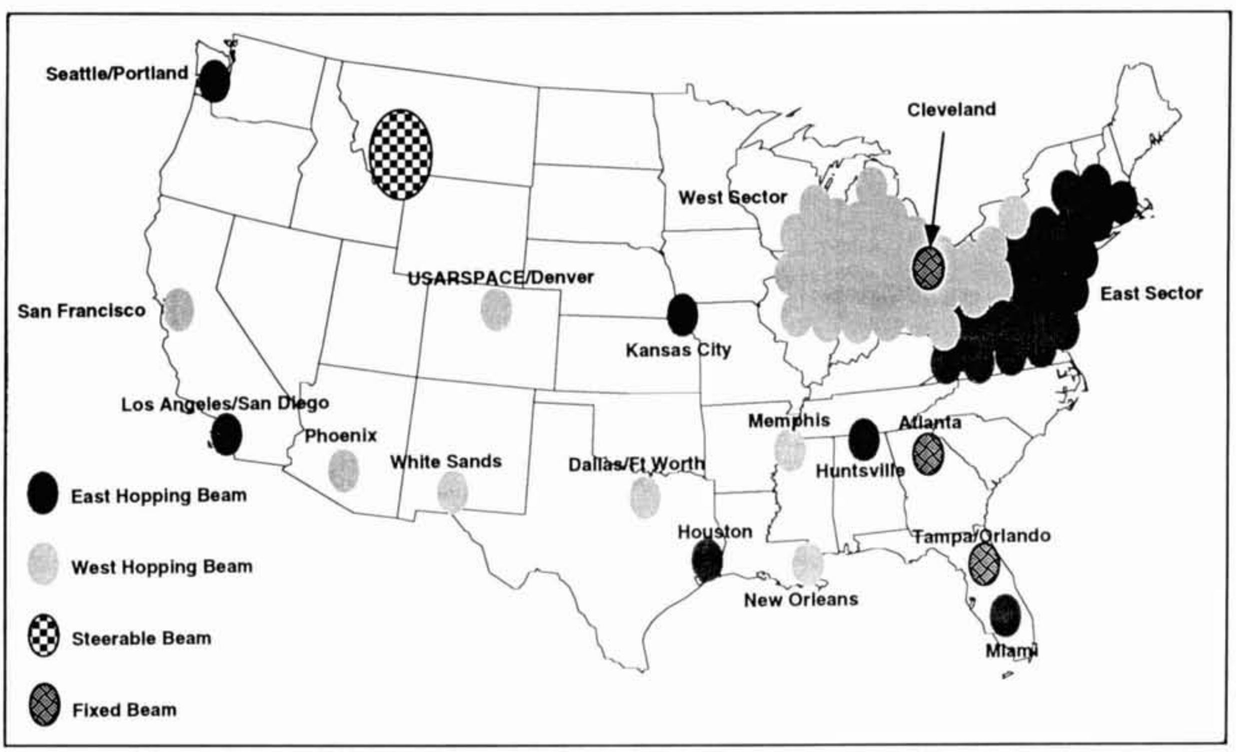

Figure 2. ACTS multibeam antenna coverage.

nals, and the Ka-band command transmitter and telemetry receiver. The master control station provides networking control for the baseband processor and also serves as the backup spacecraft control center. The satellite control center is located in East Windsor, New Jersey.

When the ACTS is in repeater mode, the satellite operates as a classic transponder with two exceptions. The ACTS system controller can designate spot coverage by dynamic assignment of the microwave switch matrix. The matrix lets the controller hop from one footprint to another in one microsecond. Also, the sharp focus of the spot beam provides very high gain on both the uplink and downlink allowing the operation of ultra-small aperture terminals (USATs). NASA is developing a USAT that can transmit and receive at a data rate of 2.4 kb/s—a handheld unit, capable of supporting low data rate digital voice. This handheld unit is approximately the size of a portable telephone and uses a small phased array antenna (approximately three inches square).

In baseband processor mode, the ACTS scans the eastern or western zones in a single millisecond. The beam switches from footprint to footprint, picking up data bursts from the T1 very small aperture terminals (VSATs), which are designed to operate with the ACTS processor. The amount of dwell time on a zone is dependent on the offered traffic load and is measured in microseconds. The minimum dwell time is six microseconds and the maximum dwell time is one millisecond. The uplink data rate from these terminals is 27.5 Mb/s and the downlink data rate is 110 Mb/s. A terminal may use a maximum of 28, 64 kb/s channels. The user can send and receive packets from any zone. For example, a terminal using 12 64 kb/s channels would receive a dwell of approximately 28 microseconds. The formula for calculating dwell time is:

$$DT = \left[\frac{1000\left(\frac{\text{dwells}}{\text{seconds}}\right) \cdot BR}{UT} \right]^{-1}$$

Where:
DT = Dwell time (s)
BR = Burst rate (b/s)
UT = User throughput (b/s)

The T1 VSAT uses an offset feed parabolic reflector either 1.2 or 2.4 meters in diameter. Using the 2.4 meter antenna, the terminal will have a peak effective isotropic radiated power (EIRP) of 66 dBW at duty cycles of 33 percent or less, and 64 dBW at duty cycles above 33 percent. When equipped with the small antenna, the earth station peak EIRP is 60 dBW at duty cycles below 33 percent and 58 dBW at duty cycles above 33 percent. Spectral variations in transmit power across the operating channel bandwidth won't exceed 1 dB. The EIRP is manually adjustable in nominal 1 dB increments to 9 dB below the peak levels.

The T1 VSAT transmits carriers on either 29,236.032 or 29,291.328 MHz and receives the downlink carrier on 19,440.000 MHz. The uplink's bandwidth is 41.5 MHz and the downlink's bandwidth is 165.9 MHz. The modulation format for both the uplink and downlink is serial minimum shift keying (SMSK).

The earth station automatically applies or removes forward error correction coding (FEC) at the direction of the master control station. The FEC code is a rate 1/2, constraint length 5, convolutional code. When the code is engaged the burst rate is halved, but the user throughput rate is unaffected. Although engaging the FEC code does not affect an individual user's throughput, it may affect the overall network. The master control station reserves time, within each frame, in a "rain fade pool." The master control station allocates time from the rain fade pool to terminals using the FEC coding, thus increasing their dwell time. The increased dwell time allows the terminal to maintain its user throughput even though the burst rate is halved. Exhaustion of the rain fade pool results in a reduction in the overall satellite throughput. Rain or other atmospheric disturbances that could degrade link performance will cause the master control station to initiate FEC coding on an uplink. (Operating with the FEC coding engaged is similar to operating in AMTOR mode B.)

The bit error rate (BER) performance of the T1 VSAT is at least 5×10^{-7} on both the uplink and downlink. During rain fades up to 10 dB the terminal will maintain a BER performance of at least 5×10^{-7}. The earth station will operate over a 15-dB signal range with dynamic level variations up to 0.5 dB per second without loss of data.

The T1 VSAT uses a rubidium timing source. This ensures that the earth station clock, used for timing uplink and downlink bursts, has a short-term (300 ms) stability of + 1 part in 10^{-9} and a long-term (2-year) accuracy to within ± 1.64 parts in 10^{-9}. The short-term stability of the satellite clock, used for timing uplink and downlink bursts, will not exceed ± 2.2 parts in 10^{-9}, and its long-term accuracy will be within ± 4 parts

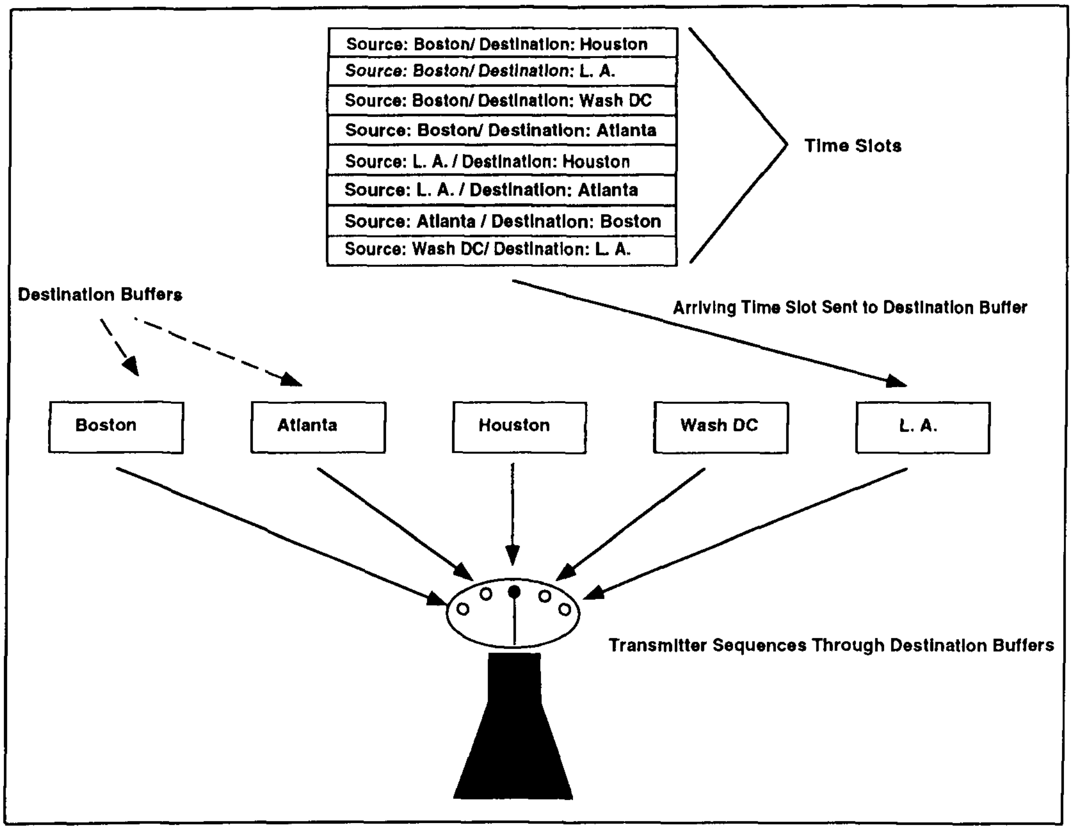

Figure 3. ACTs baseband processing.

in 10^{-10}. The master control station will maintain the long-term accuracy of the satellite clock with a Cesium standard.

Figure 3 is a simple example of the baseband processing operation of ACTS. Earth stations time transmission bursts so the burst arrives at the satellite when the appropriate feed horn is active. The satellite demodulates the burst and sorts the packets into the destination buffers. When the satellite activates a feed horn for a given footprint, the data buffer for that destination is burst on the downlink. The switching speed gives the terminal users a virtual circuit to any footprint. The processing delay in the satellite is on the order of 3 milliseconds—insignificant with respect to the round-trip path delay of approximately 250 seconds.

In the baseband processing mode, the ACTS uses a time division multiple access (TDMA) frame that is 1.000 milliseconds duration with an accuracy of ± 4.5 parts in 10^{-6}. All beam hopping sequences repeat frame-by-frame. Changes in beam hopping sequences take place at superframe boundaries. A superframe contains 75 frames.

Each frame contains 1,728 consecutively numbered time slots. Time slots are approximately 0.579 microseconds in duration; this corresponds to the time occupied by a single 64-bit word clocked at 110 Mb/s. Antenna dwells and burst assignments occupy an integer number of slots.

Guard slots prevent burst collisions and provide time for beam switching. Uplink bursts are nominally timed to arrive at the satellite within ± 60 nanoseconds of the arrival assignment. Terminal bursts arriving outside the normal timing interval receive an early or late indication, and the offending terminal is notified.

The master control station controls the duration and position of all bursts. Terminals receive instructions on outbound orderwires and send circuit requests and status on inbound orderwires. The master control station maintains two reserved regions in each frame. The "fade pool" carries orderwires and provides the additional time slots needed by terminals operating in coded mode. The "satellite acquisition window" is used to bring terminals on line.

A discussion of the United States Army's technology demonstrations

The United States Army Space Command (USARSPACE) plans to use the ACTS system to demonstrate the capabilities that commercial processing satellite systems can provide the Army. In particular, Army Space Command's interest lies in highlighting the capabilities of VSATs and their application to tactical field units. To meet their objectives, the Army will use a T1 VSAT terminal, modified into a transportable configuration, and the ACTS baseband processor. Under contract to USARSPACE, The MITRE Corporation has designed and will build two prototype terminal systems for the Army technology demonstrations. These systems will include the Harris ruggedized terminal and all the demonstration equipment, packaged in a sturdy transportable configuration.

The existing T1 VSATs consist of an outdoor antenna unit and a small indoor rack unit. The indoor rack unit is a standard 19-inch rack about four feet high. USARSPACE is planning to modify six terminals. Modifications include placing the indoor electronics into carrying cases and using a quick reaction antenna design. The Army's modified terminal will be transported by truck and require less than one hour to set up and make contact with the satellite.

The Army will demonstrate:

1. Connection of graphics workstations for imagery,
2. Common-user, two-wire, facsimile and voice traffic with audio conferencing,
3. Video teleconferencing,
4. ACTS connection to the Army Maneuver Control System (MCS),
5. ACTS connection to the Army Mobile Subscriber Equipment (MSE).

The first demonstration involves transferring imagery data between workstations. This imagery data will include satellite reconnaissance photographs, topographic maps, and computer enhanced images. The Army will show that the ACTS system can supply on demand communications capability for providing classified imagery data between workstations. Tactical headquarters will use the workstations to exchange imagery data between commands, higher headquarters, or intelligence organizations.

A SUN SPARCstation using a high data rate serial interface card will interface the ACTS terminal. The high resolution image files will reside on the workstation's hard drive. When an image transfer is required, the ACTS terminals will request service from the satellite. Next the satellite will establish a circuit between the sending location and the receiving location. The workstation will then synchronize the encryption units and send the file. Custom software controls the encryption unit and divides the image file into packets. Error detection and correction are performed on transmitted data packets. If a packet arrives with uncorrectable errors, the workstation will request a retransmission of the packet. The SPARCstations will interface with the ACTS terminal via a channel service (CSU). This CSU is manufactured by Tylink and has four ports that can accomodate clear channel bandwidths from 64 kb/s to 1.544 Mb/s in increments of 64 kb/s.

The second demonstration concerns providing on-demand common-user, two-wire, telephone circuits with audio conferencing. Using secure telephone unit (STU) III instruments, the Army will provide secure voice and facsimile for point-to-point circuits. Audio conferencing requires a conferencing "bridge." The audio conferencing bridge is a standard user-defined card that the Army will obtain from NASA, integral to the ACTS terminal. The conferencing bridge allows up to eight parties per conference.

At this time, the Army requires only black and white facsimile transmissions. Office facsimiles normally interface (CCITT V.27/29) with analog telephone loops. A number of facsimile manufacturers provide a digital interface (RS-232C) on their facsimiles. The Army is selecting a facsimile with a digital interface and will connect this unit to a STU III. This will provide secure facsimile capability.

The Army's third demonstration involves a video teleconferencing configuration that will support classified interactive video teleconferencing between a video "monitor" and a designated viewer. Additional participants receive classified audio and video from the monitor, but cannot respond. A CSU port for the video teleconferencing equipment will be configured to support 256 kb/s. An encryption device will provide the required communications security for classified conferences.

The fourth demonstration makes use of the Army's maneuver control system (MCS)—a suite of equipment and ancillary software. At the core of the MCS lies the Miltope Bobcat rugged transportable computer unit (TCU). The Bobcat TCU is based on the Hewlett-Packard 9000 series 300 computers. The Army will interface the ACTS terminal via a CSU to the Bobcat TCU at a serial I/O port. The serial I/O ports on the Bobcat TCU are RS-232C serial data ports that support data rates up to 230 kb/s. The information transfer between MCS equipment is at a data rate of 192 kb/s. This is the highest data rate that can be supported, as the CSU supports data rates in increments of 64 kb/s and the

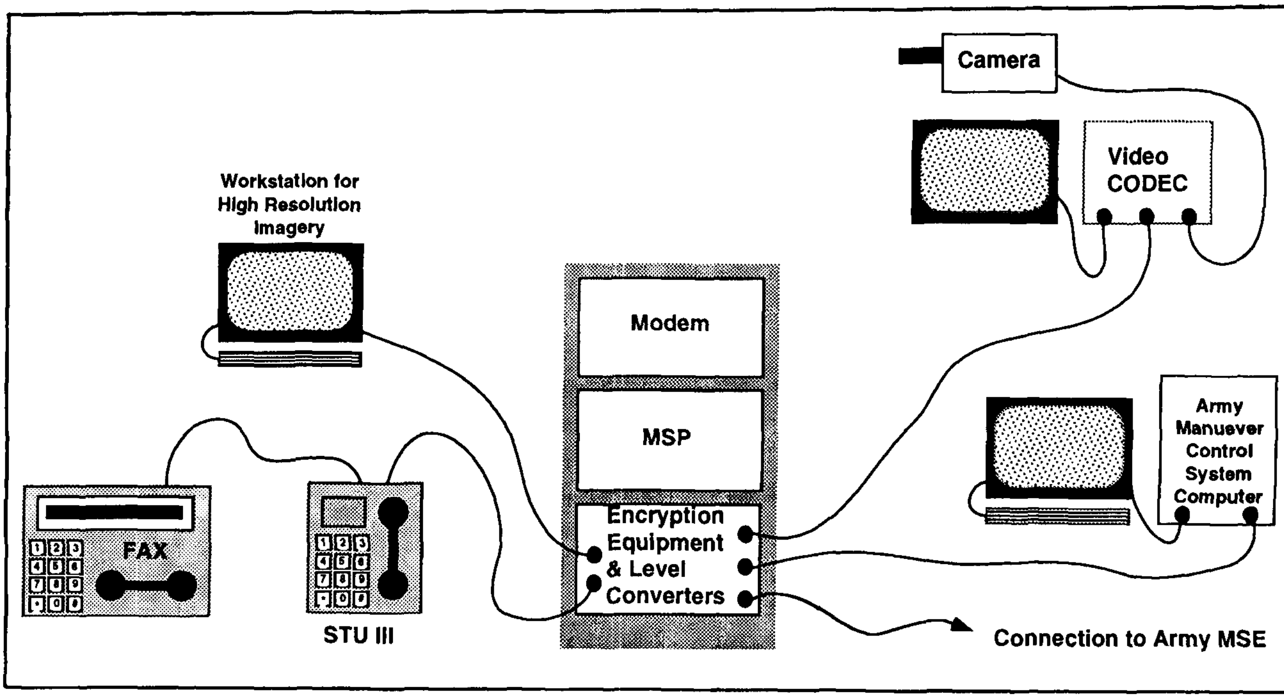

Figure 4. Experiment configuration.

RS-232C I/O port can support a maximum data rate of 230 kb/s. The CSU accepts data through its RS 449 I/O port, so an interface adapter will convert the RS-232C signals to an RS 449 format.

The final USARSPACE demonstration illustrates the integration of Army's mobile subscriber equipment (MSE) with the ACTS terminal. The Army's MSE is similar to that of the civilian cellular telephone system; however, its cell sites aren't fixed but move as the Army advances. The Army will use the ACTS system to provide fixed trunking and demand-assigned circuits between MSE circuit switches.

Figure 4 shows an artist's conception of the experiment configuration and **Figure 5** is a system level block diagram. The design configuration supporting the Army's demonstrations uses a customer service unit (CSU) to provide access ports with high data rates (e.g., 256 kb/s). This configuration lets the operator choose any three of the following four high data rate experiments:

High resolution imagery,
Video teleconferencing,
MCS interconnection,
MSE interconnection.

While supporting any three of the above experiments, the configuration will also provide secure facsimile, secure voice, and non-secure audio conferencing.

The number of available time slots on the digital termination equipment (DTE) bus of the modular switching peripheral (MSP), and the number of available channel slots for the MSP, limit the number of experiments that can be conducted simultaneously.

The DTE bus of the MSP has 30 available time slots. Allocation of these time slots, to user defined cards in the MSP chassis, follows a simple priority algorithm. This algorithm assigns the highest priority to the user-defined card requiring the greatest number of time slots. User-defined cards requiring few time slots are assigned a low priority. For example, a T1 clear channel card set consists of only two cards. However, each T1 card requires 12 time slots, while a line circuit card requires only 4 time slots. Consequently, the T1 cards' time slots are given a higher priority.

Although the MSP has 30 time slots on the DTE bus, there are only 24 channel slots in the Army terminals. Therefore, there is routing for only 24 DTE time slots across the satellite (i.e., trunked), the remaining six must be either idled or programmed as local loops. The DTE time slots determine the type and quantity of user-defined cards that can be serviced, and the channel slots determine the number of 64 kb/s digital signaling zero-format channels (DS0s) that can be trunked.

Example: Let the MSP be populated with a fully active T1 clear channel card set (i.e., two cards) and a single line circuit card. This configuration occupies 28 DTE time

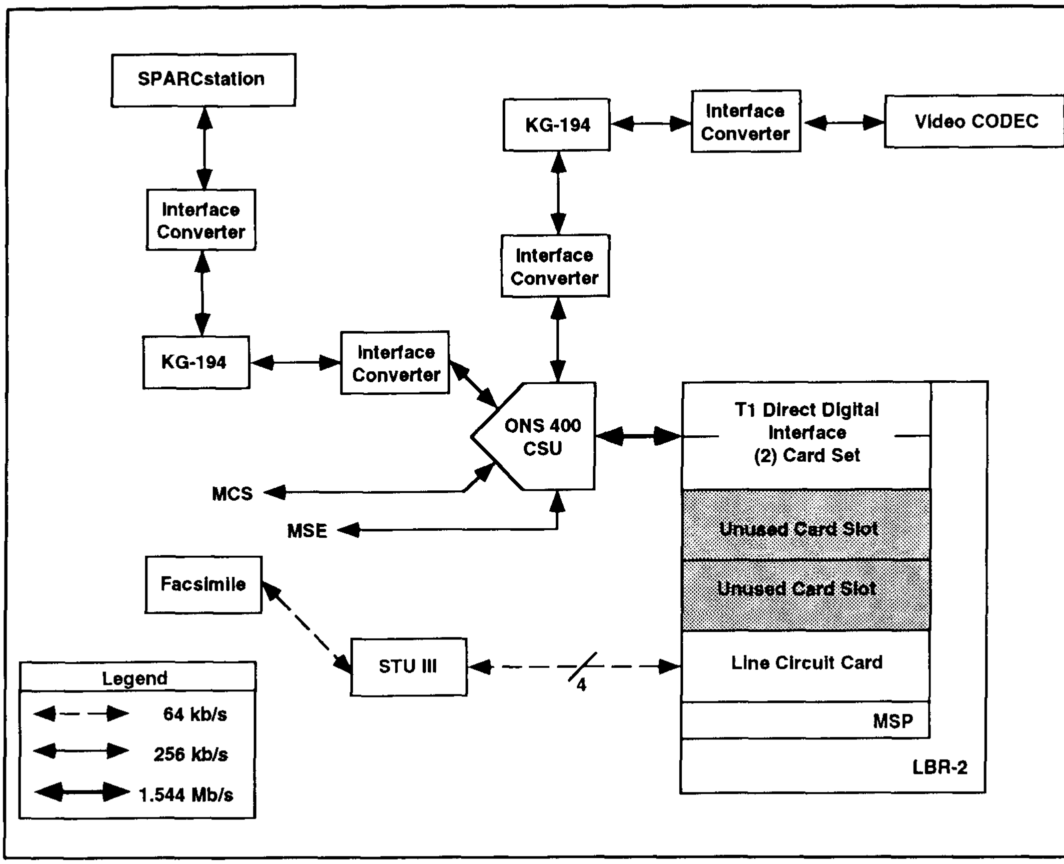

Figure 5. System level block block diagram.

slots; one time slot for each active 64 kb/s DS0 in the T1 card set (24, since all are active) and 4 time slots for each of the four circuits in the line circuit card. However, only 24 of these circuits can be trunked over the satellite due to the availability of only 24 channel slots. Any four circuits can either be idled or assigned as local loops (for instance, 24 DS0s from the T1 card are trunked and the line circuits are idled, or N line circuits are trunked and 24-N T1 DS0s are trunked and the remainder assigned as local loops). **Figure 6** graphically illustrates these examples.

In the Army's design configuration the MSP is populated and programmed as follows:

(1) Clear channel T1 card set with one card active (12 DS0s active),
(1) Eight party additive conference board,
(1) Line circuit card.

This configuration allocates 776 kb/s to the CSU (768 kb/s user throughput plus 8 kb/s T1 signaling overhead); 768 kb/s (12 DS0s) are available to the user. The CSU can support any three of the high data rate experiments at the same time. The MSP conference board and line circuit card provide the user with another 768 kb/s of capacity. The Army can simultaneously conduct audio conferencing, utilize three line circuits independent of the audio conference, and perform any three of the high data rate experiments.

The four port CSU is programmed and controlled from the unit's front panel display and keypad. The MSP programming is accomplished through a DTMF keypad associated with a line circuit interface.

Summary

ACTS is a declaration of the resolve of the United States to meet the international challenge in satellite communications, and is a blueprint for telecommunications into the next century. This experimental system will provide telecommunications capabilities different from those of current satellite and fiber optic systems. The four-year experiment period will furnish an opportunity for government agencies, industry, academia, and other interested parties to explore new technologies and applications.

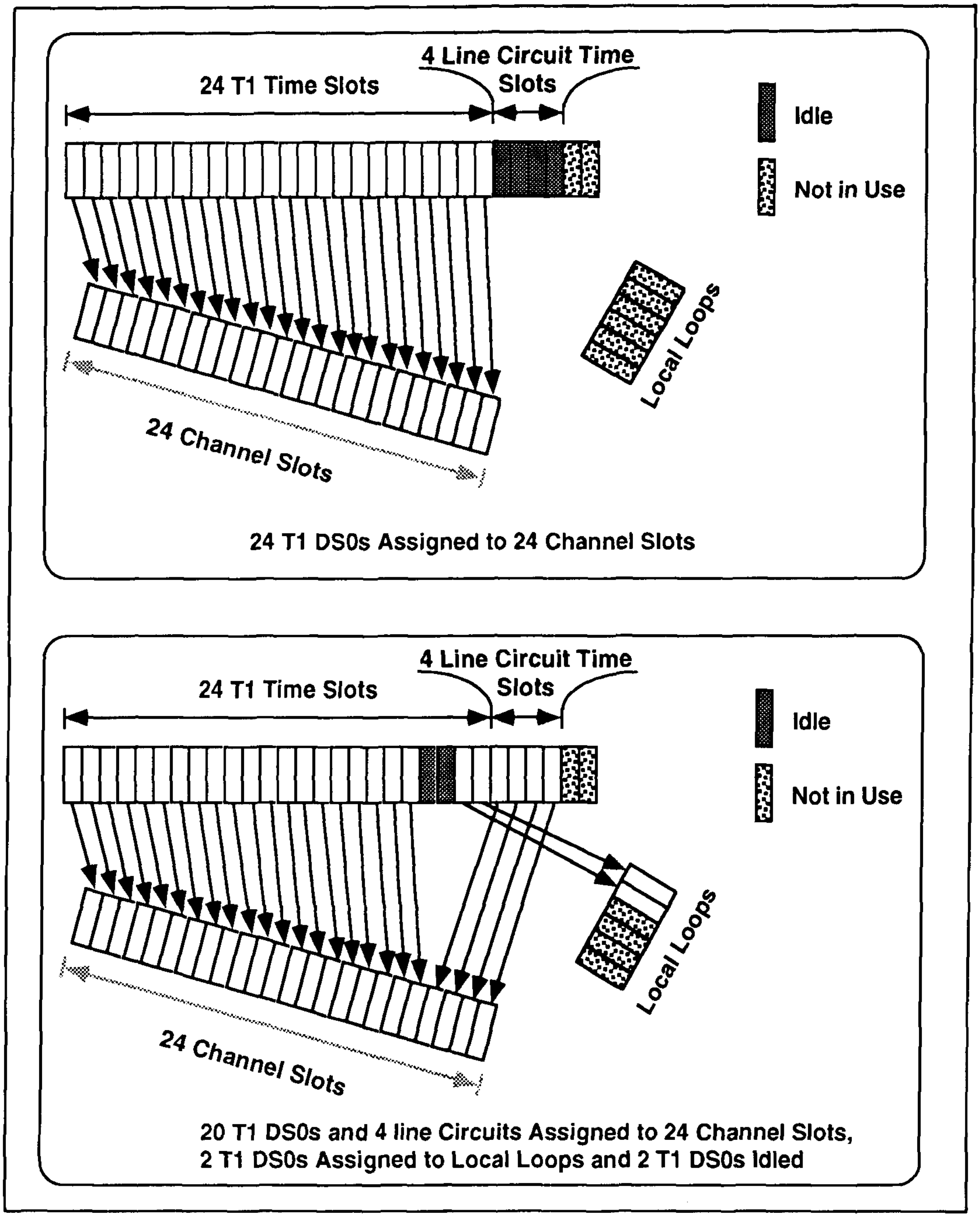

Figure 6. Time and channel slot assignments.

Although I've discussed in detail the Army's use of the high data rate, baseband processing capabilities of the ACTS system, other experiments include:

- Thin route voice and data services compatible with the basic integrated services digital network (ISDN) protocols.
- Land mobile satellite communications.
- Aeronautic and maritime applications.
- High definition television (HDTV).
- Investigation of weather effects on Ka-band satellite links.
- High speed data networks for linking supercomputers.
- Distance learning.
- Medical imagery, data, consultation, and diagnostic assistance to remote locations from urban medial centers.

The first ACTS experimenter working group meeting was held at the NASA Lewis Research Center in Cleveland, Ohio 8-9 July 1992. Forty representatives from industry, universities, and other government agencies attended the meeting to present their experiment concepts. There are currently 56 approved experimenets involving 73 organizations. The success of the first experimenter working group meeting represents the commitment from these organizations to the ACTs program. For information on how your organization can get involved, read the sidebar that accompanies this article. ■

Attention Experimenters

NASA will launch ACTS in the summer of 1993. The NASA ACTS Experiments Office is working with industry, government, and academic organizations in the development of experiment concepts. If you are interested in experimenting and using the ACTS system, please contact Mr. Ron Schertler, Chief of the ACTS Experiments Office, at (216) 433-3527 or Ms. Joanne De-Vincent of Mitre at (202) 646-9177 for further details on opportunities and involvement in the ACTS Experiments Program.

PRODUCT INFORMATION

Fluke offers guide to electrical troubleshooting

A new booklet, "Electrical Troubleshooting with Fluke Multimeters," provides a number of test techniques for troubleshooting electrical systems using Fluke DMMs. The free 20-page publication includes sections on DMM safety and protection, basic electrical measurements, troubleshooting with MIN MAX recording, power measurements and power factor, wiring and grounding, engine driven generators, motors and harmonics.

"Electrical Troubleshooting with Fluke Meters is available at Fluke authorized distributor locations, or by contacting John Fluke Mfg. Co., Inc., Service Equipment Group, P.O. Box 9090, M/S 250-E Everett, Washington, 98206, (800)87-FLUKE.

New *TMOS* Power MOSFET Selector Guide and Cross Reference Available

Motorola announces its revised *TMOS® Power MOSFET Selector Guide and Cross Reference*. The newly designed guide includes tables of the latest linear ICs available to drive power MOSFETs.

The selector guide also includes the new high-energy E-FETs™, SMARTDISCRETE™ products, surface mount devices including SOT-23 and SOT-223, MOSFETs, isolated U.L. recognized devices and SENSEFETs™, in addition to standard devices.

To obtain a free copy of the *TMOS® Power MOSFET Transistor Selector Guide and Cross Reference*, call Motorola Literature Distribution at (800)441-2447, or write Motorola Literature Distribution Center, P.O. Box 20924, Phoenix, Arizona 85063. Ask for SG56/D, Revision 11.

Spring-Loaded Needle-Point Probe Tips

Pomona Electronics new Series 5789 spring-loaded needle-point probe tips are useful for scanning test points on SMD and high-density lead circuitry. The sharp, insulated, stainless steel needle-point tip allows positive, non-slip probing of high-density lead traces while under constant pressure. The probe is 1.42 mm in diameter and 89 mm long.

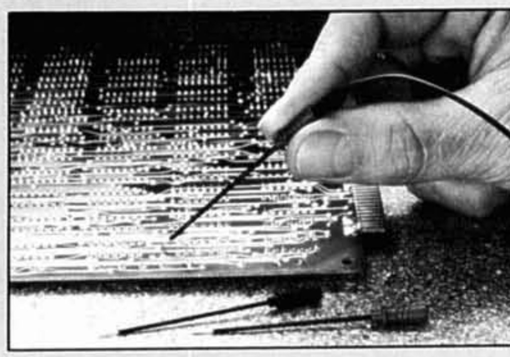

The probe tip can be attached to a variety of test equipment and cable interfaces, and connects to 0.64 mm diameter square or round sockets on test leads via gold-plated pins. The probes are rated at 50 volts, 1.5 amps maximum and weigh 0.66 grams. They are available in red or black.

For a free copy of Pomona's new 140-page catalog, contact: Customer Service, ITT Pomona Electronics, 1500 East Ninth Street, P.O. Box 2767, Pomona, California 91769. Phone: (714) 469-2900. FAX: (714) 629-3317.

Jerry Sevick, *W2FMI*
32 Granville Way
Basking Ridge, New Jersey 07920

THE 4:1 BALUN

An in-depth look at this popular design

The first article in this series on baluns[1] discussed the most popular of all baluns—the 1:1 balun designed to match 50 ohms unbalanced to 50 ohms balanced. It not only gave a review of the history, theory, and design of these broadband transformers but also my viewpoint on recently published articles[2-5] advocating "new" designs using coaxial cable (wound around a toroid or threaded-through ferrite beads) as the transmission line. As was noted, I am in considerable disagreement with the claims advanced for these "new" 1:1 baluns.

This article deals with the next most popular balun—the 4:1 balun designed to match 50 ohms unbalanced to 200 ohms balanced. I've also included the "step-down" balun matching 50 ohms unbalanced to 12.5 ohms balanced. Succeeding articles will describe many special baluns that have never been available before. Included are baluns with ratios of 1.5:1, 2:1, 6:1, 9:1, 12:1 and 16:1. Many of these baluns will match 50 ohms unbalanced to higher or lower balanced impedances.

A little history

There are really only two classic papers that have established the principles upon which the transmission line transformer (the balun being a subset thereof) is based. The first paper was by Guanella in 1944, who proposed the idea of coiling a transmission line to isolate the input from the output resulting in the (now-popular) current or choke balun.[6] The second was by Ruthroff in 1959. His analysis of these transmission line transformers is the present standard.[7] Ruthroff also introduced the unun (unbalanced-to-unbalanced transformer) and the hybrid transformer.

Interestingly enough, Guanella and Ruthroff both had different approaches to their 1:1 and 4:1 balun designs. Guanella used a two-conductor 1:1 balun design while Ruthroff used a three-conductor design. Investigators who followed[2-5] failed to recognize that Ruthroff's third conductor (which increased the low-frequency response over the two-conductor balun) was located on a separate part of a toroidal core. Their comparisons were made with a three-conductor balun that had the third wire in parallel with the other two. This then gave rise to the term voltage balun—a trifilar-wound balun (an inferior design).

But the differences between Guanella's and Ruthroff's approaches to 4:1 baluns were even more striking. Guanella's technique was to connect coiled transmission lines in a parallel-series arrangement, so in-phase voltages were summed at the high impedance side. Ruthroff obtained a 4:1 transformation ratio by summing a direct voltage with a delayed voltage that traversed a single transmission line (in a phase-inverter connection[1,8]). His 4:1 balun had a built-in high-frequency cutoff, while Guanella's didn't. This important difference was overlooked by practically everyone who followed.

In this article, I'd like to review the two different approaches used by Guanella and Ruthroff in obtaining 4:1 baluns. Of particular importance are the descriptions of the potential drops along the lengths of the transmission lines (which account for the ohmic losses) and the low-frequency model of the Guanella balun. These descriptions were probably presented for the first time in the second edition of my book *Transmission Line Transformers*.[8] I'll also present a single-core version of Guanella's 4:1 balun, which promises to have all of the properties of an efficient and broadband balun matching 50-ohm coaxial cable to a

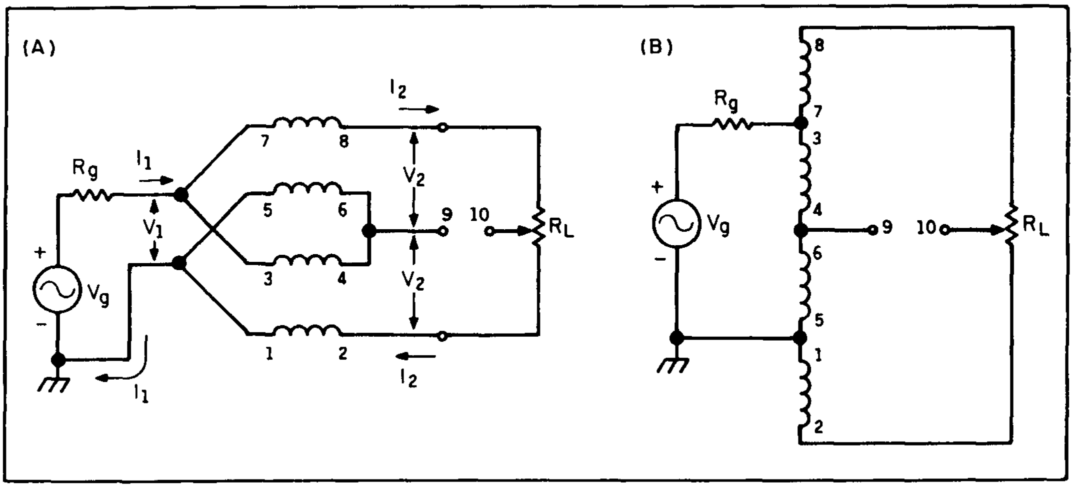

Figure 1. Electrical models of the Guanella 4:1 balun: (A) high-frequency model, (B) low-frequency model.

floating 200-ohm balanced load. Finally, I'll discuss some high and low-power designs, and comment on other 4:1 designs that are commercially available.

The Guanella 4:1 Balun

Figures 1A and **B** show the high and low-frequency models of Guanella's method of connecting transmission lines in parallel-series for obtaining a 4:1 balun. The high-frequency model (**Figure 1A**) assumes that the choking reactances of the coiled (or beaded) transmission lines are sufficient to isolate the input from the output so only transmission line currents are allowed to flow. This occurs when the reactance of windings 3-4 and 5-6 (which are in series) is much greater than R_g (at least by a factor of 10).[8] If two cores are used, the reactance is the sum of the reactances of windings 3-4 and 5-6. If a single core is used, the reactance is twice as large because of the mutual coupling between the windings. The other advantage (besides only using one core) is that shorter transmission lines can be used, resulting in better high-frequency performance.

As with all transmission line transformers, the objective is to have the transmission lines see loads equal to their characteristic impedances resulting in "flat lines." This yields the highest frequency response. Because each transmission line in **Figure 1A** sees one-half of the load, R_L, the optimum value of the characteristic impedance is $R_L/2$. In any event, the input impedance, V_1/I_1, is simply the impedance of two identical transmission lines connected in parallel. It then follows that the impedance transformation ratio is the load, R_L, divided by the input impedance.

Because the Guanella 4:1 balun sums voltages of equal delays from identical transmission lines, his balun is only limited in high-frequency performance by the deviation of the characteristic impedance of the transmission lines from the optimum values and the parasitics not absorbed into the characteristic impedance of the lines. I (and practically everyone else) had overlooked the simple and important statement, "a frequency independent transformation," which appeared in Guanella's 1944 paper,[6]—a fact that is evidenced by the scarcity of his designs in the literature. Another interesting aspect of the Guanella 4:1 balun is the analysis of his balun when the load is floating or grounded at different points. This leads to the determination of the voltage gradients that exist along the transmission lines and the various functions of which his 4:1 design is capable. Assuming a matched load or very short transmission lines resulting in $V_2 = V_1$, they are:

Floating load. With terminal 10 (which is at the center of R_L) floating, the potential gradient along the top transmission line in **Figure 1A** (windings 5-6 and 7-8) is $-1/2V_1$, and along the bottom transmission line (winding 1-2 and 3-4) it is $-3/2\ V_1$. The voltage to ground on terminal 9, V_{90}, is $-1/2V_1$. Since the bottom transmission line (in **Figure 1A**) has a voltage drop along its length three times greater than the top transmission line, it results in three times more loss because losses in transmission line transformers are voltage dependent (dielectric-type losses).[8]

Even though a single-core Guanella 4:1 balun maintains the voltages (stated above) when feeding a folded dipole (of about 200 ohms) that has a virtual-ground potential at terminal 10, it still feeds equal currents to each side of the antenna because of the series-connection at its output. Furthermore, the choking reactance of the windings also prevents antenna currents from flowing on the outside of the coaxial cable feedline.

Load grounded at center. When two cores are used and terminal 10 (the center of R_L) is grounded, the voltage gradient along the top transmission line in **Figure 1A** is zero and along the bottom transmission line it is $-V_1$. The voltage to ground on terminal 9 (V_{90}) is also zero. In fact, the core for the top transmission line is not needed. It only acts as a mechanical support for the top transmission line, which now only operates as a delay line. Also, all of the loss now occurs in the core of the bottom transmission line, where a longitudinal potential gradient exists. Furthermore, the low-frequency response, as seen from **Figure 1B**, is now determined by the reactances of windings 1-2 and 3-4. This means that the low-frequency response with a floating load is better by a factor of two over the case where the load is grounded at its center.

The single-core case is a different matter. Because the potential at terminal 9 (V_{90}) wants to be at $-1/2V_1$, connecting a ground directly to the center of R_L causes an imbalance that renders the single-core balun unusable. If the ground were placed at a point 25 percent below terminal 8 (50 ohms from terminal 8 with a 200-ohm load), no difference would be noted from a floating load. This condition also exists when two cores are used.

Load grounded at the bottom. Probably the most interesting case is when the load is grounded at the bottom (at terminal 2). The 4:1 balun (with two cores) is now converted into a very broadband unun (unbalanced-to-unbalanced transformer). Since the bottom transmission line in **Figure 1A** has no potential drop along its length, it only acts as a delay line. The voltage to ground at terminal 9 (V_{90}) is $+V_1$ and the voltage gradient along the top transmission line is $+V_1$. This results in a voltage of $2V_1$ across the load. The low-frequency response is now determined by the reactances of windings 5-6 and 7-8. This is just the opposite of the balun case where the center of the load was grounded. A single-core 4:1 Guanella balun can also be converted to an unun by adding a 1:1 balun (for isolation) in series.[8]

The reason for claiming a very broadband response for a Guanella unun (converted from his balun) is that two in-phase voltages are now summed at the high-impedance side. The only other competition for a 4:1 unun design is that of Ruthroff's[7] where a direct voltage is summed with a delayed voltage that traversed a single transmission line (and hence had a built-in, high-frequency cutoff). In fact, very little information can be found in the literature on a *Guanella 4:1 unun*.

Photo A shows two high-power Guanella 4:1 baluns designed to match 50-ohm coaxial cable to loads of 200 ohms. They both use no.14 H Thermaleze wire with a covering of Teflon® tubing giving characteristic impedances very close to 100 ohms (the objective). Their responses are flat from 1.5 MHz to well beyond 30 MHz. Both can

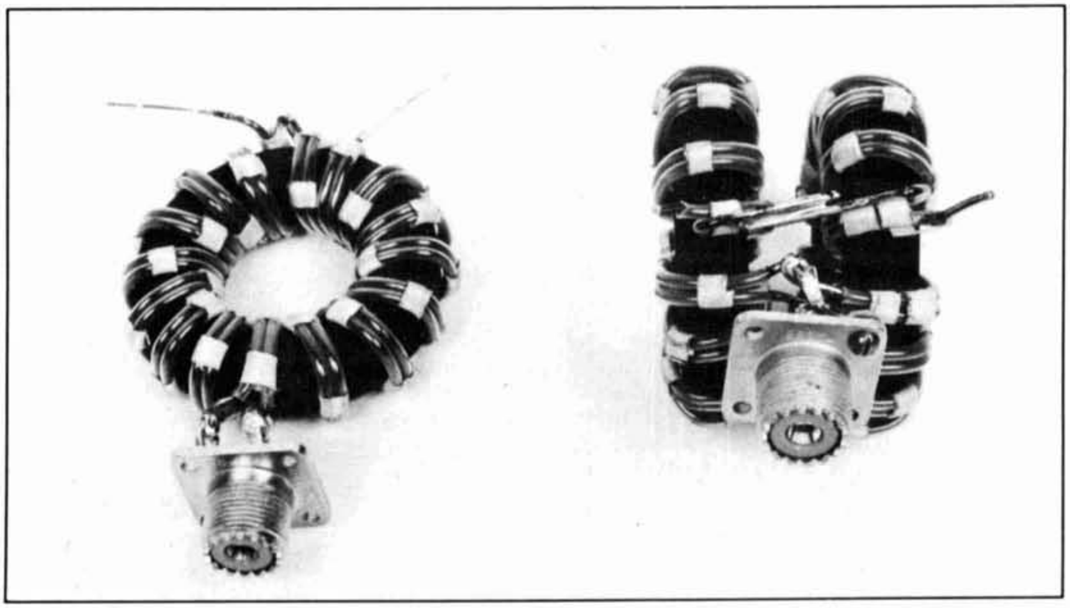

Photo A. Two high-power versions of the Guanella 4:1 balun. The balun on the left uses a single core while the balun on the right uses two cores. The connectors are on the low-impedance sides.

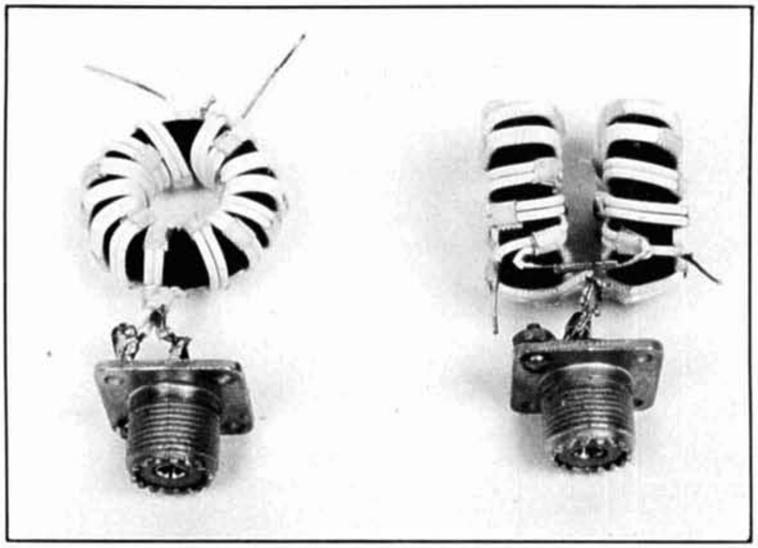

Photo B. Two low-power versions of the Guanella 4:1 balun. The balun on the left uses a single core while the balun on the right uses two cores. The connectors are on the low-impedance sides.

easily handle the full legal limit of amateur radio power.

The single-core version (on the left) has 8 bifilar turns on each of its two transmission lines. The dual-core version (on the right) has 16 turns on each core. The wires are clamped together with strips of Scotch no. 27 glass tape about every 3/4 inch. The cores are 2.4-inch OD ferrite toroids with a permeability of 250. The connectors are on the low-impedance sides. For ease of connection, the dual-core version has one winding clockwise and another counter-clockwise. Also, in the dual-core case, the spacing between the two cores (which is not critical) can be as small as 1/4 inch.

These transformers can also be wound with ordinary no. 14 (solid) house wire. The several samples I tried yielded characteristic impedances close to 100 ohms (and thus were acceptable). The major difference is in the voltage-breakdown capability. Units wound with Teflon-sleeved no.14 H Thermaleze wire have been reported to withstand 10,000 volts without breakdown! Obviously, this is beyond the capability of ordinary house wire.

Photo B shows two low-power Guanella 4:1 baluns designed to match 50-ohm coaxial cable to loads of 200 ohms. They both use no. 20 hook-up wire (solid) giving a characteristic impedance very close to the objective of 100 ohms. Their responses are flat from 1.5 MHz to well beyond 50 MHz. They are conservatively rated at 150 watts of continuous power and 300 watts of peak power. I have exposed these baluns to 500 watts of continuous power (in a matched condition) for a considerable length of time during which they experienced virtually no rise in temperature.

The single-core version (on the left) has 7 bifilar turns on each of its two transmission lines while the dual-core version (on the right) has 14 turns on each core. The wires are clamped together about every 1/2 inch with strips of Scotch no. 27 glass tape. The cores are 1.25-inch OD ferrite toroids with a permeability of 250. The connectors are on the low-impedance sides. As in the previous case, the dual-core version has one winding clockwise and another counter-clockwise.

Photo C is a step-down version of the Guanella 4:1 balun. It uses two ferrite rod cores 3/8 inch in diameter and 3.5 inches in length. Their permeabilities are 125. It uses the schematic of **Figure 1A**, but the generator (which is grounded) is placed on the right side and the load (ungrounded) on the left side. This 4:1 balun is designed to match 50-ohm coaxial cable (on the right side) to a floating load of 12.5 ohms. Each rod has 13.5 bifilar turns of no. 14 H Thermaleze wire. Again, for ease of connection, one rod is wound clockwise and the other, counter-clockwise. The response is flat from 1.5 MHz to well over 30 MHz. This balun is fully capable of handling the legal limit of amateur radio power. Also, the connector is on the high-impedance (50 ohms) side.

It should be mentioned again that the three dual-core baluns mentioned here also make excellent broadband ununs. They only sacrifice a little in low-frequency response. But because of their conservative designs, they can still handle the 160-meter band. Furthermore, all of the components (as kits or completed units) are readily available.*

The Ruthroff 4:1 balun

Figure 2 shows the high and low-frequency models of Ruthroff's approach for a 4:1 balun. The high-frequency model (**Figure 2A**) assumes that the choking reactance of the coiled (or beaded) transmission line is sufficient to isolate the input from the output in such a way that only transmission line currents are allowed to flow. This occurs when the reactance of winding 3-4 (or 1-2 since they are the same) is much greater than R_g (at least by a factor of ten).[8]

As you can see in **Figure 2A**, the transmission line is connected in a phase-inverter function.[1,8] That is, a $-V_1$ voltage gradient now exists along the length of the transmission line. Therefore, the voltage across R_L

*Amidon Associates, Inc., 2216 East Gladwick Street, Dominguez Hills, CA 90220.

now becomes $V_1 + V_2$. Although Ruthroff analyzed his 4:1 unun in his classic paper,[7] his results also apply to his balun because both devices sum a direct voltage with a delayed voltage. In essence, he used loop equations on the input and output and transmission line equations to eliminate one set of variables (I_2 and V_2). He also used a maxima technique (setting a derivative to zero) to solve for the optimum characteristic impedance of the transmission line. As in the Guanella case, he found the optimum value to be $1/2R_L$.

An inspection of **Figure 2A** shows that the left side of R_L (terminal 3) has a direct voltage, V_1, to ground and the right side (terminal 2) a delayed voltage, $-V_2$, to ground which traveled the length of the transmission line. You can also see, that if the line is electrically one-half wavelength long, the output is *zero*. Therefore, Ruthroff's design (which has a built-in cutoff) is sensitive to the transmission line length.

I have recently found another interesting aspect of Ruthroff's design.[8] If the center of the load is grounded, the high-frequency performance is vastly improved. The built-in high-frequency cutoff is eliminated because the balun now takes on the character of a Guanella balun which sums voltages of equal delays. Therefore, with a load that is center-tapped-to-ground, Ruthroff's designs could be the 4:1 balun of choice.

Photo D shows a high-power (on the left) and a low-power (on the right) version of Ruthroff's 4:1 balun. The high-power balun has 16 bifilar turns of no. 14 H Thermaleze wire on a 2.4-inch OD ferrite toroid with a permeability of 250. The wires are also covered with Teflon tubing giving the optimum characteristic impedance of 100 ohms. With the load floating, the response is flat from

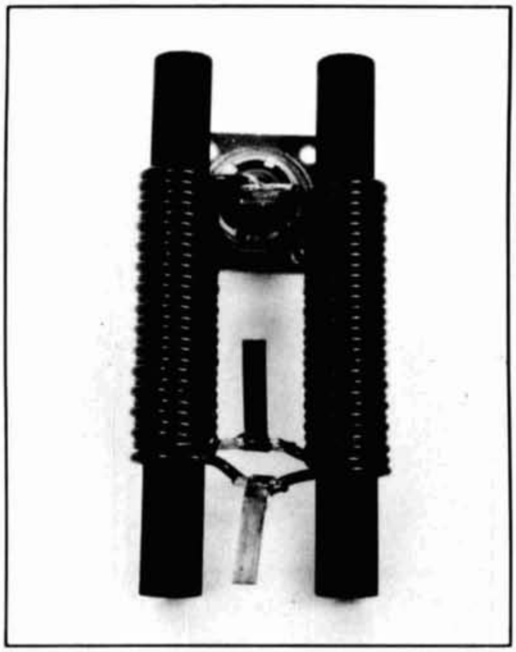

Photo C. A dual-core (rods) 4:1 Guanella step-down balun designed to match 50-ohm coaxial cable to a floating load of 12.5 ohms. The connector is on the 50 ohm, unbalanced side.

1.5 to 15 MHz. With the load center-tapped-to-ground, it's flat from 1.5 to over 50 MHz! This balun can easily handle the full legal limit of amateur radio power.

The low-power balun has 14 bifilar turns of no. 20 hook-up wire (solid) on a 1.25-inch OD ferrite toroid with a permeability of 250. When the load is floating, the response is flat from 1.5 to about 21 MHz. When the load is center-tapped-to-ground, it's flat from 1.5 to over 50 MHz! This small balun is conservatively rated at 150 watts of continuous power and 300 watts of peak power.

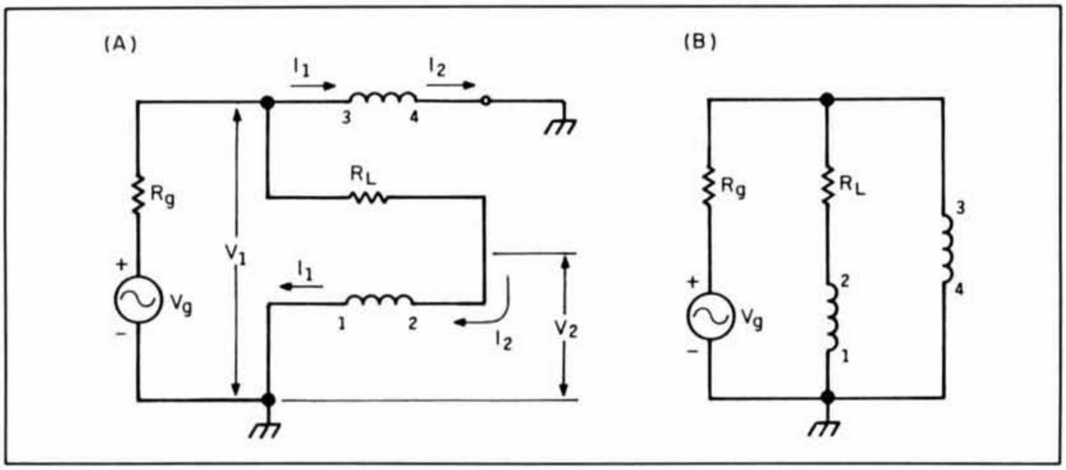

Figure 2. Electrical models of the Ruthroff 4:1 balun: (A) high-frequency, (B) low-frequency.

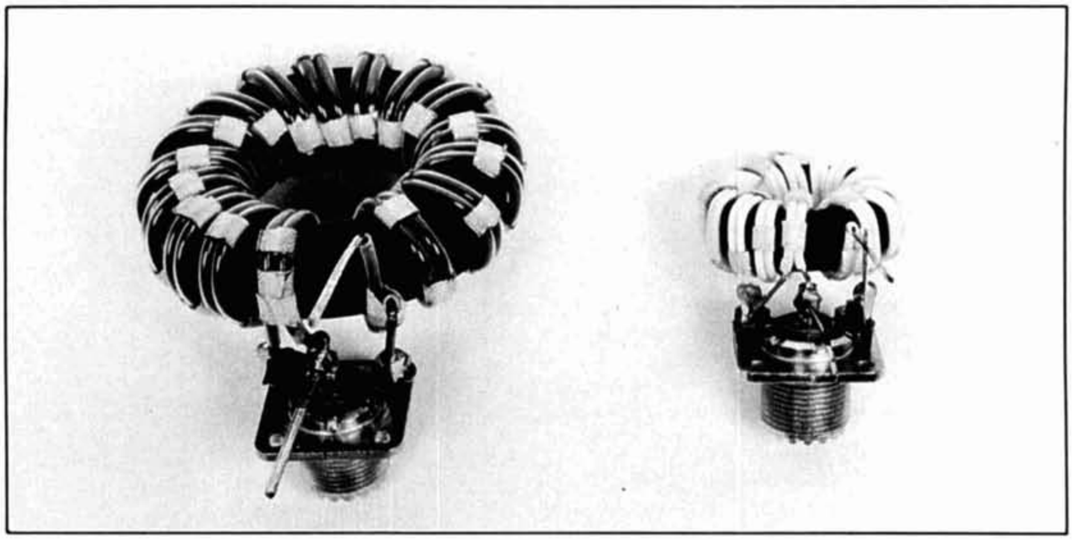

Photo D. High-power (left) and low-power (right) versions of Ruthroff's 4:1 baluns. The connectors are on the low-impedance sides.

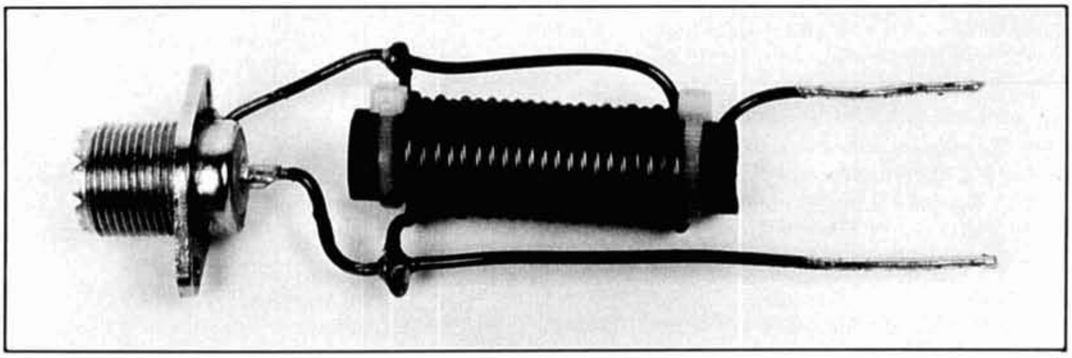

Photo E. A typical 4:1 rod-type voltage balun (*HI-Q*).

Comparisons with other baluns

After completing the study on 4:1 baluns, I thought it would be interesting to characterize other baluns that are commercially available or that have been recently described in the amateur radio literature. My findings are as follows:

The 4:1 rod-type Ruthroff balun. Photo E shows the typical rod-type 4:1 balun, which has been practically the only one available over the past two to three decades. The balun in the photograph happens to be the *HI-Q Balun*. It is the Ruthroff design (now called a voltage balun[2]) with 10 bifilar turns of no. 14 wire on a 1/2-inch diameter rod 2 inches in length. In terminating this balun with 200 ohms, I found the useful range to be only from 7 to 15 MHz. Below 7 MHz, the input impedance showed a considerable inductive component indicating autotransformer action and flux in the core (which could be harmful). Above 15 MHz, the transformation ratio increased and became complex. I found the optimum impedance level when matching 100 ohms to 25 ohms (indicating a characteristic impedance of the windings of only 50 ohms). The useful frequency range at this impedance level increased to 3.5 to 30 MHz.

When matching 50-ohm coaxial cable to a 20-meter folded dipole at a height of 0.17 wavelengths (resulting in a resonant input impedance of 200 ohms), I found the VSWR curve was indistinguishable from that of the best Guanella 4:1 (current balun[2]) baluns. This balun also presented no difficulty in handling the full power limit. But, as was mentioned in the first article in this series,[1] the rod-type balun has the following disadvantages: 1) It uses the Ruthroff design that is not recommended with a floating load; 2) it uses a rod core with only 10 bifilar turns, which gives insufficient choking at the lower frequencies (80 and 160 meters) to prevent harmful core flux (and *saturation*); and 3) it is susceptible to voltage breakdown. This type of balun is certainly *not* recommended.

4:1 current baluns. I also characterized several so-called current baluns,[2] that have recently appeared on the market. These are my findings:

- They are the dual-core (toroids) version of the Guanella balun that sums voltages of equal delays.
- The electrical performances of these baluns are vastly superior to the rod-type balun described earlier.
- These baluns should meet their electrical and power-rating specifications.
- The only criticism is that they could have more of a safety margin at the low-frequency end where excessive core flux (due to higher than expected impedances) could take place. I recommend more inductance in the windings.

The beaded-coax 4:1 balun. A recent design in an amateur radio journal[3] advocated using beaded coaxial cable (of 100 ohms) in a 4:1 Guanella design. Various claims were advanced for this "new" approach. I constructed one of these baluns using no. 14 wire with Teflon sleeving resulting in the required 100-ohm characteristic impedance. Here are my findings:

- The excellent electrical performance of this balun verified my analysis (expressed earlier) with the high and low-frequency models and the subsequent voltage gradients. In fact, the high-frequency performance exceeded the capability of my simple test equipment.[8]
- The major disadvantage is in efficiency. Because high-permeability (2500) beads are required in order to obtain the required choking reactance in the HF band, this balun had considerably more loss than coiled-type baluns using low-permeability (less than 300) ferrite toroids.[8] A soak-test[8] (transformers connected back-to-back and about 500 watts applied into a dummy load) with the dual-core low-power unit in **Photo B** showed that the smaller balun ran considerably cooler! The beaded transmission line technique is only recommended for baluns (and ununs) in the higher-frequency bands.

And finally, other conclusions from this study which warrant repeating are:

- With sufficient choking, the major loss (ohmic) is voltage dependent. Therefore, even well-designed 4:1 baluns can be very lossy when mismatched with high-impedance loads that present high voltage gradients.
- From an over-all standpoint, the dual-core 4:1 Guanella design is the balun of choice. It can provide the largest safety margin at the low-frequency end (against flux in the core) and is the least susceptible to mismatched and unbalanced loads.
- The single-core Guanella 4:1 balun matching into a floating load and the Ruthroff 4:1 balun matching into a center-tapped-to-ground load look very interesting. They also have the advantage of using only one core.
- The 4:1 Guanella balun can easily be converted into an unun with the broadest possible bandwidth. ■

References

1. Jerry Sevick, W2FMI, "Baluns Revisited," *Communications Quarterly*, Summer 1992, page 13.
2. Roy Lewallen, W7EL, "Baluns: What They Do and How They Do it," *The ARRL Antenna Compendium*, Vol. 1, Amateur Radio Relay League, Newington, Connecticut, 1985, pages 12-15.
3. J.S. Belrose, "Transforming the Balun," *QST*, June 1991, pages 30-33.
4. M.W. Maxwell, W2DU, *Reflections*, Amateur Radio Relay League, Newington, Connecticut, 1990, Chapter 21.
5. Joe Reisert, W1JR, "Simple and Efficient Broadband Balun," *Ham Radio*, September 1978, pages 12-15.
6. G. Guanella, "Novel Matching Systems for High Frequencies," Brown-Boveri Review, Vol. 31, September 1944, pages 327-329.
7. C.L. Ruthroff, "Some Broad-band Transformers," *Proceedings of the IRE*, Vol. 47, August 1959, pages 1337-1342.
8. Jerry Sevick, W2FMI, *Transmission Line Transformers*, 2nd edition, Amateur Radio Relay League, Newington, Connecticut, 1990, Chapters 7, 9, 11.

PRODUCT INFORMATION

High-Speed CMOS ICs Available

Philips ECG has added high-speed CMOS ICs to its semiconductor line. The line now includes 61 of the most popular HCMOS logic types.

The 74HC and 74HCT device families are part of the ECG® Replacement Semiconductors product line, which contains over 4,000 distinct solid-state devices. The 74HC series is used in buffered, high-speed CMOS applications; the 74HCT series is used in TTL input-compatible applications, as well as for TTL and CMOS interface.

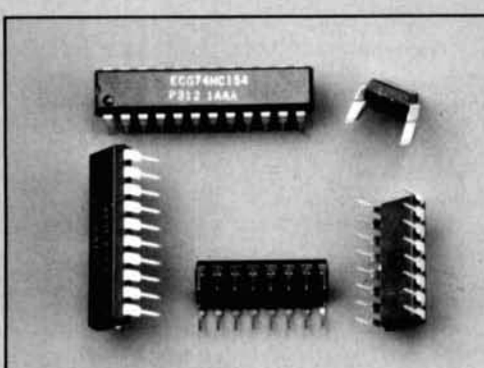

Bob Rylatt, *G3VXJ*
Reprinted with permission from
Radio Communication
May 1992

THE EXJAY

Resonant multi-band antenna system

Although an HF enthusiast, I have never regarded beam antennas a realistic possibility for normal suburban reasons. Equally, family and career commitments have caused patchy activity over the first twenty-odd years of my licensed existence.

However, 1989 was a high spot of activity with sunspots peaking, work load under control, and children as partially independent teenagers. Some time for radio was thus a distinct possibility. The antenna system which had evolved over a decade comprised two delta loops (see later) strung in series by a traditional method from a chimney to a distant tree and fed with tuned feeders so that, by phasing, a degree of electronic rotation was possible.

My opinion was that it was quite competitive, but certainly it is difficult to describe (hence replicate!). The loops, however, contained the gem of the ideas outlined below.

Then—from a radio point of view—disaster struck. The family vote was to move QTH to another suburban location! This clearly would involve the "education" of new neighbors and I would have to start with simpler arrays than previously in use. This approach also made sense as I wanted to be up and running as soon as possible after the move, so as not to miss the sunspot peak. Also little extra time would be available in the light of the painting, digging drilling, etc. required at the new idyllic family home.

What was required was a three-band HF antenna with general all round coverage. A commercial ground plane was quickly fitted to the chimney and commissioned. Equally quickly a TVI problem appeared on a rather sensitive setup next door. It proved necessary to move to horizontal polarization, and a half size G5RV was utilized. The TVI was now gone and G3VKJ was free to operate, but in comparison with the ground plane, signals were significantly down—particularly on 21 MHz. I decided to try something different.

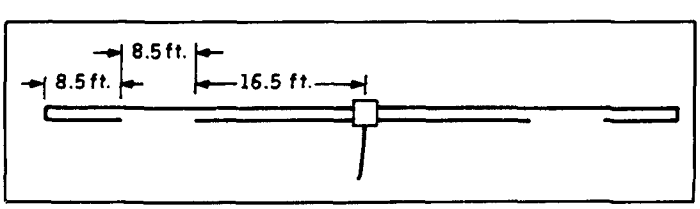

Figure 1. Basic configuration for 14 and 21 MHz.

The first attempt—or, *How things didn't work the first time.*

Fortunately, my junkbox always has plenty of slotted 300-ohm twin feeder in it, due to a history of antenna experimenting. This was used for all experiments, but any twin cable of suitable strength can be used. It was decided to try a $3\lambda/2$ for 21 MHz in parallel with a $\lambda/2$ dipole from 14 MHz and then try to get 28 MHz going with "stopping stubs." The general arrangement is shown in **Figure 1**.

This worked fine on 14 and 21 MHz, but with no amount of adjustment could I get this arrangement to resonate on 28 MHz.

The second attempt—or, *the discovery.*

The arrangement shown in **Figure 1** implies that two sections of the twin feeder had been cut away. This, in fact, was not the case, and by a quirk of lazy serendipity, I had left the wire isolated between the 14-MHz dipole and the 28-MHz stubs. In frustration, these 28-MHz $\lambda/4$ lengths were connected to the 21-MHz $3\lambda/2$ at the ends of the 14-MHz dipole and—bingo!—28 MHz resonated. The design at this stage appeared as in **Figure 2**.

The analysis—or, *Why did it work?*

Although I had never seen any such ar-

Frequency	SWR
14.0	1.9:1
14.15	1.4:1
14.3	1.9:1
21.0	1.4:1
21.15	1.0:1
21.3	1.6:1
28.0	1.1:1
28.15	1.1:1
28.3	1.2:1
28.45	1.2:1
28.6	1.3:1

Table 1. Final dimensions and SWR performance figures for the three-band horizontally polarized antenna shown in *Figure 3*.

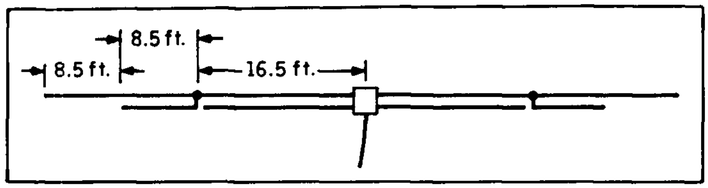

Figure 2. Stubs added for 28 MHz operation.

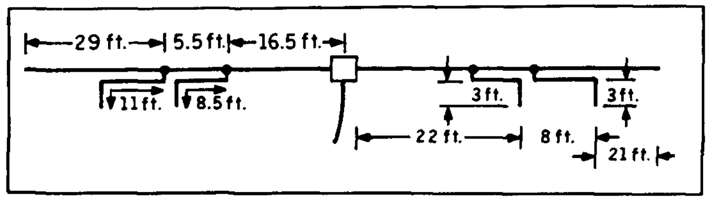

Figure 3. Dimensions shown give low SWR on three bands.

rangement published before, the 28-MHz operation appeared intuitively obvious. When several λ/2 dipoles are connected together onto a common feeder, the dipole for a selected band takes the power because it is fed from a low impedance current antinode into a resonant λ/4. The 8.5-foot stub on the 21-MHz antenna provided a stub for 28-MHz operation at exactly an equivalent low impedance position, assuming the center feedpoint position to be a current antinode.

If this theory was correct, λ/4 stubs for any band could be positioned at the appropriate current antinode position on a wire and resonance would occur. It was decided to try this out.

The third attempt—or, *When things really worked out.*

Just to remind ourselves, what was really needed was a three-band horizontally polarized antenna offering all round coverage. I decided that a 3/2λ pattern mounted east/west (my only option) would be my best compromise.

Using the new-found technique, the three-band version shown in **Figure 3** was erected. The ends of the 21 and 28-MHz dipoles were turned down as shown for three reasons. First this facilitated tuning of the ends to bring each band to resonance. Second, separating the voltage node from adjacent wires reduced capacitive detuning. Finally, for 28-MHz, these turn downs allow the 21-MHz λ/4 to be connected at the right position.

After some time adjusting the 3/2λ lengths for each band, the final dimensions (shown together with SWR performance in **Table 1**) were achieved. The SWR was no surprise considering 3/2λ center fed has an input impedance a little above the 50-watt feed.

Performance—or, *Did it really work?*

Having got the antenna resonant and in the air at 20 feet, some considerable time was spent listening, comparing the new antenna performance to the ground plane. Very little difference was noted in any direction or on any band with the slight difference illustrating the six peaks of the 3/2λ radiation pattern shown in **Figure 4**, so the first objective of all round performance on three bands with horizontal polarization has been achieved.

Now came the time to use the antenna in anger—after all, the original objective had

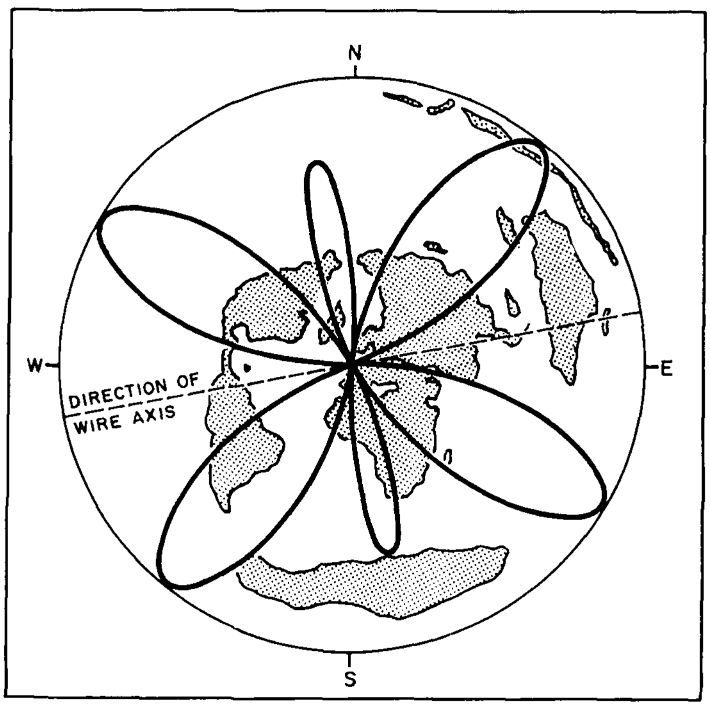

Figure 4. Radiation pattern with the antenna horizontally polarized.

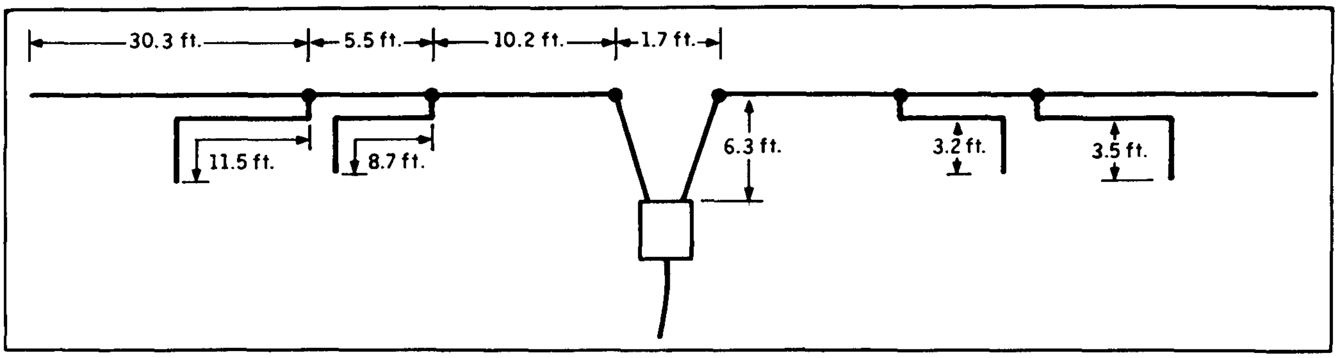

Figure 5. Conversion to form a three-band double extended zepp.

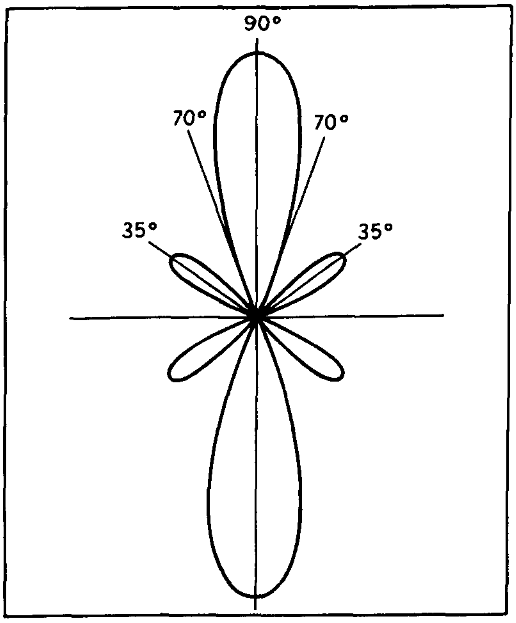

Figure 6. Theoretical radiation pattern for the above antenna.

been to get going quickly and simply at the new QTH. In the six months from December 1989 to May 1990, the antenna was used with 100 watts of CW and 250 watts PEP of SSB. A "shout list" is not the best way of illustrating an antenna performance, but for illustration, the following half-dozen prefixes worked on each band is given:

14 MHz: KH5J, XU8, T32, FW, 3Y5, ZD7
21 MHz: 1S0, 7O1, JD1, 3W, V85, 3D2 Conway
28 MHz: ST0, ZZ0 Trindade, ZS8, VR6, FH5, XW8

These results compared very well with other wire antennas used previously, as these were all new countries for me.

Development--or, *What else can be done with that idea?*

It was noticed that the 14-MHz length was a little shorter than expected, and the 28 MHz a little longer. I decided it was therefore possible to create a 2 × 5/8λ three-band double extended zepp by folding back the center to give a north/south radiation pattern with a theoretical gain of 3 dB. **Figure 5** shows the general arrangement and **Figure 6** the theoretical radiation pattern.

To bring the antenna to resonance the ends had to lengthened slightly as shown, but the SWR improved to 1.1:1 on 14 MHz, 1.2:1 on 21 MHz, and 1.1:1 on 28 MHz. More importantly, the radiation pattern sharpened north/south, as predicted, when compared to the ground plane.

An idea not implemented at G3VXJ was to mechanize the change from 3/2λ to double extended zepp format by the use of pulleys, as shown in **Figure 7**, so that the radiation pattern could be changed at will. However, my shack is not at the center!

Another version I tried briefly was a loop version comprising a delta loop on 14 MHz and folded 3/2λ for 21 and 28 MHz. (The arrangement had been used successfully at my original location.) The arrangement is shown in **Figure 8**, together with the current distributions for the 3/2λ version. This was a little unsightly by my required standards and was quickly replaced.

The eight bander—or, *the ultimate?*

Before starting to explain it should be noted that my garden is not long enough to accommodate this antenna, so dimensions reflect a "bent end" version of this arrangement. Others experimenting with a straight antenna in the clear will, no doubt, have to adjust dimensions.

After experimenting with independent wires, the relationships shown in **Table 2** were developed.

It can be easily seen that on bands marked with the same letters, a single wire will resonate on both bands. For instance, note A shows a length which resonates at 3.6 MHz and 18.1 MHz. Length B was selected to support the system as the end effects shortened the length a bit. From this, the eight-

Frequency MHz	Length λ	Feet	Notes	
3.6	1/2	131.2	A	
18.1	5/2	134.8	A	
10.1	3/2	134.9	B	Corrected length for end insulators
24.9	7/2	133.8	B	Corrected length for end insulators
28.3	7/2	121.0	C	
14.1	3/2	103.3	D	
7.05	1/2	67.0	E	
21.1	3/2	69.0	E	

Table 2. Relationships developed as a result of experimentation with independent wires. (See text for explanation of notes.)

band antenna shown in **Figure 9** was built.

The overlap shown at * in **Figure 9** was made by threading an additional third wire through the slotted 300-ohm feeder. This stub provides the 18-MHz λ/4, while the overall length including the stub is the 3.5-MHz antenna.

The antenna exhibited an SWR of 2.5:1 or better on all eight bands (after some trimming). I am confident that in a straightforward environment a better result would be achieved, but I returned to the three-band version which fits the garden.

Conclusion—or, *Was it really a good idea?*

I have not seen the simple use of λ/4 stubs in my thirty years of amateur radio, but little is new under the sun, so maybe it has been used before. It seems to work well in a number of antenna applications and hence, no doubt, it can be used by others to help in multi-banding where required. From my point of view, the basic three-band HF variant has been reinstated and continues to serve me well.

Many multi-band dipole antennas have been proposed over the years. What is different about this technique is that the antenna is truly resonant on each band. This is achieved without the use of traps (which introduce losses) and provided correct matching to coax feeder reducing other losses.

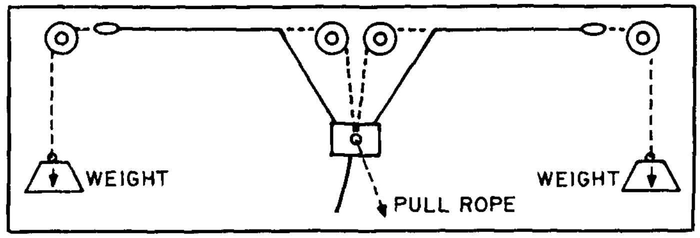

Figure 7. Suggested mechanical arrangement to change characteristics.

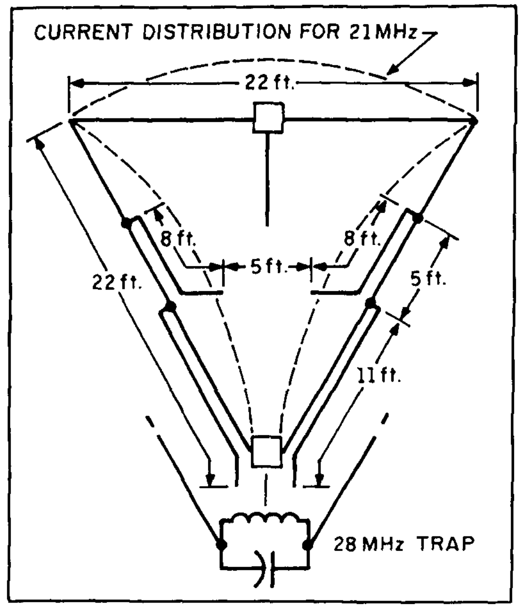

Figure 8. Loop version of the antenna uses a 28-MHz trap.

When correctly adjusted, the antenna can be directly connected to rigs with solid-state power amplifiers.

At G3VXJ there are other criteria. The three-band antenna was an important part of solving a TVI problem while at the same time providing horizontal polarization and good all round coverage.

Probably equally important is that it is "scenic" in the suburban environment. Three-hundred ohm twin feeder shows little more than a single wire at 30 feet, and the turned down ends are equally minimal in their visual impact. In particular, no adverse comments have been received from the new neighbors. ■

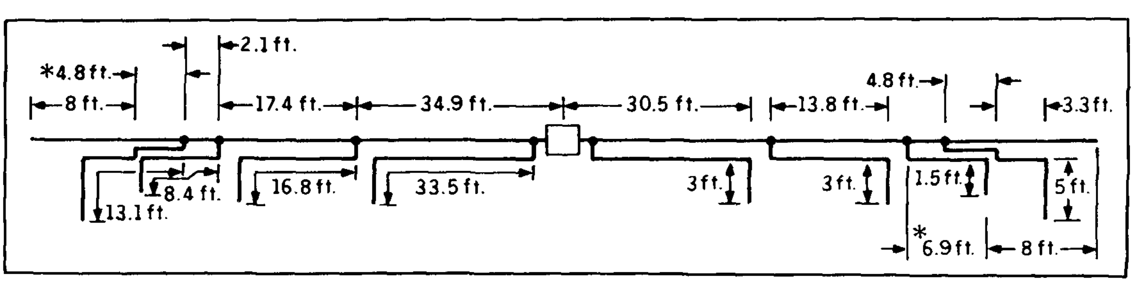

Figure 9. Final dimensions of the eight-band version.

Bob Brown, *NM7M,*
504 Channel View Drive
Anacortes, Washington 98221
Condensed for publication by:
Ward Silver, *N0AX*
P.O. Box 927
Vashon, Washington 98070

LONG-PATH PROPAGATION

Background, introduction, and details of the study

Aside from the inherent curiosity bred by "long path" (LP), it has provided determined DXers on the West Coast with those rare Middle Eastern zones that are so elusive when working with just short-path propagation. I wonder how many of us who are interested in long path have thought about how it really works and may vary within a year or even a solar cycle. I started pondering those questions a while back and finally decided to work out answers as best I could, on the air and with my computer. It took almost twelve months on the 20-meter CW band working nothing but long path and performing some computer exercises.

This is a condensation of the details of my year-long study of long-path propagation from the northwest corner of the United States. During this time, from April 1, 1991 to March 21, 1992, I made almost 1,700 long-path contacts on the 14-MHz CW band in the early morning hours.

I analyzed these long-path contacts by groups according to the level of geomagnetic disturbance and the season in which they were made—either spring/summer or fall/winter, when the sun was above or below the equator. The data show the time distribution of long-path contacts and how their frequency of occurrence was affected by geomagnetic activity during months 55 to 67 in Solar Cycle 22.

When making LP contacts, I used a Ten-Tec Corsair as my transceiver, a linear amplifier running about 200 to 250 watts output, and a generic 3-element tri-band Yagi at 38 feet above ground. All this amounts to a midscale DXer's setup. However, my QTH is a bit different in that it's located on an island—truly a low-noise site!

At the same time I was operating, I was collecting all the solar and geophysical data that NOAA and others had to offer; information I'd need to interpret the results. Using my computer to work out regression analyses and various details like distance, heading, and paths to DX stations, I think I've pulled the various aspects of long-path propagation into a coherent whole. In what follows, I'll summarize my own experience and suggest some guidelines for others to use in working with this fascinating mode.

Some details of the study

In dealing with LP propagation, it's necessary to discuss details of the great-circle paths, some solar astronomy, and invoke properties of ionospheric charts—those critical frequency maps for FoF2 used in the past. Let's take the matter of the great-circle paths first, followed by solar astronomy. After that, we'll take a closer look at geomagnetic indices.

To begin, note that at my QTH (48.5 N,

122.6 W) in the northwest corner of Washington, one looks southward to work LP into Africa and beyond. For the time period mentioned, about 1200 to 1500 UTC, I made contacts with 4S7s, VU2s, and 3B9s in the spring/summer season by pointing the beams somewhat east of south toward the sunlit hemisphere. I contacted the rest of that southerly region, from Mauritius (3B8) to Capetown (ZS1), by pointing the beam west of south toward the dark hemisphere. Note that there are seasonal effects here—especially for the 4S7s, VU2s, and the 3B8s—which I'll discuss later.

For those areas where amateur operators are most active, say in the African region as well as off into the Indian Ocean and toward Southern Asia, one can calculate the beam headings and distances, all in excess of 20,000 km, for each DX site. One can even calculate details of the great-circle paths to the locations, including the distance of closest approach to the southern geographic and geomagnetic poles.

As the seasons change, illumination along the paths will also change, affecting signal strength. This is a slow steady process, but HF propagation can often be disrupted suddenly, frequently without warning, by disturbances of solar origin. Thus, there's also a question as to whether signals following those great circle paths will be adversely affected if they enter the far reaches of the Southern Hemisphere.

The experienced DXer knows the evils of which I speak: magnetic storms, auroral absorption (AA), and polar cap absorption (PCA) events. They take their toll on HF signals without regard to hemisphere, but not always equally. So the next task is to explore those possibilities as well, finding how close the great-circle paths come to the southern magnetic pole (78.98 S, 109.1 E) before turning northward again toward Africa, the Indian Ocean, or Europe.

For this discussion, paths were categorized as being sub-auroral in latitude, in the auroral zone, or into the polar plateau—according to their maximum southerly excursion. The dividing lines are taken as below 60 degrees southern geomagnetic latitude for sub-auroral (Sub-AZ) paths, from 60 to 70 degrees for auroral zone (AZ) paths, and finally from 70 to 90 degrees southern geomagnetic latitude for (Polar) paths into the geomagnetic polar plateau. This is a natural separation for paths as auroral absorption (AA) events occur largely in the 60 to 70-degree range and polar cap absorption (PCA) events affect HF propagation paths which go across the polar plateau.

Antipodal considerations

I should proceed by presenting more of the results, but I'd like to digress to make an interesting point. In particular, great-circle paths are the locus of intersections of planes which pass through the center of the earth. For a particular point of reference, say my QTH at 48.5 N, 122.6 W here in Northwest Washington, all great circles that pass through this location also pass through its antipodal point located diametrically opposite my QTH at 48.5 S, 57.4 E. Indeed, one can think of all the great circles through my location, no matter what their heading, as having a common diameter on the line joining my QTH and its antipodal point.

So what's so special about antipodal points? Well, Crozet Island (FT4W) is close to being antipodal to my QTH! Its coordinates are 46.4 S, 51.9 E—only 465 km from my antipodal point. In essence, all the great-circle paths from my location pass close to that location. Put another way, Crozet Island is close to being along all the paths **toward** my QTH for signals from all the other stations in the long-path directions I'm interested in!

This alone put Crozet Island in a special category, but it was also important because of the near-constant activity of Jean, FT4WC, during the spring/summer season. In *The DX Bulletin*, Jean was listed as one of the "Resident Amateurs on Regularly" and, being near the focus of the paths to my QTH, he served as a beacon for me. More important, it has been suggested that antipodal focusing is involved in LP contacts—so I examined contacts in the same manner as other contacts over larger areas, say Africa, the Indian Ocean, and Europe.

In a more general sense, the azimuthal equidistant map in **Figure 1** can be used to distinguish between the categories of paths. Thus for this QTH, great-circle paths that go across the polar plateau are found at headings between 158 and 231 degrees east of south, and between 231 and 254 degrees west of south. Finally, paths with headings less than 135 or more than 254 fall in the sub-auroral zone category.

And some solar astronomy

We all know the sun creates the ionosphere and that there are seasons for the ionospheric layer, as well as for the neutral atmosphere, depending on whether the subpolar point is above or below the equator. In presenting the results of the LP study, I'll consider only two seasonal divisions—spring/summer and fall/winter. These divisions have a

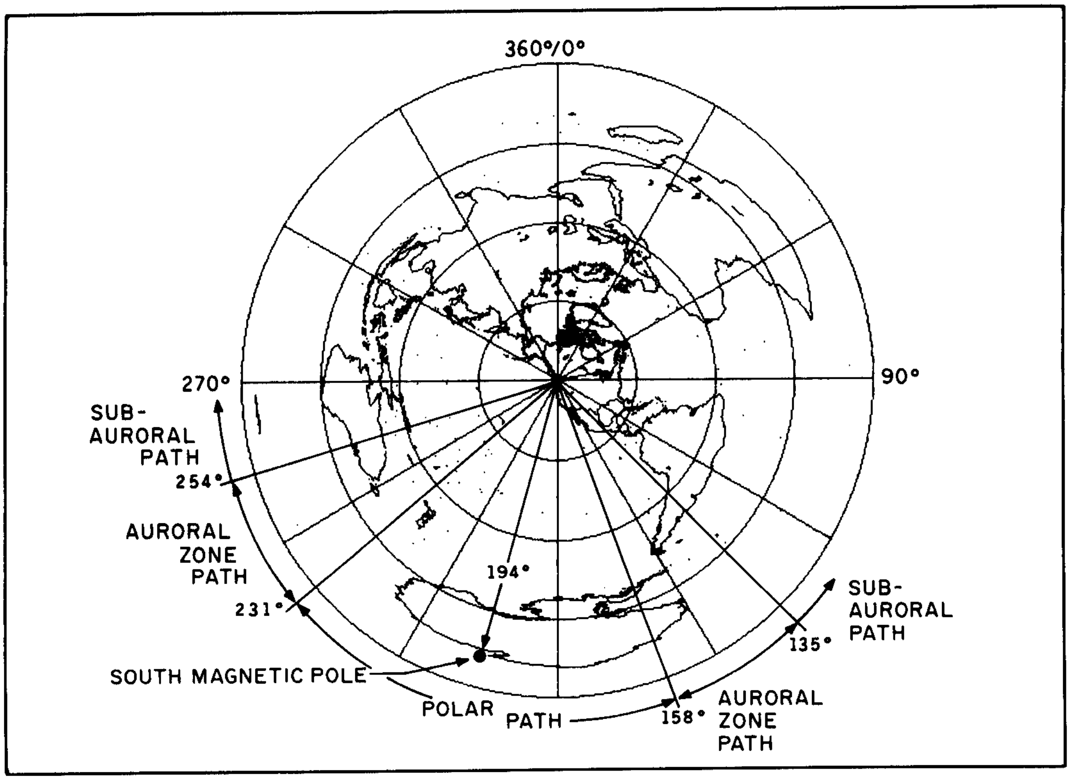

Figure 1. Azimuthal equidistant map showing path categories.

bearing on regions of ionospheric absorption in the D region as well as the details of the critical frequency maps for FoF2. To proceed, let's start with the gray line—a region of twilight along the terminator.

The gray line has enjoyed a prominent role in long-path discussions. One can explore that role in detail using the GEOCLOCK program or, more simply, by using the plastic slides of *The DX Edge.* I prepared **Figures 2** and **3** from *The DX Edge* using the months of June and December, respectively, choosing times corresponding to those when the mean monthly terminator or gray line passed close to my QTH.

As **Figure 2** indicates, paths to India and Sri Lanka are close to the gray line around 1230 UTC in June, and it's not surprising

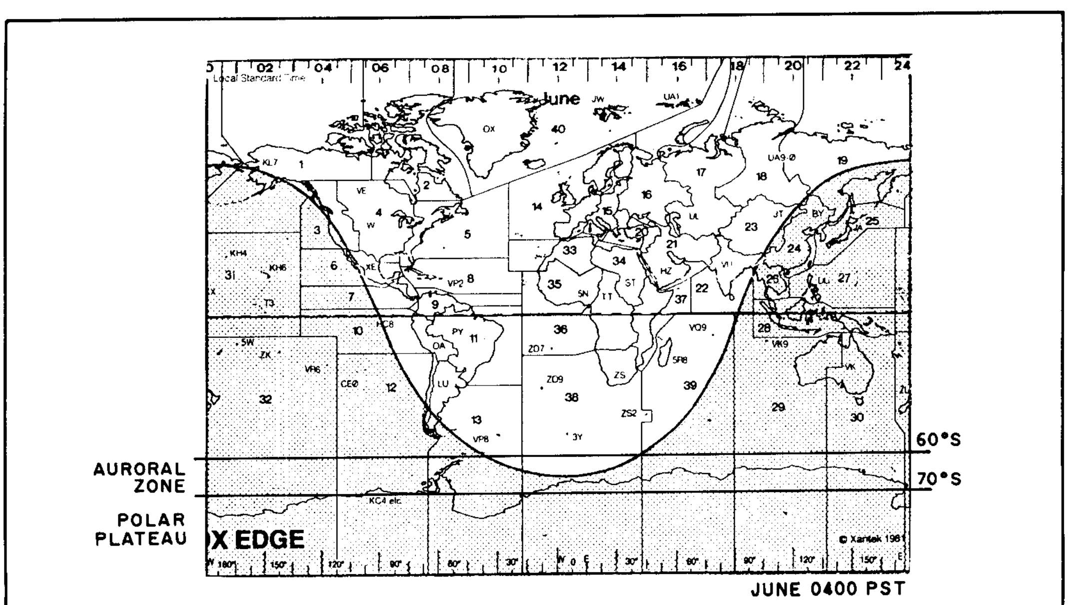

Figure 2. Gray line for June, as shown by The DX Edge.

that I was able to contact both 4S7s and VU2s regularly at the outset of an LP session during the early months of the LP study. Those contacts were consistent with what might be called "conventional wisdom," the path being sheltered from solar illumination by its location in the twilight along the gray line.

However, there were differences with seasons of the year and levels of geomagnetic activity. While the seasonal effects were gradual, the changes weren't small or subtle, and were quite evident when you look at the times when LP DX was coming in and consider the prefixes heard on the band. Geomagnetic activity, however, was sporadic in time, varied markedly in degree, and had an effect on the ionospheric conditions.

The main change with seasons was that stations in the Indian Ocean area, say in Sri Lanka and India, were no longer heard when the Southern Hemisphere went into its summer season. This was the result of increasing ionospheric absorption as their long paths to my location became more illuminated. Thus, paths that went off into the east from here, toward the sunlit hemisphere, soon became ineffective as the summer season progressed in the Southern Hemisphere.

That same shift of the subsolar point resulted in the winter season in the Northern Hemisphere, and had another effect on LP signals that went to the west from this QTH. In particular, for signals to and from Europe, the shift in seasons actually reduced the illumination on the portions of the paths over Europe. As a result, more of Europe was open and those contacts on LP became much more frequent. **Figure 3** illustrates December sunlight conditions.

All in all, the loss of the signals from the Indian Ocean area, as well as the appearance of more European signals, had the effect of shifting the time distribution of LP contacts toward later hours. This result was quite striking, as seen in **Figure 4** where the time distribution of contacts for the two seasons are displayed in 15-minute intervals. That shift also involved a change in the calls contacted, from those in Eastern Europe to those in Western Europe. Part of the shift is sociological in origin, having to do with the difference in time of the end of a work day.

Geomagnetic indices

From the standpoint of principle, it would be more desirable to use indices from the Am network, with its extended distribution of magnetometers, in examining magnetic disturbances of LP propagation. As a practical matter, however, the application of those results would be difficult to bring down to the level of everyday operations. Part of this is due to the fact that the Am network isn't well known outside the tight circle of professional geomagneticians. Further, even though it is prepared under the auspices of IAGA by the Institut de Physique du Globe in Paris, the assembly and analysis of data takes a good deal of time. As a result, the tables for the Km, Am indices reach NOAA about 2 to 3 months after data collection is completed.

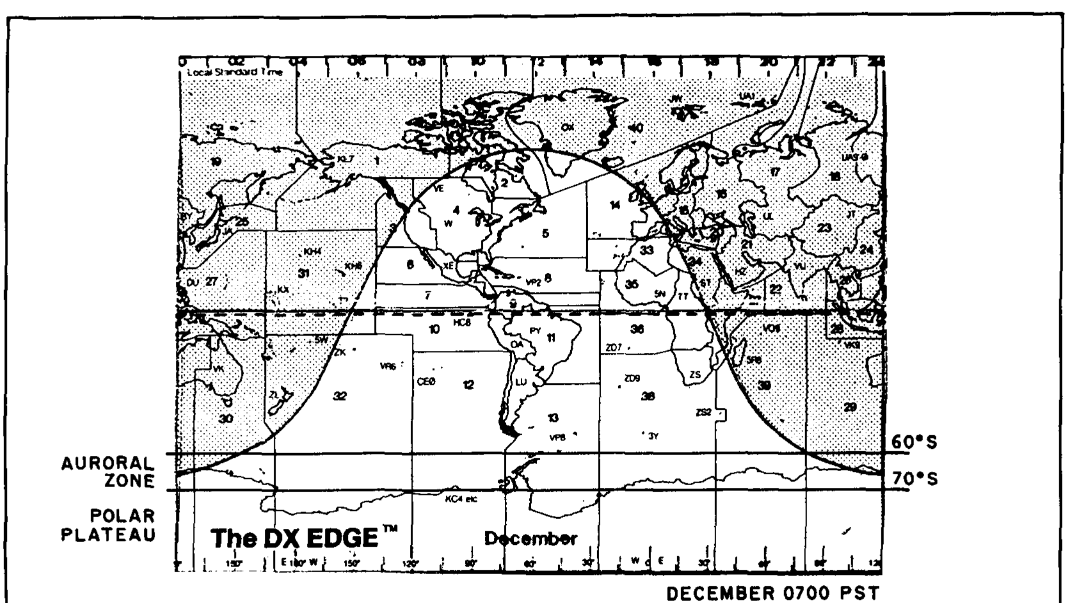

Figure 3. Gray line for December, as shown by The DX Edge.

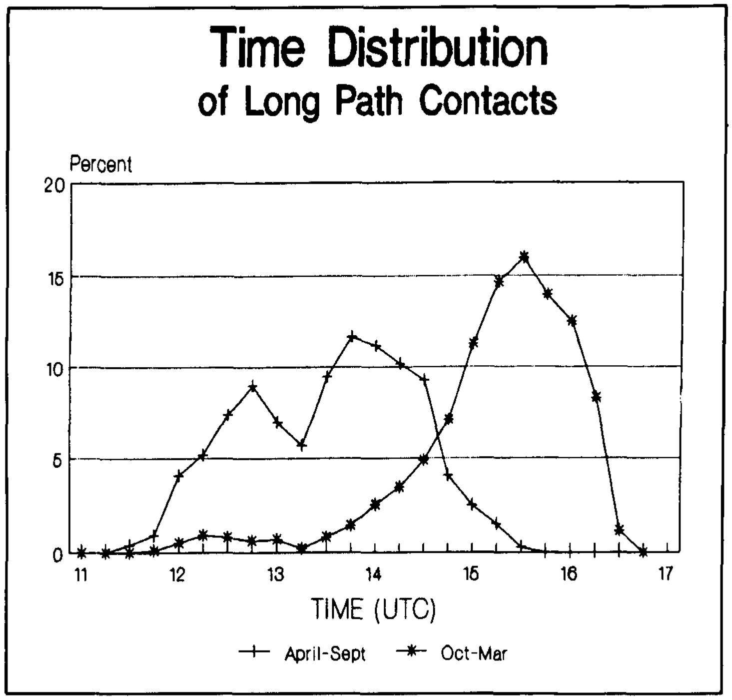

Figure 4. Time distribution of long-path contacts.

On the other hand, the Ap index is better known and Ap estimates are forecast three days in advance on the NOAA BBS—a distinct advantage to the DXer. With a strong statistical correlation between Ap and Am, one can use the Ap index with confidence. Thus, if the DXer has a sense of the Ap values that will support propagation, it should be possible to adopt a plan of operation, be it for contesting or DXing, that takes into consideration possible changes in conditions.

With those remarks, I'll conclude my discussion of geomagnetic indices. From this point onward, I'll use only the Ap index in my analysis. Those who are interested in the question of three-hour K indices and daily A indices might like to read the article by Menvielle and Berthelier.[1] It might also be interesting to review the other geomagnetic data that the NOAA BBS provides: K and A indices from over 20 observatories, albeit usually 3 to 4 days after the fact and without any sort of overall analysis or interpretation.

Long-path propagation in a nutshell

The serious DXer knows that LP is a dawn-dusk affair—one that is essentially controlled by ionospheric absorption in the D region. Thus, the times of any LP opening or closing are set by solar illumination on the extreme ends of the path. More specifically, competing factors are: 1) sunrise on the F region in the winter hemisphere, which raises the MUF and opens the path, and 2) signal absorption in the D region on the morning portion that grows at a faster rate than the absorption decreases on the dusk end, ultimately closing the path.

Any sort of geomagnetic activity that decreases the ionization in the F region at refraction points along the path can only shorten the duration of the opening or close it altogether. The same is true of any solar event that increases the ionization in the D region—say a sudden burst of solar X-rays (SID), or the arrival of solar protons in the polar cap (a PCA event). But during quiet conditions, the local times of LP openings will shift with the seasons. Openings will occur earliest near the summer solstice and latest around winter solstice, starting about 2 to 3 hours later for a path that's open year round, as is the case from the West Coast to Europe.

Long-path openings vary in duration, from about 3 to 4 hours in the spring/summer season to 1 to 2 hours in the fall/winter season. During the spring/summer season, a dawn opening is really a series of shorter openings that overlap in time. Here on the West Coast, it starts with signals from 80 degrees East Longitude—say UJ8s, VU2s, or 4S7s—and then moves steadily westward with the sun toward stations in Central Europe—say UB5s, YUs, or LZs. With that variety of locations, some paths from the

West Coast go off to the east of south and toward the sunlit hemisphere, but are protected by the winter darkness in the Southern Hemisphere. The other paths toward Europe go off to the west of south into the dark hemisphere and depend on the level of solar activity for critical frequencies to support propagation.

During the fall/winter season, the more easterly stations are just not heard on LP as their signals have been wiped out by solar illumination on the portions of the paths in the southern hemisphere. The other paths, that went westward across a darkened ionosphere in the spring/summer season, now come close to fitting the conditions for gray line propagation. As a result, the majority of LP contacts during this period are with Europe, opening with UB5s and HAs and then finally closing with Fs, Gs and LAs in Northern Europe.

From the standpoint of propagation, however, contacts with the southern portions of Africa are still possible, simply few in number. This is because intense afternoon thunderstorm activity shifts from the equatorial regions of Africa into the southern and eastern portions of the continent with the coming of their summer.

For LP DXing from other locations, like the East Coast or elsewhere, the possibilities and problems are best examined using a propagation program like the new MINIPROP PLUS. Of course one can cite possibilities, say the East Coast to Australia and Japan, as noted in ARRL publications, but those are only individual cases and somewhat limited when it comes to variety of DX. More general cases, offering greater opportunities, are from Australia to Europe or Indonesia to South America.

In any event, whatever the path, the experience from month 55 to month 67 in Solar Cycle 22 indicates that LP contacts can be made year-round on 14 MHz, the only exception being days during major magnetic storms. Thus, there will be days when the LP signal strengths are amazing and other days when LP signals, or ANY signals for that matter, are not heard.

Between these two extremes of LP propagation, there's a moderate negative correlation (−0.43) with magnetic activity, at least on paths that go through the auroral zone. Thus, when the Ap index rises, LP signals are weaker and less numerous. Consequently, the number of contacts one can make in a day will decrease. However, some LP will still be open; you just have to work harder at it.

The problems that lead to weaker and less numerous LP signals result from ionization changes in the auroral and polar F regions, when solar wind and plasma impinges on the outer boundary of the earth's magnetic field. A separate analysis of LP contacts during the recent spring/summer season indicates that paths which only reach sub-auroral latitudes (from Southern California to South Africa, for example) are more successful for LP propagation than the other paths which run more poleward, as is the case for the northwest.

Given that the spring/summer season is the most rewarding time for working "New Ones," any operation on LP in the fall/winter season is like weight training; it keeps you in shape for the upcoming DX season. A bit of practice busting through pileups won't hurt either!

At this point in Cycle 22, the sunspot number is high enough that MUF considerations are important only on the higher bands like 21 and 28 MHz. That situation will gradually change as we move closer to the solar minimum. Long path contacts on 14 MHz will become more spotty in time and LP DXing will slowly shift to 7 MHz. Seven-MHz LP DXing is already a "winter sport" with its own loyal following, but because of the lower frequency, it's only feasible from QTHs where the DX paths stay within darkness in the Southern Hemisphere.

The mention of paths and their relation to darkness brings up another important point in LP DXing: one really needs a good atlas, *The DX Edge*, or better yet, a good propagation program like the MINIPROP PLUS. While *The DX Edge* is helpful in giving rough indications of the geometry in LP propagation, a program like MINIPROP PLUS goes further and gives not only MUF information, but also signal-strength data. It also shows the geometry for both short and long paths in relation to the terminator.

With the aid of a computer and a good LP program, it's possible to understand what's on hand at any moment, and to plan ahead for future DXpeditions. The "back door" via LP can be quite effective in avoiding short-path QRM from stations between you and the DX in those difficult zones. Additionally, all the tools mentioned in the preceding paragraph are essential for operators who wish to explore the LP possibilities from their locations, say Australia to Europe or Europe to the Orient.

As for the other tools needed to be effective in the pursuit of LP DX, at a minimum they start with a good transceiver, complete with RIT and XIT, and a beam antenna (for example, a 3-element Yagi that is at least a half-wavelength above ground and well removed from nearby objects). With that sort of setup, you're in business, ready to leap out of bed when the alarm goes off and start looking for LP DX.

The LP signals you hear will have that "DX sound," but they are quite steady considering they often pass through high magnetic latitudes in the south. From time to time, however, you'll hear various forms of multipathing. This happens most often in the fall/winter season when both short and long-path propagation can be in effect simultaneously.

Finally, we come to the marvel of the strength of LP signals, from more than half the way around the world. When you hear them, you can think of the challenge that they present to theoretical understanding. There are ideas of focusing and chordal hops to consider, but they cannot be invoked willy-nilly as some sort of ionospheric structure must be involved, like that found with the equatorial anomaly. So ponder the signals you hear and think of how they can be explained. It's a challenge! ■

REFERENCES

I. M. Menvielle and A. Berthelier, "The K-Derived Planetary Indices: Description and Availability," *Re. Geophys.*, 29, 1991, pages 415-432.

A Bit About the Author and His Work

Who is Bob Brown? First licensed as W6PDN in 1937 and later as N7GDZ, Bob became NM7M in 1981. He is best known for his "Propagation" column in *Worldradio*. Bob was an instructor and professor of physics from 1952 to 1982. During this time he wrote 80 papers on atmospheric and ionospheric physics.

In its original form, Bob's study on long-path propagation covered more than 60 pages. Consequently, I have divided the work into two parts. This first section presents some details about how the study was done and under what conditions. A qualitative summary covering the basic conclusions of the study ends Part 1.

Part 2 covers the data obtained during the study in more detail. It discusses some of the analyses, as well as factors affecting long-path propagation. The second installment also explores special topics like Gray Line, Off-Great-Circle paths, and Extreme Long Path, and presents a detailed quantitative summary of the data.

For those readers interested in obtaining a typeset and bound copy of the full report, copies are available from Bob Brown, NM7M, 504 Channel View Drive, Anacortes, Washington 98221.

de N0AX

PRODUCT INFORMATION

Non-CFC Gas Duster

Philips ECG has an ozone-conserving aerosol duster with easy control of gas flow.

OZ1100 Jet Air Cleaner is a CFC-free, dry, inert, nonabrasive, nonflammable gas duster equipped with a human-factors engineered trigger valve. The product can be used to remove dust, lint, oxide particles, and other particulate matter in applications where conventional solvents can't be employed. It is safe for most delicate instruments, sensitive equipment, memory disks, tapes, and films. The cleaner is available in a 12-ounce aerosol can, complete with trigger valve and extension tube for difficult-to-reach areas.

For more information on OZ1100 Jet Air Cleaner, look for your nearest ECG product distributor under "Electronic Equipment & Supplies" in the telephone directory yellow pages or call (800) 526-9354.

J. Robert Witmer, *W3RW*
146 Forest Trail Drive
Lansdale, Pennsylvania 19446

A "SYNTHESIZER-SIMULATOR" FOR 6-METER FM OPERATION

Use surplus 2-way commercial equipment to operate on 6 meters

Six meters is a largely under-used band that provides a wide range of propagation capabilities. Amateur radio manufacturers are just starting to rediscover 6 meters, but equipment tends to be on the pricey side. Used 2-way commercial equipment is available at reasonable cost, but the majority is crystal controlled and, as a result, has limited frequency flexibility. Also, it often lacks the "bells and whistles" we're accustomed to seeing on the latest FM equipment. The synthesizer-simulator is a 2-to-6 meter transverter, optimized for operation with used 2-way commercial service transceivers. The unit effectively translates your 2-meter FM equipment's capability to 6 meters. You can also use this approach without a commercial transceiver (more on that later).

The Solution

In the early days of 2-meter FM, the lack of frequency flexibility was circumvented by adding an external synthesizer. Because of the current proliferation of synthesized equipment, external synthesizers are generally not available to help with the 6-meter flexibility problem. I think the synthesizer-simulator provides a unique solution.

The synthesizer-simulator, used with a synthesized 2-meter transceiver, (see **Figure 1**), provides the same drive to a crystal-controlled transmitter that an external synthesizer would have. On receive, the front end of the commercial rig is used as the RF stage in a converter that converts 6-meter signals to 2 meters. By using this approach, you obtain all the bells, whistles, and capabilities of the latest 2-meter rigs plus the quality of the critical RF sections of commercial-grade equipment (that is, Motorola, General Electric, and RCA). The approach requires minimum modification of the commercial equipment.

Good used commercial equipment is available

Used commercial 2-way rigs in operating condition are often available at hamfests (even solid-state units!). Many have simply been retired from service in favor of newer equipment. I won't address the realignment and tuneup of used commercial equipment because this subject is beyond the scope of this article, but you'll find summary information for selecting equipment for conversion in a later section.

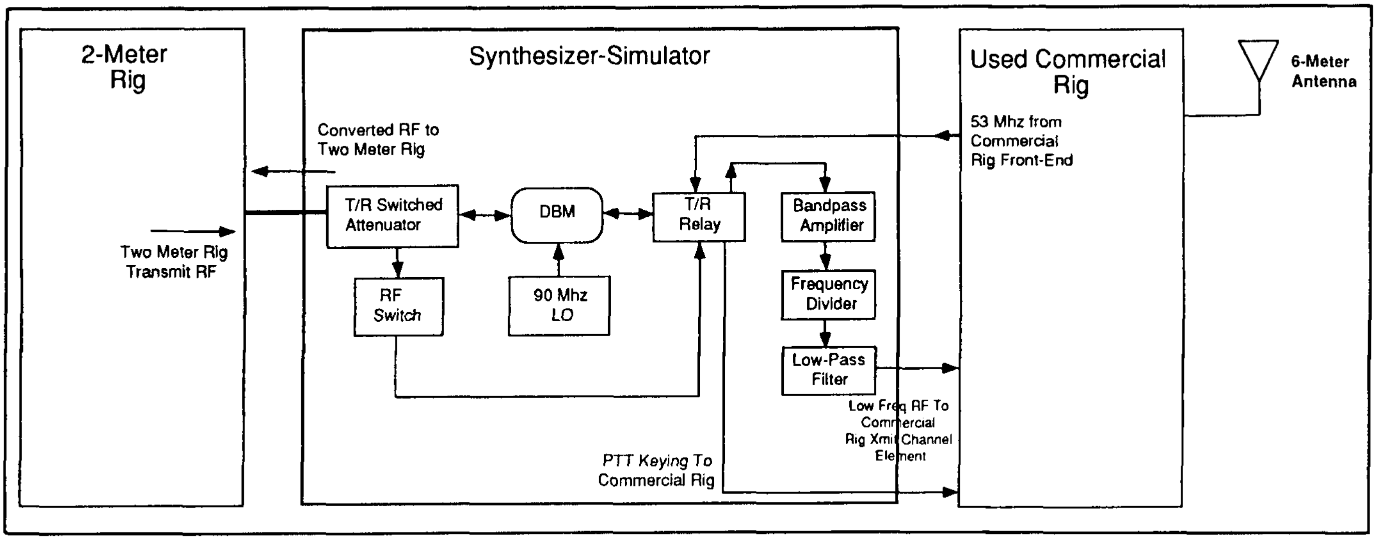

Figure 1. Synthesizer-simulator/interface diagram.

Operation

When you use your 2-meter rig in conjunction with the synthesizer-simulator, operate just as you normally would in the low-power position. Program the CTSS and repeater split required by the 6-meter repeaters you plan to use. **Table 1** shows the relationship between the 6- and 2-meter frequencies.

When connected to a dual-band (144/444 or 144/222) transceiver with cross-band repeat capability, the synthesizer-simulator approach can also provide you with "remote-base" type operation. Since 6-meter HTs aren't readily available, this approach can add HT accessibility to 6 meters.

How it works

Figure 1 is a block/interface diagram of the synthesizer-simulator. **Figure 2** is a top level schematic of the unit. The 2-meter rig is found on the left side of the diagrams shown in **Figures 1** and **2**. The used commercial rig, which has been realigned for 6-meter operation, is on the right side. In transmit, the signal from the 2-meter transmitter is mixed to 52.01 MHz. After bandpass amplification, it is divided by the factor needed to provide the required equivalent crystal frequency for the commercial rig's transmitter. The receive side of the synthesizer-simulator operates just as receive converters normally do. A 90-MHz local oscillator simplifies the frequency translation process between 2 and 6 meters; for example, 52.00 MHz becomes 142.00 MHz. A more detailed discussion of transmit and receive operation, and the workings of the individual circuit elements, follows.

Receive operation

During receive, the 6-meter receive signal (53.01 MHz) from the 6-meter antenna is routed via the commercial rig's internal T/R relay to the RF amplifier. The output of the RF amplifier is connected to the receive side of the synthesizer-simulator T/R relay. From the T/R relay, the signal is connected to the DBM, where it's mixed with the 90-MHz local oscillator injection signal, creating sum and difference signals at 143.01 MHz and 36.99 MHz, respectively. These signals are routed to the T/R switched attenuator connected to the 2-meter rig. The 2-meter rig rejects the 36.99-MHz signal and receives the 143.01-MHz signal with minimum attenuation.

Transmit operation

The 2-meter transmit signal (142.01 MHz) is input to the synthesizer-simulator's T/R switched attenuator, where it's attenuated by approximately 33 dB and passed to the DBM. The 142.01-MHz signal is mixed in the DBM, creating outputs of 52.01 MHz and 232.01 MHz. The DBM outputs are connected via the T/R relay to the input of the bandpass amplifier, which amplifies the 52.01-MHz signal and attenuates the 232.01-MHz signal. The bandpass amplifier raises the 52.01-MHz signal to a level sufficient to trigger the first CMOS buffer in the digital divider.

The 52.01-MHz signal is divided by 6 in the digital divider, producing a 8.6683-MHz signal. This signal is routed through the output filter of the synthesizer-simulator to the modified transmit channel element of

6-Meter RPT / Simplex		Local Osc	2-Meter Rig Frequencies		Synthesizer Simulator Frequencies		
Output Freq	Input Freq	Mhz	Receive	Transmit	Xmit DBM Out	F-out @ U2a	F-out to Cmcrl Rig
53.01	52.01	90	143.01	142.01	52.01	26.005	8.66833
53.03	52.03	90	143.03	142.03	52.03	26.015	8.67167
53.05	52.05	90	143.05	142.05	52.05	26.025	8.67500
53.07	52.07	90	143.07	142.07	52.07	26.035	8.67833
53.09	52.09	90	143.09	142.09	52.09	26.045	8.68167
53.11	52.11	90	143.11	142.11	52.11	26.055	8.68500
53.13	52.13	90	143.13	142.13	52.13	26.065	8.68833
53.15	52.15	90	143.15	142.15	52.15	26.075	8.69167
53.17	52.17	90	143.17	142.17	52.17	26.085	8.69500
53.19	52.19	90	143.19	142.19	52.19	26.095	8.69833
53.21	52.21	90	143.21	142.21	52.21	26.105	8.70167
53.23	52.23	90	143.23	142.23	52.23	26.115	8.70500
53.25	52.25	90	143.25	142.25	52.25	26.125	8.70833
53.27	52.27	90	143.27	142.27	52.27	26.135	8.71167
53.29	52.29	90	143.29	142.29	52.29	26.145	8.71500
53.31	52.31	90	143.31	142.31	52.31	26.155	8.71833
53.33	52.33	90	143.33	142.33	52.33	26.165	8.72167
53.35	52.35	90	143.35	142.35	52.35	26.175	8.72500
53.37	52.37	90	143.37	142.37	52.37	26.185	8.72833
53.39	52.39	90	143.39	142.39	52.39	26.195	8.73167
53.41	52.41	90	143.41	142.41	52.41	26.205	8.73500
53.43	52.43	90	143.43	142.43	52.43	26.215	8.73833
53.45	52.45	90	143.45	142.45	52.45	26.225	8.74167
53.47	52.47	90	143.47	142.47	52.47	26.235	8.74500
52.49	52.49	90	142.49	142.49	52.49	26.245	8.74833
52.525	52.525	90	142.525	142.525	52.525	26.2625	8.75417
53.55	52.55	90	143.55	142.55	52.55	26.275	8.75833
53.57	52.57	90	143.57	142.57	52.57	26.285	8.76167
53.59	52.59	90	143.59	142.59	52.59	26.295	8.76500
53.61	52.61	90	143.61	142.61	52.61	26.305	8.76833
53.63	52.63	90	143.63	142.63	52.63	26.315	8.77167
53.65	52.65	90	143.65	142.65	52.65	26.325	8.77500
53.67	52.67	90	143.67	142.67	52.67	26.335	8.77833
53.69	52.69	90	143.69	142.69	52.69	26.345	8.78167
53.71	52.71	90	143.71	142.71	52.71	26.355	8.78500
53.73	52.73	90	143.73	142.73	52.73	26.365	8.78833
53.75	52.75	90	143.75	142.75	52.75	26.375	8.79167
53.77	52.77	90	143.77	142.77	52.77	26.385	8.79500
53.79	52.79	90	143.79	142.79	52.79	26.395	8.79833
53.81	52.81	90	143.81	142.81	52.81	26.405	8.80167
53.83	52.83	90	143.83	142.83	52.83	26.415	8.80500
53.85	52.85	90	143.85	142.85	52.85	26.425	8.80833
53.87	52.87	90	143.87	142.87	52.87	26.435	8.81167
53.89	52.89	90	143.89	142.89	52.89	26.445	8.81500
53.91	52.91	90	143.91	142.91	52.91	26.455	8.81833
53.93	52.93	90	143.93	142.93	52.93	26.465	8.82167
53.95	52.95	90	143.95	142.95	52.95	26.475	8.82500
53.97	52.97	90	143.97	142.97	52.97	26.485	8.82833
53.99	52.99	90	143.99	142.99	52.99	26.495	8.83167

Table 1. Typical synthesizer-simulator operation frequencies.

the commercial rig, where it's processed just as an original crystal-generated signal would have been. This results in a commercial rig output on 52.01 MHz. **Table 1** shows the typical frequencies associated with operating the synthesizer-simulator with a 90-MHz local oscillator frequency.

The 2-meter rig transmit signal also activates the transmit DC switch that applies +12 volts DC to the T/R relay bandpass amplifier and output frequency divider interface. The T/R relay provides a contact closure for the commercial rig's PTT line to actuate the commercial rig's transmitter.

Detailed functional block circuit operation description

Input attenuator/RF switch (see Figure 3). The input of the synthesizer-simulator consists of a quarter-wave transmission line/diode-switched RF attenuator, D4-D8, and TT_1 and TT_2. The quarter-wave transmission line/diode switch bypasses the attenuator during receive operation. I designed the attenuator using approximate resistor values found in *The ARRL Handbook*[1] to provide approximately 33 dB of attenuation. This reduces 2 watts of input power to

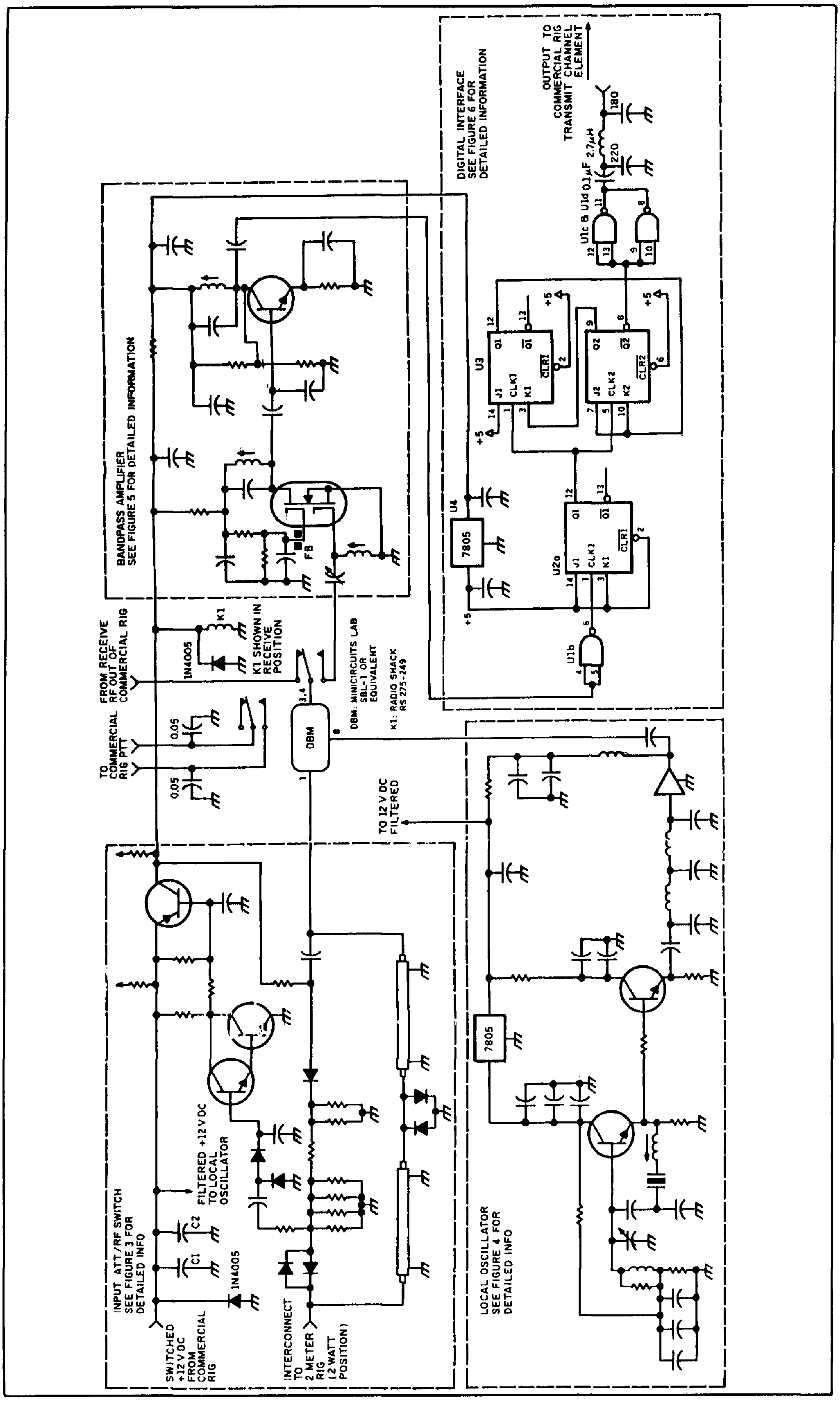

Figure 2. Synthesizer simulator schematic.

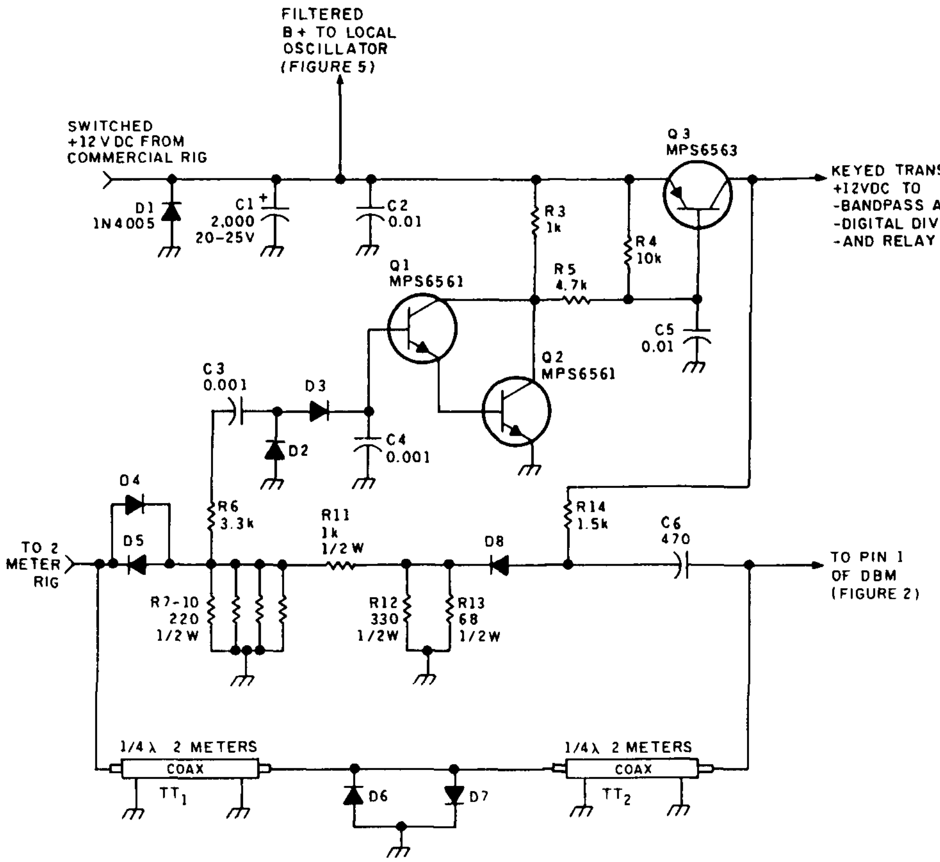

Parts List: Input Attenuator/RF Switch

Capacitors
All capacitors are 16 to 20-volt disc ceramic unless otherwise noted.

Diodes
D2-D8—1N914 silicon

Resistors
All resistors are 1/4-watt carbon film unless otherwise noted.

Transistors
Q1,Q2—MPS6561 (NPN)
Q3—MPS6563 (PNP)

TT_1, TT_2 Electrical 1/4-wavelength of 50-ohm coax at center of intended 2-meter transmit operating band.

Figure 3. Input attenuator/RF switch schematic.

the recommended maximum linear rated input of the DBM, which is 1 mW or 0 dBm. The attenuator input section consists of 4 paralleled 220-ohm 1/2-watt resistors, R7-R10. Mount these resistors for easy access in case they get fried by an accidental application of high input power (that is, in case you forget to set your equipment to the low power position).

The *RF sensing circuit* consists of a circuit using a diode voltage doubler, D2 and D3, and a Darlington transistor configuration, Q1 and Q2. A PNP transistor, Q3, acts as the Transmit B+ DC switch that keys K1, the PTT keying and 53-MHz switching relay.

Mixer (see Figure 2). The mixer circuit takes advantage of the DBM's bidirectional performance characteristic. This allows IF and RF port mixing to occur in either direction, with minimum performance difference. The DBM's ports are selected to match the appropriate frequency ranges of the circuit. The IF, or lowest frequency,

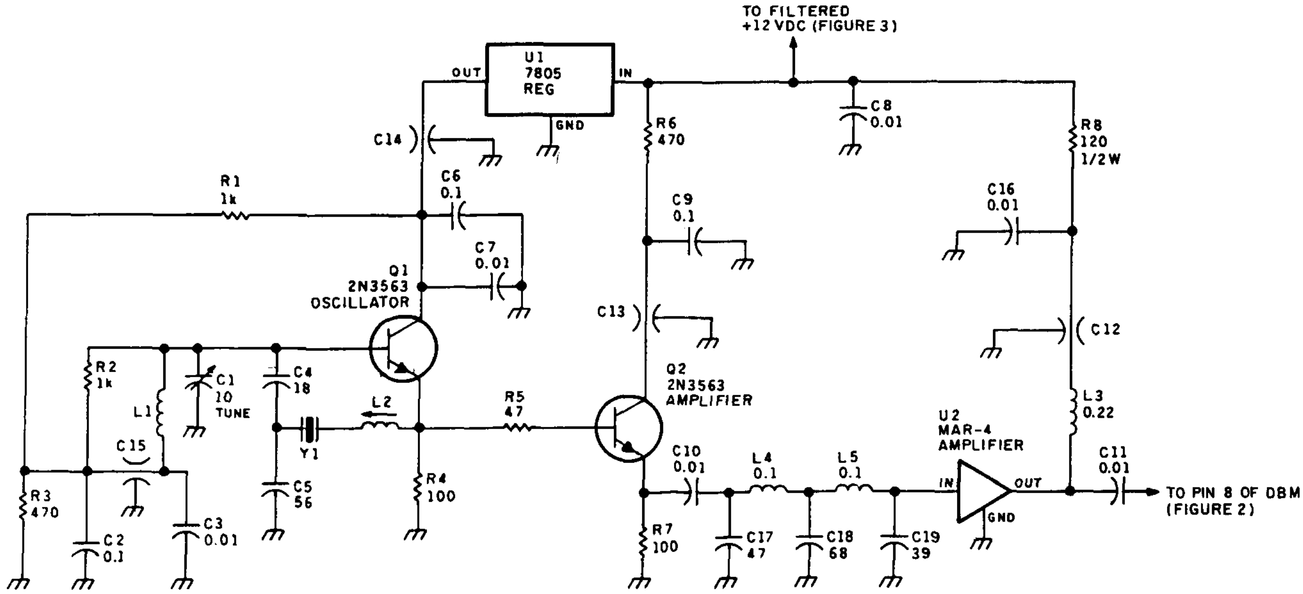

Parts List: Local Oscillator

Capacitors
C1—8 to 10-pF trimmer
C12-C15—1,000-pF feedthrough bypass

All capacitors are 16 to 20-volt disc ceramic unless otherwise noted.

Crystals
Y1—90-MHz, 5th-overtone, series-resonant crystal (see text).

Inductors
L1—Five turns no. 28 enamel wire, 3/16-inch ID close wound
L2—Three turns no. 28 enamel wire, 3/16-inch ID slug-tuned coil form.
L3—0.22-μH miniature RF choke.
L4,L5—0.1-μH miniature RF choke.

Integrated Circuits
U1—5-volt, 3-terminal regulator, 7805 or equivalent
U2—Mini-Circuits Labs MAR-4 MMIC

Resistors
All resistors are 1/4-watt carbon film unless otherwise indicated.

Transistors
Q1,Q2—2N3563 or equivalent

Figure 4. Local oscillator schematic. Except as indicated, decimal values of capacitance are in microfarads (μF); others are in picofarads (pF); resistances are in ohms: k = 1,000.

port (Pins 3 & 4) is used as the 50-MHz port. The LO (Pin 8) is connected to the "LO port" and the 2-meter side is connected to the "RF port" (Pin 1).

Local Oscillator (see Figure 4). The 90-MHz local oscillator circuit is taken from a *QST* article.[2] I substituted Mini-Circuits Labs' MAR-4 MIMIC for the MSA-0304 specified in the article.* You can use the circuit's capability to "free" oscillate with a 47-k resistor in place of the crystal and L2, to get the oscillator L1 and C1 components on frequency to ensure crystal oscillation. Use a frequency counter or FM broadcast receiver to check the operating frequency. L1 is non-critical. The best approach is to make a coil like that specified, try it, and if it doesn't give you the desired frequency oscillation range with C1, adjust its size. If you have an appropriate variable slug-tuned coil, try that. I used the same approach for L2, the crystal frequency trimming inductor. Once the

*Mini-Circuits Labs Manual/Catalog.

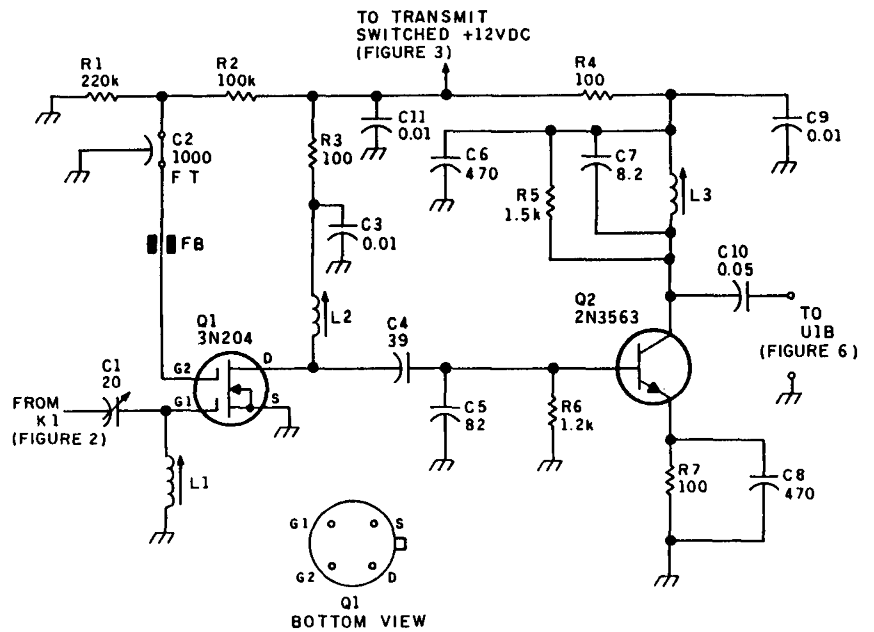

Parts List: Bandpass Amplifier

Capacitors
C1—Ceramic or piston trimmer, 20 to 25 pF maximum
C2,C3—500 to 1,000-pF feedthrough, solder-in type preferred.
C4—500 to 1,000-pF feedthrough
C5—100 to 200-pF silver-mica or ceramic

Inductors
L1—Ten turns no. 24 enamel on 1/4-inch slug-tuned coil form
L2,L3—Ten turns no. 28 enamel wire on 3/16-inch slug-tuned coil form
FB—Ferrite Bead

Transistors
Q1—Dual-gate MOSFET such as the 3SK51 or 3N204
Q2—2N3563 or equivalent

Figure 5. Bandpass amplifier schematic. Except as indicated, decimal values of capacitance are in microfarads (μF); others are in picofarads (pF or $\mu\mu$F); resistances are in ohms: k = 1,000, M = 1,000,000.

oscillator free-runs in the right range, remove the 47-k resistor and install the crystal and L2. Monitor the current to the oscillator and adjust C1 for a peak in current drain that indicates that oscillation is occurring. Adjust L2 for on-frequency operation and peak C1 for maximum current (there is some interaction between these adjustments). There's a 5-section lowpass filter (L4, L5, C12, C13, and C14) between the output of the oscillator (Q1 and Q2) and the MIMIC (U2).

On-frequency performance is important not only for the obvious reasons, but also to obtain maximum noise rejection by the 2-meter receiver. Six meters is considered by some to be the "optimal" band for susceptibility to manmade interference. This is one area where the synthesizer-simulator approach may suffer if you plan mobile operation. Most commercial low-band VHF transceivers contain receiver noise blankers. I have found that acceptable performance is obtainable on most, but not the weakest signals, with on-frequency operation.

I chose a 90-MHz, 5th-overtone crystal, Y1, for the oscillator, so the receive range for 53 to 54 MHz would convert to 143 to 144 MHz and simplify frequency readout. This also minimizes the feedthrough of high-level 2-meter signals during receive.

T/R Relay (see Figure 2). The only relay used in the synthesizer-simulator, K1, follows the DBM. I used a relay because I wanted a universal interface for keying the commercial rig's push-to-talk (PTT) circuit. PTT circuit keying requirements aren't the same in all equipment. In Motorola equip-

Op Freq	2Mtr Freq	DBM Out	U2a Out	U3 Out	C-Rig Xtal Freq	C-Rig X Factor	U2b Divide #	U3 Divide #
52.525	142.525	52.525	26.2625	4.3771	4.3771	12	2	3
52.525	142.525	52.525	26.2625	6.5656	6.5656	8	Not Used	4
52.525	142.525	52.525	26.2625	8.7542	8.7542	6	Not Used	3
52.525	142.525	52.525	26.2625	13.1313	13.1313	4	2	Not Used

Table 2. Output interface divider selection. C-Rig stands for commercial rig; X-Factor is the crystal multiplication factor.

ment, like Motracs, the PTT operation is accomplished by grounding the PTT line. In the RCA 700/1000 equipment series, the PTT function is implemented by keying + 12 volts DC to the PTT line. Using a relay was one simple way to meet both requirements. I selected a Radio Shack 12 volts DC DPDT unit (RS 275-249) and used the extra set of contacts to switch the 53-MHz RF connections to the DBM. Both PTT lines are bypassed to ground with 0.05-μF disc ceramic capacitors. The diode across the relay coil suppresses the relay's generated inductive spike.

The receive side of the 53-MHz RF comes from the output of the commercial rig's RF amplifier circuit. In the RCA Model 1000 that I modified, I made a small cut in the output circuit trace of the RF amplifier and connected a small piece of coax cable from the amplifier output to a phono connector marked "receive" on the transceiver case.

Bandpass amplifier (see Figure 5). The 52 to 53-MHz transmit side of the relay goes to a bandpass amplifier consisting of Q1 and Q2. I derived the bandpass amplifier from the 6-meter dual-gate MOSFET preamplifier in *The 1987 ARRL Handbook*, substituting a parallel-tuned circuit for the source 100-ohm resistor in the handbook circuit. This stage is followed by a single-stage bipolar amplifier that raises the voltage output to a level sufficient to trigger the CMOS divider circuitry and provides bandpass filtering of the output of the DBM. The filtering requirement isn't severe because the sum of the 2-meter drive signal and the 90-MHz LO is 232 Mhz—sufficiently high that the CMOS divider circuitry won't trigger. The difference of the 2-meter signal and the second harmonic of the 90-MHz LO is typically in the 38-MHz range. If this signal level is high enough to trigger the divider, it will be divided by 6, generating output at approximately 6.3 MHz—outside the bandpass of the transmit stages of the commercial rig tuned for 6-meter operation.

Digital divider/transmitter output interface (see Figure 6). The transmitter output section of the synthesizer-simulator uses an initial divide-by-two circuit consisting of one half of a 74HC73 dual J-K flip-flop, U2a, to bring the 52 to 53-MHz output of the DBM into the 26 to 26.5-MHz range. The sections of a dual J-K flip-flop (74HC73, U3) are connected to select the correct output frequency to match the frequency/multiplier characteristics of the commercial rig transmitter (see **Table 2** for typical divider selections). The divider shown is connected to provide a divide-by-3 factor. The output of the divider is fed to paralleled buffer stages U1c and U1d (74HC00), which drive the output filter.

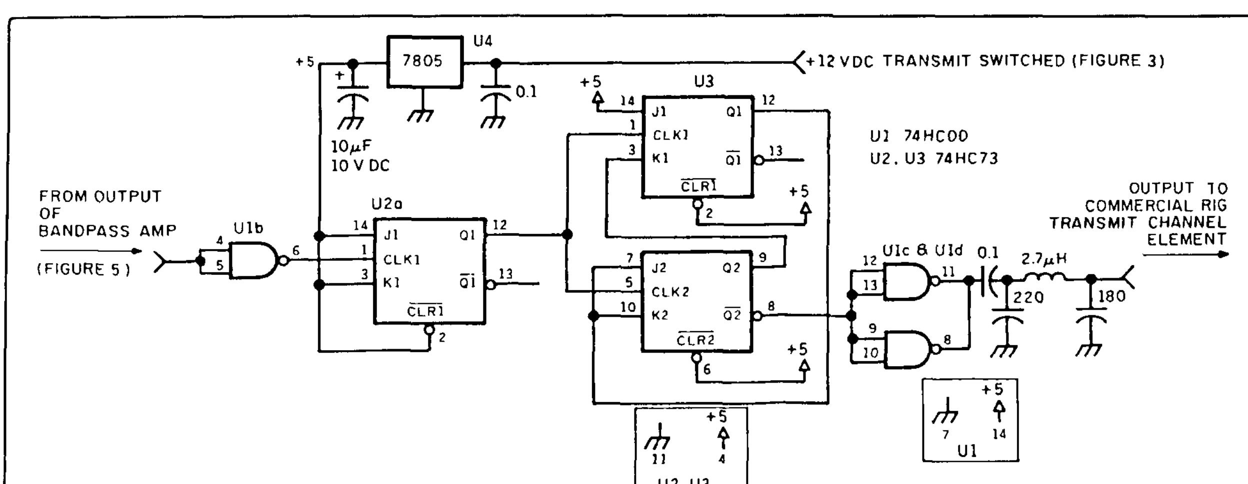

Figure 6. Output digital interface.

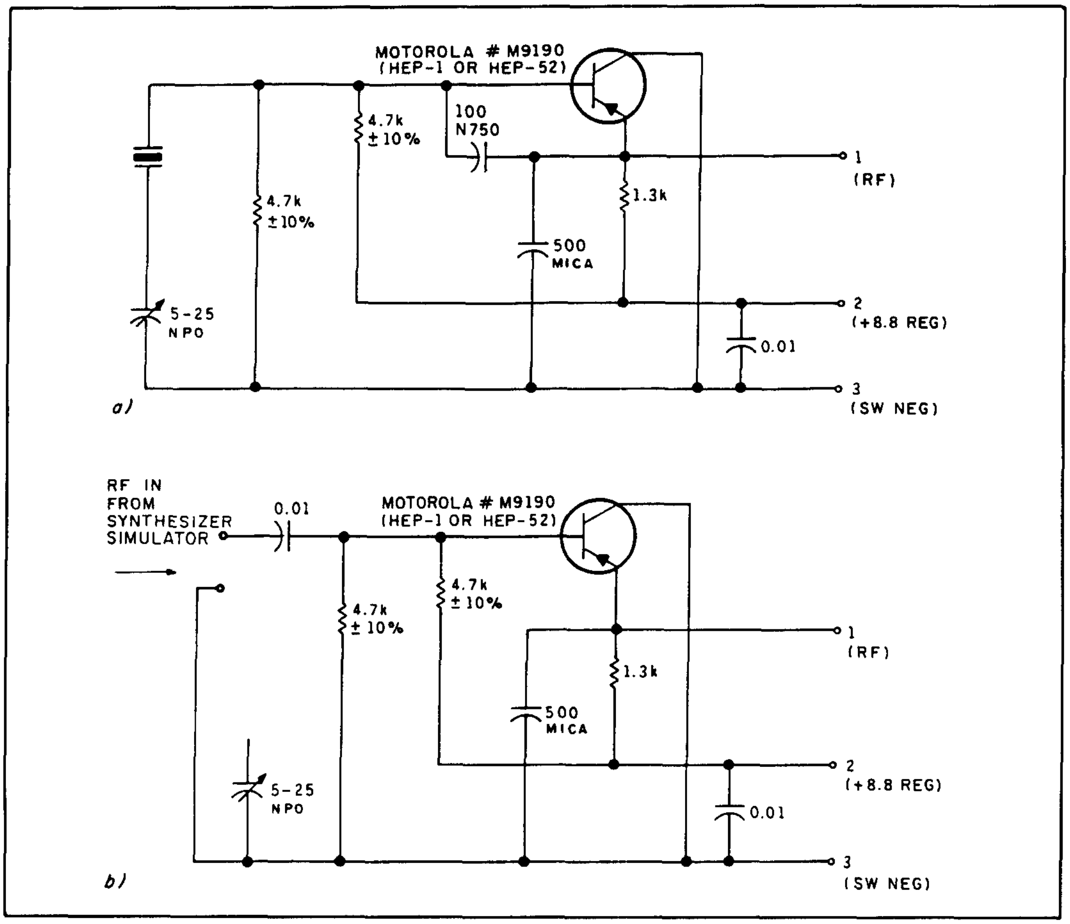

Figure 7. Channel element schematics. (A) Typical unmodified Motorola-style channel element (no. TLN 1083). (B) Modified channel element.

This output provides sufficient drive to a modified channel element in the commercial rig's transmitter. I've had good luck coupling the synthesizer-simulator output to the base of the channel-element oscillator transistor via a 0.01-μF coupling capacitor. I also modified the channel element by removing the oscillator feedback capacitor usually found connected between the base and emitter of the channel-element oscillator transistor, as in **Reference 3**. **Figure 7A** shows the schematic of a typical transmit channel element from **Reference 3**. **Figure 7B** shows how the channel element is modified to interface with the synthesizer-simulator.

Construction

The synthesizer-simulator may be constructed in sections to ease the building task. Use construction techniques appropriate for each individual section. My unit fits nicely in a 9 X 7 X 2-inch aluminum chassis. **Figure 8** shows an approximate layout of the unit in this chassis. Descriptions of the construction approach used for each section follow. Small diameter 50-ohm coax such as RG-174 (RG-188 Teflon® preferred) is used for RF interconnection of the subassemblies.

Input attenuator/RF switch. I built the input attenuator/DC switch on an old pc board that had circuit pads in most of the desired places for the RF components. I soldered terminal strips to the ground foil to support construction of the DC switch components. Mount the input attenuator resistors so you can access them easily in case they are damaged by an accidental application of high input power.

Local oscillator. In building the local oscillator, I employed a technique I've used for several years for RF circuits. With a piece of double-sided G-10 circuit board material as the base, I glued small pieces of single-sided board material cut to the size required for the particular pads. I used feedthrough bypass capacitors for bypass requirements. When using this approach, the primary DC power distribution is executed on the opposite side of the circuit board from the RF components. Grounding is accomplished by soldering directly to the ground plane, keeping the RF circuit ground leads as short as possible. If a change is required, you can pry the desired pad loose and glue it in the new location.

Bandpass amplifier. The bandpass amplifier follows the layout in *The ARRL Handbook*. I chose this layout because the preamplifier could be used with the bipolar stage added per the previously mentioned technique using scraps of pc board material for pads.

Output interface digital divider. I built the output interface digital divider using a Radio Shack number 276-891 circuit board. I used low-profile sockets and made the required interconnects with jumper wires. Then I glued quarter-inch wide strips of single sided pc board material to the long dimension, component side edges of the main board. These strips are used for RF ground connections. I built the 5-volt regulator for the digital circuitry on a 3-terminal strip mounted on the input side pc board strip. The output lowpass filter components are mounted on the output side strip using the glued pad construction technique.

Check-out tips

As mentioned in the local oscillator discussion, you can check LO operation with a broadcast FM radio. You can also use an FM broadcast receiver to monitor the output of the synthesizer-simulator in the transmit mode (tuned to the second harmonic). The synthesizer-simulator can serve as a receive converter with just the LO and DBM connected.

Two-meter equipment considerations.

Output power. The input attenuator for the synthesizer-simulator is designed to handle 2 to 3 watt power levels. This corresponds to typical HT output levels. Base/mobile rigs usually have a higher low power setting—typically 5 watts. My Kenwood 4100A originally had a 5-watt low power setting. I found from reviewing the manual that both high and low power settings of the rig were independently adjustable, so I adjusted the low power output to approximately 2.5 watts. Before you change the synthesizer-simulator input attenuator to handle 5 watts, check to see if the rig's power level is adjustable.

Frequency coverage. To take advantage of the 90-MHz frequency local oscillator approach to readout translation, your 2-meter rig needs extended coverage capability. Coverage should extend down to 142 Mhz—lower if you want to take advantage of the new lower frequency repeater subband. If your rig doesn't have this capability use a 93-MHz LO crystal for Y1 instead.

Odd-offset split capability. The synthesizer-simulator doesn't have built-in transmit offset capability. Any receive-transmit offset must come from the 2-meter rig. Because the standard repeater offset for 6 meters is 1.0 MHz, rather than the standard 2-meter 0.6-MHz offset, you'll need to operate the 2-meter rig in a nonstandard or odd offset split mode to access the typical 6-meter repeater. This shouldn't be a problem because many manufacturers now provide 2-meter rigs that can handle an odd offset on every channel. Even some of the earliest synthesized equipment could handle odd offsets.

Interfacing the synthesizer-simulator to commercial equipment

Transmitter interfacing. To interface the synthesizer-simulator to the commercial equipment transmitter, you must select the synthesizer-simulator's divide ratio and connect the divider's output to the transmitter. Depending on the type of commercial equipment you use, it may also be necessary to make adjustments in the deviation/microphone/CTCSS sections. As a final step, connect the synthesizer-simulator to the commercial equipment's PTT circuit.

Output divide ratio. Make sure the divide ratio of the synthesizer-simulator's output divide circuitry matches the frequency range of the original crystal oscillator operation. My RCA Model-1000 uses a channel-element crystal of 8.718333 MHz for 52.31-MHz transmit operation (which means the transmitter has a multiplication factor of 6). This means that my synthesizer-simulator output divide circuitry must also be connected provide a 8.718333-MHz output when the transmit input signal to the unit is 52.31 + 90 MHz (see **Table 1** for typical frequency values). In this example, the output divide ratio is 3. **Table 2** lists output interface divide ratios.

Microphone/CTCSS/modulation considerations. The transmitter acts on the synthesizer-simulator output in the same manner as it would the output from the original crystal oscillator. Consequently, the original modulation circuitry in the commercial equipment may still be functioning. This is true of equipment using phase modulators; the modulator circuitry usually follows the crystal oscillator/channel element. In equipment using direct FM modulation, the modulation is often applied to the channel element and synthesizer-simulator operation will disable the original modulation function. By not using the original microphone with a phase-modulation transceiver, you have essentially disabled the original modulation function. But the internal tone generation circuitry is still functional. You can disable this by removing the tone reed or turning down the tone modulation level adjustment. If you don't disable these functions, the modulation generated by the commercial equipment might be mixed with the modulation from the 2-meter transceiver. This could cause a problem (tone beating) if the repeater requires CTCSS access.

PTT interface. I used a spare microphone connector to connect to the PTT circuit through the now unused matching connector on the control head.

Receive interface. The RCA equipment mentioned in the preceding paragraphs uses internal phono style connectors to connect the T/R relay to the input of the receiver. This simplifies the receiver interface to the synthesizer-simulator.

Cross-band repeat operation

You can operate the FM synthesizer-simulator with a dual-band transceiver that has cross-band repeat capability, to create a "poor-man's" 6-meter remote base. In this mode, you can access 52.525 MHz or any other simplex frequency compatible with the synthesizer-simulator frequency scheme and your dual-band transceiver cross-band repeat capability. Repeater remote access may be possible depending on your receiver's cross-band repeat capability. Be sure to review the FCC requirements and regulations before initiating this kind of operation.

Options/alternatives

Two-meter rig frequency range—local oscillator crystal frequency. Many of today's 2-meter rigs will operate, or can be modified to operate, down to 142 MHz—permitting the approach described using a 90-MHz crystal LO. If your rig won't make this range, I recommend using a 93-MHz crystal. This will translate the most active 6-meter repeater output section of the band (usually the lower half of the 53.01 to 53.97 range) to the repeater input/simplex section of the 146 to 147-MHz band. My original version of this synthesizer-simulator uses a 94-MHz oscillator that puts this section of the band in the low end of the 147 to 148-MHz range—the repeater output section of the 2-meter band. Local 2-meter signals are often strong enough that you may notice some bleed-through during base operation with an outside antenna, if you use this frequency scheme.

Stand-alone operation. There's no reason why the synthesizer-simulator couldn't be used for 6-meter operation without a used commercial rig; just add dedicated receive and transmit circuitry. One approach would be to use a 6-meter preamplifier for the receiver front end and add transmitter power stages following the DBM like those in **Reference 4**.

Commercial rig considerations.

The expression "commercial equipment" in this article refers to FM radio equipment used for commercial communications service; i.e., police, fire, business, and so on. Used commercial equipment is commonly available at hamfests and varies in vintage and condition. Equipment for this service has been manufactured by a number of companies, but the best documentation and experience base exists for equipment manufactured by General Electric, Motorola, and RCA. (Though RCA is no longer in this business, used RCA equipment has been plentiful.) The following sections discuss equipment characteristics you should consider when selecting commercial rigs.

Equipment selection. I recommend that you ask around at your ham club meetings, or build the receive converter part of the FM synthesizer-simulator and listen in on local 6-meter activity, to find out what type of commercial equipment enjoys local popularity. Usually there's a source for used commercial equipment and/or local hams who are familiar with particular equipment types and sources. Because relatively little equipment is manufactured for amateur service on 6 meters, the use of commercial service equipment is still quite popular on this band.

Equipment identification. Used commercial equipment is usually available in three bands corresponding to the commercial service bands normally referred to as VHF low, VHF high, and UHF. VHF low typically covers 25 to 54 MHz, VHF high covers from 138 to 174 MHz, and UHF covers from 402 to 512 MHz. It's important to be aware of this because the equipment often looks the same externally, no matter what band it covers. The other variable associated with commercial equipment is frequency

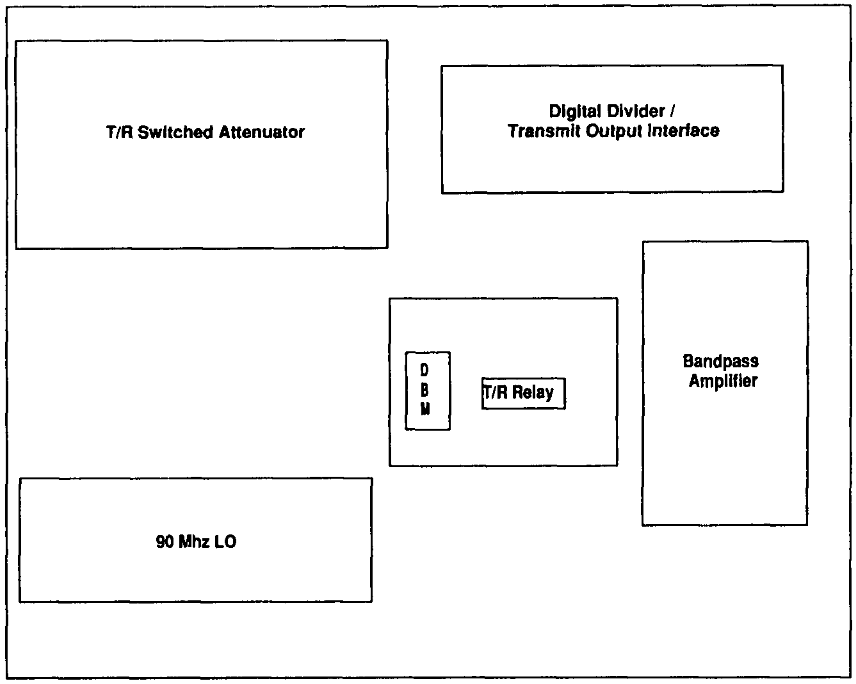

Figure 8. Approximate synthesizer-simulator layout.

channel capacity. Older equipment typically has one to two channel capacity standard with some equipment having four channel capability. Some newer equipment provides capacity for eight channels and up. You only need one channel for use with the synthesizer-simulator, so channel capacity is not an issue.

To complicate matters, the low VHF band is usually subdivided into three band splits: low, middle, and high. For conversion to 6 meters you'll want low VHF band, high-split equipment. The best way to tell what band the equipment is on is to look at the installed crystals. Usually, your best bet is to choose equipment that has just been removed from service (replaced with more modern equipment), which should still have the original crystals installed and be operational. Equipment which is operational in approximately the 43 to 50-MHz range can probably be converted by simple realignment. Some equipment requires component value changes in some circuits for 6-meter operation.

Before obtaining equipment, be sure you have a source for the tune-up information you'll need for ham-band realignment. If you can borrow a set of crystals for tuneup, the realignment will be simplified. Before beginning realignment, establish that the equipment is operating properly with the installed crystals on its original frequency.

Beware of any equipment that has visible rust or missing parts. Sometimes transceivers that were too difficult to repair became spare parts sources for the repair of other units. These "bone-pile" transceivers can find their way to hamfests, and the person selling the units may not know much about them—so buyer beware!

Equipment configurations. Commercial equipment is usually designed for two types of installations: "trunk-mount" and "dash-mount." Trunk-mount equipment designs permit the large bulky part of the equipment to be installed at a distance from the operator's location—often in the trunk. In addition to the main equipment, trunk-mount rigs come with "accessories," which consist of a "control-head" and interconnecting cable, along with a microphone and speaker. In the dash-mount configuration, the control head is integrated into the main equipment package as it is in most 2-meter equipment. (It's interesting to see the number of new multi-band FM transceivers that provide a kind of remote or "trunk-mount" installation capability.) When making an equipment deal, be sure all the components for the unit (i.e., trunk/main unit, control head, cable, microphone, and speaker) are included. These accessories are usually not interchangeable, so be sure you get the correct components.

Operating bandwidth. One disadvantage of the older commercial equipment is limited transmit operating bandwidth. This is especially true of older total-tube equipment that is typically limited to 200 to 500-kHz transmit bandwidth. This could be a problem if the repeater inputs in your area are widely separated in frequency and/or widely separated from 52.525, the national simplex frequency. Transmit stages can be stagger-tuned to obtain some wider operational capability, but each piece of equipment has its own quirks. The later model solid-state equipment provides wider operating capability. My Model-1000 RCA is all solid-state and provides acceptable operation over the entire 52 to 53-MHz transmit range when used with the synthesizer-simulator. (The synthesizer-simulator by itself has transmitter drive capability from under 51 to over 54 MHz when driven by the proper 2-meter rig frequency.) Receive bandwidth limitations aren't as much of a problem. Receiver front end bandwidth can usually be widened by increasing the value of interstage coupling capacitors, or by adding an external pre-amplifier.

Interface considerations. The synthesizer-simulator has been used successfully with RCA Model-1000 and Motorola U51LHT Motrac equipment. Interfacing shouldn't be a problem with any similar equipment, especially that which uses channel elements for frequency control. A channel element consists of circuitry dedicated to providing crystal-controlled operation on one channel. It typically has a single transistor crystal oscillator and associated circuitry for trimming the oscillator on-frequency and compensating the oscillator for temperature changes. **Figure 7** shows the schematic of a typical Motorola transmit channel element oscillator before and after modification. The 700 and 500 RCA series use the same channel elements, so interfacing should be easy. (Note that some 500 series models used "quick-heat" tubes that are very expensive to replace.)

Summary

The synthesizer-simulator provides a new approach to obtaining "synthesizer-like" operation on 6 meters when interfaced with a 2-meter rig and a used commercial rig realigned for 6-meter operation. Because of the unique transmitter interface circuitry in the synthesizer-simulator, minimal modifications to the commercial rig are required. I've been using this approach for over four years and find it's flexibility hard to beat!

REFERENCES

1. *The ARRL Handbook*, Chapter 25, Table 6, Amateur Radio Relay League, Newington, Connecticut, 1987.
2. Richard Campbell, "A Clean, Low-Cost Microwave Local Oscillator," *QST*, July 1989.
3. Thomas McLaughlin, "Building Motran and Motrac Channel Elements," *Ham Radio*, December 1972.
4. Carl Martens, "A 40W 6-Meter FM/CW Mobile Transmitter," *73*, May 1972.

PRODUCT INFORMATION

A guide to troubleshooting automotive electrical systems available

John Fluke Mfg. Co., Inc. offers "Beat the Book with Fluke Meters," a new, updated application note on automotive electrical troubleshooting. This free 16-page color booklet describes and illustrates time-saving procedures for servicing electrical systems safely and accurately using DMMs.

In addition to DMM information, "Beat the Book" also includes sections on automotive electrical diagnosis, the charging system, the starting system, the ignition system, current drains and shorts, cooling systems, and computer sensors.

This free publication is available at Fluke authorized distributor locations, or by contacting John Fluke Mfg. Co., Inc., Service Equipment Group, P.O. Box 9090, M/S 250-E, Everett, Washington, 98206, (800)87-FLUKE.

Newsletter for Spread Spectrum Enthusiasts


SPREAD SPECTRUM SCENE

EDITORIAL

FCC Grants the Buaas Spread Spectrum STA on April 17!

GOOD NEWS AND BAD NEWS

Watch for SS Legislation Soon!

Spread Spectrum Scene covers PCN/PCS, digital cellular phone, CDMA/TDMA, networking, packet, and experimental ham spread spectrum communications. The newsletter carries information on new products, how-to articles, basic technical information, and industry news. For a free sample, send S.A.S.E. to Randy Roberts, KC6YJY, P.O. Box 2199, El Granada, California 94018-2199.

Peter O. Taylor
AAVSO Solar Division
P.O. Box 5685
Athens, Georgia

THE SOLAR SPECTRUM

Gamma rays and solar flares

One of the more interesting and exciting aspects of the current astronomical scene is the ability of today's advanced space technology to provide information about some of the more exotic ramifications of solar and stellar phenomena. These special techniques have radically altered the science of astronomy, especially in the ways that the universe is viewed and research is conducted.

A graphic example of this sophisticated approach to data gathering was recently announced by NASA.[1] During April 1991, the space shuttle Atlantis deployed the Compton Gamma Ray Observatory, a project developed and managed by Goddard Space Flight Center in Greenbelt, Maryland. Since that time, radiation sensors aboard the Compton Observatory have obtained an extraordinary amount of information about the gamma ray sky, some of which is then computer processed into images that closely resemble conventional photographs.

Photo A. NOAA/USAF Sunspot Region 6659 photographed on June 10, 1991, by Dr. Jean Dragesco from the South of France.

The work is carried out by the Energetic Gamma Ray Experiment Telescope and Imaging Compton Telescope. Operation of the instruments is a cooperative effort by the Max Planck Institute for Extraterrestrial Physics in Germany, and the University of New Hampshire.

Normally, these instruments collect data from stellar and extra-galactic sources. However, when the situation calls for it —say, the eruption of an intense solar flare or the prediction of unusually high solar activity to come—the equipment is automatically signaled to direct its attention toward the Sun.[2,3]

The Compton Telescope is capable of observing flare activity in two modes: imaging (0.8 to 30 Megaelectronvolts or MeV) and burst (0.1 to 10 MeV). When the equipment is alerted to a strong flare, the telescope mode is readjusted so solar neutron events carry a high priority in the data collection process. Meanwhile, the burst mode continually integrates gamma ray spectra from two detector modules. One operates in the low 0.1 to 1.0 MeV range, and the other in the high energy, 1 to 10 MeV, arena. The system is fully capable of detecting upward and downward motion, and of separating gamma rays from neutrons through an analysis of their respective electron or proton energy loss.

Solar flare associated gamma rays have been monitored from satellites since the early 1970s, but only in the high energy range.[4] Gamma ray spectra were first detected in the great flares that occurred during early August 1972 (Chupp, 1973)[5] by an instrument designed by Professor E.L. Chupp of the University of New Hampshire, and flown on the OSO-7 spacecraft. In the period 1980-89, a number of these events were detected with the Gamma Ray Spectrometer aboard the Solar Maximum Mission satellite. However, for a variety of reasons—both technical and opportunistic—imaging gamma ray telescopes have never before been directed toward the Sun (Kambach et al., 1992).[2]

During the past year and a half, NASA's Compton Observatory has filled this gap by gathering data on many of these events. Especially intriguing are the effects that were spawned by the powerful class X flares that occurred in NOAA/USAF Sunspot Region 6659 (**Photo A**) during June 1991. During this unusual opportunity, the spacecraft itself was reoriented and its instruments configured into the solar fare mode. Thus, the equipment was not dependent upon an automated response to the dramatic surge in activity.

Three class X solar flares were observed by the Compton Observatory instruments during June.[3] These were extremely intense phenomena, ranked from X10 to X12+. (X12 is the most powerful X-ray classification for a flare event. Flares that exceed this intensity swamp the GOES satellite detectors.) The events that occurred on the 9th and 11th were observed beginning with their impulsive phases, since both erupted during orbital sunrise. Because of orbital considerations, observations of the June 15th flare began 50 minutes after the event began.

Perhaps most intriguing of all, the impulsive stages of the flares that occurred on the 11th and 15th were followed by a gamma ray "afterglow" that lasted for more than five hours after the first event, and for more than ninety minutes after the June 15th flare. **Photos B** and **C** demonstrate how the mighty flare eruption (X12+) on the 11th caused the Sun to become an extraordinarily bright object in the gamma ray sky. (See "Outlining June's Strong Flare Activity," in the Summer 1991 issue of *Communications Quarterly* for additional information about these events and their terrestrial consequences.)

According to Dr. James Ryan of the University of New Hampshire, co-principal investigator of the Compton Telescope project,[1] one explanation for this phenomenon seeks to tie the long duration afterglow to protons raised to extremely high energies by the flare explosion, and stored in a series of magnetic loops—a type of coronal arcade or "magnetic slinky"—in the solar atmos-

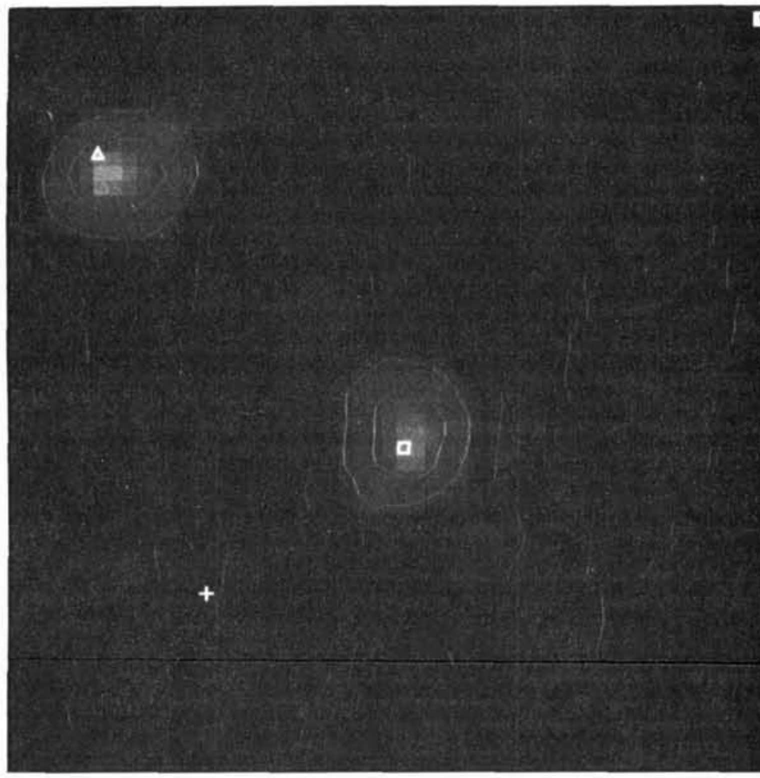

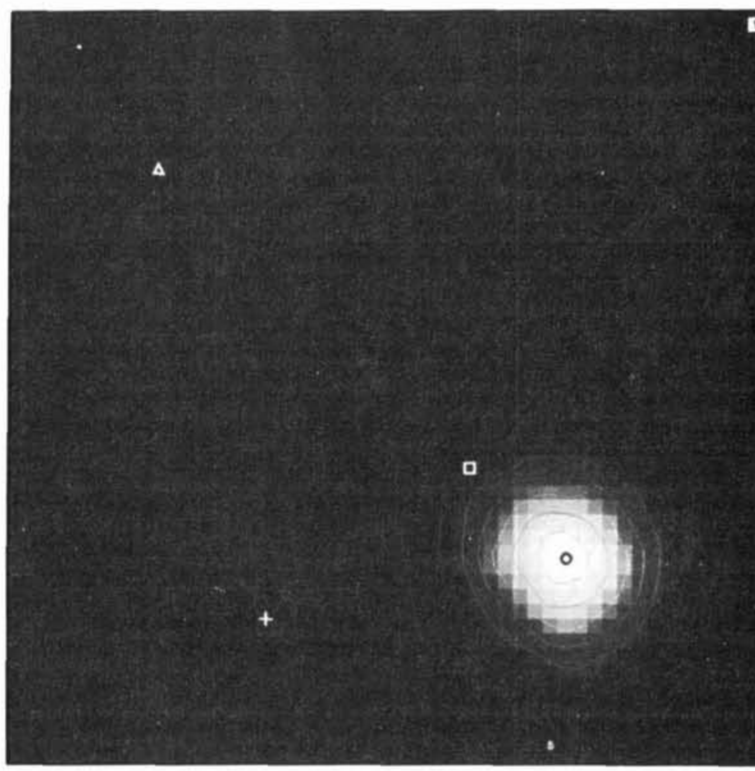

Photos B and C. Two images from the Energetic Gamma Ray Experiment Telescope onboard the Compton Gamma Ray Observatory. The top picture was taken before the powerful class X flare erupted. The symbols represent (Δ) the gamma ray pulsar Geminga, (□) the Crab Nebula—believed to be the remnants of a star that exploded in A.D. 1054, and (+) the quasar PKS0528+134. The second image is a 4-hour exposure that began over an hour after the June 11th flare. The Sun (○) shows up prominently in this picture, demonstrating the strength and persistence of gamma ray emission from the flare. Images courtesy of NASA.

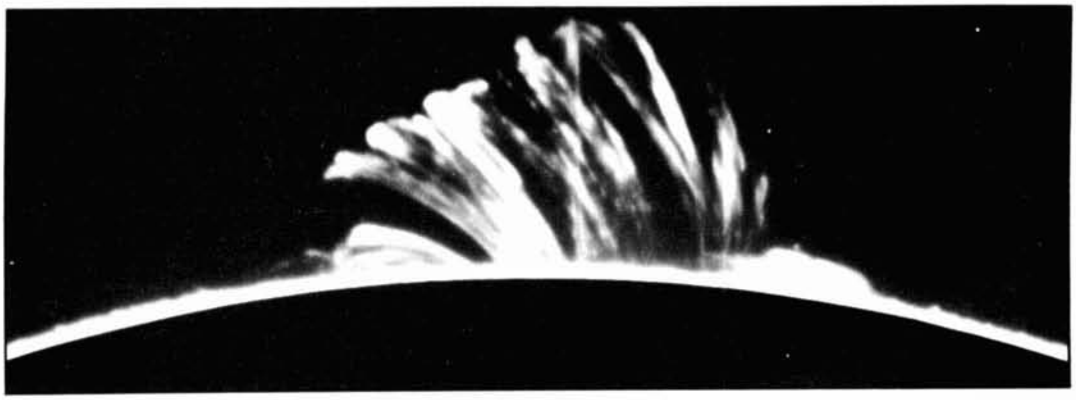

Photo D. A few hours after the June 15th flare ended, these brilliant prominences were photographed by Dr. Dragesco using a telescope equipped with a narrowband Hα filter.

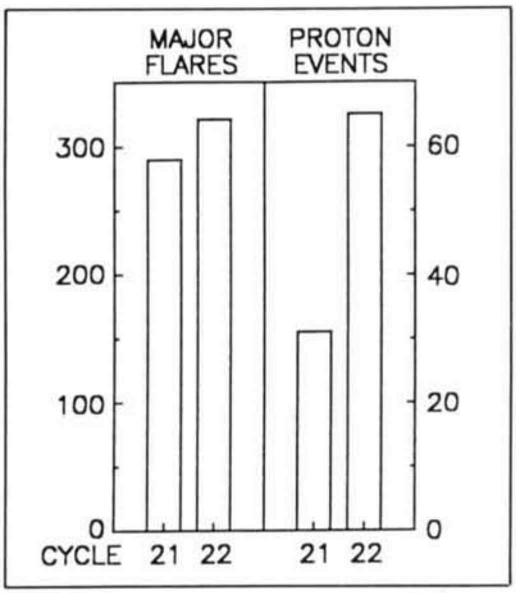

Figure 1. A comparison of major flare ($\geq$m5 X-ray intensity) and proton events through the first 69 months of solar cycles 21 and 22. Proton events are associated with the emission from large flares; they can dramatically affect the Earth's environment.

phere. The brilliant Hα loop prominence system that appeared above Region 6659 shortly after the June 15th event is shown in **Photo D**. This structure could represent a type of magnetic storage mechanism.

Dr. Ryan believes that if this theory is correct, protons are stored at the Sun in a manner similar to the way they are in the Earth's Van Allen radiation belts. On the Sun however, they slowly escape, causing the long-lasting glow observed by the Compton instruments. Such a scenario could substantially increase our knowledge of the behavior of particles at the Sun.

The Compton Observatory has also secured the first image of a celestial object (the Sun) in the "light of neutrons."[1,6] The neutrons were produced in nuclear collisions at the Sun. When they arrived at Compton, the neutrons spawned flashes of light that were first recorded by photomultipliers in the project and then computer-processed into an image. Dr. Ryan believes that such an image capture—through the transmission of matter rather than electromagnetic radiation—is a true "technological breakthrough."[1]

We wish to express our appreciation to Dr. James Ryan for providing us with detailed information concerning the Compton Observatory and observations, and to NASA for furnishing the photographs of gamma ray activity.

Recent activity and short-term outlook*

As predicted by Space Environment Services Center forecasters, the Sun became more active during the fall. However, the increased level of activity that began during September with the occurrence of thirty-three class M and two class X flares, is expected to be relatively short-lived. The production of major solar flares and number of proton events for the first 69 months of cycles 21 and 22 (through June 1992) is compared in **Figure 1**.

Hereafter, a general decline to a minimum sometime in 1996 or 1997 is expected. Some prediction models suggest an even earlier minimum—perhaps up to one year earlier. However, cycles of such short duration (nine years) are fairly rare in the historical record of the solar cycle. ■

*A portion of this information was taken from the *SELDADS* data base.

REFERENCES

1. NASA News Release 92-112 (7/15/92), Washington, D.C.
2. G. Kambach, et al., *Astronomy & Astrophysics Supplement Series 1*, 1-99 (2001), 1992.
3. M. McConnell, et al., *COSPAR Paper E.3-S.5.06*, 1992.
4. H. Zirin, *Astrophysics of the Sun*, Cambridge University Press, New York, New York, 1988.
5. E.L. Chupp, *Nature*, 241, 333, 1973.
6. J. Ryan (private communication and preprints), 1992.

L.B. Cebik, *W4RNL*
1434 High Mesa Drive
Knoxville, Tennessee 37938-4443

THE EFFECTS OF ANTENNA HEIGHT ON OTHER ANTENNA PROPERTIES

A computer study

While examing the properties of some interesting antennas based on the extended double Zepp (EDZ), I had occasion to review a 12-meter phased array consisting of two EDZ elements cut to the standard formula (0.64 wavelength each side of center feed), spaced 1/8 wavelength (4'11"), and fed 180 degrees out of phase. At 35 feet, a reference dipole using copper wire showed a calculated gain of 6.9 dBi, while a single wire EDZ showed a gain of 9.6 dBi. The phased array had a gain of 12.6 dBi, which was 3.0 dB better than the simple EDZ and 5.7 dB better than the simpler dipole. I was surprised at the relatively large gain of the array over the single wire antennas. It wasn't consistent with results I had calculated for variations on the EDZ theme. Then it hit me: 35 feet was 7/8 of a wavelength on the 12-meter band. In examining the characteristics of antennas at low heights typical of those used by amateurs with limited funds and space, I had learned that the results of calculations performed at 7/8 wavelength weren't always consistent with those achieved above and below that height.

To confirm my suspicion, I performed a series of calculations via ELNEC for a collection of 12-meter wire antennas at heights of 20 to 70 feet (in 1-foot increments) above medium ground (average earth), using copper wire losses.* My present stock of models, logged into a Quattro spreadsheet file for convenience, includes dipoles, 2 and 3-element Yagis, 2-element 180-degree phased arrays, 135-degree phase-fed beams, and delta and quad loop beams. Data gathered includes main-lobe take-off angle, gain, feedpoint impedance, and front-to-back ratio, wherever relevant. Gain figures use the lowest main lobe at its maximum. Except for the lowest heights investigated (20 to 25 feet), the differences in take-off angles varied too little to note in the body of this study, but see **Appendix 1** for a few notes on the subject. In any event, this study makes no claim as to the DX performance of any antenna. In fact, many of the models are far from optimized, having been chosen to test hypotheses related to their properties at various heights.

Taking the time to study the patterns of

*ELNEC is available from Roy Lewallen, W7EL, P.O. Box 6658, Beaverton, Oregon 97007.

ANTENNA HEIGHTS BETWEEN 1/2 AND 1 3/4 WAVELENGTH, 20 THROUGH 10 METERS

Frequency in MHz	Antenna Height in Feet per 1/8 Wavelength Increase: 1/2	5/8	3/4	7/8	1	1 1/8	1 1/4	1 3/8	1 1/2	1 5/8	1 3/4
14.2	34.63	43.29	51.95	60.61	69.27	77.92	86.58	95.24	103.90	112.56	121.21
18.11	27.16	33.94	40.73	47.52	54.31	61.10	67.89	74.68	81.47	88.26	95.04
21.2	23.20	29.00	34.80	40.60	46.39	52.19	57.99	63.79	69.59	75.39	81.19
24.95	19.71	24.64	29.57	34.50	39.42	44.35	49.28	54.20	59.13	64.06	68.96
28.5	17.26	21.57	25.88	30.20	34.51	38.83	43.14	47.45	51.77	56.08	60.39

Table 1. 1/8-wavelength increments of antenna height for a selected frequency within each ham band from 20 through 10 meters.

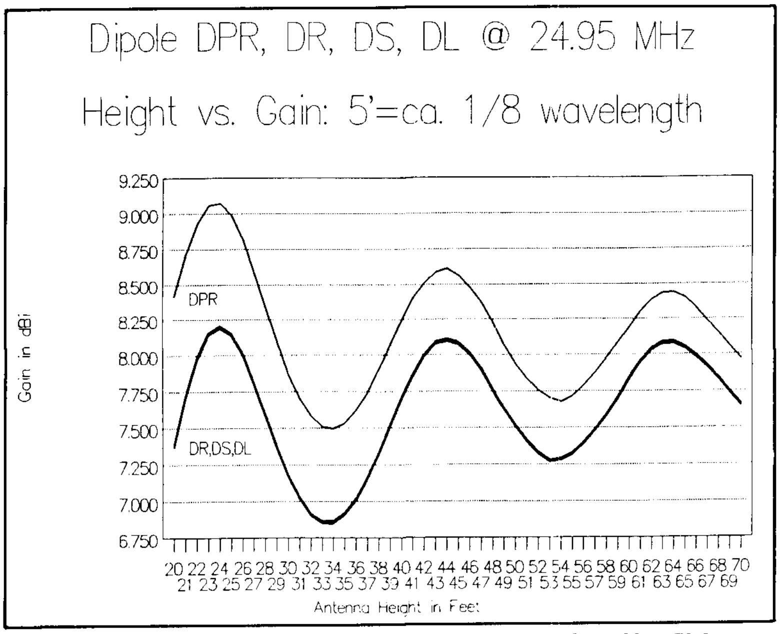

Figure 1. Gain variations in dipoles DPR, DR, DS, and DL from 20 to 70 foot heights.

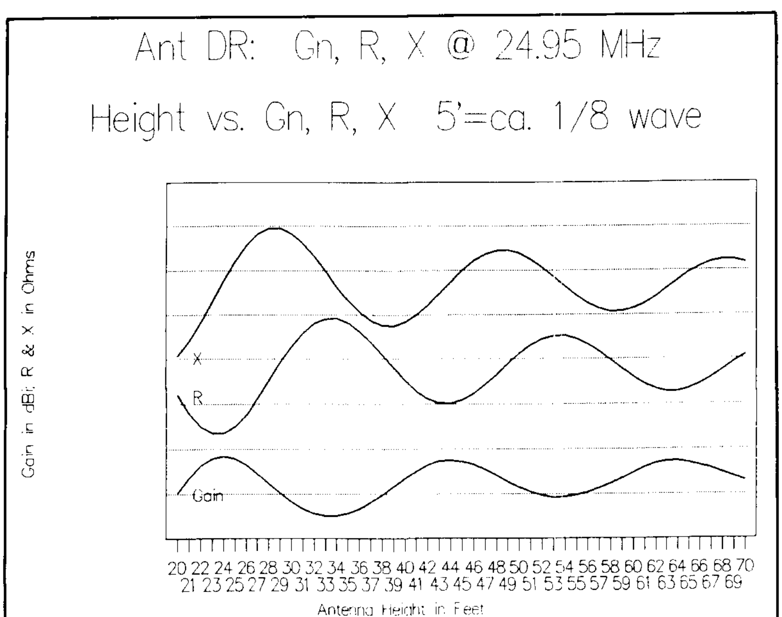

Figure 2. Gain versus resistance and reactance for a 1/2-wavelength dipole from 20 to 70 foot heights.

antenna properties as the height of the antenna is varied has proven very instructive to me. Antenna specifications, whether presented by hams or commercial manufacturers, usually appear as a single set. Sometimes writers use free space numbers, sometimes real earth numbers. Some specify gain in dBi, others use dBd, still others use a real dipole at the same height as their standard. None, however, specify antenna performance over a range of heights, but perhaps they should. In any event, if we understand how the performance of various types of antennas varies with height, we can have more realistic expectations when we build or buy an antenna and install it at home.

Twelve meters is an interesting band to use for calculating antenna performance at the heights of typical amateur installations. In the United States, we tend to work in increments of 5 feet, which is close to 1/8 wavelength at 12 meters. **Table 1** lists the heights that correspond to 1/8-wavelength increments from 1/2 to 1-3/4 wavelengths for a selected point in each of the ham bands from 20 through 10 meters. The results derived for the antenna models at 12 meters can be translated to other bands with adjustments for height. The effects of yard clutter, uneven terrain, and other variables limit the precision with which models can be realized in practice. So, too, do construction practices. Hence, gain and other figures are useful only for *generalized* comparisons. Their absolute values are relatively unimportant. Indeed, most of the information in this study appears in graphic form, as the shape of the curves may be more educational than tables of numbers from which the graphs derive. For reference, each antenna model type is accompanied by one or more free space azimuth pattern. Where relevant, some elevation patterns also appear. In the end, the line graph gives you an indication of antenna performance.

Applying the figures from this study to other bands requires conversion by reference to wavelengths and fractions of wavelengths above ground. Extrapolating the 12-meter results to other bands is necessarily limited by at least two factors. First, practical building limitations restrict extrapolations to 20 through 10 meters. On 6 and above, the lowest antennas are typically higher than 1-3/4 wavelengths up. Similarly, on 80, the highest antennas are below the half-wavelength point. Second, the average or medium soil model from which these figures result becomes nonlinear at the lower HF frequencies. To this second factor we may add the problem of changing depths to which antenna currents penetrate in the lower HF region, which troubles any assumption of coherent soils underlying an antenna system. **Appendix 2** provides some additional details on these limitations of extrapolation.

Any study like this, undertaken in spare time, is subject to specific data point errors. Modeling each antenna for between four and seven data points per step and 51 steps per model opens the door to transcription errors. Only gain numbers were allowed the three decimal places given by ELNEC in order to smooth gain curves. Other data were rounded on the fly to one decimal place—except for the takeoff angle and certain very high reactances, which were recorded as integers. A second opening for transcription error occurs in manually entering the data into a spreadsheet for analysis (a time consuming and fatiguing task).* Simple antennas, like the dipoles, took about 1 minute per step to run and record; simplified quad and delta loops took about 3.5 minutes per step. Fully tapered-element loop antennas took close to 9 minutes per step, even with a coprocessor on a 20-MHz computer; therefore, they were only spot checked for coincidence with the substitute models. Nonetheless, what I learned in the process made the fatigue worthwhile, and I apologize in advance for any data point errors.

Dipoles

As long as I can remember, amateur literature on 1/2-wavelength dipoles has recorded the fact that the feedpoint resistance and reactance change as one moves the antenna upward. Less prominent (indeed, invisible) in most literature is the fact that dipole gain, as a function of a comparison to an isotropic source, also changes with height. In fact, gain minima and maxima may be greater than 1.3 dB apart. Unlike NBS standards for length and weight, the dipole is a highly variable standard.

*For those who would like to examine the data, a copy of the spreadsheet file is available, if you can read a compressed Quattro file on your own spreadsheet. To receive the file, send a preformatted IBM disk in a self-addressed mailer with sufficient return postage. If you send a disk capable of more than 600 KB, I shall supply the uncompressed file as well, if you request it. Regrettably, I can not format the file for other spreadsheet systems or to non-IBM-compatible computers, nor can I take the responsibility for the readability of the file. I can only copy the file and hope for the best.

DIPOLES: (all antennas computed at 30 segments per wire)

Antenna Description	Designator	Material	Element	Length	Free Space Characteristics Gain dBi	R	X	Source
Dipole, resonant perfect ground	DPR	#18 Cu	Only	19.2 feet	2.066	73.5	+1.9	Formula
Dipole, resonant	DR	#18 Cu	Only	19.2 feet	2.066	73.5	+1.9	Formula
Dipole, short	DS	#18 Cu	Only	19.0 feet	2.057	71.1	−13.6	Formula
Dipole, long	DL	#18 Cu	Only	19.4 feet	2.075	75.9	+17.5	Formula
Dipole, thick	DT	¼-inch Al	Only	19.4 feet	2.116	76.3	+21.0	Formula
Dipole, very thick	DVT	1-inch Al	Only	19.4 feet	2.156	79.8	+27.5	Formula
Extended Double Zepp	EDZ	#18 Cu	Only	25.25 feet	4.905	124.9	−678	Formula

Table 2. Dipoles modeled in this study.

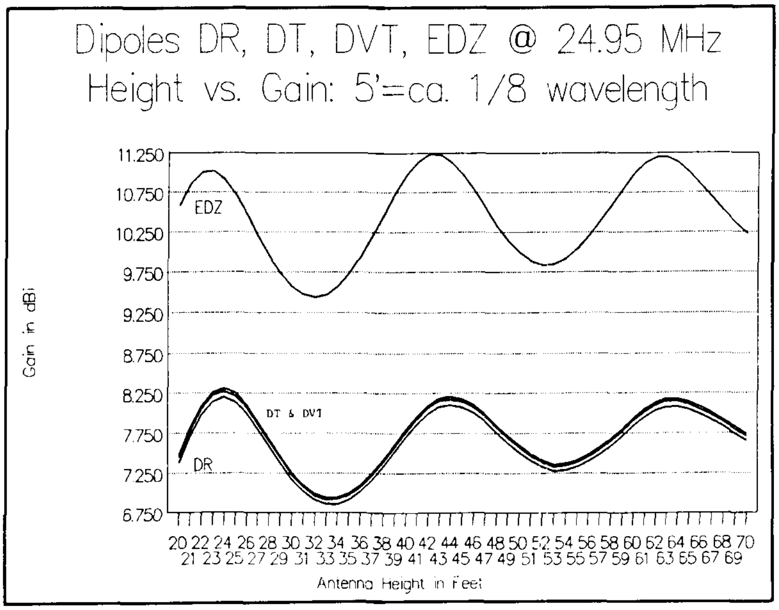

Figure 3. Gain variations in dipoles DR, DT, DVT, and EDZ from 20 to 70 foot heights.

Table 2 lists the dipole models evaluated via ELNEC. The reason for the large number of models is simple: they answer some interesting newcomer questions about variations in dipole performance. First, does the quality of ground make a difference in the position of maxima and minima? Second, does the length of a 1/2-wavelength dipole make a difference? Antenna models DPR, DR, DS, and DL answer these two questions unequivocally. No! **Figure 1** graphs the gain of four no. 18 copper dipoles at 24.95 MHz over medium ground. The upper curve traces the gain change of DPR, the dipole over perfect ground. We may note in passing that gathering data on any antenna over perfect ground is more difficult than over real ground. The reason is that higher angle lobes may show higher gain figures than the lowest lobe when above perfect ground. The current state of MININEC programs re-

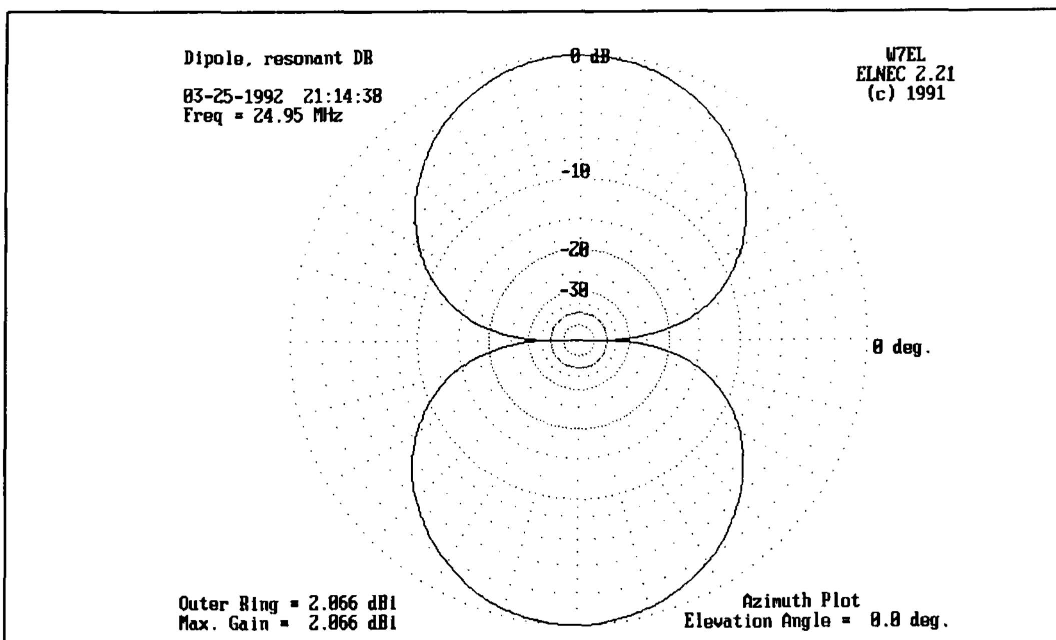

W7EL ELNEC 2.21 Dipole, resonant DR		03-25-1992 21:14:38
Azimuth plot Elev angle = 0.0 deg Outer ring = 2.066 dBi Reference = 0 dBi	Frequency = 24.95 MHz Ant Ht = 0.000 ft Wire Loss: Copper Rstvty = 1.74E-08 Rel Perm = 1	Max Gain = 2.066 dBi Source 1 impedance = 73.465 + J 1.941 SWR (50 ohm) = 1.471 (75 ohm) = 1.034
1 Wire Wire 1: 30 segments Length = 19.200 ft 1 source No loads	Free space	Gain: 2.066 dBi Angle: 90 deg F/Side: 99.990 dB Bmwidth: 78 deg -3dB: 51, 129 deg Slobe: 2.066 dBi Angle: 270 deg F/Slobe: 0.000 dB

Figure 4. Free space pattern for a 1/2-wavelength dipole.

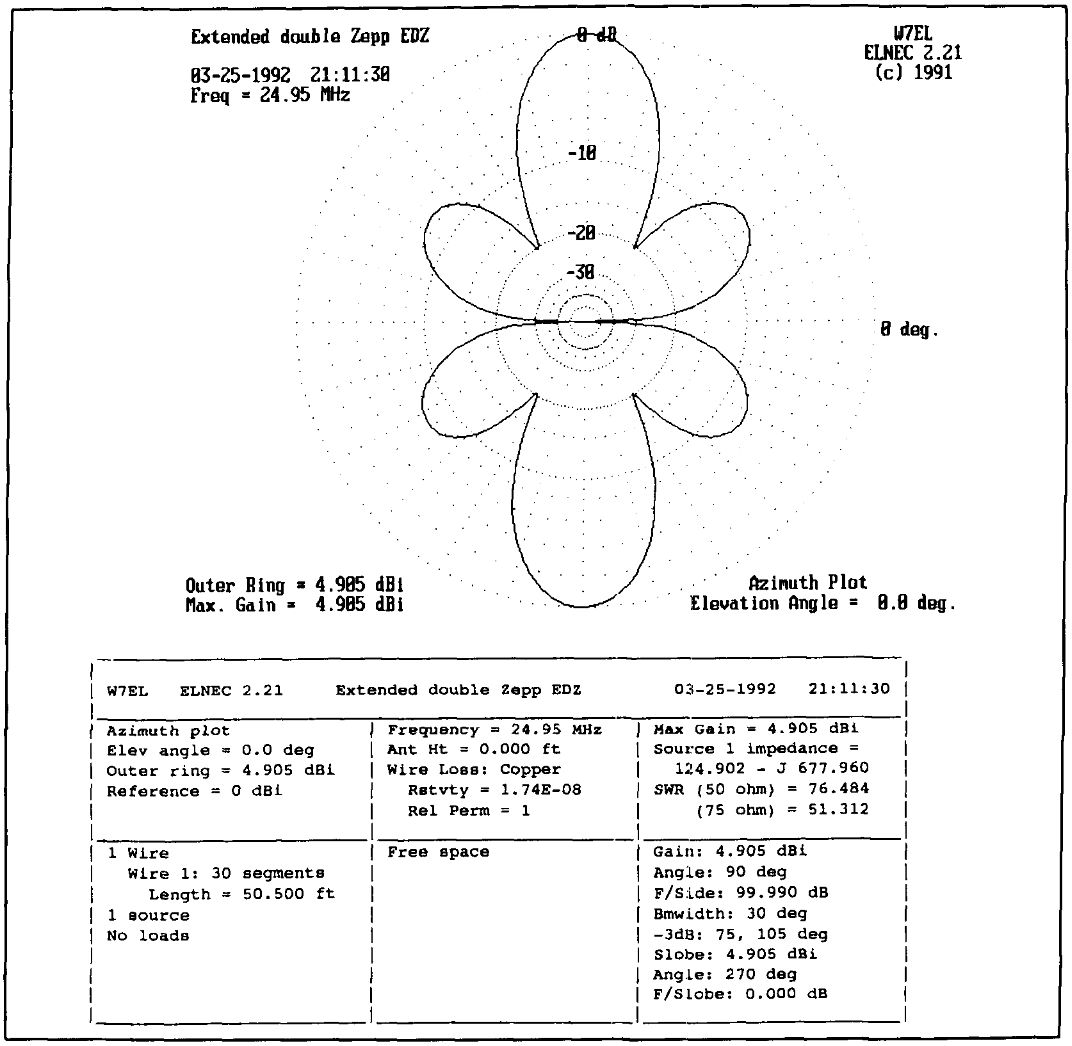

Figure 5. Free space pattern for an extended double Zepp dipole.

quires that one go hunting for the gain of the lowest lobe.

The lower curve of **Figure 1** is actually three traces so close together as to be inseparable. Antenna DR is roughly resonant in the sense of having its reactance alternate between capacitive and inductive as the antenna goes up. DS presents a varying capacitive reactance at all heights, while DL presents an inductive reactance at all heights. Regardless of whether the antenna is slightly short or slightly long, the gain maxima and minima remain in the same places. Small but significant amounts of reactance don't displace these points any more than does the nature of the ground. In general, for 1/2-wavelength dipoles, the gain maxima coincide with the minima of the resistive component of the feedpoint impedance, as shown in **Figure 2**.

A related question concerns the effect of element thickness upon maxima and minima. Antennas DT and DVT used 1/8-inch

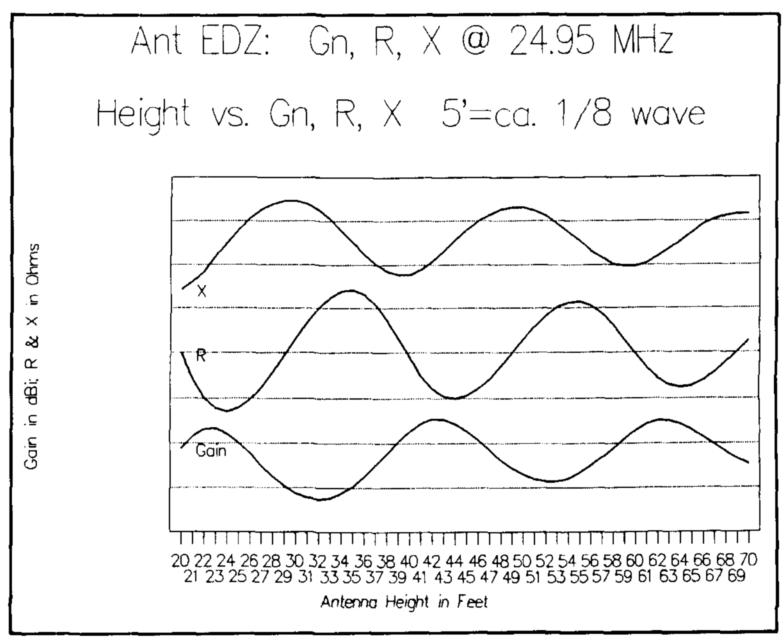

Figure 6. Gain versus resistance and reactance for an extended double Zepp dipole from 20 to 70 foot heights.

180-DEGREE PHASE-FED ARRAYS: (all antennas computed at 10 segements per half wavelength)

Antenna Description	Designator	Material	Element	Length	Space to Previous Element	Free Space Characteristics Gain dBi	R	X	Source
Double W8JK 180 degree phase fed	D8JKP	#18 Cu	DE	19.7 feet		6.847	1455	−6786	Formula
			Refl.	19.7 feet	4.9 feet				
Double EDZ 180 degree phase fed	DEDZP	#18 Cu	DE	25.25 feet		7.695	19.3	−654	HB, 92, p 33-11
			Refl.	25.25 feet	4.9 feet				
Double Quad Loop 180 degrees phase fed	DQLp	#18 Cu	DE	40.32 feet		5.830	19.7	+8.5	Formula 1005/f
			Refl.	40.32 feet	5.0 feet				
Double Quad Loop 180 degrees phase fed	DQLp-A	#18 Cu	DE	(41.60 feet)		5.880	20.2	+6.5	Sub. model for DQLP 1038/f
			Refl.	(41.60 feet)	5.0 feet				

Notes: HB = 1992 ARRL Handbook.

Table 3. 180-degree phase-fed arrays modeled in this study.

and 1-inch diameter aluminum elements, respectively. **Figure 3** shows the results of modeling these thick and very thick dipoles. Although gain increases enough to be barely visible, nothing else changes in the variation of gain as a function of antenna height.

For resonant or near-resonant 1/2-wavelength dipoles, the actual positions of the gain maxima and minima are slightly short of true 1/8-wavelength points. Maxima occur near, but before the 5/8, 1-1/8, and 1-5/8 wavelength points, while minima occur just before the 7/8 and 1-3/8 wavelength points. The difference is roughly 1 foot at 12 meters, or about 0.025 wavelength. The next question is whether this holds true for all dipole antennas.

Figure 4 shows the free space pattern of a 1/2-wavelength dipole, with its well-known pinch-waisted pattern. **Figure 5** shows a much longer dipole, the extended double Zepp (EDZ), also modeled on no. 18 copper wire. Each leg of this dipole is about 0.64 wavelength long. Because the antenna is nonresonant, it exhibits a large reactance at the feedpoint. At a total length of 5/4 wavelengths, the reactance is capacitive. This effective antenna shows a displacement of maxima and minima between 2 to 3 feet lower—more than 0.06 wavelength lower—than the 1/2-wavelength antenna, as seen in **Figure 3**. As **Figure 6** shows, the maxima and minima are not directly related to either the resistance or reactance at the feedpoint, but to intermediate points.

Another more subtle difference between the 1/2-wavelength dipole and EDZ appears in **Figure 3**. All 1/2-wavelength dipoles display their highest gain at about 5/8 wavelength and their lowest gains at 7/8 wavelength. The graph approximates the voltage curve for a dampened oscillator. Above 3 wavelengths of antenna height, the difference between maxima and minima drops to about 0.2 dB or less. The EDZ follows a slightly different gain pattern, reaching its maximum level at 1-1/8 wavelength. The increase of gain with height between the 5/8 and 1-1/8 wavelength points is common for many other antennas that lack the oscillation of values shown by the dipoles. The EDZ shows characteristics of being a mixed-breed antenna.

There are some lessons to be learned from even the limited analysis performed here. The lessons apply to almost any antenna design one might disseminate to others. In the real world of antennas, there are perhaps no standard antennas, not even the 1/2-wavelength wire dipole. There are only *ceteris paribus* references; that is, references if all other things are equal. Hence, even the wire dipole is not a blank standard for horizontal antennas. Rather, the dipole serves as a reference at the same frequency, at the same height, over the same type of earth, in the same orientation, and made of the same material. As a baseline for comparisons, it is not a number, but a graph against which other antennas can be plotted.

180-degree phase-fed arrays

If dipole antenna configuration has little or no effect upon the variations in main lobe gain until we reach the very high reactance of the EDZ, even though feedpoint resistance and reactance display similar but displaced variations, then another question arises. What creates the variations in gain? The question receives a partial answer from the group of antennas listed in **Table 3**. All the antennas have two elements, fed 180 degrees out of phase with each other. The double W8JK is a classic and has been built with spacing from 1/8 to 1/4 wavelength. The double EDZ is of more recent vintage and appears in *The ARRL Handbook*. The double quad loop is a conceptual invention designed to add one more antenna to the lot; its performance doesn't justify construction by anyone. In fact, because loops require so much computer time to run when accurately modeled (using the element tapering feature of ELNEC), I ran a substitute. Its parenthetical model-only dimensions allowed me to track the same performance within reasonable limits while using only six segments per wire.

Figures 7 and **8** show the free space azimuth patterns for the D8JKp and DEDZp antennas, respectively. Analysis of the dimensions of the double W8JK would show its elements to be slightly long under any conditions, even though they are traditionally considered to be 1 wavelength long. A precise 1-wavelength dimension for any given amateur frequency would yield an antenna without reactance at that frequency. However, even a small frequency excursion would cause a reactance jump. Similarly, small changes of length, such as those

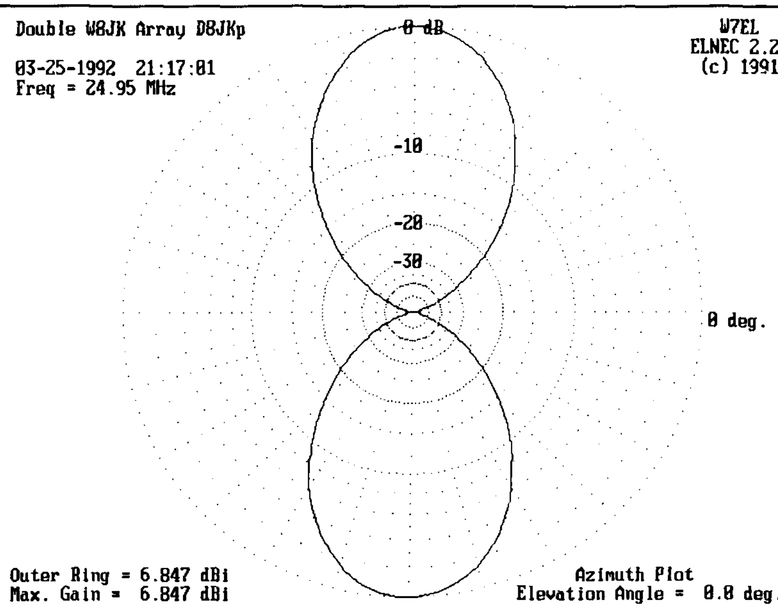

W7EL ELNEC 2.21 Double W8JK Array D8JKp 03-25-1992 21:17:01		
Azimuth plot Elev angle = 0.0 deg Outer ring = 6.847 dBi Reference = 0 dBi	Frequency = 24.95 MHz Ant Ht = 0.000 ft Wire Loss: Copper Rstvty = 1.74E-08 Rel Perm = 1	Max Gain = 6.847 dBi Source 1 impedance = 1455.37 - J 6786.10 SWR (50 ohm) > 100 (75 ohm) > 100
2 Wires Wire 1: 20 segments Length = 39.400 ft 2 sources No loads	Free space	Gain: 6.847 dBi Angle: 90 deg F/Side: 99.990 dB Bmwidth: 42 deg -3dB: 69, 111 deg Slobe: 6.847 dBi Angle: 270 deg F/Slobe: 0.000 dB

Figure 7. Free space pattern for a double W8JK array.

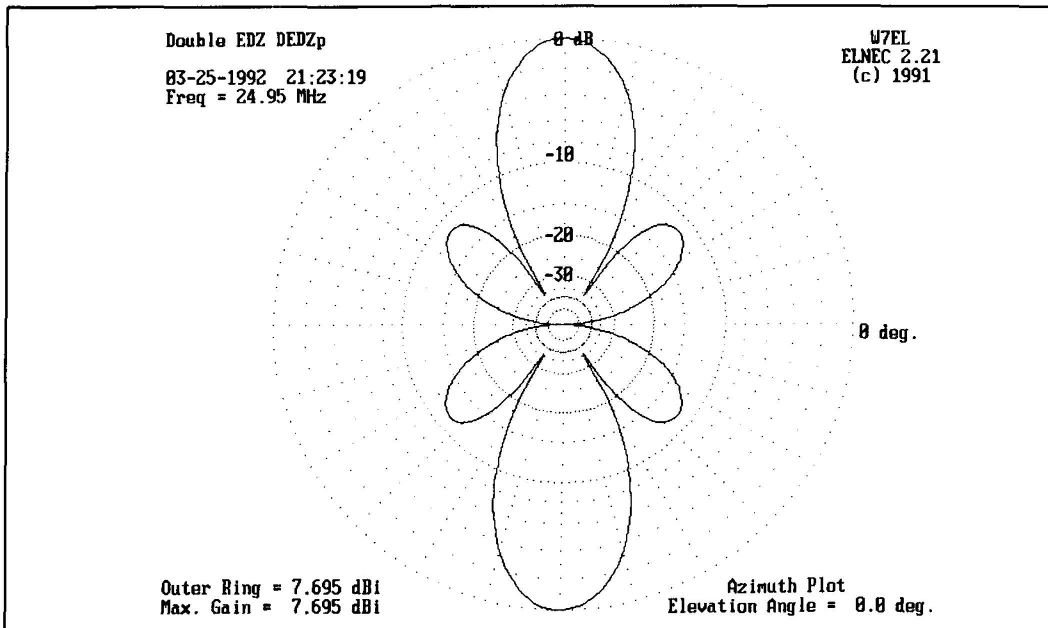

W7EL ELNEC 2.21 Double EDZ DEDZp		03-25-1992 21:23:19
Azimuth plot Elev angle = 0.0 deg Outer ring = 7.695 dBi Reference = 0 dBi	Frequency = 24.95 MHz Ant Ht = 0.000 ft Wire Loss: Copper Rstvty = 1.74E-08 Rel Perm = 1	Max Gain = 7.695 dBi Source 1 impedance = 19.308 - J 654.268 SWR (50 ohm) > 100 (75 ohm) > 100
2 Wires Wire 1: 30 segments Length = 50.500 ft 2 sources No loads	Free space	Gain: 7.695 dBi Angle: 90 deg F/Side: 99.990 dB Bmwidth: 28 deg -3dB: 76, 104 deg Slobe: 7.695 dBi Angle: 270 deg F/Slobe: 0.000 dB

Figure 8. Free space pattern for a double extended Zepp array.

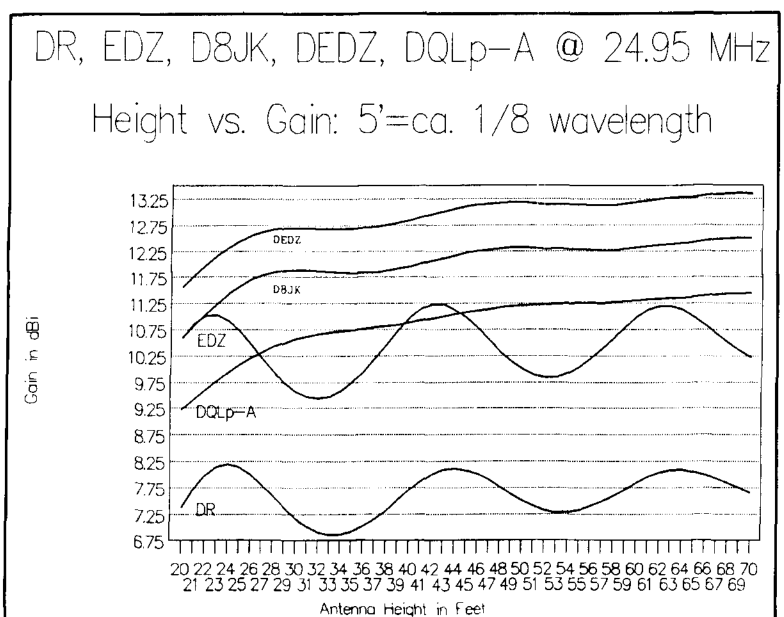

Figure 9. Gain variations in antennas DR, EDZ, D8JKp, DEDZp, and DQLp-A from 20 to 70 foot heights.

created by element sag due to gravity, create the same effect. Varying the model element length between 37.6 and 37.8 feet produced a resistive feedpoint impedance component around 30,000 ohms, while the reactive component went from 10,700 ohms inductive to 4,400 ohms capacitive—a change of more than 15,000 ohms in about 2-1/2 inches. The longer 39.4-foot elements produce a large, but stable, capacitive reactance without pattern distortion. In contrast, the double EDZ array has more gain, but a more complicated pattern of radiation.

Figure 9 shows the results of modeling these arrays with their 180-degree feed systems. Resonant 1/2-wavelength dipole and EDZ patterns are shown for the contrast. With all three phase-fed arrays, the gain patterns show little peaking and may be considered "well-behaved." These same patterns also show up in the impedance figures. Above three quarters of a wavelength (30 feet at 12 meters), both the resistive and reactive components of the double quad loop vary less than 1 ohm each. The peaks and valleys in the patterns of the other two arrays vary only slightly, but do show an inverted co-variance with the resistive component. That is, feedpoint resistance peaks as gain dips. **Figure 10** shows the phenomenon for the double W8JK. The double EDZ isn't worth graphing in this regard, since its reactance varies back and forth by 1 ohm throughout the height range investigated.

There seems to be a pretty good reason for the lack of gain and impedance variation among the antennas of this group. **Figure 11** shows the elevation pattern of the double EDZ antenna at the 40-foot level. Compare the high angle radiation immediately above the antenna to **Figure 12**, the elevation pattern of the resonant dipole at the same height. Without high angle radiation to reflect off the ground and back to the antenna, variations in antenna currents and phase angles, with consequential altera-

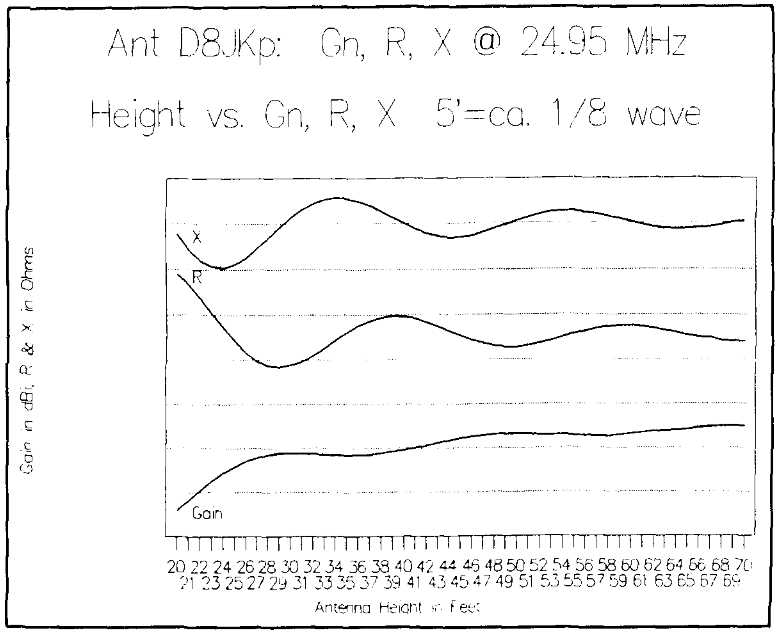

Figure 10. Gain versus resistance and reactance for a double W8JK array from 20 to 70 foot heights.

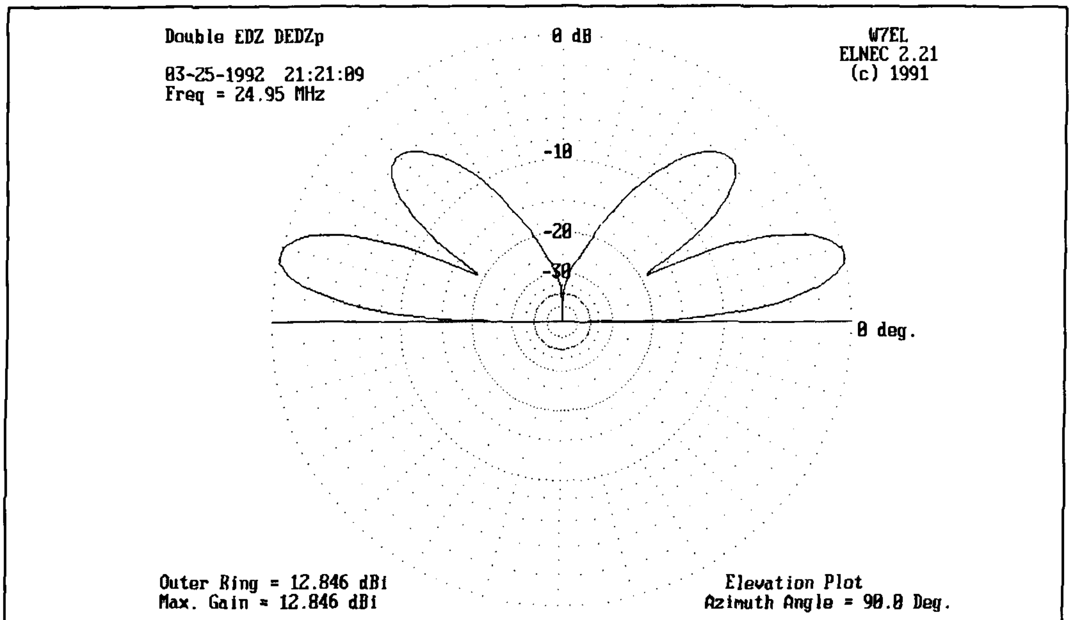

W7EL ELNEC 2.21 Double EDZ DEDZp 03-25-1992 21:21:09

Elevation plot Azimuth angle = 90.0 deg Outer ring = 12.846 dBi Reference = 0 dBi	Frequency = 24.95 MHz Ant Ht = 40.000 ft Wire Loss: Copper Rstvty = 1.74E-08 Rel Perm = 1	Max Gain = 12.846 dBi Source 1 impedance = 19.691 - J 654.611 SWR (50 ohm) > 100 (75 ohm) > 100
2 Wires Wire 1: 30 segments Length = 50.500 ft 2 sources No loads	Real ground 1 medium, 0 radials Medium 1: Cond = 2.000E-03 Di Const = 1.500E+01	Gain: 12.846 dBi Takeoff: 14 deg Bmwidth: 13 deg -3dB: 7, 20 deg Slobe: 12.846 dBi Angle: 166 deg F/Slobe: 0.000 dB

Figure 11. Elevations pattern of the double EDZ array at a height of 40 feet.

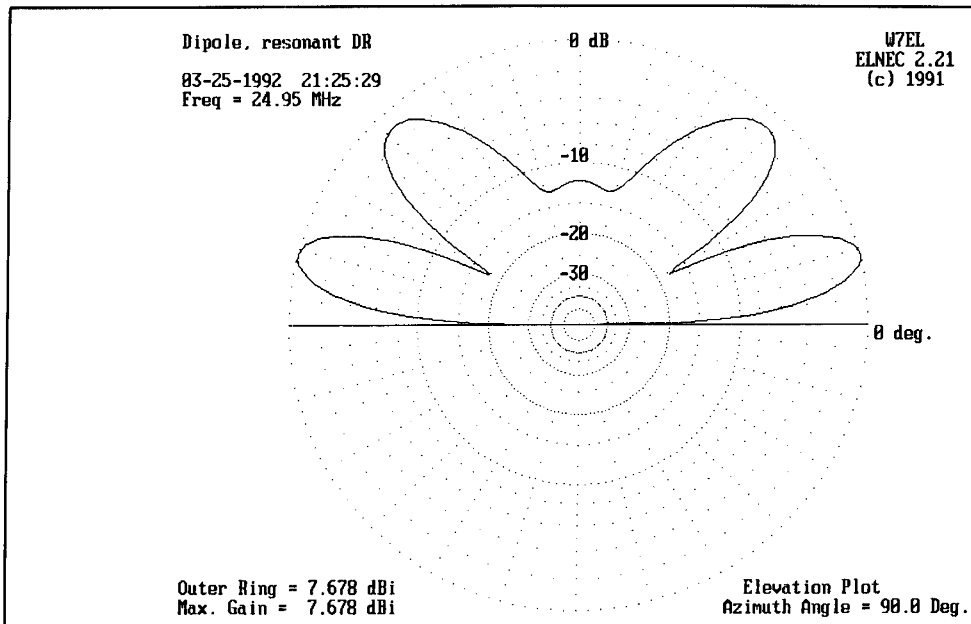

W7EL ELNEC 2.21 Dipole, resonant DR		03-25-1992 21:25:29
Elevation plot Azimuth angle = 90.0 deg Outer ring = 7.678 dBi Reference = 0 dBi	Frequency = 24.95 MHz Ant Ht = 40.000 ft Wire Loss: Copper Rstvty = 1.74E-08 Rel Perm = 1	Max Gain = 7.678 dBi Source 1 impedance = 70.180 - J 6.553 SWR (50 ohm) = 1.428 (75 ohm) = 1.119
1 Wire Wire 1: 30 segments Length = 19.200 ft 1 source No loads	Real ground 1 medium, 0 radials Medium 1: Cond = 5.000E-03 Di Const = 1.300E+01	Gain: 7.678 dBi Takeoff: 14 deg Bmwidth: 14 deg -3dB: 7, 21 deg Slobe: 7.678 dBi Angle: 166 deg F/Slobe: 0.000 dB

Figure 12. Elevation pattern of the resonant dipole (DR) at a height of 40 feet.

tions of antenna feedpoint impedance and gain, aren't possible. The 180-degree feed system cancels high angle radiation (both up and down). The dipole near the (real) ground treats the ground as a lossy "image" element (that is, a driven element with the horizontal component of the current 180 degrees out of phase with that in the real antenna element). As we shall see, the addition of parasitic elements to the antenna can add further complexities to the variations in antenna performance with height.

Comparing the performance of a dipole or EDZ with either the W8JK or the double EDZ array can be misleading unless one is clear about the gain variables involved. **Table 4** illustrates the point by showing gain comparisons at the 7/8-wavelength point and the 1-1/8 wavelength point. The arrays show about 3/4 dB better comparative performance at the lower height than at the upper. Of course, both numbers are equally wrong as single value comparisons. The comparisons simply are not transferrable from one height to another. Only comparative graphing reveals the true picture of one antenna over another. Even if we add the qualification that the exact figures cannot usually be obtained in practice, numbers lead to expectations, and rational expectations require full explanations.

2-element Yagi beams

As **Table 5** shows, this study modeled four 2-element Yagis to get a sense of their gain patterns with changing height. All the Yagis in this study used 1-inch diameter aluminum elements to simplify modeling. The Yagis added a new specification to check: front-to-back ratio. Some may find results of the modeling surprising; others may not.

Of the four models, two used reflectors and two used directors. The reflector Yagis included a close-spaced model (about 1/8

COMPARISON OF ANTENNA GAIN EXTREMES AT 2 SELECTED HEIGHTS

Height Feet	Wavelength	Gain Dipole	Gain EDZ	Gain Double W8JK	Gain Double EDZ	W8JK Over Dipole	DEDZ Over Dipole	W8JK Over EDZ	DEDZ Over EDZ
35	7/8	6.91	9.73	11.83	12.68	4.92	5.77	2.10	2.95
45	1 1/8	8.08	10.97	12.22	13.11	4.14	5.03	1.25	2.14
Difference in Gain Advantage Due to Height Change from 35 to 45 feet:						**0.78 dB**	**0.74 dB**	**0.85 dB**	**0.81 dB**

Table 4. Comparison of antenna gain extremes at 2 selected heights.

wavelength) and a wide-spaced model (a bit under 1/4 wavelength). The close-spaced model had been designed for a gamma match by Bill Orr, W6SAI, and showed considerable capacitive reactance. The wide-spaced model proved to be a close match for 50-ohm coax, with a consequent reduction in both gain and front-to-back ratio.

The results of setting the beams through 1-foot steps appear in **Figure 13**. The gain curves for both Yagis are "well-behaved," with only small ups and downs. Like the phased arrays, the curves show a relatively steady increase in gain with height (contrary to the collection of dipoles). It's interesting to note that the small peaks for both antennas occur in the same place as those for dipoles: about 0.025 wavelength prior to the 5/8, 1-1/8, and 1-5/8 wavelength points (25, 45, and 65 feet at 12 meters). Gain maxima coincide closely with the lowest values for the resistive component of the feedpoint impedance. However, the minima occur up to 3 feet earlier. Nonetheless, the presence of a parasitic element appears to protect the gain from much of the variation induced in dipoles.

Front-to-back ratio, however, is another matter. As **Figure 13** demonstrates, both Yagis show great fluctuations in front-to-back ratios as height increases, although the maxima and minima decrease with height. Roughly, the peaks and valleys occur at the 1/4-wavelength marks. Y2R-2, the 50-ohm model with near resonance, more closely hits those marks, while the heavily reactive model, Y2R-1, leads by a consistent foot (0.025 wavelength).

The director models of the 2-element Yagi were designed by reference to formulas taken from two different handbooks without regard to whether they were good antennas to build. Their overall gain and front-to-back ratio figures compare favorably with the reflector models, but matters such as bandwidth were not checked. Both models are fairly close-spaced, with one excelling in gain, the other in front-to-back ratio. More importantly, one was significantly capacitively reactive, the other in-

2-ELEMENT YAGI BEAMS

Antenna Description	Designator	Material	Element	Length	Space to Previous Element	Free Space Characteristics Gain dBi	F-B dB	R	X	Source
2-element Yagi DE + Refl.	Y2R-1	1-inch Al	DE	17.8 feet		6.716	10.1	23.0	−27.7	CQ, 12-90,
			Refl.	19.6 feet	4.8 feet					p. 83, scaled
2-element Yagi DE + Refl.	Y2R-2	1-inch Al	DE	18.2 feet		6.442	8.7	50.2	+0.3	AB, 16 Ed,
			Refl.	19.4 feet	8.7 feet					p. 11-2 ff
2-element Yagi DE + Dir.	Y2D-1	1-inch Al	Dir.	18.04 feet		6.640	10.2	27.7	−9.7	RHb, 21 Ed,
			DE	19.08 feet	4.81 feet					p. 29.4
2-element Yagi DE + Dir.	Y2D-2	1-inch Al	Dir.	18.50 feet		7.208	8.8	18.4	+24.0	AB, 16 Ed,
			DE	19.88 feet	3.94 feet					p. 11-7

Notes: CQ = CQ Magazine, December, 1990, p. 83; AB = ARRL Antenna Book, 16th Ed.; Rhb = Radio Handbook, 21st Ed.

Table 5. 2-element Yagi beams modeled in this study.

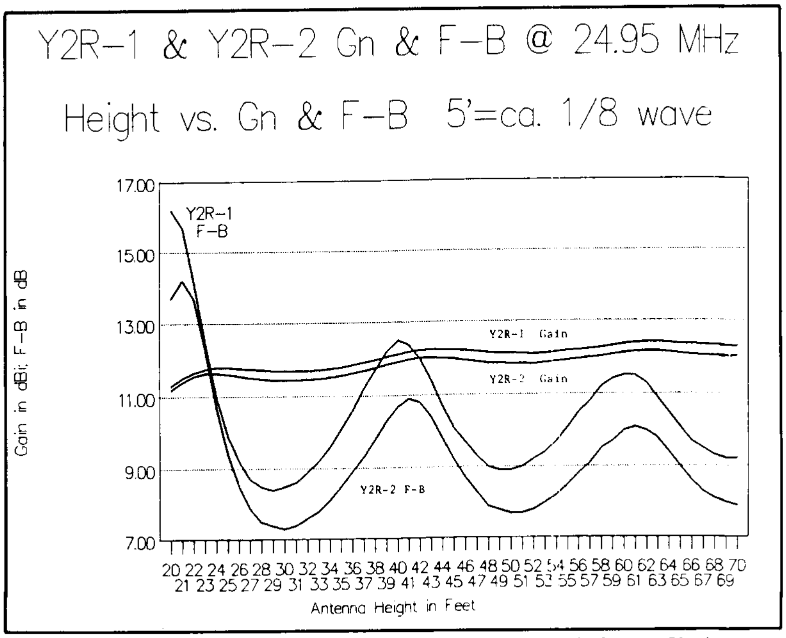

Figure 13. Gain and front-to-back ratio versus height for two 2-element Yagis with reflectors.

ductively reactive. For reference and comparison, **Figures 14** and **15** show free space patterns of Y2R-1 and Y2D-1.

Figure 16 displays the results of modeling the director Yagis. Like their reflective cousins, these antennas display well-behaved gain curves, with maxima and minima closely placed at the 1/8-wavelength positions. However, the gain maxima and minima of these directive Yagis coincide directly with the peaks and valleys of the resistive component of the feedpoint impedance, in direct opposition to both dipoles and 2-element Yagis with reflectors. The higher the antenna, the more closely feedpoint resistance coincides with gain peaks.

Again, like their reflective cousins, the directive Yagis show front-to-back ratios that vary widely over the range of antenna height. Y2D-2, the significantly inductive model, reaches its peaks 1 to 2 feet ahead of the gain peak. The capacitively reactive model tends to be late, reaching its front-to-

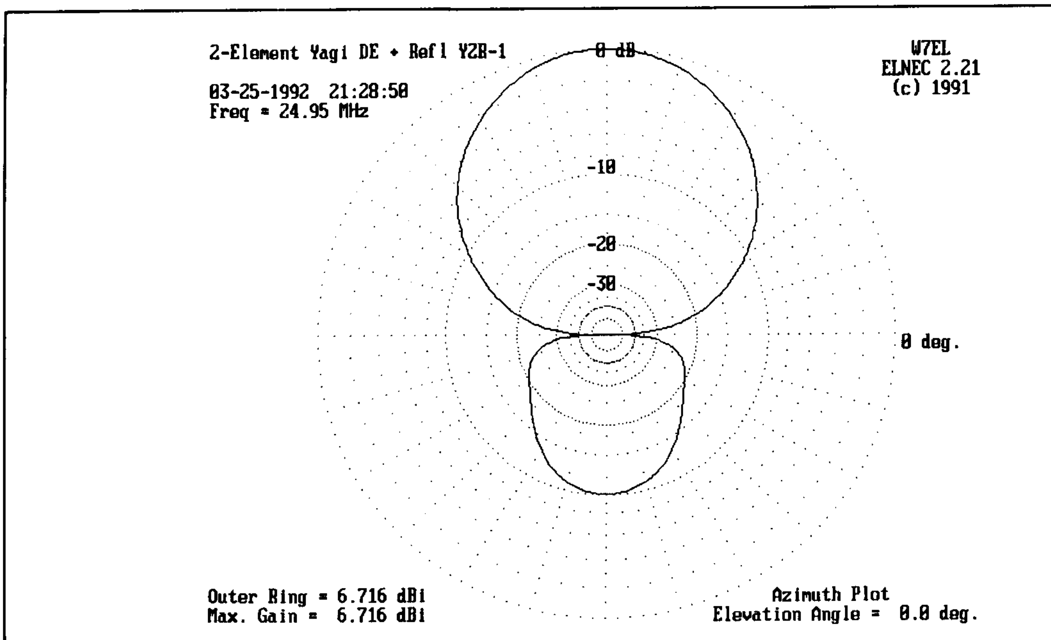

W7EL ELNEC 2.21	2-Element Yagi DE + Refl Y2R-1	03-25-1992 21:28:50
Azimuth plot Elev angle = 0.0 deg Outer ring = 6.716 dBi Reference = 0 dBi	Frequency = 24.95 MHz Ant Ht = 0.000 ft Wire Loss: Aluminum Rstvty = 4E-08 Rel Perm = 1	Max Gain = 6.716 dBi Source 1 impedance = 23.069 - J 27.673 SWR (50 ohm) = 2.954 (75 ohm) = 3.733
2 Wires Wire 1: 10 segments Length = 17.800 ft 1 source No loads	Free space	Gain: 6.716 dBi Angle: 90 deg F/B: 10.082 dB Bmwidth: 68 deg -3dB: 56, 124 deg Slobe: -3.367 dBi Angle: 270 deg F/Slobe: 10.082 dB

Figure 14. Free space pattern for YR2-1, a 2-element Yagi with reflector.

back ratio peaks after the gain peak. In this model, where the reactive component is approximately equal to the resistive component, the front-to-back ratio peaks coincide even more closely with the resistive peaks than the gain peaks do. In the case of Y2D-1, where the feedpoint resistance is about 3 times the reactance, the gain, front-to-back ratio, and resistance peaks tend to cluster together.

The most significant difference between the reflective and the directive Yagis is the position of the front-to-back ratio peaks. Roughly speaking, they are out of phase with each other. Where the directive Yagi peaks its front-to-back ratio, the reflective Yagi hits a valley. We may ignore gain, which changes little with height, but like the arrays, climbs slowly. A directive 2-element Yagi will tend to show a better front-to-back ratio than its reflective cousin in the following ranges: 25 to 30 feet, 45 to 50 feet, and 65 to 70 feet (5/8 to 3/4, 1-1/8 to 1-1/4, and 1-5/8 to 1-3/4 wavelength high). The reflective 2-element Yagi shines at under 25 feet, 35 to 42 feet, and 55 to 62 feet (1/2 to 5/8, 7/8 to 1, and 1-3/8 to 1-1/2 wavelengths high). These performance notes, of course, are relative to the general performance capabilities of 2-element Yagis.

3-element Yagis

The 3-element Yagi holds the potential for much superior performance with respect to both gain and front-to-back ratio. In this day of computer-optimized Yagis, I had some difficulty coming up with a variety of designs to test. **Table 6** shows the three models used. The first, Y3-1, is scaled from an *ARRL Antenna Book* design. The second, Y3-2, uses formulas from an older handbook and represents a wide-spaced model. The third, Y3-3, derives from formulas in the ARRL book, but strives for equal close-spaced elements. **Figure 17** pre-

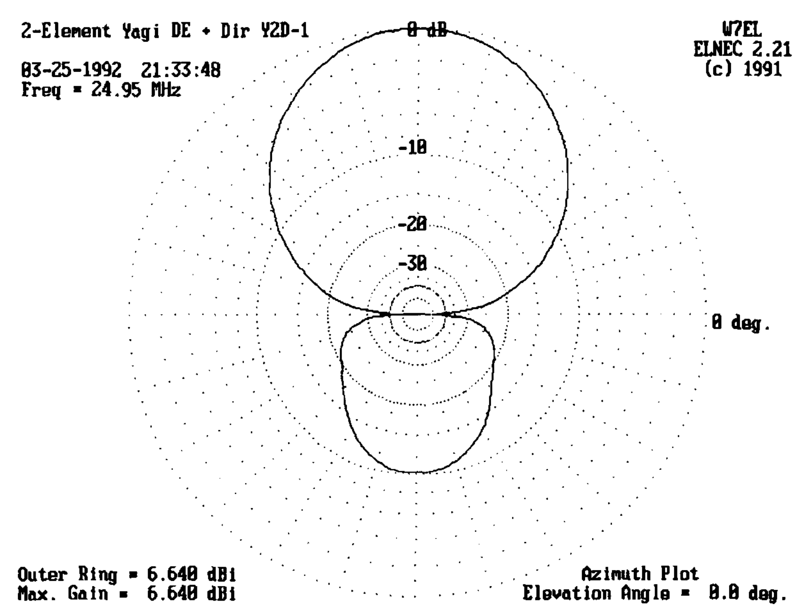

W7EL ELNEC 2.21	2-Element Yagi DE + Dir Y2D-1	03-25-1992 21:33:48
Azimuth plot Elev angle = 0.0 deg Outer ring = 6.640 dBi Reference = 0 dBi	Frequency = 24.95 MHz Ant Ht = 0.000 ft Wire Loss: Aluminum Rstvty = 4E-08 Rel Perm = 1	Max Gain = 6.640 dBi Source 1 impedance = 27.719 - J 9.689 SWR (50 ohm) = 1.899 (75 ohm) = 2.758
2 Wires Wire 1: 10 segments Length = 18.040 ft 1 source No loads	Free space	Gain: 6.640 dBi Angle: 90 deg F/B: 10.180 dB Bmwidth: 66 deg -3dB: 57, 123 deg Slobe: -3.540 dBi Angle: 270 deg F/Slobe: 10.180 dB

Figure 15. Free space pattern for Y2D-1, a 2-element Yagi with director.

sents a free space azimuth pattern of Y3-3 for reference. The three models together yield both higher and lower resistive components to the source impedance and both inductive and capacitive reactance, distributed among the various models.

The 3-element Yagi is a fairly complex antenna in terms of element interaction. Many builders have despaired of having gain, front-to-back ratio, and bandwidth merge. Other properties of the antenna also diverge as one changes dimensions. Interestingly, the model antennas tend to split according whether their elements are close-spaced or wide-spaced.

Like the 2-element Yagis and the phased arrays, the gain of the 3-element Yagis climbs rapidly between the 1/2-wavelength height and the 3/4-wavelength point, as shown in **Figure 18**. For models Y3-1 and Y3-3, the close-spaced beams, the gain continues to rise, changing only in the rate of increase. The wide-spaced beam, Y3-2, shows an overall increase in gain, but passes through peaks and valleys in the process. In fact, its rapid rise phase is delayed by 1/8 wavelength compared to the other 3-element Yagis. It would appear that wide element spacing does not permit the parasitic elements as effectively to isolate the gain from the effects of reflected high angle radiation. This condition is also confirmed in the variations of feedpoint resistance and reactance, both of which vary by up to 20 percent. In contrast, the close-spaced Yagis exhibit a total resistance and reactance range of around 1.5 ohms, which reduces to a range of 1 ohm or less above the 3/4-wavelength height.

Turning to **Figure 19**, we discover an obverse condition in the front-to-back ratios. The wide-spaced beam, Y3-2, shows the least variation in front-to-back ratio values, although they are the lowest of the group. The close-spaced Yagis exhibit significant maxima and minima, with the optimized model, Y3-1, showing sharp peaks just above the progressive half-wave heights. Interestingly, both the close-spaced beams have front-to-back maxima that coincide closely with the feedpoint resistance maxima, while Y3-2 shows a reasonable coincidence between inductive reactance maxima and front-to-back ratio peaks.

The complex interactions among the elements of these Yagis permit no unqualified generalizations. Element spacing around 1/8 wavelength produces beams with certain consistent characteristics, but those properties change as the element spacing approaches a quarter wavelength. Whether even computer optimization can produce a 3-element Yagi that performs consistently with respect to gain and front-to-back ratio at all reasonable heights may be doubtful. The lesson, if any, is this: a beam optimized for one height requires reoptimization before installation at another.

135-degree phase-fed antennas

An interesting class of antennas consists of two elements, the rear of which is fed 135 degrees out of phase with the front. Standard element spacing is 1/8 wavelength. Traditionally made of twinlead elements with a twisted 1/8-wavelength twinlead phasing line from the front element,

3-ELEMENT YAGI BEAMS:

Antenna Description	Designator	Material	Element	Length	Space to Previous Element	Free Space Characteristics Gain dBi	FB dB	R	X	Source
3-element Yagi handbook design	Y3-1	1-inch Al	Dir.	18.6 feet		7.957	16.6	8.9	−7.9	AB, 16 Ed, p. 11-11
			DE	19.0 feet	4.0 feet					
			Refl	19.8 feet	6.0 feet					
3-element Yagi 0.25 wave-length	Y3-2	1-inch Al	Dir.	18.04 feet		8.649	7.3	38.1	+48.5	Rhb, 21 Ed, p. 29.6
			DE	18.96 feet	9.86 feet					
			Refl.	20.08 feet	9.86 feet					
3-element Yagi 0.15 wave-length spacing	Y3-3	1-inch Al	Dir.	18.44 feet		8.771	12.6	9.8	+10.4	AB, 16 Ed, p. 11-11
			DE	19.05 feet	5.91 feet					
			Refl.	19.88 feet	5.91 feet					

Notes: AB = ARRL Antenna Book, 16th Ed.; Rhb = Radio Handbook, 21st Ed.

Table 6. 3-element Yagi beams modeled in this study.

these are the notorious ZL-Specials. They come in two varieties. ELNEC originator Roy Lewallen, W7EL, created his Field Day Special by using two elements of equal length. Older ZL-Special designs tended to make the rear element longer to optimize gain and front-to-back ratio. A typical ZL-Special free space pattern appears in **Figure 20**. Both models appear in **Table 7**: the W7EL model (scaled) as FDSP, the older model as ZLSP.

In modeling the ZL-Specials, I followed the lead of ELNEC's originator and made each element from a single fat wire, 0.145 inches in diameter. This simulates the thickness of twinlead without the difficulties inherent in directly modeling closely-spaced parallel wires. However, the resultant feedpoint resistance and reactance values will not be those associated with twinlead models. The patterns of rise and fall, if any, will parallel twinlead values.

In general, the Field Day and ZL-Special

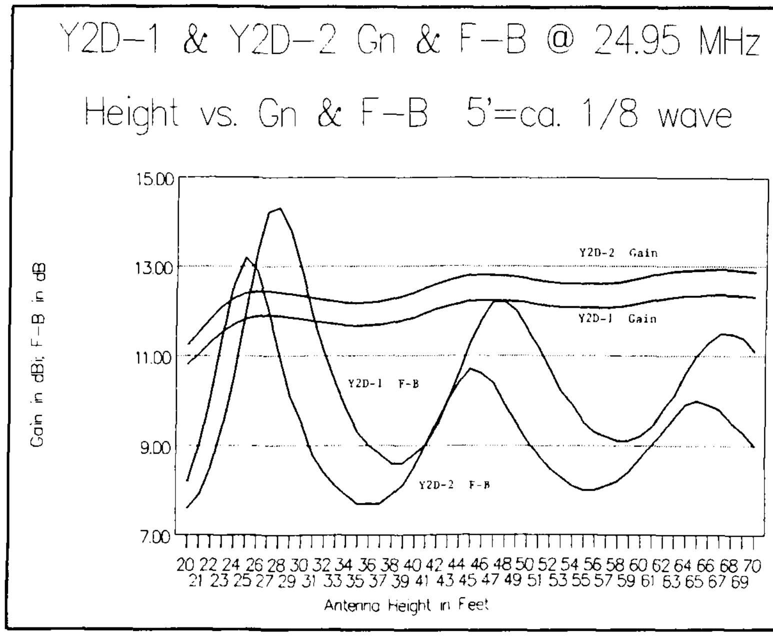

Figure 16. Gain and front-to-back ratio versus height for two 2-element Yagis with directors.

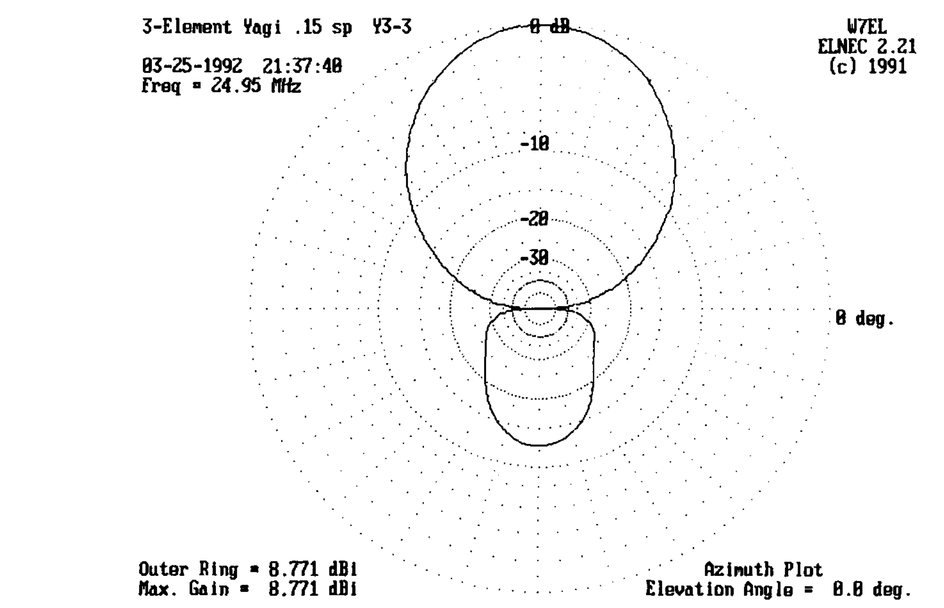

W7EL ELNEC 2.21 3-Element Yagi .15 sp Y3-3 03-25-1992 21:37:40		
Azimuth plot Elev angle = 0.0 deg Outer ring = 8.771 dBi Reference = 0 dBi	Frequency = 24.95 MHz Ant Ht = 0.000 ft Wire Loss: Aluminum Rstvty = 4E-08 Rel Perm = 1	Max Gain = 8.771 dBi Source 1 impedance = 9.809 + J 10.437 SWR (50 ohm) = 5.328 (75 ohm) = 7.797
3 Wires Wire 1: 10 segments Length = 18.440 ft 1 source No loads	Free space	Gain: 8.771 dBi Angle: 90 deg F/B: 12.646 dB Bmwidth: 58 deg -3dB: 61, 119 deg Slobe: -3.875 dBi Angle: 270 deg F/Slobe: 12.646 dB

Figure 17. Free space pattern for Y3-3, a 3-element Yagi with 0.15 wavelength element spacing.

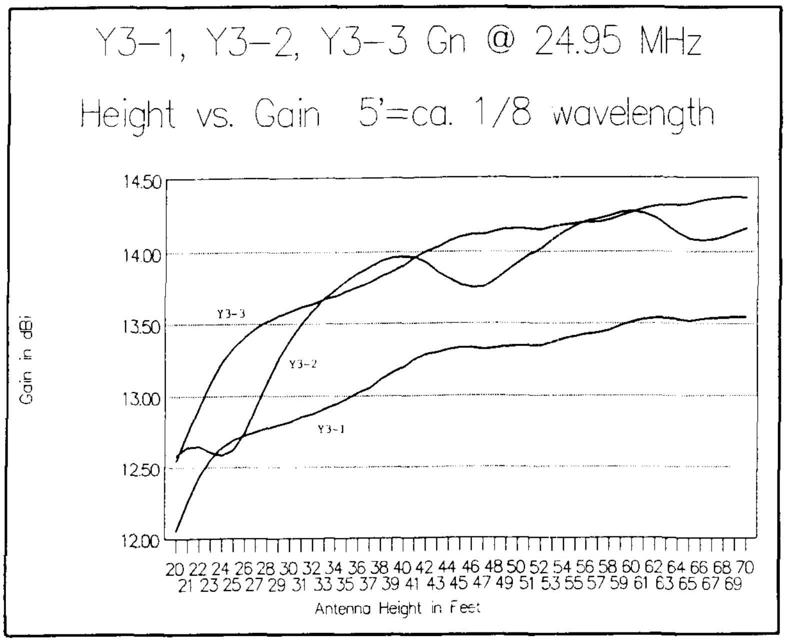

Figure 18. Gain variations in Yagis Y3-1, Y3-2, and Y3-3 from 20 to 70 foot heights.

variations have little to distinguish them. The traditional ZLSP shows a marginally higher gain and a seemingly significant increase in front-to-back ratio at any height, but that is an artifact of comparing an idealized model to a scaled actual antenna.*

*W7EL uses a program capable of evaluating Field Day and ZL Special designs using equal or unequal element lengths, so long as the elements are folded dipoles. The program yields element current calculations that are very accurate, as verified by actual element current measurements. His work is testimony to the fact that, while we may never eliminate the cut-and-try aspect of antenna construction, dedicated antenna specialists with a knack for computer programming can put us much closer to precision performance than at any time in radio history.

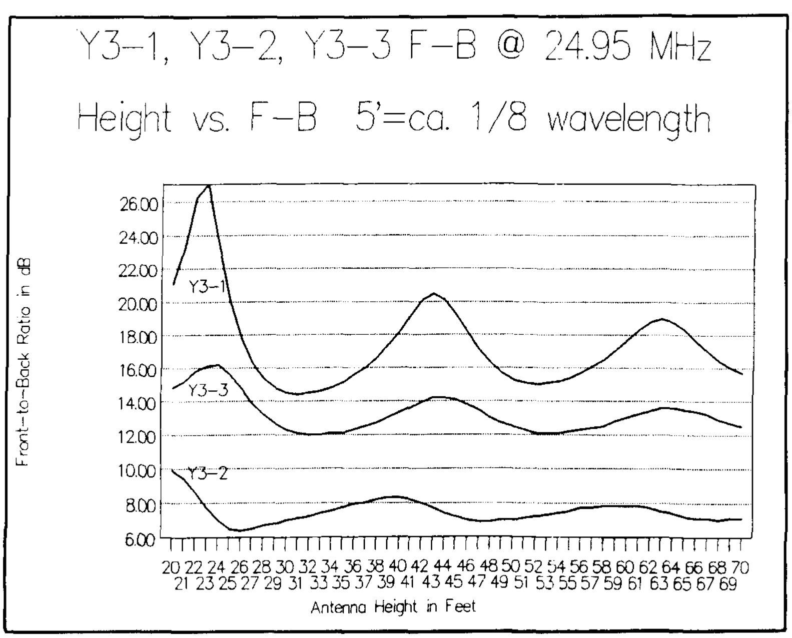

Figure 19. Front-to-back ratio variations in Yagis Y3-1, Y3-2, and Y3-3 from 20 to 70 foot heights.

Moreover, front-to-back ratios higher than about 20 dB may be of little use unless an offending station is aligned directly to the rear of the antenna. ZL-Specials show two rear side lobes, down about 20 dB from the main forward lobe. The calculated front-to-back ratio affects only the midpoint of the rear lobe, pulling it inward at higher values. The rejection of most rearward QRM is most likely to depend upon the lobes and less likely to depend upon the peak front-to-back ratio figures.

Nonetheless, 20 dB of rearward rejection is admirable not only for a 2-element beam, but for any 3-element beam as well. In crowded bands, the rejection may be more important for some hams than the half dB gain advantage offered by the 2-element Yagi. These much neglected antennas very likely deserve more attention than they currently receive, even if construction requires more ingenuity. Special attention is needed on feed methods to obtain the proper phasing. Models suggest that performance does not significantly suffer as the phase angles move from about 130 degrees to nearly 140 degrees. However, achieving even this broad condition at less that the high imped ances offered by folded dipole construction seems to have eluded the literature. Nevertheless, even in the abstract, these are interesting antennas to model.

Both versions of the ZL-Special reverse the patterns of gain and front-to-back ratio offered by the 2-element Yagi. Whereas the Yagi exhibits a well-behaved gain curve, the gain of the ZL-Special resembles a dipole with a rising gain figure, as **Figure 21** shows. Peaks and valleys occur at the same heights as for the dipole, and in about the same amount: the 1.1 to 1.4 dB range. Gain in both models appears to be roughly inversely co-variant with the feedpoint reactance. In contrast to the 2-element front-to-back ratio curve, which shows semi-sinusoidal characteristics, the ZL-Special front-to-back ratio curves (**Figure 22**) are coarser, but upward bound. Model ZLSP shows some noticeable peaks and valleys which are much flattened in the FDSP curve. Nonetheless, no decline goes more than a fourth of the way down to the preceding valley, which makes the dips of little design concern. The craggy or erratic nature of the small steps in the curve make correlation with any impedance factor more speculative than certain.

The use of 135-degree phased feed systems for elements spaced 1/8 wavelength apart does not guarantee a smooth front-to-back ratio curve. As a design exercise, I made up a phase-fed double extended dou-

135-DEGREE PHASE-FED ANTENNAS

Antenna Description	Designator	Material	Element	Length	Space to Previous Element	Free Space Characteristics Gain dBi	F-B dB	R	X	Source
"Field Day Special" (fat-wire dipole elements) 135 degree phase fed	FDSP	0.145-inch Cu	DE	18.12 feet		5.976	22.8	29.8*	– 18.1*	ELNEC file scaled *R&X indicators, not twinlead values
			Refl.	18.12 feet	4.79 feet			22.1*	– 99.4*	
ZL-Special (fat-wire dipole elements) 135 degree phase fed	ZLSP	0.145-inch Cu	DE	18.4 feet		6.238	42.5	26.7*	– 0.4*	Ant Rndp, v2, p.66 *R&X indicators, not twinlead values
			Refl.	18.9 feet	4.9 feet			23.7*	– 50.5*	
Double EDZ-ZL 135 degree phase fed	DEDZP	#18 Cu	DE	48.32 feet		8.898	24.8	89.3	– 824	Exp. design
			Refl.	51.06 feet	4.9 feet			30.9	– 680	

Notes: Ant Rndp = Antenna Roundup, vol. 2, 1966, p. 66.

Table 7. 135-Degree phase-fed antennas modeled in this study.

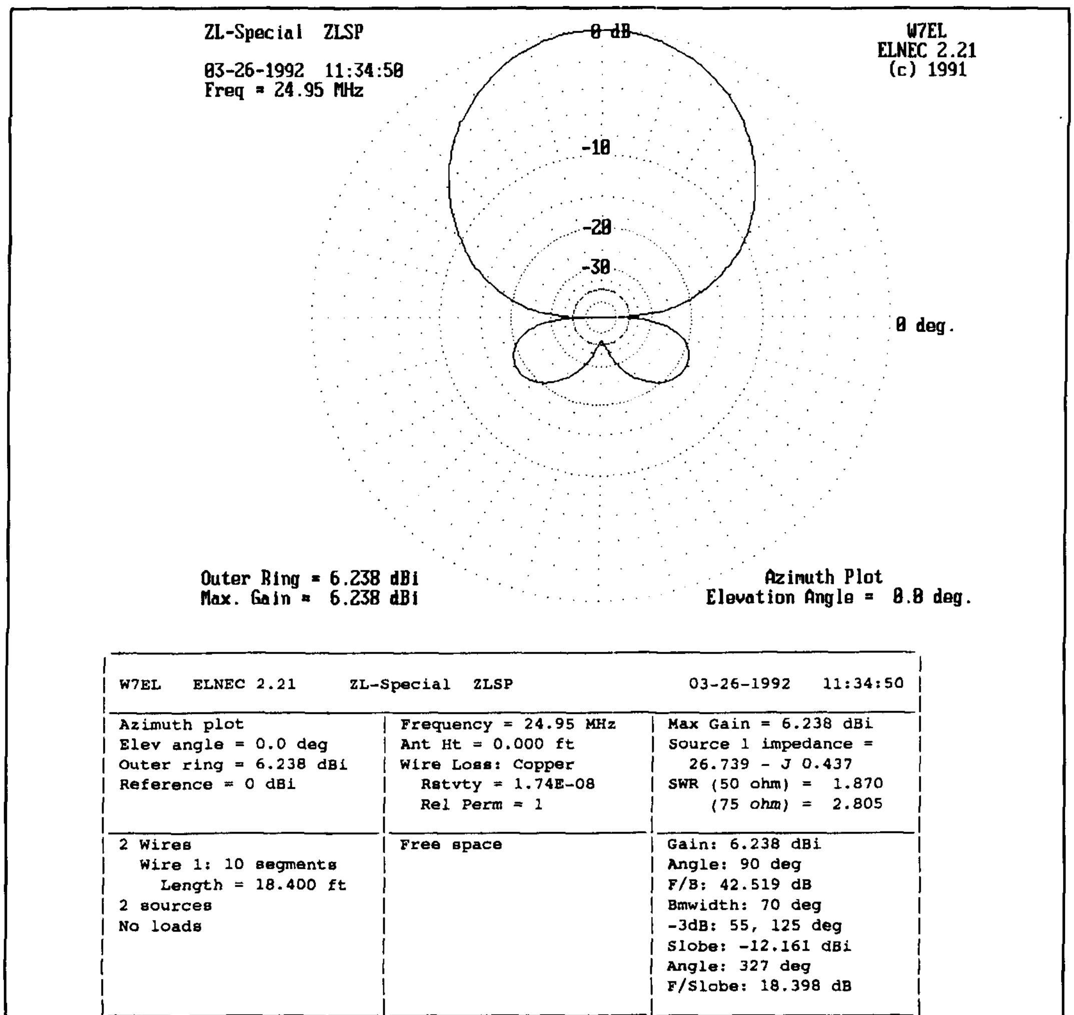

Figure 20. Free space pattern for ZLSP—a ZL-Special model using a single thick radiator to replace the folded dipole for each element.

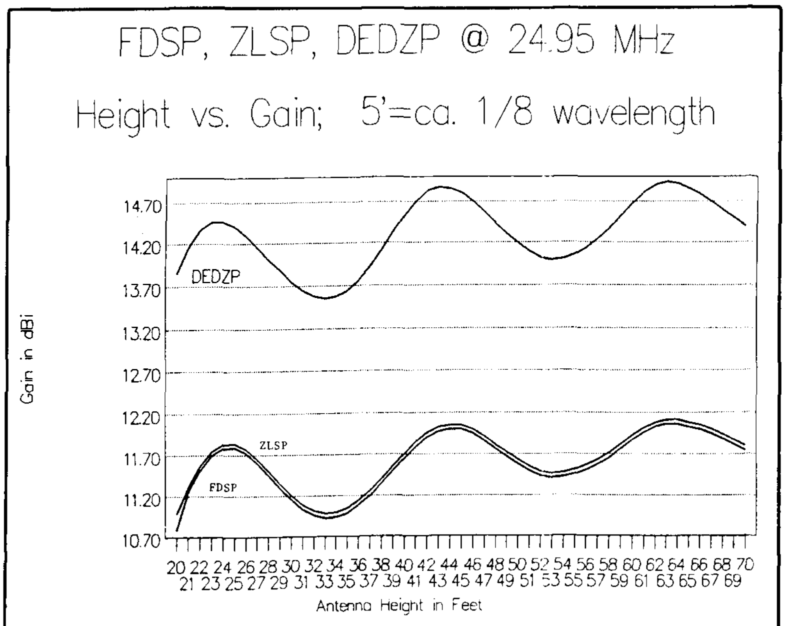

Figure 21. Gain variations in 135-degree phase-fed antennas FDSP, ZLSP, and DEDZp from 20 to 70 foot heights.

ble Zepp (DEDZP) of unequal elements. The calculated gain of the antenna appears in **Figure 21** with those of the ZL-Specials. The curve parallels the lower curves in just the way in which the EDZ curve parallels those of the dipoles. The maxima and minima appear a foot or two lower, which suggests a high value of capacitive reactance at the feedpoints, verified by **Table 7**. Like the ZL-Specials, gain appears to be roughly inversely co-variant with feedpoint reactance (when we treat the values as negative numbers so that the least capacitive reactance is a maxima; that is, the most inductive reactance). Unlike its ZL-cousins, DEDZP does not exhibit a smooth front-to-back ratio curve; in fact, just the opposite. The sharp peak values in **Figure 22** are exceptions, and the more average value is somewhat below the values for FDSP.

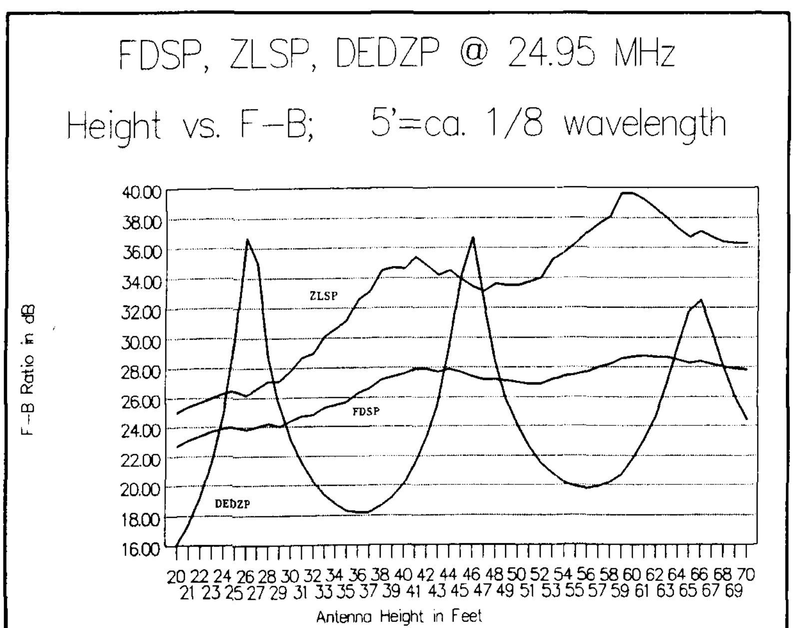

Figure 22. Front-to-back ratio variations in 135-degree phase fed-antennas FDSP, ZLSP, and DEDZp from 20 to 70 foot heights.

On the assumption that one can build and feed this antenna, perhaps its most significant use would be as a fixed wire beam set at a height to maximize front-to-back ratio. The high capacitive reactance of both elements strongly suggests a narrow bandwidth, and its pattern, shown in **Figure 23**, points to a narrow beam width. However, the multiplicity of side lobes limits absolute rejection of QRM. As a passing note, DEDZP derives from a parasitic version designed by Brian Egan, ZL1LE. It has similar gain figures, but requires an inductive load in the reflector. That factor, which requires optimizing at each height step, excluded the ZL1LE antenna from this study. However, for raw low-price gain in a fixed beam, these designs are worth considering.

Delta and quad loop antennas

The last group of basic ham antennas includes delta and quad loops. I have included a single delta and a single quad, each modeled as a parasitically fed and as a phase-fed beam. It is short and simple to alter the feed system in computer antenna modeling: it is the initial mutual impedance calculations that take so long. Had I used fully tapered elements to provide the most accurate dimensions and impedance figures, the task would have required over 7-1/2 hours per antenna. I cut that to about 3 hours per antenna by using substitute designs with fewer segments per wire. I already had a collection of quad and delta loop designs modeled in fully tapered form, but only for 7 steps between 25 and 55 feet. I chose the substitute designs with larger element dimensions for their relative coincidence of free space values and the accuracy of track with the tapered antennas. The delta loop model uses 8 segments per wire, while the quad model uses 6 segments per wire. The resulting patterns can be used with confidence, but the dimensions may not. **Table 8** lists both the substitutes and the their more accurate models. Note that the designs were selected for their close element spacing and for resonance. A further difficulty of modeling loop beams is that most builders design them for field adjustment of the reflector. That element is therefore normally too long (capacitive adjustment) or too short (inductive or fold-back adjustment) for modeling without optimizing a load for every one of the 51 height steps. The only generalization I have noted in my modeling efforts is that the traditional element formulas of 1005/f and 1030/f never appear in the same antenna. A comparison of QC-3 and DL-2 in **Table 8** illustrates the point.

Deltas and quads present special problems for analysis. Reflected high angle radiation must intercept multiple elements at different heights. Indeed, determining the height of a delta loop and a quad is itself problematic. For convenience, I used the boom or hub altitude. The quad boom is vertically centered between elements. However, takeoff angle readings suggest that the effective center of radiation is about a foot or 0.025 wavelength higher. Had I used this height, takeoff angles would have coincided closely with those for 2 and 3-element Yagis. Using the boom-hub height yields a takeoff angle lower than that of comparable antennas.

The situation is somewhat simpler for the delta loop. If one uses spider construction, with the triangle apex at the top (which is also the feedpoint), then the hub is about 1/3 the vertical dimension of the antenna. Using this figure, I found that takeoff angles paralleled closely with those for Yagis. Different construction methods, of course, will result in different relationships between the boom and the antenna. Because there is little difference in the patterns of a delta and a quad loop beam, **Figure 23**, which shows the free space pattern of the

DELTA AND QUAD LOOP ANTENNAS: (all antennas use substitute models)

Antenna Description	Designator	Material	Element	Length	Space to Previous Element	Free Space Characteristics				Source
						Gain dBi	F-BdB	R	X	
2-element Quad (tapered element model) (parasitic values shown)	QC-3	#18 Cu	DE Refl.	39.68 feet 41.60 feet	 5.0 feet	7.180	21.6	95.0	4.7	Experimental design 990/f, 1037/f substitute below
2-element Quad (6 segment/ wire model) parasitic feed	QC-3A	#18 Cu	DE Refl.	(40.80 feet) (42.88 feet)	 5.0 feet	7.261	22.5	96.9	4.3	Substitute model for QC-3 6 segments/ wire
2-element Quad (6 segment/ wire model) 135 degree phase fed	QCP-3A	#18 Cu	DE Refl.	(40.80 feet) (42.88 feet)	 5.0 feet	7.203	27.3	101.8 − 3.3	1.0 − 4.6	Substitute model for QC-3 6 segments/ wire
2-element Delta Loop (tapered element model) (parasitic values shown)	DL-2	#18 Cu	DE Refl.	40.26 feet 41.88 feet	 5.0 feet	7.080	18.4	77.8	4.7	Experimental Design 1005/f, 1045/f substitute below
2-element Delta Loop (8 segment/ wire model) parasitic feed	DL-2A	#18 Cu	DE Refl.	(41.40 feet) (43.26 feet)	 5.0 feet	7.139	18.4	88.8	− 1.7	Substitute model for DL-2 8 segments/ wire
2-element Delta Loop (6 segment/ wire model) 135 degree phase fed	DLP-2A	#18 Cu	DE Refl.	(41.40 feet) (43.26 feet)	 5.0 feet	6.967	26.7	102.2 − 2.1	− 2.5 − 13.1	Substitute model for DL-2 8 segments/ wire

Table 8. Delta and quad loop antennas modeled in this study.

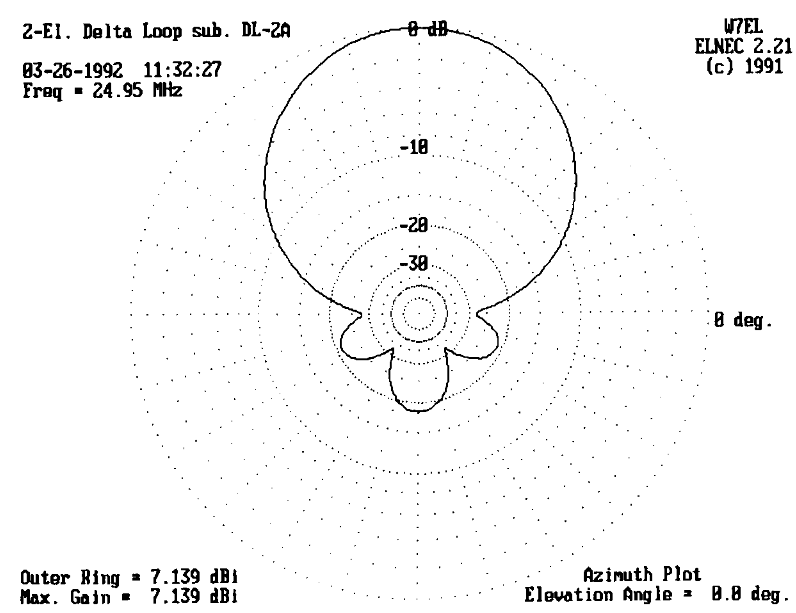

W7EL ELNEC 2.21	2-El. Delta Loop sub. DL-2A	03-26-1992 11:32:27
Azimuth plot Elev angle = 0.0 deg Outer ring = 7.139 dBi Reference = 0 dBi	Frequency = 24.95 MHz Ant Ht = 9.310 ft Wire Loss: Copper Rstvty = 1.74E-08 Rel Perm = 1	Max Gain = 7.139 dBi Source 1 impedance = 88.809 - J 1.719 SWR (50 ohm) = 1.777 (75 ohm) = 1.186
6 Wires Wire 1: 8 segments Length = 13.800 ft 1 source No loads	Free space	Gain: 7.139 dBi Angle: 90 deg F/B: 18.366 dB Bmwidth: 72 deg -3dB: 54, 126 deg Slobe: -11.226 dBi Angle: 270 deg F/Slobe: 18.366 dB

Figure 23. Free space pattern for DL-2A, a 2-element Delta Loop beam.

substitute delta loop, will suffice for both.

The gain of loop-based beams shows a more rapid and steady climb than those of Yagis, but with distinct maxima and minima. Among the antennas, there is little to choose, as the intertwining curves of **Figure 24** demonstrates. The higher pair of curves belong to the quad. They are notable only for the fact that the phase-fed model manages to exceed the parasitic model in peak values at gain maxima. The differences actually make no practical difference. Maxima and minima positions coincide with those for dipoles but depart somewhat from the corresponding maxima and minima of the feedpoint resistance.

Perhaps the most important feature of the gain curves is the manner in which gain falls off below the 5/8 wavelength point. The reputation of the quad and the delta loop is that they are relatively immune to detuning by nearby objects and the ground. This reputation does not extend to gain. At mounting heights below 5/8 wavelength, the loop beam loses its advantage over a 2-element Yagi.

With respect to front-to-back ratios, both the quad and the delta loop display very peaky patterns when parasitically fed. The two lower curves in **Figure 25** show peaks similar to those in the DEDZP pattern. The quad shows an upward displacement of its peaks and valleys that appears more significant than it is actually is: the displacement would seem less had the peaks been less sharp. In the case of both antennas, however, the front-to-back ratio, even in the valleys, rivals that of a well-designed 3-element Yagi.

Some designers have suggested that quad performance might be improved by phase-feeding the rear element in the manner of a ZL-Special. The upper curves of **Figure 25** show the improvement, were such a feed system to be feasible. Although the phase-fed delta loop beam displays initial "peakiness,'' it tends to level off at the 40-foot or 1-wavelength mark. The phase-fed quad is a paradigm of a well-behaved front-to-back curve. Nevertheless, as in the case of the ZL-Specials, there may be a limit as to the usability of extreme front-to-back ratios in antennas with rear side lobes. The lobes may better mark the limits of effective QRM rejection than the tiny but deep inset of the 180-degree front-to-back point.

If MININEC programs or computers become more efficient or more automated, further study of loop beams is both desirable and necessary. A single model of each type of loop beam is insufficient to certify the patterns as reliable enough to use. Indeed, one should at least double the number of antenna models used in this study before counting its results as more than preliminary.

Nevertheless, if this study has brought about an acquaintance with and an appreciation of the ways in which antenna performance changes with antenna height, then it has been worth the time and energy. Listing antenna specifications accurately and comparing them sensibly have always been arduous and tricky tasks. Unfortunately, I have the feeling that these notes may make the tasks a bit more difficult, even if the result is a more rational set of expectations.

Appendix 1: Take-off Angles of the Modeled Antennas

As noted early in the report, all antenna data collected refer to the lowest main lobe of radiation. As the height of any horizontal antenna is increased, the angle of maximum radiation from this lobe decreases. At the lowest heights investigated, antenna patterns show a single lobe (as viewed on an elevation plot between ground and 90 degrees straight up). As antenna height increases, other lobes appear—while the lowest lobe grows narrower. These multiple lobes may give an antenna at a set height good performance on both long skip paths and shorter domestic ones.

A full discussion of antenna elevation plots would unnecessarily lengthen this report, and several studies already exist. However, as an adjunct to this report, **Table 9** reports the take-off angles of the lowest main lobe for the antennas investigated. Antennas were grouped together if they varied from the stepping points in no more than two places. To keep the table from becoming a mere morass of numbers, I have included only the angle value when it first appears as antenna height increases. The blank spaces beneath a number have the same value. The actual angle decreases smoothly: the stepped appearance of the columns is an artifact of giving the angle value in integers.

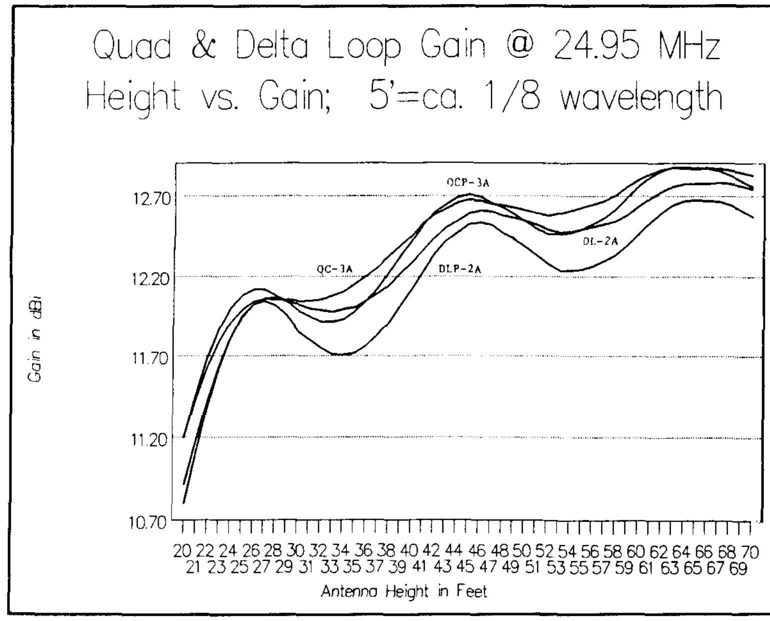

Figure 24. Gain variations in DL-2A, DLP-2A, QC-3A, and QCP-3A from 20 to 70 foot heights.

Above three-quarters of a wavelength, the actual difference in the take-off angle among the different antennas is quite small. The dipoles, the 2-element Yagis, the 135-degree antennas, and the delta loop show a close coincidence in their values, as do the 180-degree antennas, the 3-element Yagis, and the quads. The angles shown for the delta loop and the quad are functions of their mounting points, as described above. Nonetheless, the differences between the

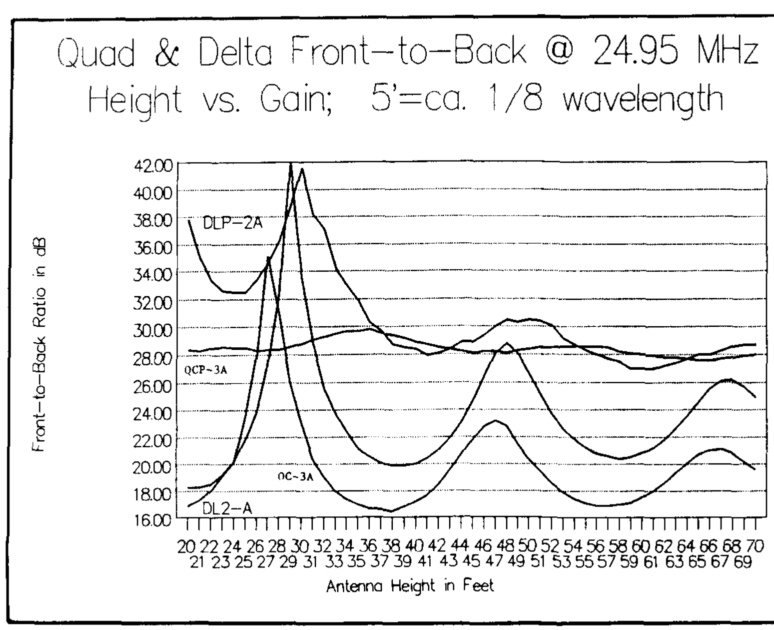

Figure 25. Front-to-back ratio variations in DL-2A, DLP-2A, QC-3A, and QCP-3A from 20 to 70 foot heights.

two groups are too small at higher mounting points to make a significant difference in antenna choice.

More significant are the differences in take-off angle for the lowest heights investigated. At 1/2 wavelength (about 20 feet at 24.95 MHz), the 4 degree difference between a dipole and a 3-element Yagi or a 2-element quad may make a significant difference in long-range performance. However, in all cases, the lobes show considerable power radiation above and below the angle of maximum radiation from the lobe. In addition, evaluating a proposed antenna and mounting height requires that one consider a number of other variables, such as the desired type of operating, the overall azimuth and elevation patterns, and the ability to install and maintain the antenna. I have added these notes only to verify the validity of comparing the antennas models investigated and to give a general

TAKE-OFF ANGLES FOR THE LOWEST LOBE OF SEVERAL TYPES OF ANTENNAS

Height		Take-off Angle in Degrees								
		Dipoles	D8JK	2-element	3-El. Yagis			FD/2LSP	DL-2A	QC-3A
Feet	Wavelengths	+EDZ	+DEDZ	Yagis	Y3-1	Y3-2	Y3-3	+DED2P	DLP-2A	QCP-3A
20	1/2	28	25	26	25	24	24	26	26	24
21		27	24	25	24	23	23	25	25	24
22		25	23	24	23	22	23	24	24	23
23		24	22	23	22	21	22	23	23	22
24		23	21	22	22	21	21	22	22	21
25	5/8	22		21	21	20	20	21	21	20
26		21	20	20	20	20				
27			19		19	19	19	20	20	19
28		20		19		18	18	19	19	
29		19	18	18	18					18
30	3/4	18				17	17	18	18	17
31		17	17	17		17	17			
32		17			16	16				16
33			16	16	16			16	16	
34		16								
35	7/8		15	15	15	15	15			15
36		15						15	15	
37			14		14	14	14			14
38				14				14	14	
39		14								
40	1		13		13	13	13			13
41				13				13	13	
42		13								
43										
44			12	12	12	12	12	12		12
45	1 1/8	12							12	
46										
47										
48			11	11	11	11	11	11		11
49		11							11	
50	1 1/4									
51										
52			10		10	10	10			10
53		10		10				10	10	
54										
55	1 3/8									
56										
57										
58			9		9	9	9			9
59		9		9				9	9	
60	1 1/2									
61										
62										
63										
64										
65	1 5/8		8		8	8	8			8
66		8		8				8	8	
67										
68										
69										
70	1 3/4									

Table 9. Comparison of antenna take-off angles for selected antennas.

impression of how take-off angle varies with antenna height.

Appendix 2: Size, Soil, and the Limits of Extrapolation

As briefly noted in the text, the ability to extrapolate the results of this study to generalities about all HF antennas, whatever their type, is limited. The patterns are reliable at best over the range from 14 to 30 MHz, and only if one assumes an obstruction-free coherent medium or average earth beneath the antenna.

Perhaps the most obvious limitation to extrapolation is that antennas below 20 meters and above 10 meters rarely hit the elevation range used in this study. The lowest limit, 1/2 wavelength, is above 140 feet at 80 meters and 70 feet at 40 meters. Likewise, 20 feet is already greater than a wavelength at 6 meters. Hence, for bands outside the upper HF frequencies, the study does not cover typical antenna heights.

There are also limitations imposed by the assumption of a coherent medium or average earth beneath the antenna. Average earth is sometimes defined as having a conductivity of 5 milliSiemens per meter (mS/M) and a dielectric constant of 13. These figures represent the default values used in ELNEC 2.21, which automatically takes into account modifications to antenna patterns created by soil conditions. One may choose other soil values most like one's home QTH by modifying the ground constants in the program. **Figure 26** demonstrates the changes in values for a half-wavelength dipole occasioned by selecting other earth constants. Included are perfect soil, very good soil of a rich pastoral nature (C = 30.3 mS/m, DC = 20), medium or average soil (C = 5 mS/m, DC = 13), poor sandy soil (C = 2 mS/m, DC = 10), and very poor industrial city soil (C = 1 mS/m, DC = 5).*

The only significant change among the lines is the gain value for each given height. For a selected frequency, in this case 24.95 MHz, the maxima and minima of gain appear at the same heights above ground. As the soil grows poorer, the take-off angle of the lowest lobe of radiation decreases slightly for any elevation, but above 5/8 wavelength, the difference is always less than a degree. The decrease in gain more than offsets the seeming take-off angle advantage. From the comparison one may conclude that soil type, while affecting antenna gain at any height, does not affect the trends under study. Nonetheless, precise analysis for any particular site will require, for precision, replication of the exercise.

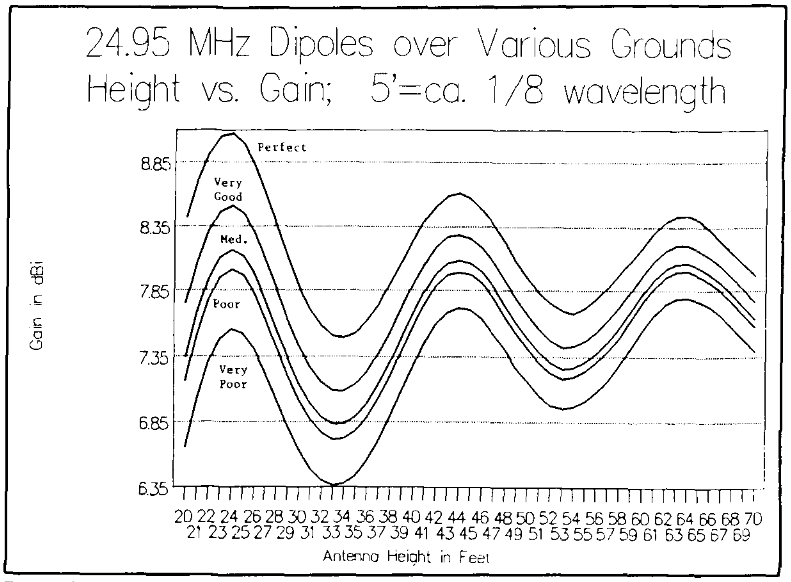

Figure 26. Gain variations in half-wavelength dipoles over various types of ground from 20 to 70 foot heights.

In addition to the differences occasioned by soil type, we must take into account the varying characteristics of soils in any typical site and the degree to which antenna currents penetrate the soils. One standard by which penetration is measured is skin depth, which increases as soils grow poorer. In the upper HF range, penetration depths to the standard measure vary from 5 to 6 feet for very good soil to nearly 40 feet for very poor soil. Consequently, scratching the surface to ordinary garden depths is insufficient to analyze the soils underlying an antenna system. Too, the assumption of coherent soil of constant characteristics is usually unwarranted by subsurface conditions.

Treating the soil as if it were a conductive surface rather than a medium is thus dangerous below the VHF range. Moreover, the degree of penetration increases rapidly at 7 MHz and below. Although the effects of ground differ according to the polarization of antennas under investigation, it cannot be ignored and becomes very significant from 160 through 40 meters. Extrapolating the results of this study to the lower HF region is thus not recommended. Rather, the study should be replicated for those frequency ranges.* ■

*These values are taken from a 1939 Federal Register on the subject of "Standards of Good Engineering Practice Concerning Standard Broadcast Stations" as reprinted by Terman in the *Radio Engineer's Handbook* (New York: McGraw Hill, 1943), page 709, and further reprinted in Gerald Hall, Editor, *The ARRL Antenna Book*, 16th Edition (Newington, ARRL), page 3-3.

*Further information on antenna ground modeling can be derived from the excellent instruction set included with ELNEC as a starter. Lewallen references the current edition of *The ARRL Antenna Book*, previously noted, which in turn will lead the reader to Terman, and perhaps beyond. All of which demonstrates that the formulas required to perform this study have been around a very long time; only the drudgery of performing them manually has deferred studies of antenna performance versus height for many antenna types.

Here's some feedback generated by Cornell Drentea's article "Improving Receiver Performance in Modern Transceivers" (Communications Quarterly, fall 1991).

Dear Cornell:

I have been meaning to write you for some time since your article appeared in *Communications Quarterly* about using PIN diodes to replace PN diodes in switching. Good job. We need more nuts and bolts type of articles like that.

I have been doing some experiments here on diode isolation. My investigation began when I was unable to obtain adequate isolation when switching filters in my old FT902DM. So having the resources available at work, I made a fixture and tested the filter board on the network analyzer. (The FT902 uses all plug in boards for major functions.) The problem became abundantly clear as shown in **Figure 1**.

With the CW filter selected, the SSB and AM filters were definitely not out! (Back in September 1981, Johnson, W4ZCB, wrote an article for *73 Magazine* about the FT902 filter isolation problem, blaming the filters themselves and not recognizing the real problem.) At that point, I began testing various PIN diodes because of their supposedly excellent off isolation. **Figure 2** shows a small collection of diodes I have tested. Stay away from the MPN3404s which were in the board when **Figure 1** was generated! Replacing the MPN3404s with HP 1N5719s did the trick, as shown in **Figure 3**.

Another factor in the filter isolation problem is the diodes switch typically in a 500-ohm environment, which further reduces their isolation effectiveness by 20 dB per port over the 50-ohm system plotted in **Figure 2**. However, pulling all the filters out only resulted in a noise floor of -78 dBm.

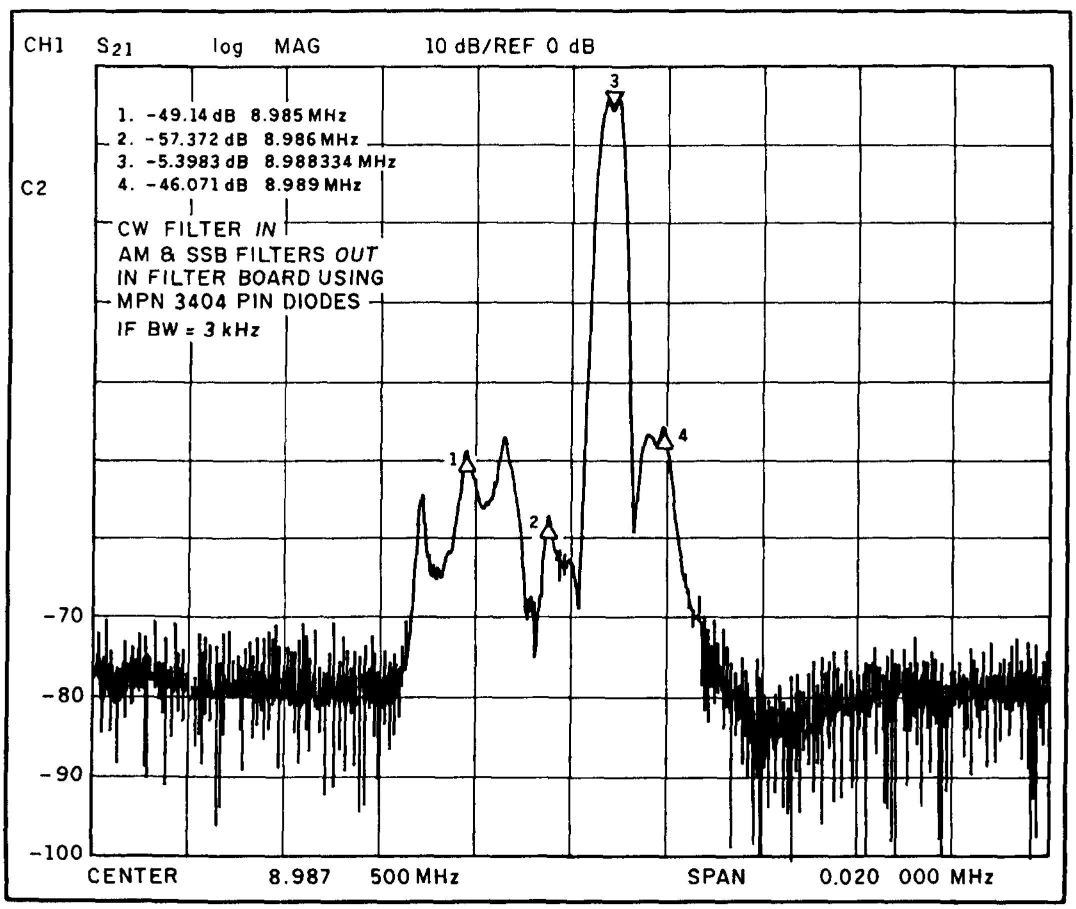

Figure 1. FT902DM filter board, using HP8753C network analyzer.

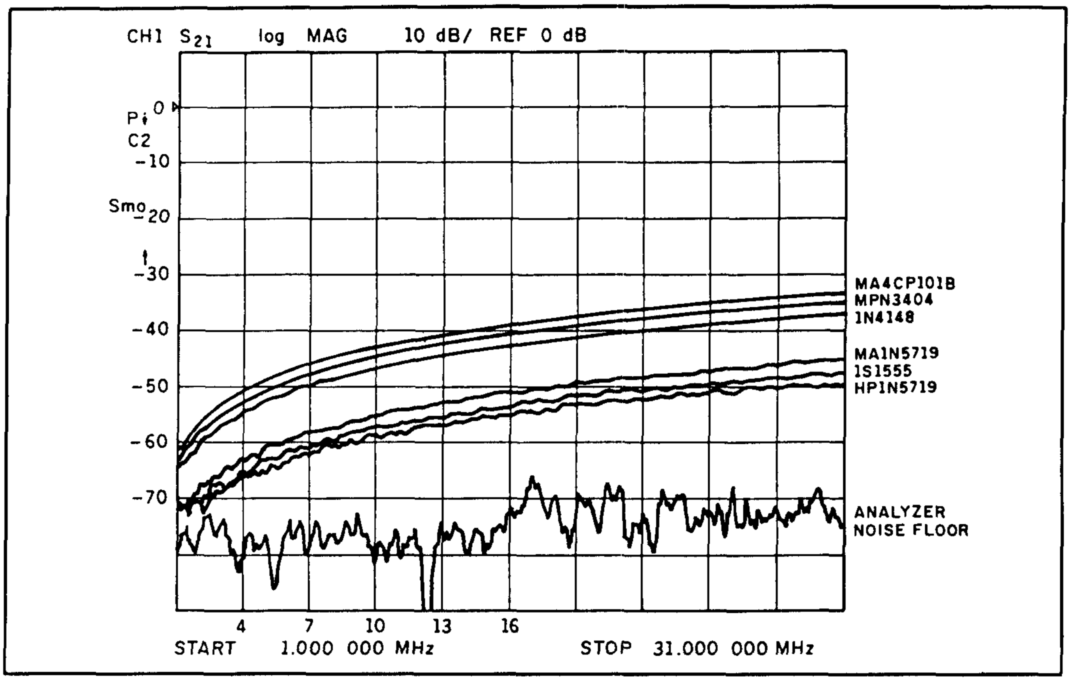

Figure 2. Isolation of PIN and PN diodes.

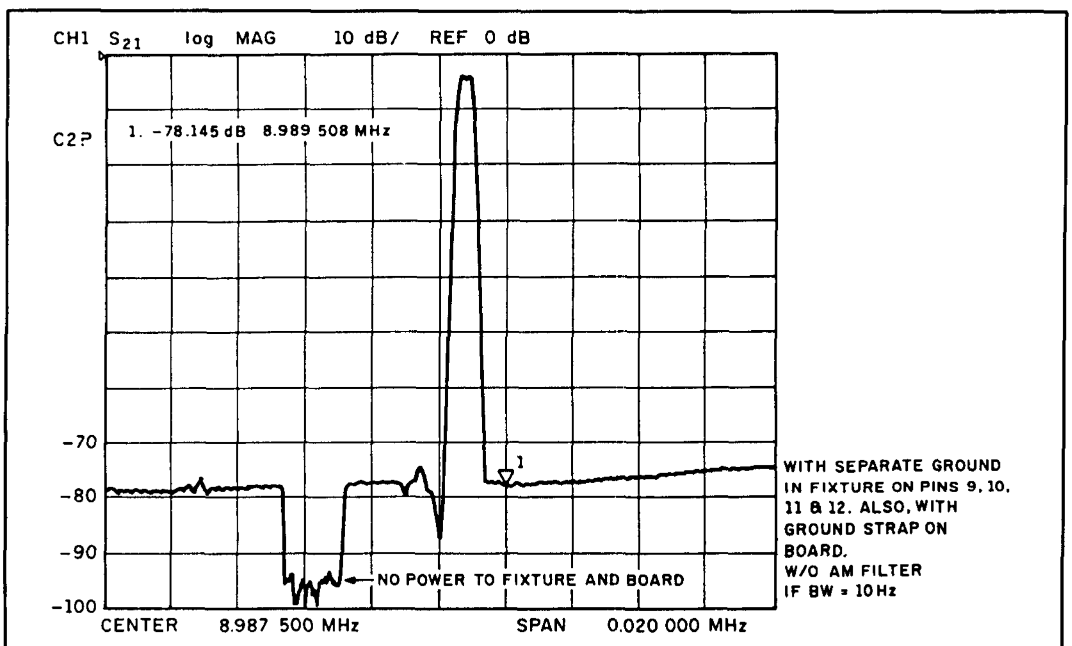

Figure 3. FT902DM filter board in test fixture using 1N5719 PIN diodes.

The culprit must be radiation across the edge connector. So I ran another test using a piece of blank edge connector material plugged into the socket and only achieved 95 dB of isolation. So much for the thought of getting 100 dB isolation with the real filter board plugged in. the poor isolation deterred me from trying to switch the diodes in a 50-ohm system. However, the diode changes on the board plus rewiring the socket in the mainframe have made a substantial improvement in filter response.

Anyway, have you run across the problems I have just stated? I would like to measure the diodes that you wrote about in the article for isolation and insertion loss if you have one to spare. I would also be curious about the reader response you received. Also, where and when do these technical information nets meet?

Currently, I am in the UHF transceiver design section at Motorola GEG doing frequency synthesizer work. Looking forward to hearing from you. Again, good article.

Hardy Landskov, N7RT
Phoenix, Arizona

Dear Mr. Landskov:

Thank you for sharing your research. With your permission, I would like to forward the information you provided to *Communications Quarterly* for publication under the "Technical Conversations" column.

You asked about isolation. It has been my experience that 95 dB isolation at the board level is quite a remarkable achievement, especially without any complex shielding which can even go inside the filters. While I have not seen anyone doing 100 dB, I would say that more often an 80 to 85-dB isolation is what is achievable across an open frame board.

About the technical nets, I am not a part of them, but I have heard them in the winter on 14.318 MHz on Sunday afternoons. I have no idea if they operate during the summer, but you can try this frequency.

I am sending you two PIN diodes, an HP 5082-3080 and 5082-3081 for your tests. I do not have any MA4P1200s since I have contributed my entire supply to a good cause. If you find anything interesting, please share your findings with us.

Regarding the reader response, some of the comments can be found in the "Technical Conversations" column of *Communications Quarterly*.

Congratulations on being involved with transceiver and UHF frequency synthesizer work. It does indeed sound like fun. Synthesizers are one of my strongest areas of expertise as I have done much with them from systems to hardware implementation in my consulting career. Again, thanks for sharing your information, and I am looking forward to hearing from you again.

Cornell Drentea, WB3JZO
JZO Research
Minneapolis, Minnesota

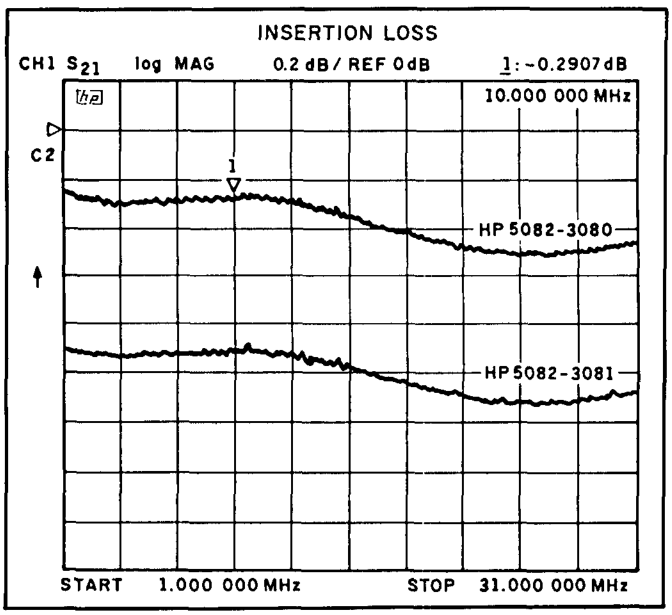

Figure 1

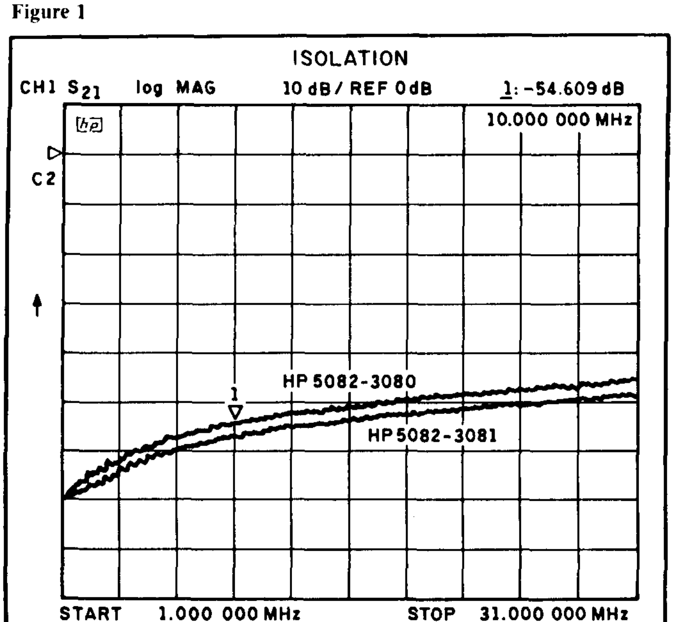

Figure 2

Dear Cornell:

I just wanted to close the loop on the PIN diodes. Here's the data from the two diodes you sent me. Same conditions as before. $I_F = 10$ mA (insertion loss) as shown in **Figure 1** and $V_R = 10_V$ (isolation) as shown in **Figure 2**.

Hardy Landskov, N7RT
Phoenix, Arizona

"Quarterly Devices" author Rick Littlefield, K1BQT, received these comments on his spring 1992 column.

Dear Rick:

I enjoyed your "Quarterly Devices" column on low-power audio amplifiers in the spring *Communications Quarterly*. You mention muting the LM386 by removing Vcc. I wonder if you have tried the method using the decoupling pin (pin 7)? G3ROO and I tried this, with success, in a recent project in *SPRAT*. See pages 21-29.

I look forward to trying the devices you described in the article. I must check out their UK availability.

Always enjoy reading your work, Rick. Keep the ideas and the circuits coming.

Rev. George Dobbs, G3RJV
Rochdale, England

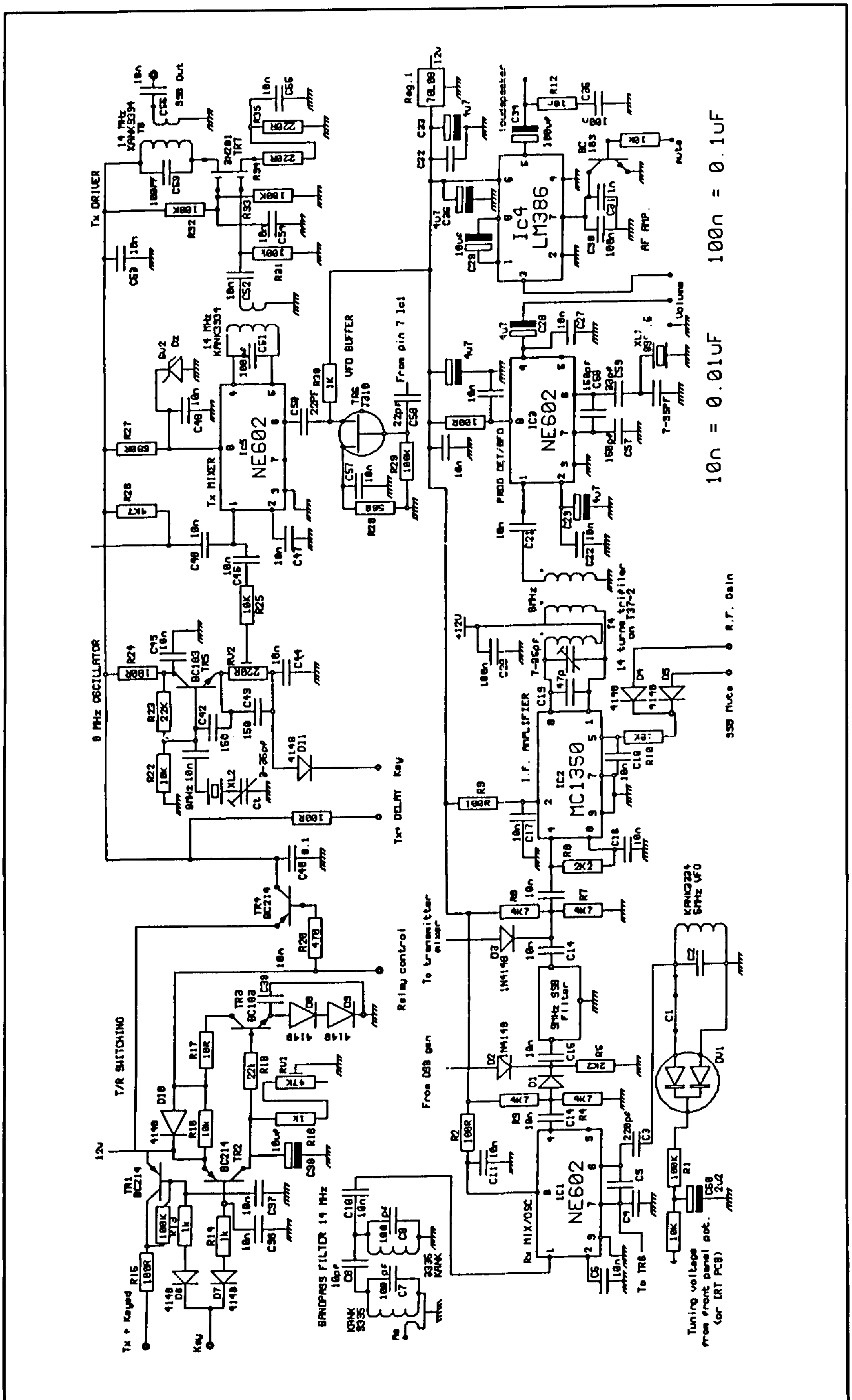

Figure 1. Muting the LM386 by using the decoupling pin (pin 7).

Reviewed by: Joseph L. Lynch, ***N6CL*****
P.O. Box 73
Oklahoma City, OK 73101

SPECIAL BOOK REVIEW

OBSERVING THE SUN

*A new book by Peter O. Taylor**

As amateur radio operators, we take a keen interest in the Sun. In many respects, we are closet Sun worshippers. We decide whether or not to turn on the radio on a particular day based on what's happening on the Sun. Hams who operate on HF frequencies want to know if a solar event has happened, so they can decide whether to bother turning on the radio. Conversely, hams who operate on VHF and above want to know about the same event because it may stimulate an aurora which may provide propagation for terrestrial communications or, may disrupt EME (earth-moon-earth) communications.

For so many facets of our hobby, we look to the Sun for its influence. Peter O. Taylor, an author whose work appears regularly in this publication, has provided a guide for our ponderings in his book, *Observing the Sun*.

In the first chapter, Taylor introduces the reader to the historical roots of solar observation. He recounts that the ancients looked at the Sun as " . . . more like that of a slave than that of a master." He cites 12th century BC Chinese writings as the first reports of what we now perceive as sunspots.

In Chapter 2, while continuing to examine the history of solar observation, Taylor discusses the invention of the telescope and how the Sun apparently stymied initial research of itself during the Maunder Minimum.[1] He goes on to cite the first scientific investigation into the properties of sunspots published in 1769, by Alexander O. Wilson, of the University of Glasgow, as the basis for modern research into sunspots. Taylor refers to amateur astronomer, Heinrich Schwabe's work as an accidental discovery of the cyclical nature of the recurrence of sunspots.

The author uses Chapter 3 to lay the groundwork for what we now know as the various cycles of the Sun. He states that the beginning of the record solar cycles, starting with Cycle Number One, is based on a system devised by the Swiss Federal Observatory in Zurich, Switzerland (and the work of Schwabe). He continues by discussing the periodicity and characteristics of the sunspot cycle, as we have been able to determine it to date. Taylor examines recent cycles and compares the even-numbered with the odd-numbered cycles. He concludes that the even-numbered cycles have longer extended maxima than the odd-numbered cycles. However, he also points out that recent odd numbered cycles have had higher maxima than their counterpart even-numbered cycles. And then he makes a prediction. While cautioning the reader, Taylor speculates that, based on recent history, ". . . if the odd-even relationship continues, the maximum of cycle twenty-three should also be a very strong one, perhaps with a peak strength which approaches 200 (in mean sunspot numbers)."[2]

Did you ever think that counting sunspots was easy? It's not. Sunspots are not individual dots on the Sun. Rather, they are often found in groups, or clusters, that appear at various locations on the Sun's surface. How large the cluster is and where it appears is meaningful to the Sun's observers. For example, sunspots from a new cycle will generally appear high in latitude, while sunspots from an old cycle will appear lower in latitude. In Chapter 4, Taylor describes the two methods of sunspot counting, the Zurich and Mount Wilson sunspot group classifications, and the differences and similarities between the two.

In Chapter 5, Taylor begins his discussion of the effects of the Sun on the Earth. Among the topics covered are the solar

*Cambridge University Press, 1991, 159 pages, $29.95.
**Mr. Lynch is the VHF editor for our sister publication *CQ* magazine. His review of Mr. Taylor's book appears here courtesy of that publication. Though it is not generally our policy to run book reviews, we thought those of you who enjoy Mr. Taylor's column "The Solar Spectrum" might also be interested in his latest book. Ed.

wind, solar flares, and coronal holes, and their relative effects on the earth's geomagnetic field. Taylor discusses the A and K indices and how they are derived.[3] He also examines the visible effect, the aurora, and its relationship to high geomagnetic indices, and why aurorae are more likely to occur during the decline of the solar cycle. Because we are in the decline of Cycle 22, one can imagine what we have to look forward to over the next few years. We have already seen some samples with the fireworks show during the period of 8-10 November 1991.[4] Taylor continues by discussing the Sun's effects on the Earth's weather patterns. The reader is left to contemplate the possibility of changes in the Earth's average temperature in relationship to the changes in the sunspot cycle.[5]

In Chapter 6, Taylor looks at the equipment needed for naked eye observation of the Sun. He warns us that solar filters, and not polarizers, must be used for direct naked eye observation. The reader is cautioned that use of the wrong equipment can severely damage one's eyesight. Taylor considers actual pieces of equipment used for observation and gives the pros and cons for each. Among the types of telescopes discussed are the catadioptric and the Newtonian reflector. Taylor also addresses direct viewing of the Sun and the differences between photographing versus drawing the image of it. In addition, he describes the use of hydrogen-alpha (Hα) filters. These filters, which transmit light centered around 6563 angstroms, in the red portion of the spectrum, have become relatively inexpensive, and thus more available to the amateur observer. By using these filters, the observer can view solar flares, coronal holes, sunspot regions, prominences, and filaments[6] from a different perspective. Taylor also examines the safest way of observing the Sun, that of projecting its image onto a surface, and how to use this indirect method of observation with the most success.

In order to keep accurate records of positions of sunspots and other objects of interest, it is necessary to know how to view the Sun and its orientational relationship with Earth. In Chapter 7, Taylor addresses orienting the image of the Sun in relationship to the observer. Among the topics covered are the projected image, the direct image, and the determination of a sunspot's position mathematically.

Chapter 8 covers what to look for and how to look for it when observing sunspots. The reader is taught how to count the sunspot groups and is advised to be consistent when making daily observations.

In Chapter 9, Taylor discusses the use of the Porter Disk for aligning the Sun's equator with the observer's equatorial position relative to the Sun.

Chapter 10 focuses on the rare white solar flares. Taylor notes that when such flares occur, they can cause massive effects on Earth. Known as WLFs, these flares have been known to trigger immense aurorae. Taylor states that WLFs that occur in the Northern Solar Hemisphere tend to begin between one and two years before the peak of the sunspot cycle. He also explains that Southern Hemisphere WLFs tend to begin approximately one year after the peak. (This is yet another aspect of the Sun we can look forward to during this cycle's decline.) The reader who is serious about observing WLFs is given information on where to send documentation of such observations.

In Chapters 11 and 12, Taylor deals with detecting solar flares electronically. Chapter 11 discusses the effects on the magnetic field. We, as amateur radio operators, should find most of the contents of this chapter very familiar. How well we know of polar cap absorptions, sudden ionospheric disturbances (SIDSs), and the effects of solar activity on the F and E layers of the atmosphere. However, we know less about the effects these events have on the D layer.

We do know that the D layer begins to materialize after sunrise, increases in intensity during the daytime to a maximum around local noontime, and then declines towards sunset. When present, it absorbs signals in the MF and low HF range (absence of long distance communications on 80 and 160 meters). At night the D layer disappears, making long distance (or skip type) communications on these frequencies more probable. Conversely, what is not as well known to amateurs, is that within the VLF spectrum, the D layer acts as a waveguide, providing ducting for signals to travel long distances. Because the D layer does not hold ionization well without the Sun's (or other) reinforcement, the effect of solar flares on that layer is one of rapid ionization and deionization. These changes can be detected on receivers tuned to VLF radio stations[7] set up, for just such purposes, within the 5 to 50 kHz range. Using a strip chart recorder, one can detect a change in amplitude in the signal during such ionization and deionization of the D layer.

Those who'd like to build just such a VLF receiving station will be interested in Chapter 12. Here Taylor describes how to construct such a station and gives the frequencies to listen for while conducting your

VLF observations.[8] He also describes how to make a magnetometer for detecting disturbances in the Earth's magnetic field.

In Chapter 13, Taylor exposes the reader to equations used for calculating relative sunspot numbers, the Sun's relative rotation, and other statistical factors.

In the last chapter, Taylor covers eclipses of the Sun. While the ancients regarded the event with suspicion and mistrust, modern research into the phenomenon has contributed much to the study of the Sun. Taylor quotes two stories as examples of the historical misgivings associated with eclipses. First, Taylor recounts one incident where two Chinese astronomer's apparently lost their heads for being too consumed with wine and failing to "drive off the dragon," or accurately forecast a particular eclipse. In the second incident, Taylor reports that the five year war between the Medes and the Lydians ended abruptly after an eclipse.

Taylor discusses various types of eclipses (partial, annular, and total) and what is necessary for each to occur. For example, a total eclipse can only occur when the moon is at perigee. Taylor proceeds to compare the lunar orbit with the Earth's and the Sun's. He states that total eclipses are rare sights for the casual observer because most occur over water. The one recent exception was the total eclipse of 11 July 1991, which occurred over several large metropolitan areas. (I just missed seeing the eclipse in Costa Rica, arriving some six hours after the event.) He gives instructions and warnings on how to view an eclipse safely (the same warnings on viewing the unblocked Sun apply[9]) and what to expect when viewing it. Taylor reports that the appearance of Baily's Beads, the streams of the remaining sunlight around the lunar limb, during the total portion of the eclipse is one of the more fascinating aspects of the event.

Taylor's book provides an excellent primer for those amateur radio operators who want to know more about the most influential aspect of our hobby of communications.

Can we harness the Sun and make it a slave for our hobby as the ancients attempted to do? Probably not. However, we can, with Taylor's book, make new, more respectful observations of the Sun. ■

REFERENCES

1. For more information on the Maunder Minimum see "Do Sunspots Ever End?," by Aaron J. Fishman, K1BAF, *Communications Quarterly*, Winter 1991, pages 52-54, "The Maunder Minimum," By Joseph L. Lynch, WA6PDE, *QST*, July 1976, pages 24-26, and the original work, "The Maunder Minimum," by John A. Eddy, *Science* magazine, volume 192, 18 June 1976, pages 1189-1202.
2. It is interesting to note that indirect correlation to this prediction existed some 17 years ago. In a phone conversation I had with Eddy, during the course of writing my article for *QST*, he expressed the feeling that we were headed for another Grand Maximum of a long-term solar cycle that stretches into 200-300 years in periodicity, and that this maximum would probably occur during the 21st century.
3. These indices are part of the Solar Activity Report that is broadcast on WWV at 18 minutes past the hour and WWVH at 45 minutes past the hour.
4. For more information on the solar events surrounding those days, see Taylor's article entitled "The Solar Spectrum," that appeared on pages 46-49 in the Winter 1992 issue of *Communications Quarterly*.
5. While neither Fishman nor I discussed weather effects caused by the Sun, Eddy does so on page 1199 of the previously cited article in *Science*.
6. For more information on solar flares, coronal holes, prominences and filaments, and the use of the Hα filter, also see Taylor's article entitled "The Solar Spectrum."
7. The D layer is very sensitive to ionization from other events, such as meteor storms. A group of Brazilian scientists, headed by Pierre Kaufmann, used data from these VLF radio stations to confirm the existence of an invisible meteor storm that was detected on the moon during late June and early July 1975, and the storm's effects on the Earth. The results of their work was published in *Science* magazine, volume 246, 10 November 1989, pages 787-790.
8. Much of the material contained in this chapter pertaining to building the VLF receiving station, plus additional material related to setting up a BASIC program for computer plotting of the VLF signals, can also be found in Taylor's and Arthur J. Stokes, N8BN's article entitled "Recording Solar Flares Indirectly," that appeared on pages 29-35, in the Summer 1991 issue of *Communications Quarterly*.
9. Recent solar eclipses have brought this warning home to amateur photographers as well, through cautions of not looking through SLR (single lens reflex) cameras without proper filtering. The magnification of the camera lens can burn, and thus, permanently destroy, part of the retina.

PRODUCT INFORMATION

NHT Symbol Libraries

New Horizons Technologies, Inc. is now shipping NHT Symbol Libraries 2.1, which are tailored to the industrial and facilities engineering fields. Libraries for architectural, electrical, structural, AWS weld symbols, piping, valves, instrumentation, hydraulic, pneumatic, and geometric tolerancing symbols are included. There are over 2300 symbols in all for facilities layout, detail, and schematic drawings.

NHT Symbol Libraries are available in versions for AutoCAD (9 through 12) and MicroStation (3 and 4) and include both screen and tablet menus, complete documentation and instructions, and a user-friendly installation program. The libraries are also available in DXF format for use with other CAD programs. However, the DXF set does not include menus or installation program.

For more information on NHT Symbol Libraries contact New Horizons Technologies, Inc. at (517) 789-6908, FAX (517) 789-6973.

Rick Littlefield, *K1BQT*
109 A McDaniel Shore Drive
Barrington, New Hampshire 03825

QUARTERLY DEVICES

Solve RF design problems with elegant simplicity using MMICs.

Like a good political candidate, the MMIC (acronym for Monolithic Microwave Integrated Circuit) has achieved widespread name recognition. However, MMICs are still new enough so that most of us haven't had the opportunity to actually apply them in circuits we have designed. In this edition of "Quarterly Devices," I'll explore the essentials you need to know to put these little powerhouses to work.

Gain block

The MMIC is a multi-stage bipolar RF amplifier housed in a small transistor-like package. Typically, a MMIC provides:

- broad frequency response—DC to over 1 GHz,
- near-constant gain over the entire operating range,
- 50-ohm Z_{in}/Z_{out} without external matching networks,
- drop-in convenience, few external components,
- good immunity against damage from static,
- high stability,
- excellent directivity.

These building block qualities allow the MMIC to satisfy a variety of amplification functions in cellular phones, two-way radios, data links, antenna preamps, line drivers, mixer followers, instrumentation amplifiers, and much more.

An inside view

Looking inside (see **Figure 1**), the MMIC schematic reveals nothing mysterious; only a simple two-stage bipolar DC-coupled amplifier. The real magic behind the MMIC lies in the precise nature of the manufacturing process. Mini-Circuits literature notes that MMICs are "fabricated with nitride self-alignment ion-implantation for precise control of doping and passivation to achieve high reliability." According to Mini-Circuits, this process yields the close tolerances and unit-to-unit uniformity required for an amplifier of this type. Suffice it to say, this alchemy works—and works economically. Most MMICs are priced from below $1 in quantity.

Although the MMIC comes in a four-lead package, a close look at **Figure 2** reveals that it's really a three-pin device. One tab provides an RF-input connection to the base of Q1. A second tab handles both RF-output and DC power at Q2 (an externally-connected bias network at R_c and C_{out} provides the necessary isolation between the DC and RF paths). The remaining two tabs provide

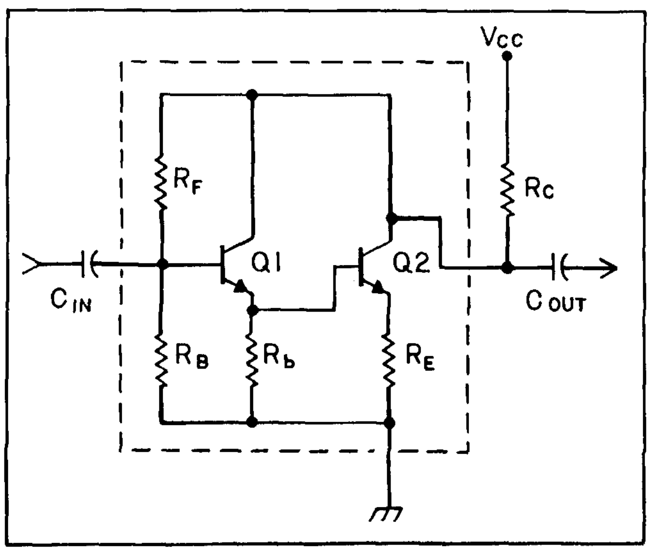

Figure 1. General schematic for MAR amplifier.

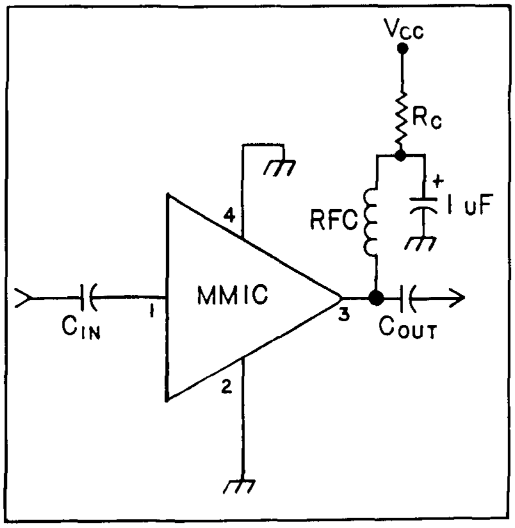

Figure 2. Pinout and biasing configuration for MMIC amplifier.

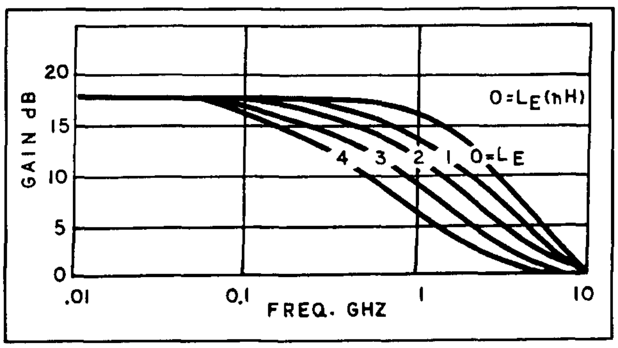

Figure 3. Effects of emitter inductance on amplifier gain for the MAR-1.

a low-inductance path to the pc-board ground plane.

When designing and laying out MMIC circuitry, there are five key areas to take into account. These are:

- •pc groundplane,
- •input and output RF paths,
- •bias resistor,
- •RF choke,
- •DC blocking capacitors.

We'll take a more detailed look at each of these areas.

The groundplane

MMICs deliver a lot of gain at extremely high frequencies (well beyond the 1 to 2 GHz cutoff). This means your layout will require a large and solid groundplane to keep return paths as short as possible. If platethroughs are used for these returns, Mini-Circuits recommends they be located directly below the ground leads, and as close to the device body as possible. If you prototype with standard two-sided board, use wire feedthroughs.

Providing a good groundplane is essential. At 1 GHz, only 2 nH of stray emitter inductance will result in over 1 dB of loss. As the graph in **Figure 3** illustrates, stray inductance very quickly becomes a major problem above 1 GHz.

The type of pc board you select can affect MMIC amplifier performance. Standard G-10 glass board generally works well through the UHF range, but you should choose a more suitable "microwave" material when working at higher frequencies (PTFE-woven glass is recommended for applications up to 2.5 GHz). Always avoid hygroscopic pc materials that pick up and retain moisture.

RF signal paths

At higher frequencies, 50-ohm stripline is the best way to feed RF in and out of the MMIC (almost anything else will introduce parasitic inductances that adversely affect amplifier performance). **Table 1** provides line widths for etching 50-ohm stripline onto various pc-board materials.

Here are some tips for laying out your signal path:

•Avoid angles and bends in stripline unless you are familiar with proper chamfering techniques to prevent unwanted reactance.

•Provide tapered transitions down to MMIC tabs, RF connectors, or other narrow component contact surfaces (a 45-degree angle is good). Abrupt or ragged trans-

Board Material	Dielectric Constant	Board Thickness	W/H Ratio	Track Width
G-10 Glass Epoxy	4.80	0.62″	1.75	.108″
PTFE-Woven Glass Fiber	2.55	0.010″	2.55	.025″
	2.55	0.031″	2.55	.079″
	2.55	0.062″	2.55	.158″
RT/Duroid 5870	2.30	0.015″	2.90	.044″
Alumina/E10	10.00	0.025″	0.95	.024″
	10.00	0.050″	0.95	.048

Table 1. 50-ohm stripline width for various pc board materials.

itions introduce parasitic inductance. Also, *provide the correct stripline gaps for any* chip components (capacitors, resistors, inductors).

•When mounting the MMIC, keep tabs on an even plane with the stripline and surrounding land area by drilling a hole in the pc board to accommodate the MMIC case.

Selecting a bias resistor

In order to hold operating current constant over a wide range of temperatures, the MMIC's internal transistors require an external collector resistor (R_c in **Figure 1**). This "stabilization resistor" compensates for changes in transistor beta as a function of temperature by adjusting the collector voltage. Mini-Circuits recommends a drop of around 2 volts across R_c to ensure flat gain response over the widest possible temperature range (–10 to +100°C). As **Table 2** illustrates, without bias compensation, the MMIC fails to amplify at low temperatures and self-destructs at high temperatures. Mini-Circuits recommends using a standard carbon-composition resistor for R_c. *These have a positive temperature coefficient* that complements the negative-coefficient of the chip resistors inside the MMIC.

When calculating the correct resistive value for the MMIC stabilization resistor, use the formula:

$$R_c = \frac{V_{cc} - V_d}{I_d} \text{ Ohms} \quad (1)$$

where:

V_{cc} = power supply voltage applied to R_c in volts,
V_d = voltage at the DC input terminal of the MMIC in volts,
I_d = quiescent bias current drawn by the MMIC in amps.

Recommended levels of V_d and I_d for each MMIC device are provided in the specification sheet. Most often, a 1/4-watt resistor will provide sufficient dissipation at R_c. However, to calculate dissipation, use the formula:

$$P_{dis} = I_d^2 \times R_c \text{ watts} \quad (2)$$

See the chart in **Table 3** for recommended resistor values at various levels of V_{cc} for MAR-series amplifiers. Note that R_c dissipation may exceed 1/4 watt for some MMICs operating at higher supply voltages.

MAR-1 Operating Voltage = 5.07 V

Voltage Drop, volts	Resistor Value, ohms	Temperature degrees C	Bias Current, mA	Power Gain @100 MHz, dB
0	0	–10	9.5	–0.5
		25	18.4	18.8
		100	**	**
1.5	82	–10	14.2	17.0
		25	17.3	18.3
		100	24.1	19.0
2.0	100	–10	16.3	18.5
		25	18.9	18.9
		100	24.6	19.0
7.0	412	–10	16.1	18.3
		25	16.6	18.1
		100	18.3	17.5

** Device destroyed due to excessive current draw.

Table 2. Effects of R_c on Performance over Temperature

Amplifier	Bias Current	Bias Voltage	Approximate Bias Resistor (Ohms)				Resistor Dissipation (Watts)
	I_B (mA)	$+V_O$	+5V	+9V	+12V	+15V	$+V_{CC}$=12V
MAR-1	17	~5	—	235	412	588	.12
MAR-2	25	~5	—	160	280	400	.18
MAR-3	35	~5	—	114	200	286	.25
MAR-4	50	~6	—	60	120	180	.30
MAR-6	16	~3.5	98	344	531	719	.14
MAR-7	22	~4	45	227	364	500	.18
MAR-8	36	~8	—	—	111	194	.14

Table 3. Typical Values for R_c at Common V_{cc}'s

Selecting a choke

In low-frequency applications, the resistance provided by R_c may be sufficient to isolate the MMIC's RF signal path from ground. However, as frequency increases, carbon-composition resistors become increasingly reactive—potentially degrading amplifier performance by 3 dB or more. To counter this, you must install an RF choke in series with R_c. As a rule-of-thumb, choose a value which provides at least 500 ohms of reactance at the lowest frequency of operation. In practice, a 10-μH molded inductor will isolate the amplifier's signal path down to 10 MHz. For VHF and higher frequencies, a few turns of enameled wire on a ferrite bead will do the trick.

In addition to installing the choke, Mini-Circuits suggests providing a ground path for any AC signals leaking through the choke by installing 1-μF capacitor from the junction of the choke and R_c to ground.

DC blocking capacitors

Because the MMIC is DC coupled, you must install external DC blocking capacitors

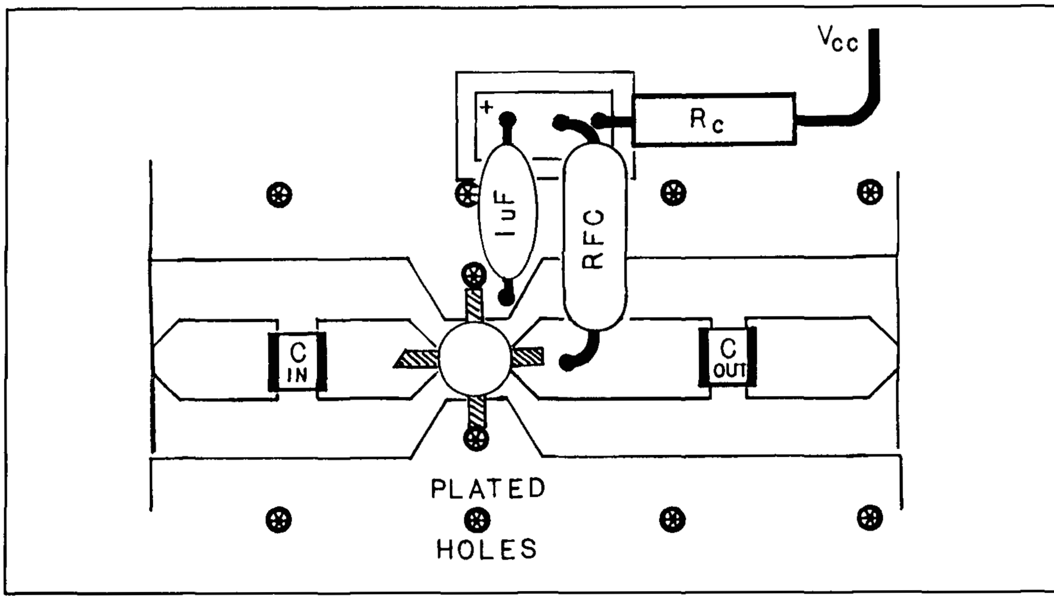

Figure 4. Recommended layout for MMIC amplifier stage.

Broadband Monolithic Amplifiers

Case Styles:

RAM MAR MAR-SM MAV VAM

Specifications:

	MODEL NO.	•FREQ. MHz (f_L f_U)	GAIN, dB Typical (at MHz) 100	500	1000	2000	MIN	MAXIMUM POWER, dBm Output (1dB Comp.)	Input (no damage)	DYNAMIC RANGE NF dB Typ.	IP3 dBm Typ.	VSWR In	Out	MAXIMUM RATING (25°C) I(mA)	P(mW)	DC POWER at Pin 3 Current (mA)	Volt. Typ.
MAR	MAR-1	DC-1000	18.5	17.5	15.5	—	13.0	+ 1.5	+20	5.5	+14.0	1.3:1	1.3:1	40	200	17	5.0
MAR	MAR-2	DC-2000	12.5	12.3	12.0	11.0	8.5	+ 4.5	+20	6.5	+17.0	1.3:1	1.4:1	60	325	25	5.0
MAR	MAR-3	DC-2000	12.5	12.2	12.0	10.5	8.0	+10.0	+20	6.0	+23.0	1.5:1	1.7:1	70	400	35	5.0
MAR	MAR-4	DC-1000	8.3	8.2	8.0	—	7.0	+12.5	+20	6.5	+25.5	1.6:1	2.0:1	85	500	50	5.25
MAR	MAR-6	DC-2000	20.0	18.5	16.0	11.0	9.0	+ 2.0	+20	3.0	+14.5	1.5:1	1.4:1	50	200	16	3.5
MAR	MAR-7	DC-2000	13.5	13.1	12.5	11.0	8.5	+ 5.5	+20	5.0	+19.0	1.4:1	1.5:1	60	275	22	4.0
MAR	MAR-8	DC-1000	32.5	28.0	22.5	—	19.0	+12.5	+20	3.3	+27.0	*	*	65	500	36	7.8
MAR-SM	MAR-1SM	DC-1000	18.5	17.5	15.5	—	13.0	+ 1.5	+20	5.5	+14.0	1.3:1	1.2:1	40	200	17	5.0
MAR-SM	MAR-2SM	DC-2000	12.5	12.3	12.0	11.0	8.5	+ 4.5	+20	6.5	+17.0	1.5:1	1.4:1	60	325	25	5.0
MAR-SM	MAR-3SM	DC-2000	12.5	12.2	12.0	10.5	8.0	+10.0	+20	6.0	+23.0	1.5:1	1.7:1	70	400	35	5.0
MAR-SM	MAR-4SM	DC-1000	8.3	8.2	8.0	—	7.0	+12.5	+20	7.0	+25.5	1.5:1	1.9:1	85	500	50	5.25
MAR-SM	MAR-6SM	DC-2000	20.0	18.5	16.0	11.0	9.0	+ 2.0	+20	3.0	+14.5	1.7:1	1.7:1	50	200	16	3.5
MAR-SM	MAR-7SM	DC-2000	13.5	13.1	12.5	11.0	8.5	+ 5.5	+20	5.0	+19.0	1.7:1	1.7:1	60	275	22	4.0
MAR-SM	MAR-8SM	DC-1000	32.5	28.0	22.5	—	19.0	+12.5	+20	3.3	+27.0	*	*	65	500	36	7.8
RAM	RAM-1	DC-1000	19.0	17.5	15.5	—	13.0	+ 1.5	+20	5.5	+14.0	1.3:1	1.3:1	40	200	17	5.0
RAM	RAM-2	DC-2000	12.5	12.0	11.8	11.0	8.5	+ 4.5	+20	6.5	+17.0	1.2:1	1.4:1	60	325	25	5.0
RAM	RAM-3	DC-2000	12.5	12.2	12.0	10.5	8.0	+10.0	+20	6.0	+23.0	1.6:1	1.7:1	80	425	35	5.0
RAM	RAM-4	DC-1000	8.5	8.2	8.0	—	7.0	+12.5	+20	6.5	+25.5	1.4:1	1.9:1	100	540	50	5.25
RAM	RAM-6	DC-2000	20.0	19.0	16.0	11.0	9.0	+ 2.0	+20	2.8	+14.5	1.4:1	1.3:1	50	200	16	3.5
RAM	RAM-7	DC-2000	13.5	13.1	12.5	11.0	8.5	+ 5.5	+20	4.5	+19.0	2.0:1	1.8:1	60	275	22	4.0
RAM	RAM-8	DC-1000	32.5	28.0	23.0	—	19.0	+12.5	+20	3.0	+27.0	*	*	65	420	36	7.8
MAV	MAV-1	DC-1000	18.5	17.0	15.0	—	12.5	+ 1.5	+20	5.5	+14.0	1.4:1	1.3:1	40	200	17	5.0
MAV	MAV-2	DC-1500	12.5	12.0	11.0	10.0	7.5	+ 4.5	+20	6.5	+17.0	1.3:1	1.4:1	60	325	25	5.0
MAV	MAV-3	DC-1500	12.5	12.0	11.0	10.0	7.5	+10.0	+20	6.0	+23.0	1.3:1	1.6:1	70	400	35	5.0
MAV	MAV-4	DC-1000	8.3	8.0	7.5	—	7.0	+11.5	+20	7.0	+24.5	1.4:1	1.8:1	85	500	50	5.25
MAV	MAV-11	DC-1000	12.7	12.0	10.5	—	9.0	+17.5	+20	3.6	+30.0	1.5:1	1.7:1	80	550	60	5.5
VAM	VAM-3	DC-2000	11.5	11.5	11.0	9.5	7.5	+ 9.0	+20	6.0	+22.0	1.5:1	1.7:1	60	240	35	4.7
VAM	VAM-6	DC-2000	19.5	18.0	15.0	10.0	8.0	+ 2.0	+20	3.0	+14.0	1.6:1	1.5:1	40	125	16	3.3
VAM	VAM-7	DC-2000	13.0	12.6	12.0	9.8	7.8	+ 5.5	+20	5.0	+18.0	1.5:1	1.5:1	50	175	22	3.8

-8 models not 50 ohms, see mini-circuits data.

Table 4. Broadband monolithic amplifiers.

to keep MMIC bias levels off the signal path. Always use high-Q chip capacitors for this purpose, as even very short component leads introduce parasitic inductance onto the stripline. In addition to eliminating unwanted lead inductance, chip capacitors self-resonate at much higher frequencies—increasing the top-end operating range of the amplifier.

When choosing a value for DC blocking capacitors, you may tailor C_{in}, C_{out} to roll-off the MMIC's low frequency response. For example, to prevent strong local FM stations from overloading a 800-MHz scanner preamp, select a value for C that is reactive at 100 MHz but flat at 800 MHz (33 pF, for example). Note that installing a low-inductance decoupling choke at R_c will further roll off unwanted LF response.

The layout—putting it all together

Figure 4 shows a typical single-stage UHF amplifier layout following Mini-Circuits guidelines. The layout occupies about 1.5 × 1.0 inches, providing ample land area around the device. Note that a number of platethrough holes (or wire feedthroughs) are provided on each side of the stripline to solidify the groundplane. If you lay your MMIC amplifier out carefully and select the right parts, you'll have little trouble implementing your design.

Choosing the right MMIC for the job

Not all MMICs are created equal. A quick scan of the specification chart shown in **Table 4** reveals some devices with attractive preamp noise figures, others with particularly high third-order intercepts, and even some that deliver transmitter-strip power levels. The one you choose depends upon what you need to accomplish.

By way of example, suppose you want to make an inexpensive mast preamp for a 400-MHz UHF-band scanner antenna. Looking at the numbers, you can see the MAR-6 develops 18.5 dB gain at 500 MHz with a noise figure under 3.0 dB. Although slightly noisier than a GaAsFET, the MAR-6 should do a respectable job of overpowering feedline loss and delivering a decent signal to the other end of your feedline. In another situation, you may want a block of RF gain to boost the output of a synthesizer board to the recommended drive level for a UHF-FM power module. For this job, the MAV-11—which provides a 12-dB boost and over 50 mW of output (+17.5 dBm)—might just be the ticket! Look for even more diversity in the future, as MMICs continue to evolve.

The bottom line

If you work (or play) with RF networks, the MMIC could become a great addition to your design repertoire. For more detailed MMIC technical data, order the Mini-Circuits *RF/IF Designer's Handbook*. In addition to MMICs, the handbook covers the full range of Mini-Circuits products, including mixers, splitters, amplifiers, chip capacitors, attenuators, terminations, directional couplers, filters, phase detectors, switches, and RF transformers (a veritable smorgasbord of products for the RF designer). To obtain a free copy, direct your request to Mini-Circuits, P.O. Box 350166, Brooklyn, NY 11235-0003.

Mini-Circuits also offers several MMIC designer kits to help you get started. The DAK-3 kit provides the widest variety of MMIC samples—a total of 48 pieces for $59.95. Specifically, you get six each of the following devices: SM-1, SM-2, SM-3, SM-4, MAR-6, MAR-7, MAR-8, MAV-11. Three of each type have standard mounting tabs, and three of each type have special surface mount tabs.

Conclusion

The MMIC is a miniature gain block that drops into 50-ohm networks without the need for transformers or tuned matching circuits. Whether you are building a simple preamp for your scanner, or a state-of-the-art military communications transceiver, MMICs can be real problem solvers. Best of all, they are inexpensive, forgiving, and very easy to use. ■

Scott D. Prather, *KB9Y*
2776 S. Monroe Street
Denver, Colorado, 80210

THE DRAKE R-8 RECEIVER

Evolution in design and simplicity

Electronics is an evolutionary art. Good designs often involve the reuse of time-proven circuits and the implementation of current state-of-the-art designs. With the release of the R.L. Drake R-8 receiver last year, Drake's engineering department took this evolutionary concept to heart. The R-8 is a blend of old and new technology, with some elegant simplicity thrown in for good measure. In this article, I'll take a close look at the design similarities and differences between the Drake R-8 and its highly respected predecessors, the R-7 and the SPR-4.

The Drake R-8: an overview

The R-8 is a communications receiver designed to cover 100 kHz to 30 MHz continuously. An optional VHF converter provides additional coverage from 35 to 55 MHz and from 108 to 174 MHz. The receiver will demodulate AM, SSB, CW, RTTY, and FM transmissions. Five degrees of selectivity are available: 6.0 kHz, 4.0 kHz, 2.3 kHz, 1.8 kHz, and 0.5 kHz. The IF bandwidth can be selected independently of mode with the exception of FM, where it is fixed at 12 kHz. The unit features a total of 100 memories, into which the user may program not only a given frequency, but also the mode, bandwidth, AGC hang time, preamp/attenuator setting, synchronous detector mode, noise blanker mode, step size, notch filter, and antenna. The user may view and select information in memory through a 16-key pad or through a conventional rotary tuning knob. An RS-232

Photo courtesy of R.L. Drake

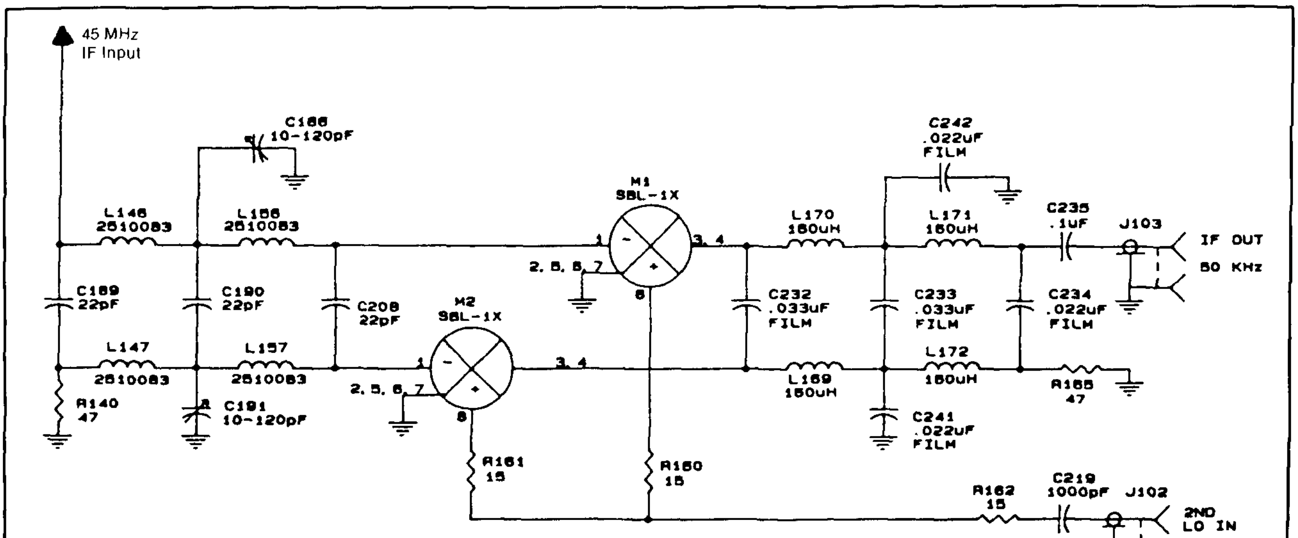

Figure 1. R-8 Image rejecting mixer.

I/O port provides control over all major functions of the R-8, as well as enhanced memory capabilities. Communication with the receiver over this port is possible with any communications program, or Drake can supply special IBM-compatible software at a nominal cost.

On the surface, the unit looks like most other communications receivers of recent vintage. But a close look inside reveals some very interesting and innovative circuit designs.

The R-8 front end

Most of the front end in the R-8 appears to have been borrowed from the design of the R-7. Nine PIN-diode switched Chebyshev bandpass filters provide selectivity for the RF preamp and mixer. Drake also used the same transistor for the RF preamp in the R-8 as they did in the R-7. A roofing filter to improve the first IF rejection precedes the first mixer. As was the case in the R-7, Drake used a double-balanced mixer (DBM) to up-convert to a 45-MHz IF (the R-7 used 48.05 MHz). A non-AGC controlled JFET amplifies the 45-MHz IF from the DBM before it's routed to a four-pole crystal filter. This 45-MHz filter provides a 12-kHz bandwidth at the -3 dB points. From the crystal filter, the 45-MHz IF signal is routed either to the AM or the FM IF chain. I'll return to the FM portion of the receiver later, for now I will concentrate on the AM IF.

A unique mixer design

Conventional up-conversion receiver design has typically dictated conversion from an IF in the 45 MHz (or above) range to a second IF in the 2 to 9 MHz range, and a second mixer to take the IF down to 455 kHz or lower. In the R-8, the 45-MHz IF signal is further amplified and routed to a pair of double-balanced mixers set up as an image rejecting mixer (IRM, see **Figure 1**). In this configuration, the local-oscillator (LO) injection frequency to the IRM is 45.05 MHz, converting to a second IF of 50 kHz directly.

One of the benefits of eliminating a mid-IF stage is an improvement in the receiver's dynamic range. Although a number of design factors affect dynamic range, it is directly related to the overload characteristics of the nonlinear stages in a receiver. Mixers are nonlinear by design. Eliminating an additional mixer stage and its associated IF amplifiers helps to improve the dynamic range and minimize the generation of spurious responses.

Another benefit gained from the elimination of an additional mixer stage is that by converting to a 50-kHz IF directly, no expensive bandpass filters are required for a second IF in the 2 to 9-MHz range. L/C filtering that provides excellent selectivity is easy to design for an IF frequency this low, eliminating the cost of expensive mechanical or crystal filters in the IF altogether.

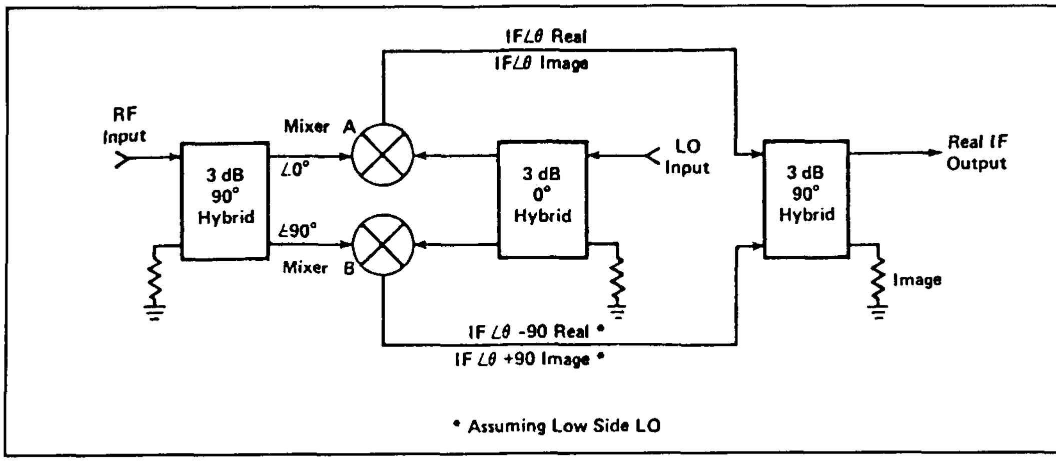

Figure 2. Image rejecting mixer block diagram. Reprinted from *Microwave Solid-State Circuit Design* by Inder Bahl and Prakash Bhartia (see *Reference 2*).

The IRM design used in the R-8 isn't a new concept. An original paper describing this mixer design for microwave frequencies in the 1 to 12 GHz band was presented in 1970 by Kurpis and Taub in the *IEEE Transactions on Microwave Theory and Techniques*.[1] However, Drake's adaptation of this design is the first I've seen in a consumer communications receiver.

How the image rejecting mixer works

The IRM consists of two gain and phase matched double-balanced mixers fed in phase from the LO (see **Figure 2**). A 45-MHz hybrid network feeds the signal input to DBM A with no phase shift while DBM B is fed −90 degrees out of phase with the incoming signal. Since DBM A is fed in phase with the incoming signal, its output displays a 0 degree phase shift for both the desired and the image frequency. However, the output from DBM B has a +90 degree phase shift for the desired signal and a −90 degree phase shift for the image (the R-8 uses high-side LO injection, therefore these angles are reversed from **Figure 2**). The outputs from the two DBM are then combined in a second 45-MHz hybrid network. Here, the desired signals from each DBM combine in phase at the IF port of the hybrid and are passed on to the IF stages. However, the image signals from DBM B cancel with those from DBM A at the image port, where a resistive load is used to terminate the image power.[2]

According to Kurpis and Taub, this mixer design will provide a minimum of 20 dB of image rejection. In the Drake alignment procedure, they claim a minimum image rejection at 45.1 MHz of 30 dB, which can be considered typical for this mixer in a narrowband application. This degree of rejection can only be realized with DBMs and hybrids that are carefully phase and amplitude matched.[3] **Figure 3** shows the critical relationship between these two parameters and image rejection of the mixer.

Second IF

Drake's concept of simplicity didn't end at their design of a dual conversion receiver with a 45-MHz first IF and a 50-kHz second IF. They took advantage of the low-frequency second IF to provide selectable IF bandwidth without the high cost of crystal or mechanical filters. In the R-8, the 50-kHz second IF signal is amplified by an AGC-controlled IF amplifier and routed through one of five four-pole Chebyshev L/C filters. These filters are very similar to the second IF filters used in the SPR-4.

The 6.0, 4.0, 2.3, and 1.8 kHz filters in the R-8 were designed for a −60/−6 dB shape factor of better than 2.2. The 500-Hz filter is limited to a −60−/−6 dB shape factor of less than 4.0. Response curves for the IF filters are available. Send an S.A.S.E. to Communications Quarterly, P.O. Box 465, Barrington, NH 03825. Insertion loss varys widely according to the filter selected; passband ripple is less than 2.9 dB peak-to-peak on the widest bandwidth, and the ultimate selectivity exceeds −95 dB. Shape factor performance and insertion loss were somewhat compromised with this design; however, these are impressive numbers for L/C filters. By comparison, mechanical filters typically provide a −60/−6 dB shape factor of between 1.5 and 2.5 for −6 dB bandwidths in the 2 to 6 kHz range, and 1.7 to 3 for a −6 dB bandwidth of 500 Hz. Mechanical filters typically display passband ripple of about 2 dB, and an insertion loss of between 3 and 6 dB.

The crystal filters in the R-7 provide a $-60/-6$ dB shape factor comparable to mechanical filters, except at the 500-Hz bandwidth, were they approach 2.2. Again, careful circuit design provided the R-8 with an IF filter whose performance approximates that of mechanical filters, at a fraction of the cost.

After passing through the selected 50-kHz L/C filter, the signal is amplified by an AGC-controlled IF amplifier stage and routed to a second set of five L/C filters. From there, the signal is routed to the final stages of IF amplification and on to the AGC circuitry and AM/SSB detector. The AGC was designed to compensate for the varying insertion loss presented by the L/C filters, maintaining a constant S-meter reading without regard to the setting of the bandwidth or passband tuning.

AM synchronous detector

Another area in which the R-8 differs from its predecessor is found in its AM synchronous detector. When AM signals are propagated through the ionosphere, the carrier is sometimes lost while the sidebands remain strong. In a conventional envelope detector, this results in apparent overmodulation, often creating extreme distortion. In a synchronous detector, a locally generated carrier is phase locked to the incoming carrier frequency and injected into the detector. During periods of deep fading, this locally injected carrier replaces the "missing" carrier, reducing distortion. Although advertised as having an AM synchronous detector, the Drake R-7 actually used a low-distortion envelope detector for AM with no recovered-carrier reinsertion. The result was a receiver that fared no better than most of its day on deeply fading signals.

The synchronous detector in the R-8 is a true synchronous detector (see **Figure 4**). The frequency of the incoming 50-kHz carrier is doubled by U109 sections B,D and routed to the carrier-reinsertion phase-locked loop U112. In addition to tracking the incoming carrier frequency, the carrier-reinsertion PLL also tracks the setting of the passband tuning control (PBT), permitting the detector to stay in synch as the PBT is used to suppress interference. The phase-locked regenerated 100-kHz carrier from U112 is then divided by two in U108 and applied to the carrier input of the SSB/AM detector chip U103.

The importance of an efficient synchronous detector shouldn't be underestimated.

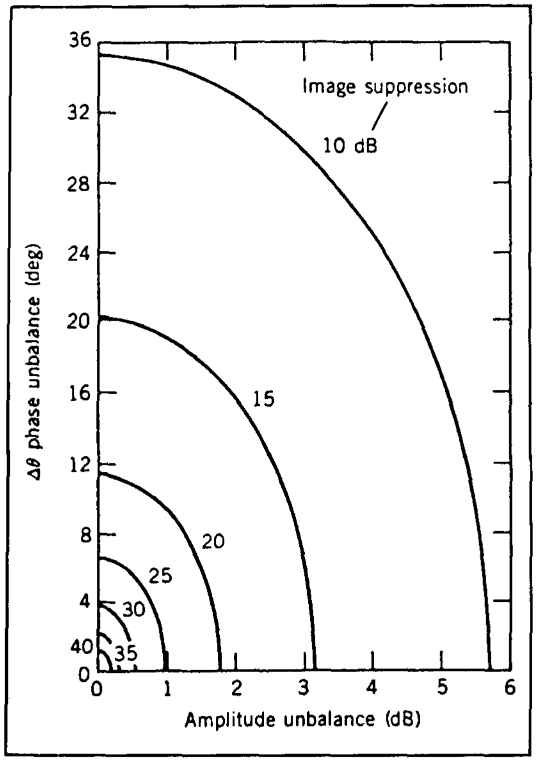

Figure 3. Image rejection as a function of circuit amplitude and phase errors. Reprinted from *Microwave Circuit Design Using Linear and Nonlinear Techniques* by George Vendelin, Anthony Pavio, and Ulrich Rohde (see *Reference 3*).

In addition to greatly reducing distortion during periods of deep carrier fades, the synchronous detector is also effective when receiving two AM stations on the same frequency whose carriers are slowly beating against one another (such as during BCB DXing). The internally generated synchronous carrier eliminates this beat, dramatically improving intelligibility. The detector is also useful when trying to copy a weak signal adjacent to a strong local signal. The synchronous carrier tends to reduce the annoying interference from sideband splatter, improving intelligibility.

Noise blanker

Another area in which the R-8 exhibits superiority over the R-7 and SPR-4 is in the receiver's noise blanker circuitry. In the R-7 and SPR-4 the noise blanker was of a conventional design, employing a fixed-bandwidth, high-gain noise amplifier, and associated blanking circuitry in the 5.645-MHz second IF. However, the designers of the R-8 took a different approach. The R-8 uses a unique noise blanker chip, which includes an internal amplifier with AGC, a peak detector, a

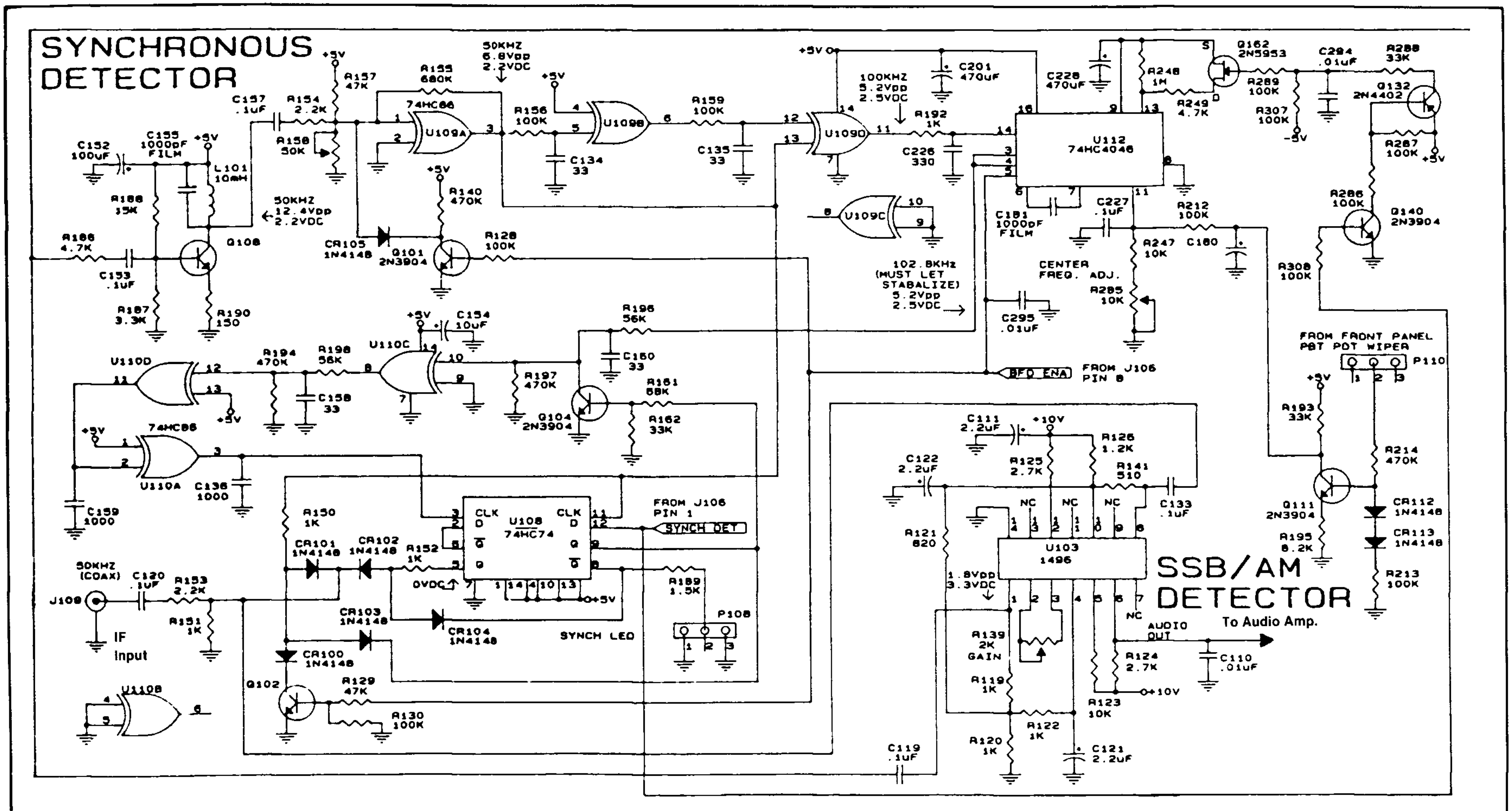

THIS DOCUMENT CONTAINS INFORMATION WHICH IS CONFIDENTIAL AND PROPRIETARY, AND IT IS NOT TO BE USED, COPIED OR REPRODUCED, IN WHOLE OR IN PART, OR DISCLOSED TO OTHERS WITHOUT THE EXPRESSED WRITTEN PERMISSION OR R.L. DRAKE COMPANY.

Figure 4. R-8 synchronous detector.

noise differentiator, an RF gate, and a audio circuit designed to fill in the blanking "holes" (see **Figure 5**). When the blanker is enabled, the differentiated noise pulses turn the RF gate off, suppressing their amplification by the remaining IF stages. At the same time the RF is gated off, audio from the detector is "held" for a predetermined time to prevent the creation of a "hole" during RF blanking. The result is an extremely efficient noise blanker that works better than anything I have ever heard before. On repetitive impulse noise (like that from fluorescent lights, SCR light dimmers, etc.) the blanker is so effective that enabling it sounds as though you have turned the interference source off! The only fault I could find in this circuit is that the blanker has no effect on weak noise pulses, because they cannot properly trigger the RF gate.

FM IF and detector

The inclusion of FM in the R-8 was unprecedented in Drake's prior receivers. The FM section is quite conventional, using a generic Motorola MC 3362 FM receiver chip of the type used in many portable FM transceivers. Incoming 45-MHz IF signals from the front end are mixed with an on-chip 34.3-MHz second LO. The result 10.7-MHz second IF is mixed with another on-chip 10.245-MHz LO to provide a 455-kHz third IF. Ceramic filters in the 455-kHz IF provide additional selectivity. An on-chip demodulator and received signal strength indicator (RSSI) circuit round out the FM portion of the R-8. This section of the receiver is simple, but there's little sense in "reinventing the wheel" when custom-application chips of this type are readily available.

Audio circuitry

The audio amplifier portion of the R-8 is quite conventional in most respects. Again, simplicity is evident in Drake's judicious use of op amps and a generic audio amplifier IC. The notch filter design differs from that used in the R-7. In the R7, the notch filter was in the 50-kHz IF. The R-8 uses an audio notch circuit instead. Unique to the R-8 is the inclusion of a tone and a squelch control. The tone control either boosts or cuts the receiver's bass response by ±10 dB. I found this control moderately useful during certain conditions.

The squelch control works in any detection mode. It can be set to trip at a certain "S-meter" reading, permitting the radio to scan a frequency band or through memory

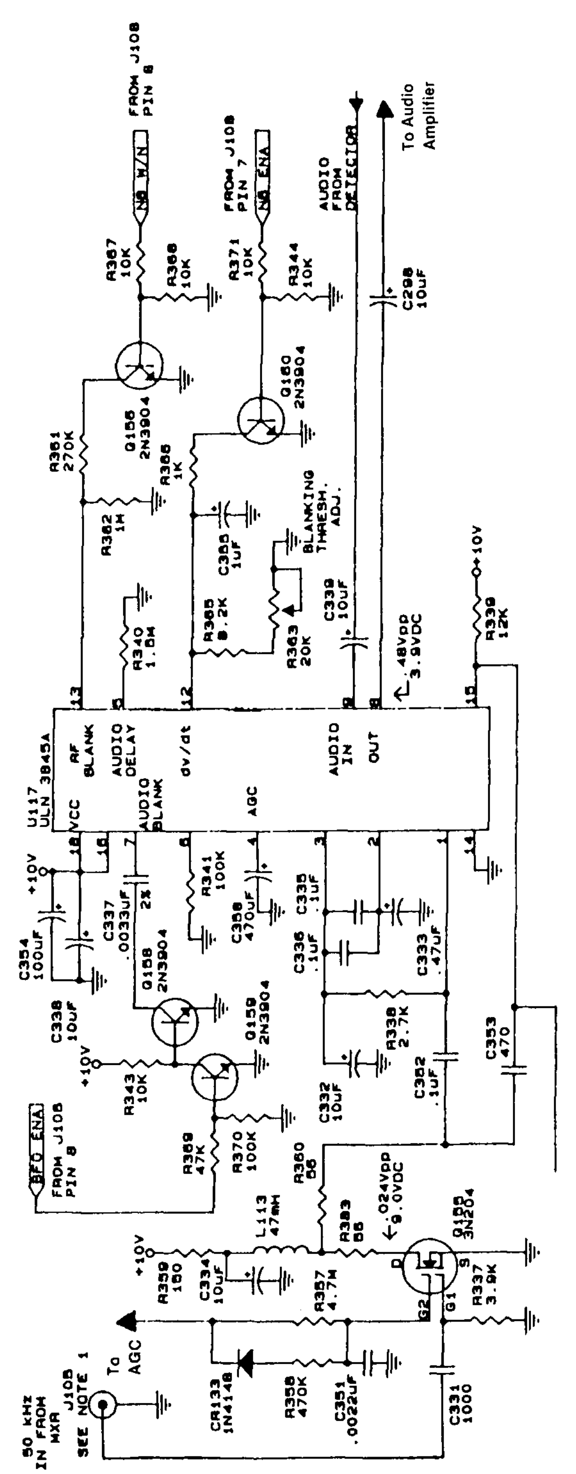

Figure 5. R-8 noise blanker.

looking for a signal whose strength exceeds a preset threshold. While I found the usefulness of this feature questionable in an HF environment, it will no doubt come in handy for some special application of the scanner.

VHF converter

The optional VHF converter is also of a somewhat unique design. The converter covers 35 to 55 MHz and 108 to 174 MHz in two separate bands. The preselector for the 35 to 55-MHz range uses a single wide-band bandpass filter. However, the preselector for the 108 to 174-MHz range is a 15-step voltage-tuned design. The receiver's microprocessor selects the appropriate front-end filter and one of six fixed-frequency synthesizers according to the frequency desired. The synthesized LO is then routed to a double-balanced mixer to convert the incoming signal to a range covered by the receiver front end.

Construction

Significant changes in the R-8 card construction and positioning make it possible to service it without an extender card. In the R-7, a total of 12 printed circuit boards plugged into two card cages in the receiver. While this provided excellent isolation between cards, it was a nightmare to repair. The Drake TR-7/R-7 extender card kit (or a homemade equivalent) was a necessity in order to work only any of the cards with power applied.

The R-8 uses a total of four cards, two of which are stacked vertically. The front-end card can be removed and made to stand on end using tabs on the board that engage with slots in the back panel. All interconnecting cables are designed to allow operation of the front-end card in this position. Holes drilled in the front end card allow access to alignment points on the second IF/audio card below it with the front end card in place.

All printed circuit boards in the R-8 are glass epoxy, and they are unusually thick. Ground-plane grids are used extensively to prevent ground loops and instability.

Other than the obvious differences in the positioning of cards, the mechanical design is quite similar to the R-7. The chassis is of heavy-gauge anodized aluminum, with a black anodized front panel. The receiver width and height are almost identical to the R-7. One nice improvement is that the front legs are retractable. This allows the user to change the elevation of the front panel without removing the bottom panel.

Ergonomics

The R-8 was designed with careful attention to the ergonomic aspects of its use. All controls with similar functions are grouped together, keeping hand motion across the front panel to a minimum. The keyboard is laid out in a conventional 10-key pattern. The keys' color coding readily identifies their secondary functions. Drake's use of the rotary tuning control as a conventional tuner or as a means for rapidly selecting memory locations is a very nice touch.

RS-232 control

Most functions of the R-8 are available via a 9600-baud serial I/O bus on the rear panel. Communication with the radio via this port can be through a computer running almost any serial communications program or through a dumb terminal. A list of programming and interrogation codes is included in the owner's manual for those who would like to write custom software to support the R-8. For those who would prefer to use computer control without writing their own software, Drake has available a quite user-friendly software package. The Drake software provides programming of up to 10,000 memory channels (with name tags for easy identification), 100 memory blocks, 100 VFO scans, and eight timer settings. The opening screen displays all the current settings on the R-8, including frequency to five decimal places.

The most useful application of the software that I could come up with is in the study of propagation. The R-8 can be programmed to turn itself (and a tape or chart recorder) on at a specific time on a specified frequency, and record a known station or beacon. It can then tune itself to WWV to record solar indices for that day, and then (if the VHF converter is installed) tune itself to NOAA on 162.55 MHz for recording local weather conditions. There are doubtless other applications for this versatile software package.

Final observations

Drake really did their homework when they designed this receiver. The design and features of the unit are such that it should appeal to a wide variety of users. The inclusion of FM, optional VHF coverage, and RS-232 control opens up an entirely new suite of possibilities. However, the lack of a narrow (300 Hz or less) IF filter takes the R-8 out of the CW competition-grade class.

The Drake team took a close look at the various shortcomings in their earlier receivers and designed these faults out of the R-8. In addition, they were well aware of the circuitry that had worked well for them in the past, and used it again where appropriate.

I used the receiver for almost one hundred hours on all frequencies and in all modes. I ran the receiver through a battery of on-air tests that quickly show front-end, noise blanker, and synthesizer design faults. The R-8 performed better overall than many receivers costing two and three times as much. All in all, the engineers at Drake deserve praise for the design of the R-8. It is truly an example of electronics evolution and design simplicity intended to eclipse any of their prior equipment.

Acknowledgements

I would like to express my sincere appreciation to John Schlipp, Bill Frost, and Steve Whitefield with the R.L. Drake Company for their assistance in procuring and providing information for this article. I'd also like to thank Lee Cornett with Rockwell International for supplying information on mechanical filters.

REFERENCES

1. G.P. Kurpis and J.J. Taub, "Wide-Band X-Band Microstrip Image Rejection Mixer," *IEEE Transactions on Microwave Theory and Techniques*, IEEE Publications, December 1970, pages 1181-1182.
2. Inder Bahl and Prakash Bharita, *Microwave Solid-State Circuit Design*, John Wiley & Sons, New York, 1988, pages 578-581.
3. George D. Vendelin, Anthony M. Pavio, and Ulrich L. Rohde, *Microwave Circuit Design Using Linear and Nonlinear Techniques*, John Wiley & Sons, New York, 1990, pages 624-628.

BIBLIOGRAPHY

1. G.P. Kurpis and J.J. Taub, "Wide-Band X-Band Microstrip Image Rejection Mixer," *IEEE Transactions on Microwave Theory and Techniques*, IEEE Publications, December 1970.
2. Donald G. Fink, *Electronic Engineer's Handbook*, McGraw-Hill, 1975.
3. Inder Bahl and Prakash Bhartia, *Microwave Solid-State Circuit Design*, John Wiley & Sons, 1988.
4. George D. Vendelin, Anthony M. Pavio, and Ulrich L. Rohde, *Microwave Circuit Design Using Linear and Nonliner Techniques*, John Wiley & Sons, 1990.
5. Ulrich L. Rohde and T.T.N. Bucher, *Communications Receivers Principles and Design* McGraw-Hill, 1988.
6. *R.L. Drake Communications Receiver Service Manual*, R.L. Drake Company, 1991.
7. Cornell Drentea, *Radio Communications Receivers*, TAB, 1982.

PRODUCT INFORMATION

QUALCOMM's Turnkey 40-MHz DDS System

QUALCOMM introduces the Q0320-1 40-MHz direct digital synthesizer (DDS) system. At the heart of the Q0320-1 DDS system is the QUALCOMM Q2220I-50N DDS, which digitally generates sine waves, as well as more complex synthesizer outputs like frequency hopping, frequency sweeping, FSK and MSK digital modulation waveforms. Also included are a high-performance 8-bit DAC, clock reference, low-pass filter, sine wave to TTL square wave converter, and 40-pin dual in line (DIL) header. Output frequencies can range from DC to 14 MHz with exact 2.0 Hz step resolution.

The Q0320-1 DDS System is fully assembled and tested, and resides on a single circuit card measuring only 3x3 inches. It needs only a +5 volts DC power supply and control interface for operation and requires less than 0.75 watts of power. The system comes with a user's manual that includes schematic diagrams.

For more information contact QUALCOMM Inc., VSLI Products Division, 10555 Sorrento Valley Road, San Diego, California 92121-1617.

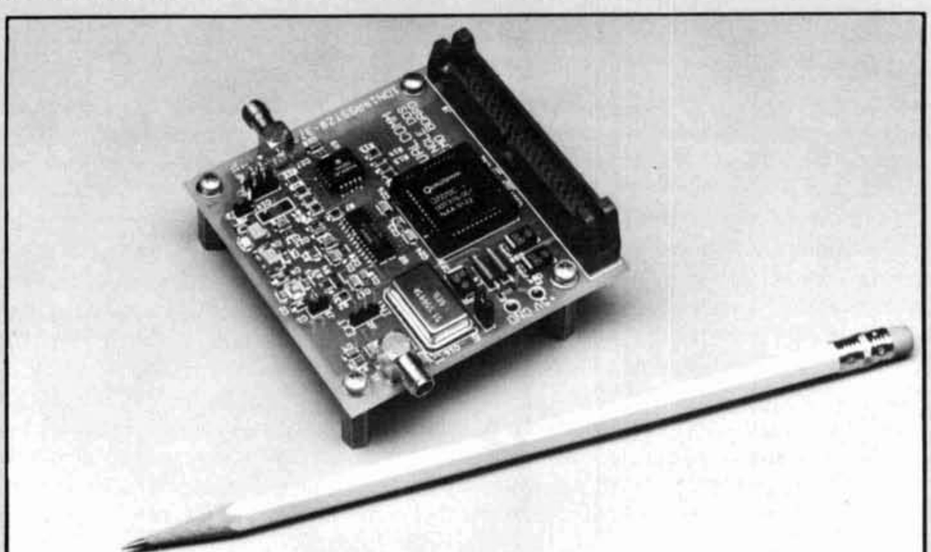

In search of a better mousetrap...

With this issue of Communications Quarterly, a new column premiers: Tech Notes. We often receive many good articles that are too short, or for other reasons just aren't suitable for use as feature presentations in the magazine. Tech Notes will showcase the best of these articles. Authors are encouraged to submit short original technical manuscripts for consideration. Peter Bertini, K1ZJH, Senior Technical Editor.

An Accessible Inductance Standard

F.P. Hughes, VE3DQB

In my youth, it was drummed into my head that any scientific work was only as good as the standards used in the measurements involved. This knowledge has stood me in good stead over the decades, enabling me to undermine rivals merely by checking their standards one against another. In an avocation where the resources available may limited, it's normal to use standards of a lesser accuracy than ideal. For instance, one uses fresh batteries from the store rather than Weston cells as voltage standards.

Resistance standards are available as commercial resistors of 1 percent accuracy. Several of these, if consistent, are acceptable as a standard to radio amateur accuracy. With a standard cell, or fresh battery, or perhaps a zener diode, and a selection of standard resistors, one can verify the readings of multimeters.

So much for DC. Standards of inductance and capacitance are harder to come by. Usually, a 5 percent capacitor is considered a standard, as is a cut off the joint of a length of commercial inductor. I used these "standards" for many years, but always thought that there ought to be something better. At last I set myself a definite aim: I would make an L or C standard to 1 percent accuracy.

Now, if you measure the resonant frequencies of two capacitors across two inductors (one at a time), what results is four equations with four unknowns. I set out to solve this on paper. Of course, it didn't work; however, it set me thinking.

A review of ancient physics books, and my copy of the *Handbook of Chemistry and Physics*, brought out that I might be able to make an inductance standard of an accuracy better than I could buy on a slim ham budget. In particular, I could make a circular ring of round wire and perhaps calculate its inductance with sufficient accuracy. A back-calculation told me that a ring of convenient size would give an acceptable resonant frequency with a 100-pF capacitor.

Contrary to my usual experience, there were no false starts when I tried this out. My ring of 16 gauge wire about 13 centimeters in diameter, soldered to a 100-pF 5-percent capacitor, resonated near 25 MHz. A larger ring and the same capacitor resonated near 22 MHz, and the calculation from both these standard inductors gave the same capacitance—within 1 percent.

Construction of the standard

The standard is constructed of bus wire—tinned copper of 16 gauge or near. The ring has to be suspended, and thinner wire might change shape perceptibly under the stress. Moveover, it's harder to measure the diameter of thin wire. The wire is formed into a circle with a diameter between 10 and 20 centimeters. Cut an ample length of wire and secure one end in the bench vice. With the needle-nose pliers, straighten the wire by grasping it loosely with the pliers held at an angle, pulling the wire taut, and sliding the pliers up the wire. Bend the wire into a gentle S by holding the pliers at an angle, so the wire is bent first one way and then the other as the plier jaws pass. Repeat this with the pliers at a different angle, so that all kinks are completely removed.

The end result is a length of wire with a graceful curve in it. Now take a circular object—a paint tin, or a bottle—of near the chosen diameter and wrap the wire most carefully round it and pull taut, so that the wire forms a circle. The two standing parts of the wire, the end in the vice and the one you're pulling on, should touch at the point at which they leave the cylinder. Release the pull carefully and remove the cylinder.

The wire will spring out to a circle of rather greater diameter than the cylinder. Cut off the standing parts to leave an accurate circle of wire.

Now solder a good quality capacitor of

near 100 pF to the ends of the circle. Cut the leads of the capacitor to half a centimeter or so. Put the wire into the vice so one end sticks up enough to solder to conveniently, and solder one end of the capacitor to one end of the wire. Then bring the other end of the wire to the other end of the capacitor and solder. The ring and the capacitor should, so far as possible, form a smooth circle. The capacitor outer plate then forms a part of the ring.

Measure the approximate diameter of the inductor, and draw a circle of this diameter on a sheet of paper. Divide the circle diametrically at 45 degree intervals. Lay the standard inductor on the circle and measure the diameter four ways, guided by the pencilled diameters. I verified my centimeter rule by checking it against a good mechanic's steel rule. It was almost a millimeter out at ten inches. Aim for 1/10th millimeter accuracy. Average these four readings.

From the remaining straightened wire, cut ten short lengths. Lay these side by side without gaps between them and measure the total of their diameters. Divide by ten to obtain the diameter of the wire. (Or you can use an optical micrometer, as I did.)

Now calculate the inductance of the circular ring of round wire from:

$$L = 0.01257 \times a[\ln(16 \times a/d) + 2 - \delta \quad \textbf{(1)}$$

Where a = radius of the ring, d = diameter of the wire, and δ is the skin depth correction. For 25 MHz, use $\delta = 0.12$, for 16 MHz use $\delta = 0.14$, and for 9 MHz use $\delta = 0.17$. Interpolate if necessary.

Using the standard

The capacitor to be measured was soldered to the wire to form the ring, so the circuitry is all ready for measurement. Suspend the ring by two threads from the ceiling, to keep the field as free as possible from interference from metallic objects.

Measure the resonant frequency of the combination with a grid-dip meter. Move the meter as far away as possible while still getting an indication. Get a rough idea of the frequency first by dipping the meter near the ring, then moving it steadily away, swinging the tuning slightly to get as accurate a dip as you can.

Measure the GDO frequency with a receiver or counter. Calculate the capacitance C using **Equation 2**:

$$C = (1¾[2\pi F])^{2}22/L \quad \textbf{(2)}$$

Where F = frequency and L = inductance.

Errors

The inductance errors to be expected in measurement of the ring can be readily calculated from the formula for L given above—especially if you can perform the calculations on your computer. As I have the capability to do so, I can state that:

An error in measurement of the diameter of 1 millimeter results in an error of 0.004 μH in the inductance at 0.4 μH. Similarly, an error of 0.1 millimeter in the measurement of the diameter of the wire results in an error of 0.007 μH. Errors in the skin effect allowance are negligible—approximately 0.0001 μH.

Errors in frequency measurement can be calculated from the formula $F = 1/2\pi \times (LC)^{-1/2}$. Consequently, an error of 0.1 MHz at 25 MHz leads to an error of 2 pF for a 100 pF nominal capacitor. Similarly, an error of 0.01 μH in the inductance of a standard of 0.4 μH leads to an error of 1.1 pF in a 100 pF capacitor.

Proof of the pudding

I built a ring of 16 gauge wire 13.16 centimeters in diameter. The calculated inductance was 0.3916 μH. I completed the ring with a 100 pF, 5 percent tolerance, capacitor. Ten measurements of its resonant frequency were made with an oscillator loosely coupled to it, the resulting mean of the measurements was 102.79 pF, with a standard deviation of 0.015 pF. Thus, there is a 95 percent probability that the true capacitance lies between 102.49 pF and 103.09 pF—well within the tolerance required for an amateur laboratory standard.

I measured a 330 $\pm$5 percent capacitor against two rings: one of 0.47723 μH, the other of 0.39246 μH. The calculated capacitances that resulted were 319.6 pF and 318.8 pF, respectively.

The much used "5 μH" standard, together with its screw-on terminals, turned out to be 4.26 μH. The 100-pF standard, complete with appendages, was 106.8 pF.

Discussion

These measurements assured me that I had attained my goal. I now have a system for constructing an inductance standard of good precision. It is certainly simpler to construct an inductance standard of high precision than a comparable capacitance standard. The capacitance calculated from the known inductance is a suitable secondary standard.

While I don't know the accuracy of the standard, it must be fairly high. However, I do know that two separately constructed standards give results for a given capacitor within the stated tolerance, the inductor is measured with an accurate rule, and the inductance is calculated from a formula derived from an impeccable theory.

Another Look at Logic Gates

Peter J. Bertini, K1ZJH

Most amateurs have had some experience with digital logic—it's hard not to find interesting applications for these devices for our shacks, repeaters, or mobile installations. The radio world is merging more with the digital domain with each new generation of radio. If you like to dabble with simple digital projects, I'm going to show you a few tricks that will greatly reduce your design time!

I'd like to discuss gates in a practical manner, avoiding Boolean algebra and other math that may apply in a more technical presentation. Like atoms in a molecule, gates are at the heart of any VLSI chip; counters, shift registers, memories, and even microcomputer chip circuitry are built around the humble gate. **Figures 1** through **4** show several common gates and their truth tables. These basic gate building blocks are available in pin-compatible DIP packages in diverse logic families as TTL, CMOS, LS, and a variety of others. I won't go into the electrical parameters or differences between these families, instead I'm going to show you how to visualize gates in a way you may not have seen before. For simplicity, I'll only discuss dual-input gates, but the techniques shown are valid for any number of like inputs. **Figure 1** shows a NAND gate; **Figures 2, 3,** and **4** show AND, NOR, and OR gates, respectively.

We're all familiar with these devices. Most of us think AND gate functions require that all inputs be in one state to enable the output state, and that OR gates need a certain level on one or both inputs of the gate to enable the desired output state. However, this assumption is incorrect; gates aren't always what they appear to be!

The symbols in **Figures 5** through **8** may be unfamiliar to many of you, but they were common back in the early days of digital logic. Their names are just as unfamiliar today. **Figure 5** shows a negated-input OR gate; **Figure 6** is a negated-input NOR gate. **Figure 7** shows a negated-input AND gate and **Figure 8** is a negated-input NAND gate. Carefully compare the truth tables of the devices in **Figures 1** through **4** with those shown in **Figures 5** through **8**. If the truth tables match, the devices are the same. Each gate shown in the first four drawings has an unlikely equal in the last four drawings. Thus, the conventional NAND gate shown in **Figure 1** is the same as the device shown in **Figure 5**, the negated-input OR gate.

You can change a gate from an OR function to an equivalent AND function by changing the symbol and inverting the inputs and output. If the inversion bubble is present on the input or output, remove it, and if it isn't there, draw it in. If the symbol is an OR, make it an AND. This works in both directions.

Yes, you can convolute an exclusive OR gate into an exclusive negated-input NAND

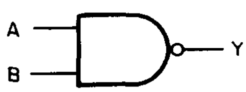

INPUTS		OUTPUT
A	B	Y
L	L	H
H	L	H
L	H	H
H	H	L

Figure 1. Symbol for NAND gate and its truth table.

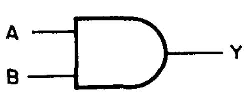

INPUTS		OUTPUT
A	B	Y
L	L	L
H	L	L
L	H	L
H	H	H

Figure 2. Symbol for AND gate and its truth table.

INPUTS		OUTPUT
A	B	Y
L	L	H
H	L	L
L	H	L
H	H	L

Figure 3. Symbol for NOR gate and its truth table.

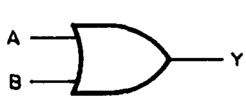

INPUTS		OUTPUT
A	B	Y
L	L	L
H	L	H
L	H	H
H	H	H

Figure 4. Symbol for OR gate and its truth table.

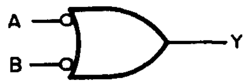

INPUTS A	INPUTS B	OUTPUT Y
L	L	H
H	L	H
L	H	H
H	H	L

Figure 5. Negated-input OR gate and its truth table. Device is actually the same as a NAND gate.

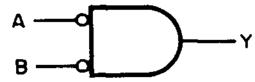

INPUTS A	INPUTS B	OUTPUT Y
L	L	H
H	L	L
L	H	L
H	H	L

Figure 7. Negated-input AND gate and truth table. Device is another function for the NOR gate.

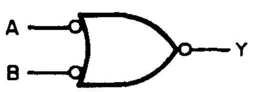

INPUTS A	INPUTS B	OUTPUT Y
L	L	L
H	L	L
L	H	L
H	H	H

Figure 6. Negated-input NOR and truth table. Device is the same as an AND gate.

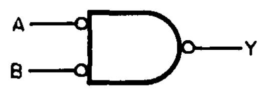

INPUTS A	INPUTS B	OUTPUT Y
L	L	L
H	L	H
L	H	H
H	H	H

Figure 8. Negated-input NAND gate and truth table. Device is really an OR gate in disguise.

gate. The truth tables will match, but there's really no practical reason for doing so (see **Figure 9**).

Let's look at a few applications. Suppose your club wants to PL the club repeater, and you wish to combine the low-going COR signal with the low-going signal from the PL decoder to produce a valid input signal indication for the repeater controller. The output signal can be high or low, a simple invertor will take care of this if need be. Draw the circuit exactly as the logic flow

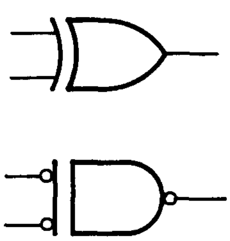

Figure 9. Exclusive OR gate can be changed into exclusive negated-input NAND gate.

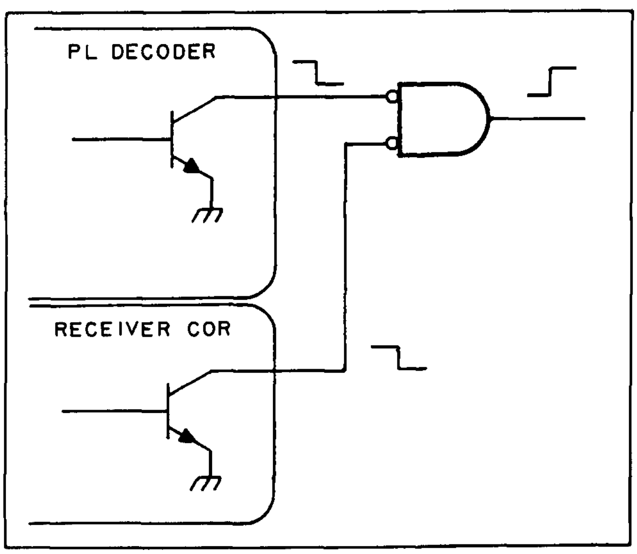

Figure 10A. Circuit senses PL and COR levels for repeater. Negated-input AND gives high output when carrier and subaudible tone are detected.

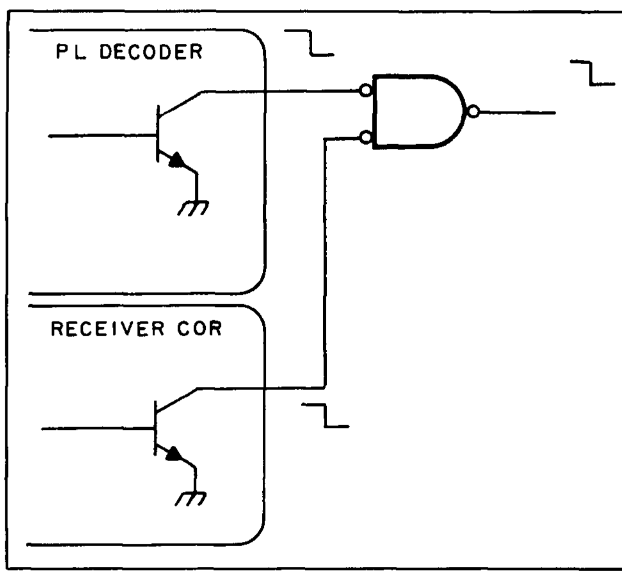

Figure 10B. Same circuit using negated-input NAND will give low active output when carrier and subaudible tone are present.

dictates. You'll want to have two lows to obtain an output. **Figures 10A** and **10B** show two circuits that meet your requirements. Note that the circuit is easier to read using the negated-input AND functions; you are looking for an output to occur when the two inputs are both in a certain identical state. Our minds have been trained to think of this as an "AND" function. Redraw the circuit by changing the gate from the AND function to an OR function and by inverting the inputs and outputs. This yields the more commonly found logic NOR or OR gate (**Figure 11**). However, the operation of the circuit is now no longer intuitive.

Inverter symbols don't change, but the inversion bubble can be drawn at either end (**Figure 12**). The inverted input version may be viewed as needing an active low for a high output. The standard type may be seen as looking for an active high to yield a low output. Buffers can be drawn with inversion bubbles at both ends. It's all a matter of perspective. If your circuit is looking for two active lows to give a high output, use the negated-input AND gate; but, if your circuit is looking for either (or both) of the inputs to go high for a low output, you'll need the NOR gate. The truth tables are the same, but each version can be used to make the operation of a circuit that's much simpler to understand. ■

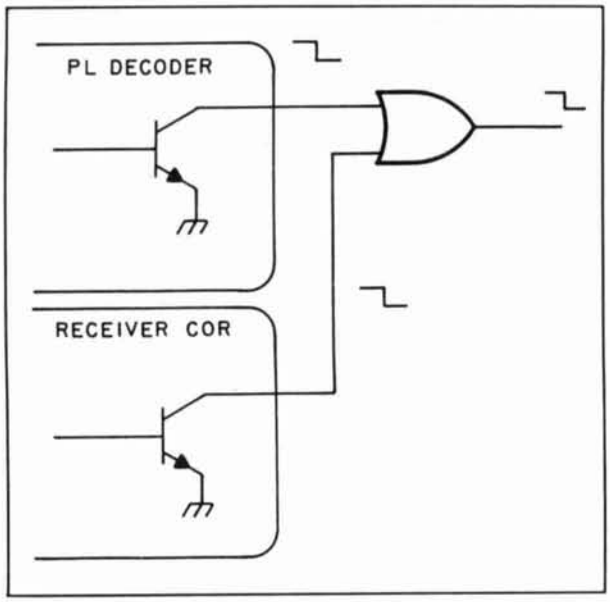

Figure 11. Conventional drawing of carrier and PL circuit uses OR gate. The function of this device is not intuitive in this configuration.

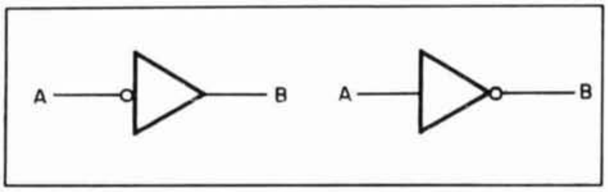

Figure 12. Inverters can be drawn either way. It's all a matter of perspective.

[redacted]

ADVERTISER'S INDEX

We'd like to see your company listed here too. Contact Arnie Sposato, N2IQO, at (516) 681-2922 or FAX at (516) 681-2926 to work out an advertising program to suit your needs.

[redacted]

FT-530
Dual Band Handheld

- **Frequency Coverage:**
  2-Meters 130-174 MHz RX
  140-150 MHz TX
  70 cm 430-450 MHz RX/TX
- 82 Memories (41 per band)
- 4 TX Power levels
  w/FNB-25: 2.0, 1.5, 1.0, 0.5W
  w/FNB-27: 5.0, 3.0, 1.5, 0.5W
- Dual in-band receive feature (V/V, U/U or V/U receive operation)
- DTMF Paging and Coded squelch included.
- AOT – Auto On-Timer with built-in clock
- ABS – Automatic Battery Saver (Super battery life, each band can have separate battery saver)
- Built-in VOX
- IBS – Intelligent Band Select (provides automatic TX band select on scan stop)
- Built-in CTCSS with dual decode
- ATS – Automatic Tone Search (displays incoming CTCSS frequency)
- Back-lit keypad and display with time delay
- Built-in cross-band repeat function
- APO – Automatic Power Off
- 5 Watts output w/ FNB-27 battery or 12 VDC
- 2 VFO's for each band
- **Accessories:**

NC-42	1-hour Desk Charger
FNB-25	600 mAh Battery (2 watt)
FNB-26	1000 mAh Battery (2 watt)
FNB-27	600 mAh Battery (5 watt)
FBA-12	6 AA Cell Holder
CSC-56	Vinyl Case w/ FNB-25
CSC-58	Vinyl Case w/ FNB-26/27
E-DC-5	12 VDC Adaptor
YH-2	Headset for VOX
MH-12A2B	Speaker Mic
MH-18A2B	Lapel Speaker Mic
MH-19A2B	Mini Earpiece Mic
MH-29A2B	LCD Display Mic with Remote Functions
MMB-54	Mobile Mounting Hanger

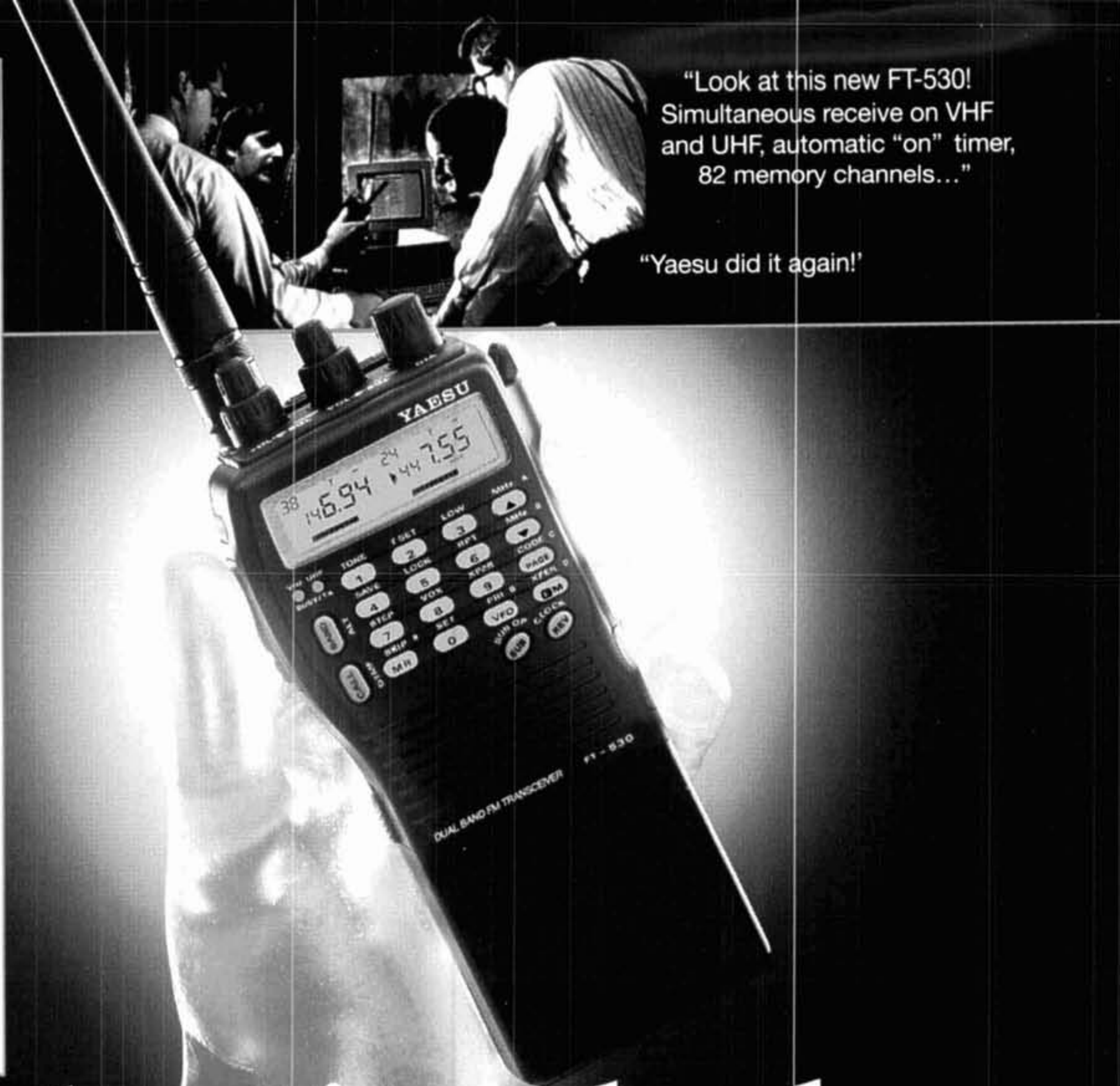

Bright minds lead to brilliant "firsts."

That's right, brilliant innovative first-time ever features which make the FT-530 our most exciting HT addition.

Exclusive break-through features, too. Like flexible in-band dual receive. Not just V/U receive. With the FT-530 you can listen to two, 2-meter signals at the same time!

Another remarkable first is the Auto On-Timer℠. Here's how it works. Choose the hour you'd like the radio to begin operating. For example, set the time for the morning, then wake up to your favorite net. What's more, the built-in 24-hour clock displays the time when the radio is off.

First out with 82 memory channels included, not an option; a real plus for storing all your favorite frequencies. With this HT, just open the box and QSO.

There's a lot of other terrific features too, such as built-in VOX and DTMF paging. And, since we know you'll find the FT-530 indispensable, we've included an automatic battery saver and voltage display – a powerful handful of exclusive features!

Be the first at your dealer's door to buy one, and the first to show off your new FT-530. What a bright idea!

NEW

Multi-Function Digital Display Speaker Mic and S Meter. *(Optional)*

YAESU

Performance without compromise.℠